Role of Rap and Rho GTPases in T-acute lymphoblastic leukaemia cell adhesion and migration

Infante, Elvira

Awarding institution:
King's College London

Title: Role of Rap and Rho GTPases in T-acute lymphoblastic leukaemia cell adhesion and migration

Author: Elvira Infante

Role of Rap and Rho GTPases in T-acute lymphoblastic leukaemia cell adhesion and migration

by

Elvira Infante

A thesis submitted to King's College London
for the degree of Doctor of Philosophy, October 2012

Randall Division of Cell and Molecular Biophysics
King's College London
2nd floor New Hunt's House
London SE1 1UL

Abstract

T-acute lymphoblastic leukaemia (T-ALL) is a common childhood cancer. Multiple genetic mutations have been identified in T-ALL patients. The most common is the mutation of the NOTCH1 oncogene occurring in more than 50% of patients. Poor prognosis has often been shown to correlate with the migration and accumulation of T-ALL cells in the tissues. Rap and Rho family GTPases play key roles in T cell adhesion and migration and are often involved in cancer progression. Most of these proteins are post-translationally isoprenylated to facilitate their anchorage to membranes, where they function to stimulate signal transduction processes.

In the first part of these studies, statins were used to reduce prenylation of GTPases, and to investigate whether the resulting alteration of GTPase membrane targeting affects T-ALL cell migration. Statins inhibited adhesion, chemotaxis and transendothelial migration of T-ALL cell lines. A similar effect was observed with geranylgeranyl transferase inhibitors and siRNA depletion of Rap1b but not Rap1a, RhoA, Rac1, Rac2 and Cdc42. These results suggest that statins and Rap1b depletion could be used to reduce tissue invasion in T-ALL.

In contrast to other Rho family proteins, the atypical Rho GTPases RhoU and RhoV are not prenylated but undergo palmitoylation for membrane targeting. They are expressed at higher levels in primary T-ALL samples compared to primary T cells, and RhoU expression was shown to be unregulated by Notch1. In the second part of these studies downregulation of RhoU and Notch1 by siRNA reduced adhesion and migration of T-ALL cell lines. Interestingly, similar functional effects were observed upon siRNA depletion of RhoV. RhoU and RhoV partially co-localized and moved dynamically between endosomes and the plasma membrane, suggesting they act together to regulate membrane trafficking. These results indicate that RhoU and RhoV could contribute to T-ALL invasion by regulating T-ALL cell adhesion and migration.

Table of contents

Abstract 2
Table of contents 3
List of figures 8
List of tables 11
Supplementary Movies 12
Abbreviations 14
Introduction 17
1.1 The immune system 17
1.1.1 T lymphocytes 18
1.1.1.1 Major histocompatibility complex and antigen recognition 18
1.1.1.2 T lymphocyte subpopulations 19
1.1.1.3 T cell receptor 20
1.1.1.4 T lymphocyte development 21
1.1.1.5 Notch1 24
1.1.2 B lymphocytes 28
1.2 T-acute lymphoblastic leukaemia 30
1.3 Ras and Rho GTPases as regulators of cell adhesion and migration 34
1.3.1 Ras and Rho GTPases lipid modification 35
1.3.2 Statins, geranylgeranyl and farnesyl inhibitors 39
1.3.3 Rap GTPases 41
1.3.3.1 Integrins and their ligands 44
1.3.4 Rho GTPases 47
1.3.4.1 RhoU 48
1.3.4.2 RhoV 50
1.4 Rap and Rho GTPases and T lymphocytes migration 53

1.4.1 Rap and Rho GTPases in adhesion 53

1.4.2 Rho GTPases and cell migration 54

1.4.3 Chemotaxis 59

1.4.4 Leukocyte transendothelial migration 61

1.4.4.1 Endothelium: the blood vessel wall 61

1.4.4.2 Rolling and adhesion 63

1.4.4.4 Transendothelial migration 64

1.4.4.4.1 Paracellular TEM 65

1.4.4.4.2 Transcellular TEM 66

1.5 Aims of the project 68

Statins inhibit T-acute lymphoblastic leukaemia cell adhesion and migration through Rap1b 69

2.1 Abstract 70

2.2 Introduction 71

2.3 Materials and Methods 73

2.3.1 Cell culture and drug treatment 73

2.3.2 Transfection 73

2.3.3 Adhesion assays 74

2.3.4 Transendothelial migration 74

2.3.5 Timelapse microscopy 74

2.3.6 Flow cytometry 75

2.3.7 Immunofluorescence 75

2.3.8 GTPase activity assays 75

2.3.9 Western blot analysis 76

2.4 Results 77

2.4.1 Statins inhibit adhesion and chemotaxis of T-ALL cell lines but not of primary T-lymphoblasts 77

2.4.2 Statins dysregulate Rap1, Rac1 and RhoA activity in CCRF-CEM cells .79

2.4.3 Low concentrations of statins do not dysregulate Rap1 activity in primary T-lymphoblasts 81

2.4.4 Rap1b is required for T-ALL cell adhesion and migration 83

2.4.5 Statins and Rap1b regulate integrin activity 85

2.4.6 Statin treatment and Rap1b downregulation inhibits transendothelial migration of T-ALL cells.....87

2.5 Discussion.....90

2.6 Supplementary materials 92

Analysis of Rho GTPase expression in T-ALL identifies RhoU as a target for Notch involved in T-ALL cell migration.....94

3.1 Abstract.....95

3.2 Introduction 96

3.3 Materials & Methods.....98

3.3.1 T-ALL patient samples and normal T-lymphocyte isolation.....98

3.3.2 Cell culture and GSI treatment 98

3.3.3 Transfection 99

3.3.4 Sample preparation and real-time SYBR-Green PCR.....99

3.3.5 Statistical analyses 100

3.3.6 Immunoblotting 100

3.3.7 Immunofluorescence.....101

3.3.8 Time-lapse microscopy.....101

3.3.9 Adhesion assay 102

3.3.10 Flow cytometry.....102

3.4 Results 103

3.4.1 Atypical Rho genes are upregulated in T-ALL 103

3.4.2 Rho gene expression patterns cluster T-ALL patients in two groups.....106

3.4.3 *RHOU* expression correlates with Notch1 signalling in T-ALL 109

3.4.4 RhoU expression is regulated by Notch1 signalling..... 113

3.4.5 RhoU regulates T-ALL cell polarization, migration and adhesion 115

3.5 Discussion..... 122

3.6 Supplementary figures 125

Roles of RhoU and RhoV in T-ALL cell adhesion and migration 127

4.1 Introduction 127

4.2 Materials and methods 128

4.2.1 Cell biology..... 128

4.2.1.1 Cell culture..... 128

4.2.1.2 Transfection of siRNAs 128

4.2.1.3 Transfection of plasmids..... 129

4.2.1.4 Adhesion assay on endothelial cells (manual counting)..... 129

4.2.1.5 Adhesion assay on endothelial (plate reader) 130

4.2.1.6 Transwell based transendothelial migration assay..... 130

4.2.1.7 Live imaging microscopy 130

4.2.1.8 Immunofluorescence microscopy 131

4.2.1.9 Analysis of filopodia and cell spreading..... 131

4.2.2 Molecular Biology 132

4.2.2.1 Generation of GFP-RhoU, GFP-RhoV and Cherry-RhoU vector 132

4.2.2.2 Restriction enzyme digestion of DNA..... 135

4.2.2.3 Agarose gel elctrophoresis..... 135

4.2.2.4 Extraction of DNA from agarose gels 135

4.2.2.5 DNA ligation..... 135

4.2.2.6 Transformation of competent bacteria..... 136

4.2.2.7 Purification of plasmid DNA from bacteria 136

4.2.2.8 Determination of DNA and RNA concentration 137

4.2.2.9 DNA sequencing 137

4.2.2.10 RNA isolation using Trizol 137

4.2.2.11 cDNA synthesis 138

4.2.2.12 Real-time SYBR-green PCR 138

4.2.3 Biochemistry 139

4.2.3.1 Immunoprecipitation 139

4.2.3.2 Western blot analysis 139

4.3 Results 141

4.3.1 RhoV expression in T-ALL cell lines and siRNA transfection in Jurkat cells 141

4.3.2 RhoU and RhoV depletion reduces adhesion of Jurkat cells to fibronectin and endothelial cells 143

4.3.3 RhoU and RhoV depletion reduces transendothelial migration 146

4.3.4 RhoU and RhoV induces morphological changes in Jurkat and SUPT1 cells. 147

4.3.5 Dynamic analysis of RhoU and RhoV distribution 151

4.3.6 RhoU and RhoV localize in part on endosomes 158

4.3.7 RhoU interacts with RhoV 163

4.3.8 The N-terminus of RhoV is not required for RhoU binding 164

4.3.9 FLIM analysis of Jurkat cells expressing cherry-RhoU and GFP-RhoV or GFP-ΔNRhoV 166

4.3.10 RhoU and RhoV form homodimers 169

4.3.11 RhoU interacts with Rac1, Rac2 and RhoV but not RhoA or Cdc42 169

4.3.12 RhoU but not Rac1 and RhoV interact with NCK1 171

4.3.13 RhoV regulates RhoU levels 172

4.4 Discussion 174

References 189

Acknowledgments 209

List of figures

Figure 1.1 Photomicrograph of the thymus.....22
Figure 1.2 Schematic representation of T cell development in the thymus. 23
Figure 1.3 Domain structure of Notch receptors.....25
Figure 1.4 Notch1 signalling.....27
Figure 1.5 Correlation of T-ALL cell lines with the normal differentiation pattern of human T-lymphocytes.....31
Figure 1.6 Phylogenetic tree of the mammalian Ras GTPase superfamily.....34
Figure 1.7 Regulation of Rho GTPase activity. 35
Figure 1.8 GTPase isoprenylation.....36
Figure.1.9 Skeletal formula of farnesylpyrophosphate (A) and geranygeranylpyrophosphate 37
Figure 1.10 Skeletal formula of 16-carbon fatty acid palmitate. 37
Figure 1.11 GTPase lipid modification.....38
Figure 1.12 Statin inhibition of prenylation.....40
Figure 1.13 Effectors, GEFs and GAPs of Rap 43
Figure 1.14 Amino acid sequences of Rap1a and Rap1b.....44
Figure 1.15 Integrin activation.....46
Figure 1.16 Amino acid sequences of Cdc42, RhoV and RhoU.....51
Figure 1.17 Domain structure of RhoU and RhoV 52
Figure 1.18 Signalling in T cell migration.....57
Figure 1.20 Schematic rappresentation of leukocyte transendothelial migration 61
Figure 1.19 Endothelial cell-cell adhesion.....63
Figure 2.1. Statins inhibit adhesion and chemotaxis of T-ALL cell lines but not of primary T-lymphoblasts.....78
Figure 2.2. Statins and GGTI increase Rap1, Rac1 and RhoA activity in CCRF-CEM cells 80
Figure 2.3. Primary T-lymphoblasts are less sensitive to statins and have higher Rap1 levels than T-ALL cells.....82
Figure 2.5. Statins, GGTI and Rap1b regulate LFA-1 integrin activity 86
Figure 2.6. Statin treatment and Rap1b downregulation reduce transendothelial migration of T-ALL cells.....88

Supplementary Figure 1.1 92
Supplementary Figure 1.2 93
Figure 3.1 Rho mRNA expression in T-ALL 104
Figure 3.2 Association of Rho expression and T-ALL disease characteristics..... 107
Figure 3.3 Association of RhoU expression with Notch1 signalling in T-ALL patients and cell lines 110
Figure 3.4 Notch1 regulates RhoU expression 114
Figure 3.5 RhoU regulates T-ALL cell morphology and migration 116
Figure 3.6 RhoU and Notch1 regulate T-ALL cell adhesion..... 118
Figure 3.7 RhoU regulates polarity..... 120
Supplementary Figure 3.2. RhoU depletion in T-ALL and effects of γ-secretase inhibition on protein expression and cell adhesion 126
Figure 4.1 Example of filopodia and a spread cell..... 132
Figure 4.2 Schematic diagram of RhoU and RhoV subcloning into pEGFP-C1..... 133
Figure 4.3 Schematic diagram of RhoU subcloning into a pmCherry-C1 134
Figure 4.4 RhoV expression in T-ALL cell lines and RhoV siRNA knockdown.... 142
Figure 4.5 RhoU and RhoV depletion affect adhesion of Jurkat cells to fibronectin 144
Figure 4. 6 RhoU and RhoV depletion affect adhesion of Jurkat cells to HUVECs 145
Figure 4.7 RhoU and RhoV down-regulation reduces TEM 147
Figure 4.8 RhoU and RhoV overexpression induce cell spreading and filopodium formation..... 150
Figure 4.9 RhoU distribution in T-ALL cells 152
Figure 4.10. RhoV distribution in Jurkat cells 154
Figure 4.11 RhoU and RhoV distribution in Jurkat cells..... 156
Figure 4.12 RhoU and RhoV co-localize..... 157
Figure 4.13 RhoU and RhoV-containing vesicles localize around the MTOC..... 159
Figure 4.14 RhoU and RhoV localize on endosomes 160
Figure 4.15 RhoU and RhoV co-localize on endosomes 161
Figure 4.16 RhoU and RhoV do not localize to the Golgi..... 162
Figure 4. 17. Coimmunoprecipitation of RhoU and RhoV..... 163
Figure 4.18 Sequence comparison between RhoV and ΔN-RhoV 164
Figure 4.19 Coimmunoprecipitation of RhoU and ΔNRhoV 165
Figure 4.20 FLIM analysis of RhoU and RhoV interaction..... 168

Figure 4.21 RhoU and RhoV homodimerize 169
Figure 4.22 RhoU co-immunoprecipitates with Rac1, Rac2 and RhoV 170
Figure 4.23 NCK1 co-immunoprecipitates with RhoU but not Rac1 or RhoV 171
Figure 4.24 RhoV regulates RhoU expression.....173
Figure 5.1Schematic mechanism of action of statins in primary-T-lymphoblast and in T-ALL cell adhesion…….183
Figure 5.2 Hypothetical model for the control of adhesion and migration by Rap1b, RhoU and RhoV in T-ALL……...187

List of tables

Table 1. Rho mRNA expression in T-ALL relative to healthy controls……..105
Table 2. Association between relative Rho expression in T-ALL and WBC……...108
Table 3. Association between relative Rho gene expression and DELTEX-1 levels in T-ALL……...112

Supplementary Movies

Movie 1	Control CCRF-CEM cells	Figure 2.6
Movie 2	Simvastatin treated CCRF-CEM cells	Figure 2.6
Movie 3	Simvastatin and mevalonic acid co-treated CCRF-CEM cells.	Figure 2.6
Movie 4	siControl CCRF-CEM cells	Figure 3.5
Movie 5	siRhoU-1 CCRF-CEM cells	Figure 3.5
Movie 6	siRhoU-2 CCRF-CEM cells	Figure 3.5
Movie 7	siControl CCRF-CEM cells	Figure 3.5
Movie 8	siNotch1-1 CCRF-CEM	Figure 3.5
Movie 9	siNotch1-2 CCRF-CEM cells	Figure 3.5
Movie 10	DMSO treated CCRF-CEM cells	Figure 3.5
Movie 11	GSI treated CCRF-CEM cells	Figure 3.5
Movie 12	pEGFP-RhoU transfected Jurkat cell	Section 4.34
Movie 13	pEGFP-RhoV transfected Jurkat cell	Section 4.34
Movie 14	pEGFP-RhoU transfected Jurkat cell	Figure 4.9
Movie 15	pEGFP-C1 transfected Jurkat cell	Figure 4.9
Movie 16	pEGFP-RhoU transfected CCRF-CEM cell	Figure 4.9
Movie 17	pEGFP-C1 tranfected CCRF-CEM cell	Figure 4.9
Movie 18	pEGFP-RhoV tranfected Jurkat cell	Figure 4.10
Movie 19	pEGFP-C1 tranfected Jurkat cell	Figure 4.10
Movie 20	mCherry-RhoU tranfected Jurkat cell	Figure 4.11
Movie 21	pEGFP-RhoV tranfected Jurkat cell	Figure 4.11

Movie 22	pEGFP-RhoV and pmCherry-RhoU co-transfected Jurkat cell	Figure 4.12
Movie 23	pEGFP-C1 and pmCherry-C1 co-transfected Jurkat cell	Figure 4.12

Abbreviations

Abi	Abl interactor
AJ	Adherens junctions
AML	Acute myeloblastic leukaemia
AML	Acute myeloid leukaemia
ANK	Ankyrin-like repeats
APC	Antigen presenting cell
ARPC	Actin-related protein
ARF6	ADP-ribosylation factor 6
BCR	B cell receptor
CCP	clathrin-coated pit
CCR9	Chemokine receptor 9
CML	Chronic myelogenous leukaemia
CNS	Central nervous system
CTLA	Cytotoxic T lymphocyte antigen
CXCL	CXC Chemokine ligand
DAAM	Dishevelled-associated activator of morphogenesis
DC	Dentritic cell
DH	Dbl-homology
DHR	DOCK homology region
Dlg	Discs large
DLL1	Delta-like ligand 1
DN	Double negative
DP	Double positive
ECM	Extracellular matrix
EGF	Epidermal growth factor
ERM	Ezrin-radixin-moesin protein
ESAM	Endothelial cell-selective adhesion molecule
ESL1	E-selectin ligand 1
ETP	Early T cell precursors
FFI	Farnesyl transferase inhibitor
FMN	Formin
FN	Fibronectin
FoxP3	Transcription factor forkhead box P3
FRET	Förster resonance energy transfer
FRL	Formin-related proteins in leukocyte
FTI	Farnesylation transferase inhibitor
GAP	GTPase activating protein
GAPDH	Glyceraldehyde-3-phosphate dehydrogenase
GAPs	GTPase activating proteins
GEF	Guanine nucleotide exchange factor
GGTI	Geranylgeranyl transferase inhibitor
GITR	Glucocorticoid-induced tumour necrosis factor receptor
GPCR	G protein-coupled receptors
GS	Intramembrane γ-secretase
HD	Heterodimerization domain
HMG-CoA	3-hydroxy-3-methylglutaryl coenzyme A

HUVECs	Human umbilical vein endothelial cells
ICAM-1	Intercellular adhesion molecule-1
Ig	Immunoglobulin antigen-binding proteins
IL	Interleukin
INF	Interferon
ITAMs	Immunoreceptor tyrosine-based activation motifs
iTreg	Induced Treg
JAM	Junctional adhesion molecule
LB	Luria broth
LBCR	Lateral border recycling compartment
LFA-1	Lymphocyte function-associated antigen/ αLβ2 integrin
Lgl	Lethal giant larvae
LN	Cysteine-rich region Notch/Lin12 domain
MAML1-3	Mastermind proteins
MAPK	Mitogen-activated protein kinase
MDS	Myelodysplastic syndrome
MHC	Major histocompatibility complex
MLC	Myosin light chain
MLL	Mixed-lineage leukaemia
MRL	Mig-10/RIAM/Lamellipodin
MTOC	Microtubule organizing centre
mTOR	Mammalian target of rapamycin
NFAT	Nuclear factor of activated T cells
NF-κB	Nuclear factor κB
NICD	Notch1 intracellular domain
NKT	Natural killer T cells
NLS	Nuclear localization signals
NPF	Nucleation promoting factor
NS	Not significant
nTreg	Natural Treg
OD	Optical density
PAK	p21 serine/threonine kinase
Pals1	Protein Associated with Lin Seven 1
PAMPs	Pathogen-associated molecular patterns
PATJ	Pals1-associated tight junction protein
PBR	Polybasic region
PBS	Phosphate-buffered saline
PC3	Prostate cancer cells
PEST	Proline, glutamic acid, serine, threonine-rich domain
PI3K	Phosphatidylinositol 3-kinases
PSGL1	P-selectin glycoprotein ligand1
qPCR	Quantitative PCR
RAM	RBP-Jκ–associated module
Rho GDI	GDP dissociation inhibitors
RIAM	Rap1-GTP-interacting adaptor molecule
ROS	Reactive oxygen species
SDF-1	Stromal-cell derived factor-1
sLeX	Sial Lewis x
SP	Single positive cells
TAD	Transactivation domain

T-ALL	T-acute lymphoblastic leukemia
TCR	T cell receptor
TEM	Transendothelial migration
Th	Helper T cells
Tiam1	T lymphoma invasion and metastasis 1
TJ	Tight junction
TLRs	Toll-like receptors
TNFα	Tumour necrosis factorα
VCAM1	Vascular cell-adhesion molecule 1
VE-cadherin	Vascular endothelial cadherin
WBC	White blood cell count
ZO	Zona occludens

1

Introduction

1.1 The immune system

The main function of the immune system is to protect against microorganisms. It uses a highly organized array of mechanisms and cell types to distinguish between foreign agents and the own body cells and molecules.

The primary defence of the human body from foreign agents is the anatomic barrier provided by epithelial surfaces. If a pathogen is able to pass this barrier, the second line of defence is provided by the innate immune system. This includes molecules that are either present in biological fluids, such as the complement system, or secreted as cells are activated. The cells of the innate immune system include monocytes, macrophages, natural killer cells, granulocytes (subdivided into neutrophils, eosinophils and basophils) and mast cells (Chaplin, 2006). Other important players of the innate immune system are the Toll-like receptors (TLRs). Mammals have a repertoire of TLRs through which they recognize a wide range of pathogen-associated molecular patterns (PAMPs). PAMPs include peptidoglycan, lipopolysaccharide, CpG DNA, and double or single-stranded RNA derived from bacterial or viral microorganisms. Interaction of TLRs with PAMPs triggers downstream signalling pathways leading to activation of other innate or adaptive processes (Kulkarni et al., 2011). A third line of defence against infection is the adaptive immune system. This is a specific response that also provides long-term protection against re-exposure to the same pathogen. The main cells of the adaptive immune system are B and T lymphocytes.

In humans, all cells of the immune system originate in the bone marrow or in the fetal liver from haematopoietic stem cells in a process known as haemotopoiesis. This process occurs in several stages and is mediated by cytokines, including interleukins, colony-stimulating factors, interferons, erythropoietin and thrombopoietin (Robb, 2007).

1.1.1 T lymphocytes

T lymphocytes originate from pluripotent precursors in the bone marrow or fetal liver and migrate to the thymus where they undergo differentiation. T cells can mature into γδ T cells and αβ T cells which subsequently differentiate into CD4+ T cells, CD8+ T cells, natural killer T cells (NKT) and regulatory T cells. Once they leave the thymus these subpopulations play different functions (Rothenberg et al., 2008).

1.1.1.1 Major histocompatibility complex and antigen recognition

In the thymus, specific patterns of gene expression lead to T cell proliferation and rearrangement of the T cell receptor (TCR). In order for T cells to recognize a foreign protein it must be degraded into small antigenic peptides that form physical complexes with the major histocompatibility complex receptors **(**MHC-I or MHC-II). The TCR can then recognize the antigens presented by MHC molecules on the cell surface. MHC molecules play a central role in enabling the immune system to distinguish self from non-self. The encounter of a naive T cell with cognate antigen on a MHC molecule initiates T cell proliferation and differentiation into memory T cells and various T cell effectors (Bjorkman, 1997). The class MHC-I molecules are glycoproteins express on the membrane of almost all nucleated cells and they are associated with β2- microglobulin. The class MHC-II molecules are heterodimeric glycoproteins mainly expressed by antigen presenting cells (APCs). The APCs include dendritic cells, macrophages, B cells, and thymic epithelial cells. APCs can internalize antigens by either phagocytosis or endocytosis and re-express a part of the antigen on the membrane surface with MHC-II molecule (Ryan and Cobb, 2012). APCs are able to induce a signal that is necessary for T helper cell activation. CD8+ T cells bind to antigens associated with MHC-I and are pre-programmed for cytotoxic functions. CD4+ T cells bind to antigens associated with MHC-II and are pre-programmed for helper functions (Xiong and Bosselut, 2012).

1.1.1.2 T lymphocyte subpopulations

CD4+ helper T cells (Th) provide regulatory functions of the adaptive immune system to respond appropriately to a particular antigen. In particular they promote and direct the differentiation and activation of B cells and cytotoxic T cells (Konig and Zhou, 2004)

Th cells include Th1, Th2 and Th17. Although other T-cell subsets, such as Th3 cells and Th22 cells, have been described, their lineage-specific transcription factors have not been identified (Maddur et al., 2012). After binding peptide on the MHC-II complex, Th cells are activated and become effectors secreting growth factors and cytokines. For example, Th1 cells secrete interleukin 2 and interferon-γ, and Th2 cells produce interleukin 4 and 5. Generally, the Th1 subpopulation induces the activation of macrophages and synthesis of IgG2b antibody by B cells. The Th2 subpopulation induces the synthesis of other antibodies including IgE (see section 1.1.2).

Recently the Th17 population has been characterized as a distinct lineage of $CD4^+$ T cells. These cells secrete IL-17 and express surface IL-23 receptor and the lineage-specific transcription factor RORγC. In addition, human Th17 cells specifically express the lectin receptor CD161. Th17 cells are important for the clearance of extracellular pathogens, however they have been associated with the pathogenesis of several autoimmune and inflammatory diseases (Maddur et al., 2012; Park et al., 2005).

Treg cells play an important role in the maintenance of immunological self-tolerance and immune homeostasis by suppressing pathological immune responses against self-antigens. These cells are CD4+ CD25+ and express glucocorticoid-induced tumour necrosis factor receptor (GITR), cytotoxic T lymphocyte antigen (CTLA)-4 and the transcription factor forkhead box P3 (FoxP3). Treg cells can either develop in the thymus or be converted in the periphery by TGF-β (Ruffell et al., 2010). Treg can be classified in natural Treg (nTreg) and induced Treg (iTreg). iTreg are induced in response to antigenic stimulation under tolerogenic conditions and thus contribute to the development of an antigen-specific immunosuppressive response. These cells can secrete TGF-β and interleukin (IL)-10 that participate in their immunosuppressive effect against conventional T cells (Menetrier-Caux et al., 2012).

As mentioned above, CD8+T lymphocytes bind MHC-I and are known as cytotoxic T cells (Xiong and Bosselut, 2012). Cytokines secreted by Th cells, induce cytotoxic T cells to proliferate and differentiate into effectors. These cells do not secrete a lot of cytokines but instead scan cells of the body that express their cognate antigen, such as virus-infected cells, tumour cells and foreign tissue graft (Chaplin, 2006).

1.1.1.3 T cell receptor

In 95% of T cells the TCR is a heterodimer consisting of an α and β chain linked by disulphide bonds. In 5% of T cells the TCR is instead formed of a γ and δ chain. The TCR forms a multisubunit complex with the CD3 complex, which is formed by CD3γ, CD3δ, CD3ε and TCRζ subunits. The CD3 subunits contain immunoreceptor tyrosine-based activation motifs (ITAMs) (van der Merwe and Dushek, 2011). ITAMs in the CD3 complex can be phosphorylated by the Src family tyrosine kinases Lck and Fyn. Phosphorylation of ITAMs allows the binding of the ZAP70 tyrosine kinase, which subsequently phosphorylates LAT and SLP-76 triggering activation of signal transduction pathways such as protein kinase C, Ras, Rac and phospholipase C (Lin and Weiss, 2001). This is important to initiate T cell responses, including proliferation and cytokine synthesis (Sommers et al., 2000).

T cells can protect from vast number of microbial pathogens as they possess specific antigen receptors, encoded a huge array of different TCR. TCR are somatically assembled from variable (V), diverse (D) and joining (J) gene elements to generate mature $V_\alpha J_\alpha$ chains and $V_\beta D_\beta J_\beta$ chains. The assembly of these gene elements is mediated by the lymphoid-specific RAG1 and RAG2 proteins that cleave the DNA near the V, D and J segments. These elements are then joined by non-lymphoid-specific DNA repair enzymes, resulting in the V, D, and J gene elements assembling in a random process and producing the huge diversity of TCR sequences (Chaplin, 2010).

As mentioned above, the TCR receptor complex expressed on the lymphocyte surface can recognize an antigen if it is presented in the context of a MHC class I or class II molecule. However, to fully activate T cells an interaction also occurs between the CD28 receptor and the CD80 or CD86 of the APC. Co-activation of a T

cell in a quiescent state via CD3 and CD28 leads to functional activation and entry into the cell cycle, leading to cell proliferation and increase in cell size. CD28 co-activation occurs in part by activation of the transcription factors nuclear factor κB (NF-κB) and nuclear factor of activated T cells (NFAT). Apoptosis is suppressed by the induction of anti-apoptotic proteins such as BCL-XL and BCL2. The phosphatidylinositol 3-kinases (PI3K) pathway is also responsible for activating the mammalian target of rapamycin (mTOR) that is required for growth (Acuto and Michel, 2003).

1.1.1.4 T lymphocyte development

In order to develop, early T cell precursors (ETP) from the bone marrow enter through the blood vessels into the cortico-medullary junction of the thymus (Figure 1.1). These precursors migrate and differentiate into double negative (DN) cells which do not express CD4 or CD8. DN cells progress through DN1 to DN4 stages (Deftos and Bevan, 2000). Development from the ETP to DN3 is coordinated with migration through distinct thymic microenvironments. ETPs and DN2 cells have a high proliferation rate, and they start to aquire their first T-cell characteristics. At DN2 stage cells initiate the rearrangement of the genes encoding the TCRβ, TCRγ and TCRδ chains. When they reach the DN3 stage they stop proliferating, and they generate the first complete rearranged TCR loci (Rothenberg et al., 2008). DN3 T cells with an in-frame TCR gene rearrangement become activated by TCR-dependent selection. Cells expressing the TCRβ undergo β-selection with the pre-T-α chain as a pre-TCR. Once a signal is transmitted through the pre-TCR, it terminates further β chain rearrengment and cells become double positive (DP), expressing CD4 and CD8. DP thymocytes begin to proliferate and form 75-88% of thymocytes. The proliferation phase contributes to T-cell diversity by generating a clone of cells with a single TCRβ-chain rearrangement. These clones can then rearrange the α-chain genes enhancing diversity (Lin and Weiss, 2001). The TCR α-chain gene rearrangement does not occur until the thymocytes stop proliferating. Completing of the TCR gene rearrangement leads to the surface expression of the TCRαβ heterodimers, which provides the substrate for the selection into single positive cells (SP) expressing CD4 or CD8, which can therefore proliferate and

migrate to the thymus periphery and function as mature αβ T cells. T cells that rearrange TCR γ and δ-chains are instead selected as γδ T cells (Hayday and Pennington, 2007) (Figure1.2).

About 99% of all thymocyte progeny die during their development in the thymus as eliminated by either positive or negative selection. The positive selection selects immature thymocytes able to interact with MHC and involves the interaction with epithelial cells in the thymic cortex. This process begins in DP thymocytes and takes several days to finalize. In the cortex the productive rearrangement of TCR in DP thymocytes results in the replacement of the pre-TCR with the clonotypic TCRαβ complex. Cells whose receptors can interact with low avidity with self-peptide-MHC expressed by cortical stromal cells receive a survival signal. DP thymocytes that fail to receive activating signals are 'non-selected' and undergo cell death in the cortex without maturing further. Positively selected DP thymocytes that gain the capability to survive differentiate into SP expressing CD4 or CD8. These cells are induced to express CC-chemokine receptor 7 (CCR7). CCR7-expressing thymocytes are attracted to the CCR7 ligands, CC-chemokine ligand 19 (CCL19) and CCL21, which are mainly localized and produced in the medulla. In the medulla, newly generated SP thymocytes are further selected by the medullary stromal cells, including autoimmune regulator (AIRE)-expressing cells, so that the cells that are reactive to tissue-specific antigens can be deleted (Ma et al., 2013; Takahama, 2006). This negative selection is crucial to eliminate thymocytes that may cause autoimmune disease. Positive and negative selections are therefore important to generate mature T cells that can interact with MHC and that are self-tolerant.

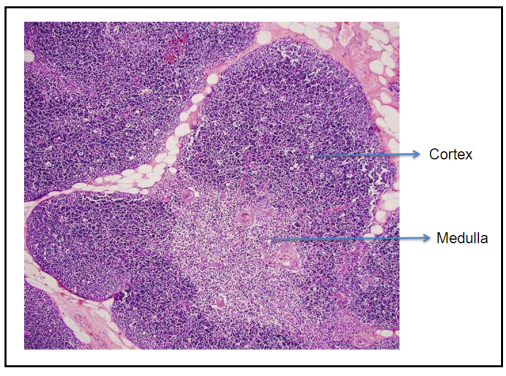

Figure 1.1 Photomicrograph of the thymus. Image shows the cortex and the medulla. (Nishino M et al., 2006)

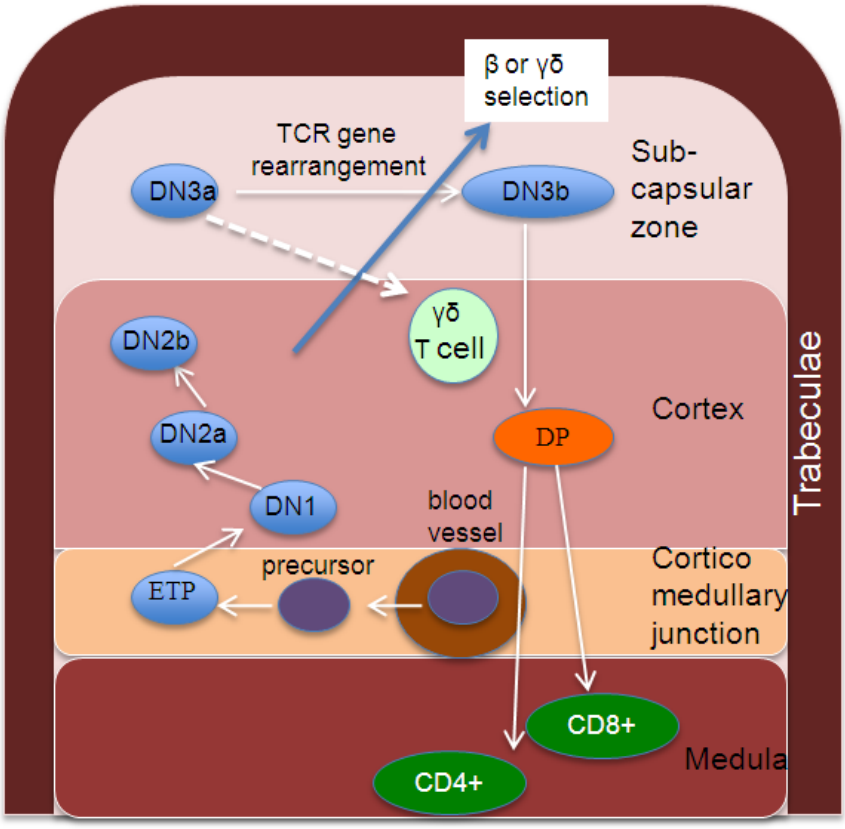

Figure 1.2 Schematic representation of T cell development in the thymus. Precursors leave the blood vessels in the cortico-medullary junction. The early T cell precursors (ETP) migrate to the cortex and differentiate to double negative (DN1). DN2 cells migrate more deeply into the cortex. In the subcapsular zone cells undergo rearrangements of the TCR β chain. For the later state of development thymocytes cross back across the cortex towards the medulla where they change from double positive (DP) to single positive (CD4+ or CD8+). Alternatively DN3 thymocytes that rearrange γδ chains of the TCR are selected as γδ T cells.

The maturation of SP thymocytes in the medulla includes the production of regulatory T cells and the expression of sphingosine-1-phosphate receptor 1 through which the cells are attracted back to the circulation that contains a high concentration of sphingosine-1-phosphate. During these stages development is coordinated by different microenvironments of the thymus epithelium, which provides receptor ligands and growth factors. Notch signalling is critical for T cell development and its pathway is stimulated by delta-like ligand 1 (DLL1) and DLL4 (Rothenberg et al., 2008).

1.1.1.5 Notch1

Notch signalling is highly conserved during evolution. Notch signalling serves as a mechanism that can regulate gene expression, and depending on the cell type, it can regulate proliferation or differentiation (Deftos and Bevan, 2000). The Notch family in humans consists of four paralogues (Notch1, Notch2, Notch3 and Notch4). They are expressed in a wide variety of tissues and they can interact with at least five Notch ligands (Jagged1, Jagged2, Delta-like 1, Delta-like 3 and Delta-like 4) (D'Souza et al., 2008).

Notch proteins are single-pass transmembrane receptors. The extracellular domain is composed of a large EGF-like repeat domain and a cysteine-rich region Notch/Lin12 domain (LN). The extracellular domain is linked to the intracellular domain by the heterodimerization domain (HD). Upon proteolytic cleavage, the intracellular domain functions as a transcription factor. It includes a RBP-Jκ–associated module (RAM), nuclear localization signals (NLS) six tandem copies of ankyrin-like repeats (ANK) and a transactivation domain (TAD). The C-terminal proline, glutamic acid, serine, threonine-rich (PEST) domain, mediates Notch protein turnover (Deftos and Bevan, 2000; Radtke et al., 2004) (Figure 1.3).

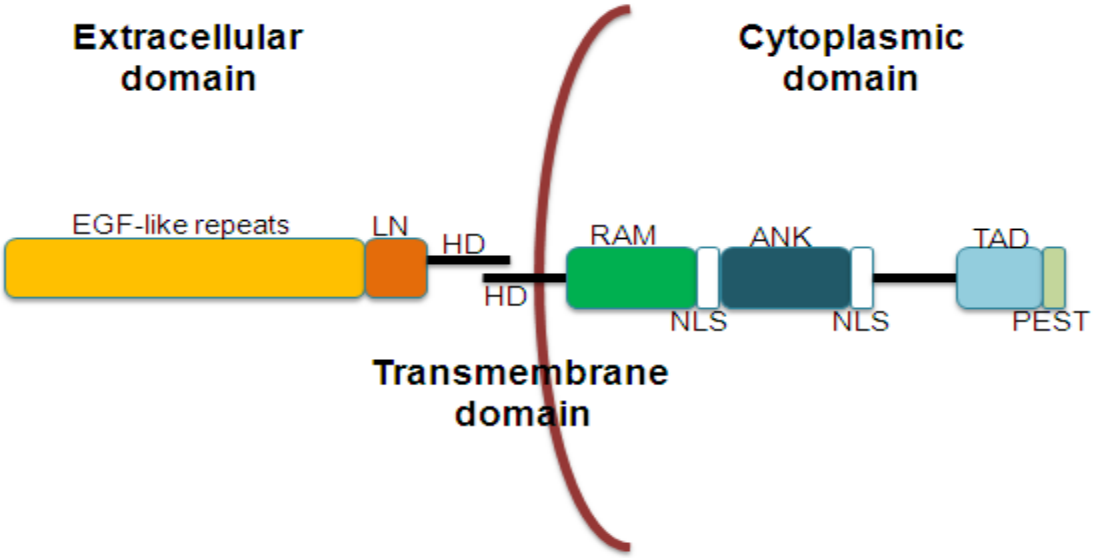

Figure 1.3 Domain structure of Notch receptors. The extracellular domain of Notch receptors contains EGF-like repeats and a cysteine-rich Notch/Lin12 domain (LN). The extracellular domain is linked to the intracellular domain by the transmembrane domain (HD). The intracellular domain is formed by the RAM domain and 6 ankyrin repeats (ANK), 2 nuclear-localization signals (NLS), followed by the transactivation domain (TAD) and a C-terminal proline, glutamic acid, serine, threonine-rich (PEST) domain.

Notch1 signalling is activated by the binding of the extracellular domain by ligands of the Delta and Serrate/Jagged families. Ligand binding induces the cleavage by the ADAM metalloproteinases of a large portion of the ectodomain exposing a site that is recognized by the intramembrane γ-secretase (GS) proteolytic complex. Cleavage by GS releases the Notch1 intracellular domain (NICD), which enters the nucleus and heterodimerizes with the DNA binding transcription factor CSL/RBP-Jκ to regulate gene expression. Once bound to CSL, NICD recruits other coactivators, including mastermind proteins (MAML1-3), which in turn recruits transcription activation complexes to induce expression of downstream target genes (Nwabo Kamdje and Krampera, 2011). These genes can either inhibit or promote maturation along particular developmental pathways. These genes include DELTEX-1. DELTEX-1 function is still not fully understood. It was recently proposed to

partecipate in T cell anergy as DELTEX-1-deficient mice have attenuated T cell activation (Hsiao et al., 2009).

Another well-known target gene of Notch1 is HES-1. HES-1 is a basic Helix-Loop-Helix (bHLH) protein that forms homodimers to repress transcription by recruiting the transcriptional co-repressor Groucho. HES-1 is required for normal T cell development, particularly in the expansion of ETP (Dudley et al., 2009) (Figure 1.4).

Notch1 was first identified as a gene involved in chromosomal translocations with the TRCβ gene in a subset of cases of T cell acute lymphoblastic leukaemia (T-ALL). The translocations result in the expression of Notch1 receptor which lacks the extracellular domain leading to constitutive activation of Notch signalling. The identification of Notch1 as a T cell oncogene and the observation that is highly expressed in the thymus suggested that it coul be involved in normal T cell development. In a mouse model, bone marrow progenitors, in which Notch1 was inactivated, enter the thymus and develop into B cells, suggesting that Notch1 can regulate a T versus B cell fate (Wilson et al., 2001). Similarly, inactivation of CSL in bone marrow progenitors inhibited T cell development which developed instead into B cells (Radtke et al., 2004). These results suggested a specific role of Notch1 in T cell commitment and development. In fact T cell commitment occurs following the interaction of T-cell precursors with Notch ligands presented by the thymus epithelium. The subsequent development of T lineage cells in the thymus requires different thresholds of Notch1 signalling. A low threshold is sufficient to suppress B cell development by thymus-seeding progenitors, whereas a high threshold is required to promote proliferation of early T lineage progenitors and their development into CD4+CD8+ thymocytes.

Notch3 was also described to play a critical role in T cell development (Bellavia et al., 2003). More specifically, in the thymus, Notch1 espression is high in the early DN thymocytes, low in DP cells and intermediate in CD4+ and CD8+ cells. Instead, Notch3 levels are significantly higher compared to Notch1 in DN thymocytes and they are down-regulated during the DN to DP transition and are really low levels in mature T lymphocytes. The different expression profile of Notch1 and Notch3 receptors indicates they might play different roles in T cell development. Notch1 has been suggested to play a role in the initial T cell lineage commitment of bone marrow progenitors and in intrathymic differentiation of T lymphoid cell lineages by favouring the CD8 versus CD4 and αβ versus γδ T cell lineage fate. Since Notch3

was shown to be mainly up-regulated in DN immature thymocytes, it has been suggested to play a role at the pre-TCR checkpoint (Bellavia et al., 2003; Campese et al., 2003). In aggrement with this, in vivo models of active transgenes have shown differences between Notch1 and Notch3. In the absence of a functional pre-TCR, Notch1 is not able to induce DP thymocyte differentiation. Notch3, instead, is able to block the pre-TCR check points forcing DN thymocyte differentiation (Allman et al., 2001; Bellavia et al., 2003; Campese et al., 2003).

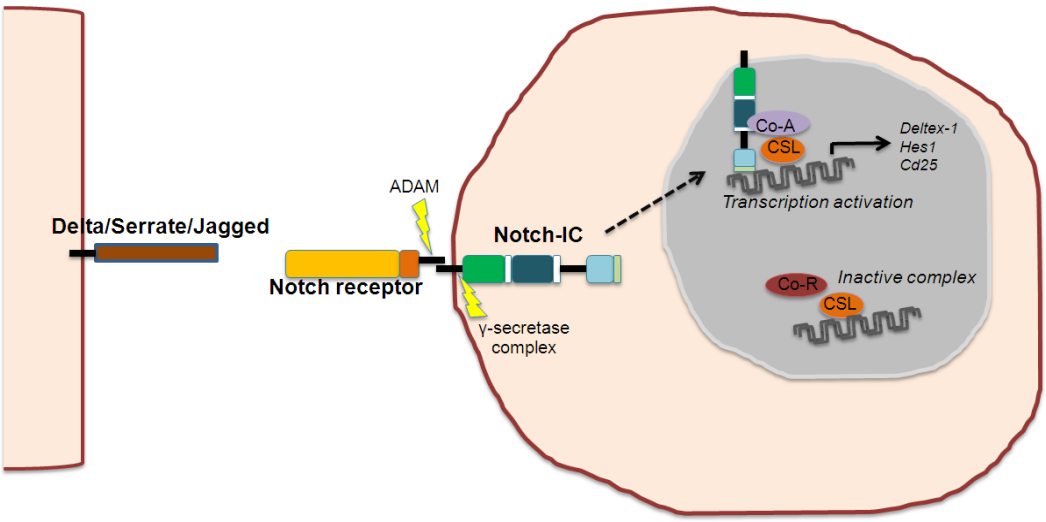

Figure 1.4 Notch1 signalling. In the thymus Notch1 is recognized by the ligands of the Delta and Serrate/Jagged families. Ligand binding induces two sequential proteolytic cleavages. ADAM-type metalloproteases cleave a large portion of the ectodomain, exposing a site recognised by the intramembrane γ-secretase proteolytic complex (GS). Subsequently, cleavage by GS releases the Notch1 intracellular domain (NICD), which enters the nucleus and binds to the transcription factor CSL. These interactions convert CSL from a transcriptional repressor to an activator by displacing co-repressors (CoR) and recruiting coactivators (Co-A). This leads to regulation of transcription of many genes.

1.1.2 B lymphocytes

B lymphocytes form 10-20% of circulating lymphocytes and are characterized by their production of the immunoglobulin antigen-binding proteins (Ig). Ig molecules are formed by two identical heavy chains and two identical k or λ light chains. The N-terminal region of the heavy and light chains varies from one antibody molecule to another and is known as V_H and V_κ or V_λ respectively. The juxtaposition of one V_H and one V_κ or V_λ domain creates the antigen-binding portion of the Ig molecule. The C-terminal portions of the heavy and light chains are constant in each subclass of antibody. The heavy chain of the C-terminal portion forms the Fc domain that is responsible for the effector functions of the Ig molecule (Chaplin, 2010).

B lymphocytes originate from haematopoietic stem cells and differentiate in the bone marrow to become mature surface IgM- and IgD- expressing cells. During differentiation their antigen receptors (surface Ig) are assembled by a RAG1/RAC2-mediated process similarly to TCRs (Jankovic et al., 2004). In peripheral lymphoid tissue, B cells carry on their maturation under the influence of cytokines secreted by Th cells to undergo isotype switching and affinity maturation by somatic mutation. The isotype switching ensures the production of antibodies of different isotypes with distinct biological effector functions but the same antigenic specificity (Chaplin, 2006). The cytokine IL-10 secreted by Th triggers a switching to IgG1 and IgG3 that bind phagocytic cells with high affinity. The cytokines IL-4 and IL-3 cause the switching to IgE. IgE binds to Fc receptors on the membranes of basophils and tissue mast cells. Localized mast-cell degranulation induced by IgE releases mediators that facilitate the recruitment of cells necessary for antiparasitic defence. IgE molecules also mediate the hypersensitivity reactions responsible of asthma or hay fever. TGF-β triggers the switching to IgA which are the main Ig of external secretions such as saliva and gut (Baumgarth, 2000). A main difference between the antigen recognition by the Ig and by TCRs is that Ig can recognize complex 3 dimensional structures, whereas the TCR can only recognize short linear peptide presented by MHC-I or II (Chaplin, 2006).

After antigen stimulation, B cells differentiate into plasma cells that secrete immunoglobulins. Each B cell receptor (BCR) expressed on the B cell surface, recognizes a specific antigen. The mature BCR form a complex which includes invariant transmembrane proteins known as CD79a (Igα) and CD79b (Igβ). The

complex also includes CD19, CD81 and CD21. The binding of an antigen induces the phosphorylation of the cytoplasmic ITAM portion of Igα and Igβ by the Src family kinase Lyn. ITAM phosphorylation induces the recruitment of different kinases and adaptor proteins depending on the state of cell maturation and antigen ligated. These signals include the mitogen-activated protein kinase (MAPK) pathway which induces cell proliferation and the Akt pathway which induces cell survival (Khan, 2009).

B cells express CD40, a member of the TNF receptor family that plays a role in the interaction of T helper cells and B cells. Activated T-helper cells express a ligand for CD40 mediating the interaction between B cells and T-helper cells (Simeoni et al., 2004)

1.2 T-acute lymphoblastic leukaemia

T-ALL is a neoplastic disorder that mainly occurs in children with a peak at 2-5 years of age. It represents 15% of paediatric and 25% of adult acute lymphoblastic leukaemia (Mathisen et al., 2013). T-ALL is characterized by clonal proliferation of malignant blast cells with an immature T lymphocyte phenotype. T-ALL cells are heterogeneous and arrested in a particular stage of maturation that can be correlated to their normal counterpart, differentiating T cells. For example the T-ALL cell line CCRF-CEM correlates with the pre-T lymphocytes. SUPT1 and Jurkat correlate with cortical T-lymphocytes (Burger et al., 1999) (Figure 1.5)

Commonly T-ALL patients present with fatigue and pallor, spontaneous bleeding and lymphadenopathy. Bone and joint pain can be observed, more frequently in children causing difficulty to walk. The pathogenesis is also characterized by a high white blood count, and infiltration of T-ALL cells into various tissues, particularly lymph nodes, spleen and central nervous system (CNS). The migration and infiltration of leukaemic cells into tissues often correlates with a poor prognosis for patients with T-ALL (Kebriaei et al., 2002). The five years survival rates are 75-80% and 35-40% for children and adult respectively. Recently, mortality has decreased due to strong chemotherapy and radiotherapy. Because the CNS is the main site of relapse, T-ALL patients usually receive cranial irradiation and intrathecal chemotherapy. This therapy unfortunately often leads to several side effects including growth impairment, neurocognitive deficit and secondary cancers. It is therefore important to develop new targeted therapies with less side effects (Demarest et al., 2008). At the stage of diagnosis T-ALL is often associated with extramedullary infiltration of leukaemic cells. This is present in 30% to 50% of children which have enlargement of the liver or spleen.

A potential mechanism in the trafficking of leukaemia cells is the interaction of the chemokine receptor CXCR4, expressed on T-ALL cells, and its ligand stromal cell-derived factor-1 (SDF-1/CXCL12) (see section 1.4.3), produced by stromal cells in bone marrow and extramedullary organs (Crazzolara et al., 2001). In a study on 11 paediatric T-ALL patients the overexpression of the chemokine receptor CCR9 and the integrin CD103 was identified in one patient. This marker was associated with relapse to the gut suggesting that CCR9 or CD103 could contribute to T-ALL location to the gut (Annels et al., 2004) (see section 1.4.3).

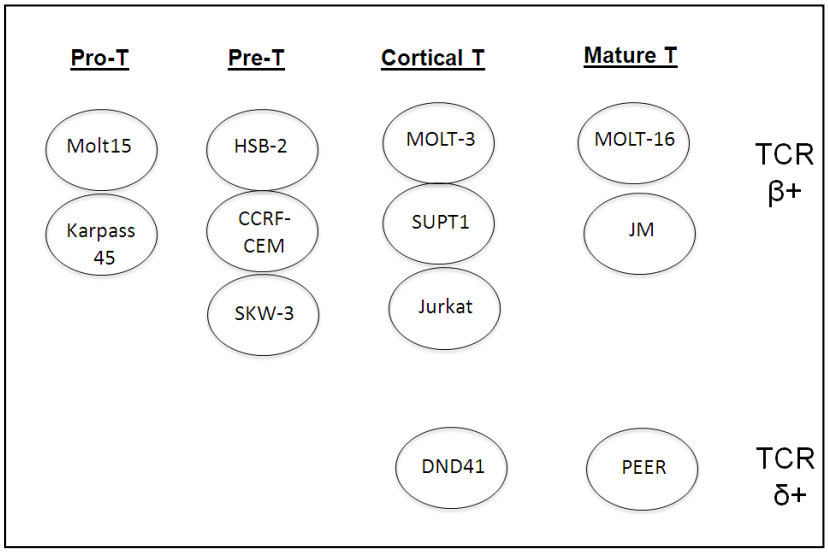

Figure 1.5 Correlation of T-ALL cell lines with the normal differentiation pattern of human T-lymphocytes. Adapted from (Burger et al., 1999)

T-ALL develops as a consequence of oncogenic mutations, in particular chromosomal translocations. The chromosomal translocations can occur during T cell development as a result of defective TCR recombination leading to aberrant proliferation and differentiation. These translocations often involve the juxtaposition of a strong promoter from TCR genes on chromosome 7 and 14 with transcriptional factor genes, such as TAL1, LMO, LYL1 and HOXA (Graux et al., 2006). Some chromosomal translocation can lead to genes encoding to chimeric proteins whit oncogenic properties as mixed-lineage leukaemia (MLL)-partner-gene fusions (Aifantis et al., 2008). Other common mutations include cryptic deletions that lead to the loss of tumour suppressor genes such as INK4 at 9p31 that leads to loss of G1 control of cell cycle (Graux et al., 2006).

Nevertheless expression microarrays, quantitative RT-PCR and whole-genome sequencing studies have identified different T-cell oncogenes that are dysregulated in T-ALL in the absence of chromosomal abnormalities (Ferrando et al., 2004; Sanz-Moreno et al., 2008; Zhang et al., 2012). Large-scale expression profiling of T-ALL

hs identified different gene expression signatures of leukaemic cells arrested at a specific stage of development. LYL1 shares 90% sequence identity with TAL1. They are expressed in the developing haematopoietic system but not in the thymus (Giroux et al., 2007). For example LYL1 is higly espressed in immature thymocytes whereas TAL1 is expressed in late cortical thymocytes (Graux et al., 2006). Interestingly, 30% of LYL1 transgenic mice develop T-cell and B-cell leukaemia with infiltration in multiple organs. LYL1 is also higly expressed in acute myeloblastic leukaemia (AML) and myelodysplastic syndrome (MDS) suggesting that it could be involved in the development of these cancers (Meng et al., 2005). TAL1 is normally expressed in a subset of haemapoietic cells, endothelial cells and cells of the central nervous system. TAL1 gene is located on chromosome 1p32. Rearrangements of this locus are present in 25% of T-ALL patients resulting in TAL1 activation. TAL1 activation is mainly due to a deletion that replaces the regulatory promoter sequence of TAL1 with that of the upstream gene SIL (Brown et al., 1990; Janssen et al., 1993).

Aberrant expression of LMO1 and LMO2 has been found in 45% of T-ALL cases. LMO1 was identified in T-ALL patients with chromosomal translocation t(11;14)(p15;q11), whereas LMO2 was found in chromosomal translocation t(11;14)(p13;q11). Transgenic mice expressing LMO1 or LMO2 develop leukaemia with an accumulation of immature DN T cells but the cancer has a long latency. This suggests that these genes are necessary but not sufficient to develop leukaemia (Aplan et al., 1997). Interestingly, some T-ALL patients have abnormalities of LMO2 and TAL1 suggesting they could act synergistically to promote tumorigenesis. Moreover, transgenic mice co-expressing LMO2 and TAL1 genes in T cells develop T-ALL 3 months earlier than mice with just the LMO2 transgene (Larson et al., 1996).

The homeobox genes normally regulate stages of embryonic development, important for morphogenesis and cellular differentiation. These genes encode highly conserved master regulators of transcription involved in the early development and regulation of haematopoiesis (Aifantis et al., 2008). Among these genes, HOXA (HOXA10 and HOXA11) is involved in a translocation associated with T-ALL. The chromosomal translocation involves the juxtaposition of TCR regulatory elements near HOXA genes or separates the HOXA gene from its regulatory elements.

Recently, Notch1 activating mutations have been identified in more than 50% of T-ALL patients (Weng et al., 2004). Most of the Notch mutations observed in T-ALL cell lines and primary T-ALL cells are located in the HD and PEST domains (Figure 1.3). Mutation of the HD domain leads to ligand-independent Notch1 cleavage and constitutive activation of Notch signalling. The mutations in the PEST domain increase the half-life of the intracellular domain (Demarest et al., 2008; Giambra et al., 2012). One of the pathways triggered by Notch signalling is PI3K/target of rapamycin mTOR pathway.

mTOR is a serine/threonine kinase that is part of two complexes, mTORC1 and mTORC2, with different biochemical structures and substrate specificity (Willems et al., 2012). mTORC2 is implicated in proliferation and differentiation of pre-T cells mediated by NF-kB and in the expression of the chemokine receptor CCR7 in leukaemic cells. CCR7 was shown to mediate leukaemic T-cells infiltration into the CNS (Buonamici et al., 2009; Lee et al., 2012).

1.3 Ras and Rho GTPases as regulators of cell adhesion and migration

Leukocyte migration is tightly regulated and requires adhesion, polarization and cytoskeleton reorganization. Key regulators of migration are Rho and Ras GTPases. Ras was the first small G-protein to be identified and is mutated in 33% of all human cancers (Baines et al., 2011). Mutations in the Ras pathway are common in myeloid malignancies. They occur in approximately 20% of adult acute myelogenous leukaemia, 40% of chronic myelomonocytic leukaemia, and 30% of juvenile myelomonocytic leukaemia cases (Mullally and Ebert, 2010).

The human Ras superfamily comprises of 154 members divided into five families: Ras, Rho, Rab, Arf and Ran families (Wennerberg et al., 2005) (Figure1.6).

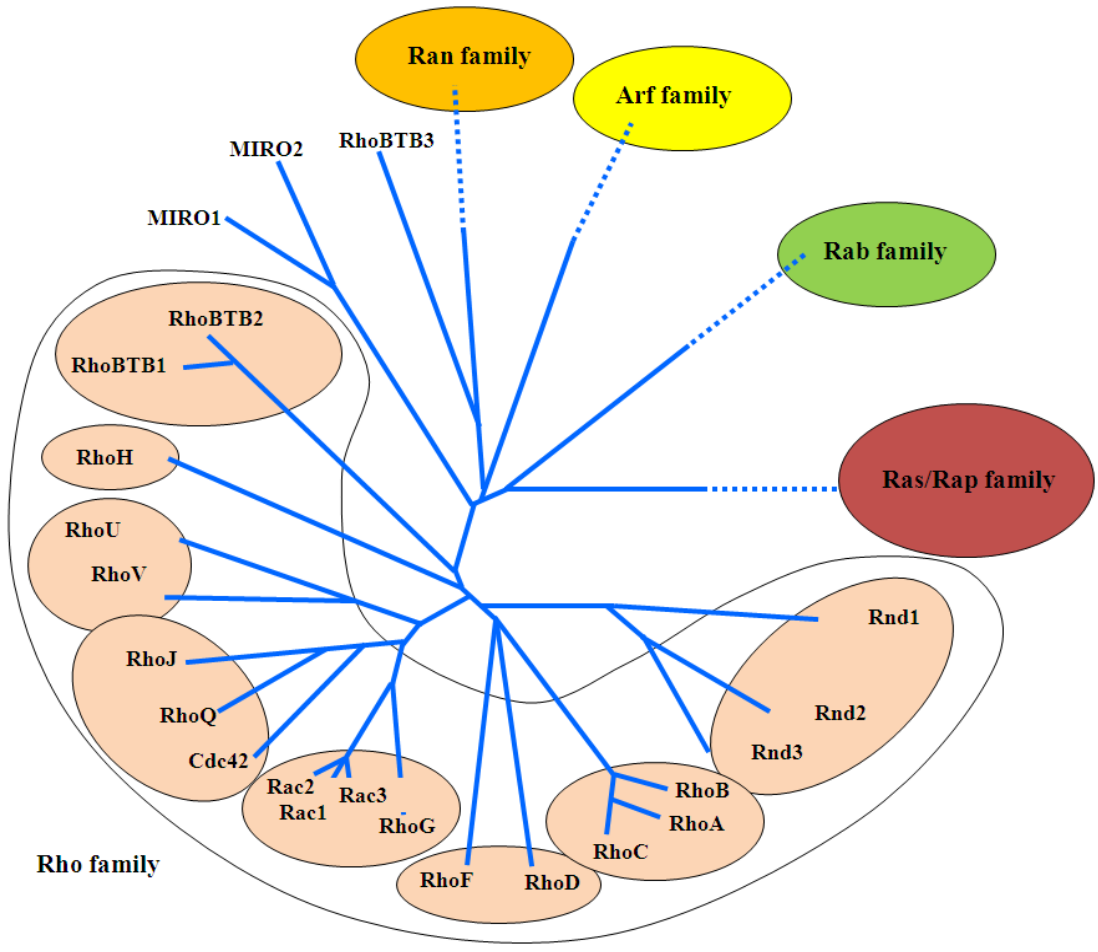

Figure 1.6 Phylogenetic tree of the mammalian Ras GTPase superfamily. There are 20 Rho GTPases classified in 8 subgroups based on sequence similarities (Vega and Ridley, 2008).

Most GTPases cycle between a GDP-bound inactive form and a GTP-bound active form that interacts with downstream effector proteins. The GTP-GDP switch is regulated by specific classes of proteins: the guanine nucleotide exchange factors (GEFs) that promote exchange of bound GDP for GTP, and GTPase activating proteins (GAPs) which promote GTP hydrolysis to GDP (Figure 1.7). .

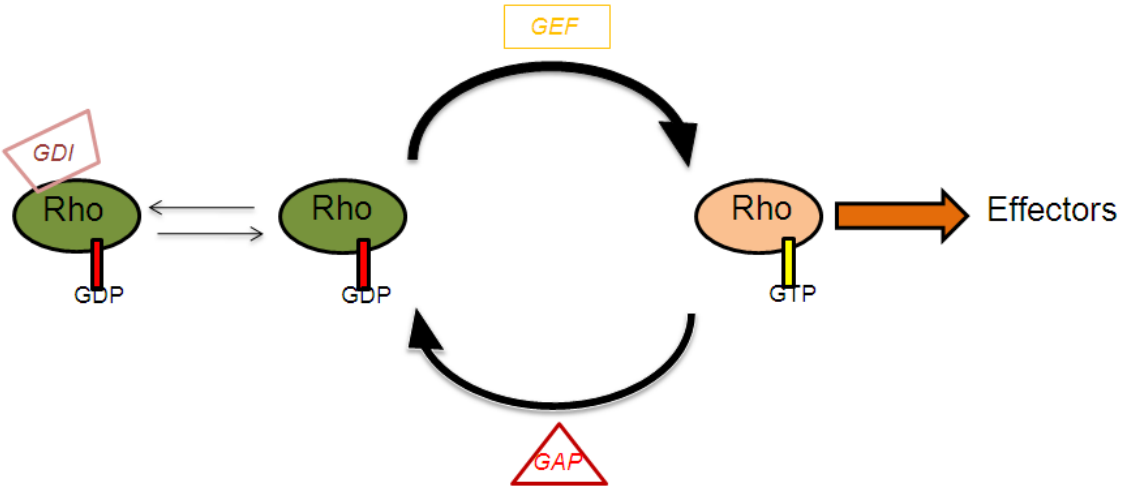

Figure 1.7 Regulation of Rho GTPase activity. Rho GTPases switch between a GDP-bound inactive form to a GTP-bound active form. This process is regulated by guanine nucleotide exchange factors (GEFs) and GTPase activating proteins (GAPs). Several Rho GTPases are also regulated by the GDP dissociation inhibitors (GDIs) which sequester them in the cytoplasm (See 1.3.1)**.**

1.3.1 Ras and Rho GTPases lipid modification

Most Ras superfamily GTPases are post-translationally modified by farnesyl or geranylgeranyl isoprenoid groups. These modifications facilitate the anchorage of these proteins to membranes where they signal to downstream effectors. Isoprenoids are lipids that can be added to the cysteine of the GTPase C-terminal CAAX

consensus tetrapeptide motif (cysteine-aliphatic-aliphatic-any). Depending on the X of the CAAX motif, GTPases can be either farnesylated or geranylated. If the X of the CAAX consensus is a leucine, the GTPase is geranylated, whereas if the X is serine or methionine, it is farnesylated (Roberts et al., 2008) (Figure 1.8).

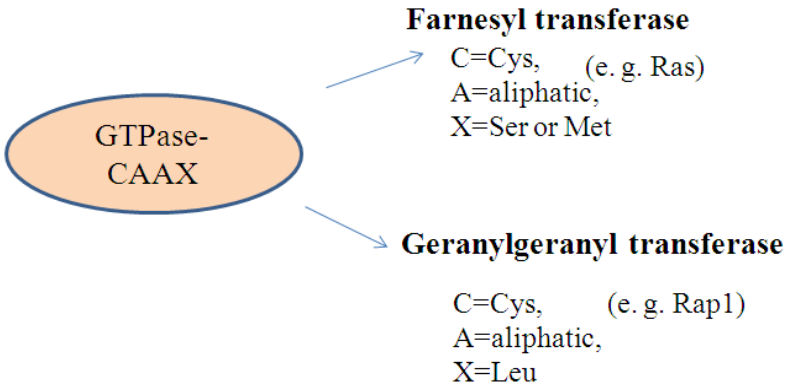

Figure 1.8 GTPase isoprenylation. Depending on the last amino acid, GTPases can be either farnesylated or geranygeranylated on the cysteine residue of the CAAX motif. Farnesyl transferase prefers a Ser or Met, geranylgeranyl transferases prefer a Leu.

Farnesyltransferase or geranylgeranyltransferase catalyse the transfer of the carbon isoprenoid chain from farnesylpyrophosphate or geranygeranylpyrophosphate to the cysteine residue. Subsequently, an endopeptidase removes the last three amino acids from the carboxyl terminus of the protein. The cysteine is then methylated by a methyltransferase (Figure 1.9)

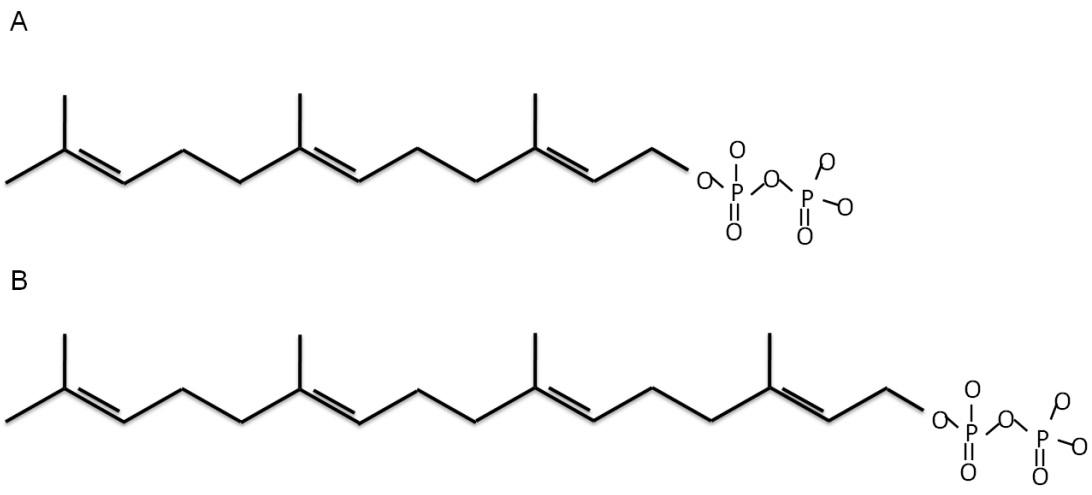

Figure.1.9 Skeletal formula of farnesylpyrophosphate (A) and geranygeranylpyrophosphate (B).

Several GTPases have a C-terminal polybasic region (PBR) with multiple lysines or arginines. This region mediates localization to membranes and interaction with some proteins. The PBR can promote the interaction with a nucleocytoplasmic shuttling protein SmgGDS. For example the PBR domain of Rac1 was found to enhance the nuclear accumulation of a protein complex containing SmgGDS and Rac1 that is too large to diffuse through the nuclear pores (Williams, 2003).

In addition to the polybasic region, some GTPases are C-terminally palmitoylated. Palmitoylation is the post-translational covalent addition of the 16-carbon fatty acid palmitate (Figure 1.10)

Figure 1.10 Skeletal formula of 16-carbon fatty acid palmitate.

The main difference from isoprenylation is that palmitoylation is a reversible process. This allows proteins to associate transiently with membranes, regulating their localization or endocytic trafficking (Navarro-Lerida et al., 2012). H-Ras has two palmitoylated cysteine residues, Cys181 and Cys184. These sites show distinct biological functions. Monopalmitoylation of Cys181 is required for H-Ras targeting to the plasma membrane, whereas monopalmitoylation of Cys184 does not permit trafficking beyond the Golgi (Roy et al., 2005). Rac1 was also recently demonstrated to be palmitoylated at Cys178. Its palmitoylation requires prior prenylation and an intact PBR. Lack of Rac1 palmitoylation induces a decrease in cell spreading and migration, suggesting palmitoylation is required for Rac1 function in actin cytoskeleton remodelling (Navarro-Lerida et al., 2012) (Figure 1.11)

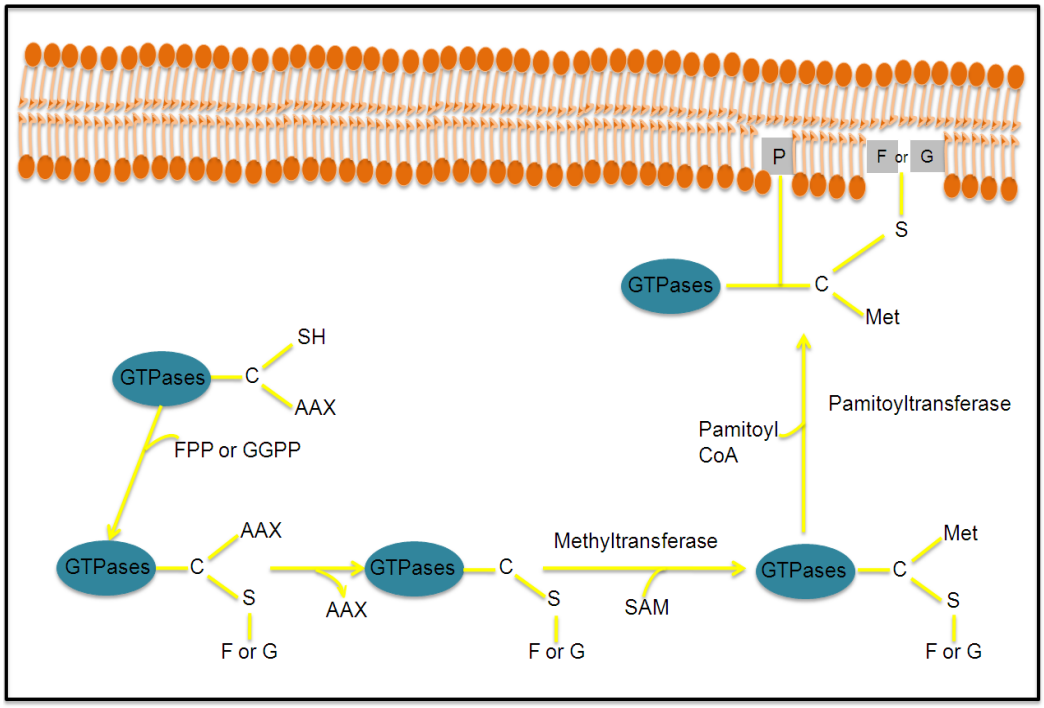

Figure 1.11 GTPase lipid modification. Farnesyl or geranylgeranyl transferase catalyse the transfer of isoprenoid groups to a cysteine residue close to the carboxyl terminus. Following isoprenylation, an endopeptidase removes the end three amino acids from the carboxyl terminus of the GTPases. The new carboxyl terminus is then methylated by a methyltransferase. In some GTPases, following transport to the plasma membrane palmitoyltransferase catalyses the addition of two palmitoyl long-chain fatty acid groups to a cysteine residue that is upstream of the isoprenylated carboxyterminal cysteine. FPP= farnesyl pyrophosphate. GGPP= geranylgeranyl pyrophosphate. F=farnesyl group. G=geranylgeranyl group. Adapted from Donward, Nat Rev Cancer 2003.

The Rho GTPases RhoU and RhoV are targeted to membranes by palmitoylation and are not prenylated (See 1.3.5.1 and 1.3.5.2).

Some Rho GTPases are regulated by GDP dissociation inhibitors (Rho GDI). The Rho GDIs in humans are GDI α, β, γ. These molecules sequester Rho proteins in the cytoplasm by binding the prenyl group at the C-terminus. This prevents the dissociation from GDP blocking the Rho protein in an inactive state (Greenwood et al., 2006) (Figure 1.7)

1.3.2 Statins, geranylgeranyl and farnesyl inhibitors

Statins are small molecules used to treat hypercholesterolemia and cardiovascular disease. They decrease cholesterol synthesis by inhibiting the 3-hydroxy-3-methylglutaryl coenzyme A (HMG-CoA) reductase that converts the 3-hydroxy-3-methyglutaryl-CoA into mevalonic acid, a substrate of the cholesterol pathway (Figure 1.12). The synthesis of mevalonate is necessary for the biosynthesis of cholesterol but also for other molecules of the mevalonic cascade, such as isoprenoids (Greenwood et al., 2006). As described above, Ras/Rho proteins are modified by isoprenoids. Suppression of isoprenoid synthesis has been considered responsible for some of the pleiotropic effects of statins.

Statins are already used to treat hypercholesterolemia, atherosclerosis and cerebrovascular disease and have shown beneficial effects in other common diseases such as neurodegeneration, osteoporosis and cancer (Fuchs et al., 2008). Randomized controlled trials for preventing cardiovascular disease indicated that statins had unexpected benefits for reducing colorectal cancer and melanoma. The reduction in isoprenylation of the Ras/Rho GTPases, preventing membrane localization, might be an important aspect in the cancer prevention properties of statins (Demierre et al., 2005).

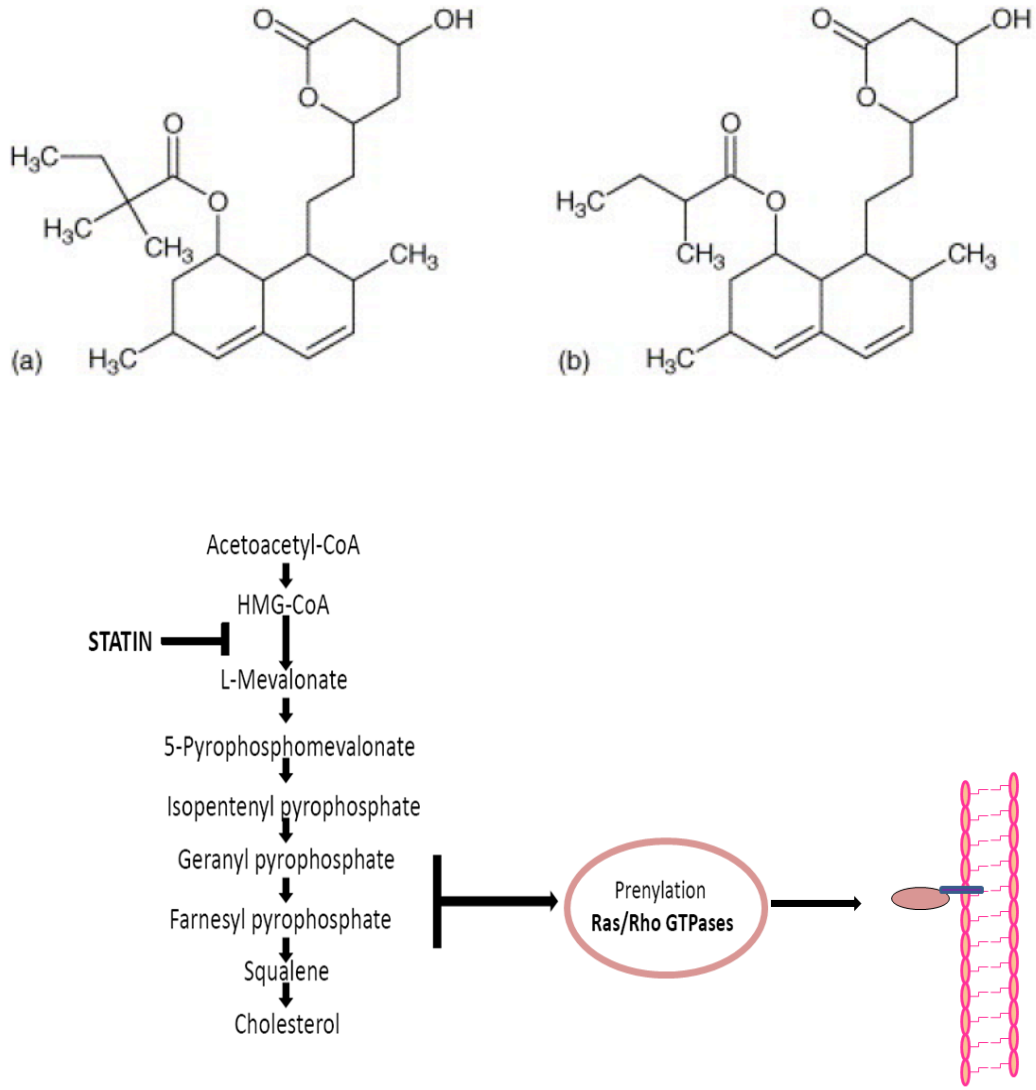

(c)

Figure 1.12 Statin inhibition of prenylation. Chemical structures of simvastatin (A) and lovastatin (B). From Barrett, J Pharm Biomed Anal. 3-Hydroxy-3-methylglutaryl-CoA reductase catalyzes the synthesis of mevalonic acid, which is required for the geranylgeranylpyrophosphate and farnesylpyrophosphate synthesis. These groups are covalently added to the Ras/Rho GTPases allowing their anchorage to membranes (C). Adapted from Grenwood, Nat Rev Immunol.

The transforming activity of oncogenic Ras requires its prenylation. For this reason farnesylation transferase inhibitors (FTIs) were developed to inhibit Ras

farnesylation. FTIs inhibit growth and induce tumour regression in Ras-dependent tumours in mice and these compounds have been tested in clinical trials in solid and haematological malignancies (Karp and Lancet, 2005). Based on initial results, these compounds were suggested to be used in combination with chemotherapy, radiotherapy or other targeted agents (Mazieres et al., 2004). However, a trial in multiple myeloma patients of the FTI inhibitor tipifarnib discouraged the use of this drug as only 23 of 36 patients showed disease stabilization (Ocio et al., 2008). The lack of success of FTI in inhibiting K and N-Ras is probably due to alternative geranygeranylation (Roberts et al., 2008; Whyte et al., 1997).

Inhibitors of geranylgeranlylation are known as geranylgeranyl transferase inhibitors (GGTIs). These compounds have also been developed as potential cancer therapies. One reason is that K-Ras, the most commonly mutated Ras isoform becomes geranylgeranylated in the presence of FTIs. Moreover, RhoC, Cdc42 and Rac1 are all geranylgeranylated and have been shown to have a role in metastasis, in same cases downstream of K-Ras. Similar to FTIs, GGTIs inhibit tumour growth in vitro and animal models and one GGTI has entered in a clinical trial in patients with advanced solid malignancy (Berndt et al., 2011).

1.3.3 Rap GTPases

Rap proteins belong to the Ras superfamily of small G-proteins. Mammals have two Rap1 (Rap1a and Rap1b) and three Rap2 (Rap2a, Rap2b and Rap2c) proteins. Rap1 and Rap2 proteins share 60% sequence homology.

Rap proteins are involved in several aspects of cell migration, controlling integrin-mediated adhesion, cell-cell adhesion, cytoskeleton organization, cell polarity and intracellular trafficking (Frische and Zwartkruis, 2010). Their effectors contain a Ras binding domain (RA)(van Dam et al., 2009). Like other GTPases, Rap proteins cycle between a GTP-bound active form and a GDP-inactive form. So far, five distinct classes of GEFs have been identified for Rap1: C3G, PDZ-GEF1 and 2, Epac1,2 and Repac, CalDAG-GEF1. Rap GAPs include Rap1GAPI and II, Spa1 and SIPA1L1/E67P1. Many of these GEFs and GAPs are not specific for Rap1 but can also act on Rap2 isoforms.

Rap1 has been implicated in β1, β2 and β3 integrin activation, a process partialy mediated by the effector molecule Rap1-GTP-interacting adaptor molecule (RIAM). RIAM belongs to the Mig-10/RIAM/Lamellipodin (MRL) family of adaptor proteins. RIAM has an RA domain that mediates the interaction with Rap1. The N-terminus of RIAM harbours a proline-rich region bracketed by two potential coiled-coil regions, whereas the C-terminus has a PH domain and a second proline-rich region (Boettner and Van Aelst, 2009). Overexpression of RIAM induces cell spreading and lamellipodium formation, and also induces activation of β1 and β2 integrin. RIAM co-immunoprecipitates with talin and expression of RIAM activates integrin through talin. siRNA depletion of RIAM in Jurkat T-cells inhibits adhesion to fibronectin. The downregulation of RIAM was also shown to decrease Rap1 membrane localization (Lafuente et al., 2004).

Although this process is not fully understood it is likely that RIAM act as scaffolding protein binding Rap, which induces talin tethering and integrin activation. Besides RIAM, the Rap1 effector RapL is also implicated in integrin activation by regulating LFA-1/αLβ2 spatial distribution (Boettner and Van Aelst, 2009). In mouse lymphoid tissues stimulated with CXCL12, RapL was found to associate with Rap1. This association induced a redistribution with LFA-1 to the leading edge, increasing adhesion to ICAM-1(Katagiri et al., 2003).

Rap1 was demonstrated to be involved in tumorigenesis. Injection of Swiss 3T3 expressing Rap1 into nude mice resulted in the formation of tumours (Altschuler and Ribeiro-Neto, 1998). Rap1 was also shown to be involved in myeloid leukaemic. Overexpression of the Rap1 GEF CalDAG-GEF in FDCP1 myeloid cells induced growth and transformation. CalDAG-GEF also increased cell adhesion to fibronectin through Rap1 (Dupuy et al., 2001). Another example implicating Rap1 in leukaemia comes from experiments on SPA-1 deficient mice. SPA-1 is a GAP of Rap1, and mice lacking this protein developed a spectrum of myeloid disorders similar to human chronic myelogenous leukaemia (CML) (Ishida et al., 2003) (Figure 1.13).

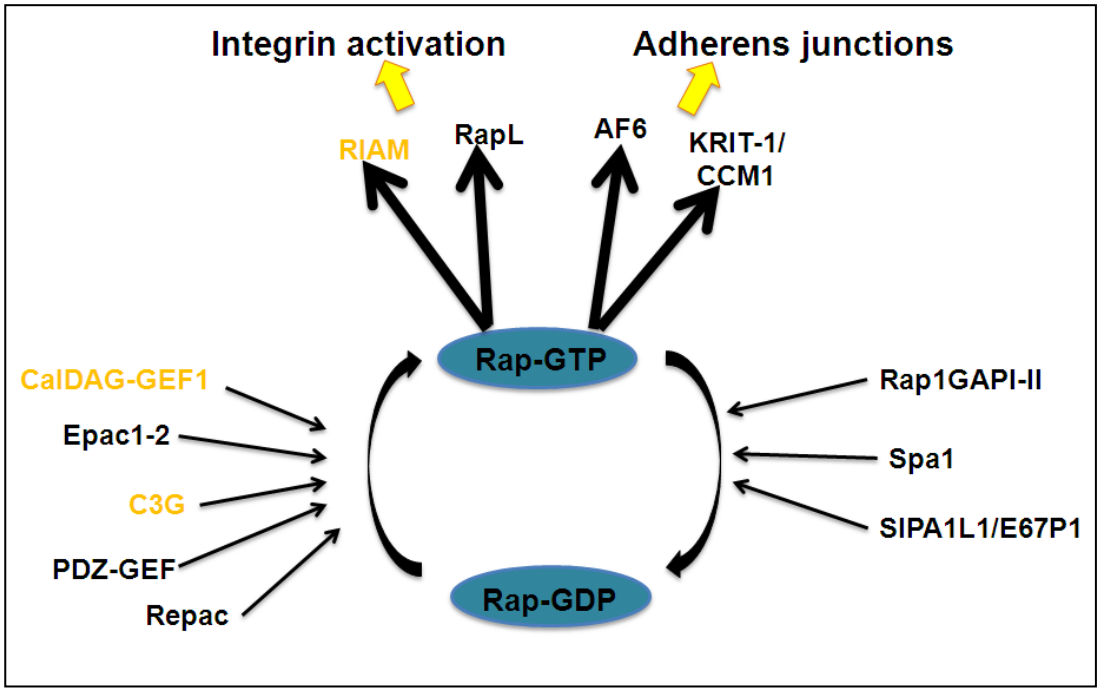

Figure 1.13 Effectors, GEFs and GAPs of Rap. Diagram showing the effectors (and their functions), GEF and GAPs of Rap. Proteins specific for Rap1 are highlighted in orange.

Rap1a and Rap1b share 95% sequence identity (Figure 1.14). They differ at just 8 amino acids located at the C-terminus (Raaijmakers and Bos, 2009). Both proteins are post-translationally modified by geranylgeranyl isopreonoids and are expressed in a variety of tissues (Wittchen et al., 2011). The distinct roles of Rap1a and Rap1b have not been clarified yet. Most studies have only used one isoform. Recently, downregulation of Rap1a but not Rap1b was reported to increase endothelial cell permeability by destabilizing cell-cell junctions. These data suggest that some cellular processes might differentially use these two isoforms (Wittchen et al., 2011).

```
Rap1a MREYKLVVLGSGGVGKSALTVQFVQGIFVEKYDPTIEDSYRKQVEVDCQQCMLE-54
Rap1b MREYKLVVLGSGGVGKSALTVQFVQGIFVEKYDPTIEDSYRKQVEVDAQQCMLE-54

Rap1a ILDTAGTEQFTAMRDLYMKNGQGFALVYSITAQSTFNDLQDLREQILRVKDTED-108
Rap1b ILDTAGTEQFTAMRDLYMKNGQGFALVYSITAQSTFNDLQDLREQILRVKDTDD-108

Rap1a VPMILVGNKCDLEDERVVGKEQGQNLARQWCNCAFLESSAKSKINVNEIFYDLV-162
Rap1b VPMILVGNKCDLEDERVVGKEQGQNLARQWNNCAFLESSAKSKINVNEIFYDLV-162


Rap1a RQINRKTPVEKKKPKKKSCLLL-184
Rap1b RQINRKTPVPGKARKKSSCQLL-184
```

Figure 1.14 Amino acid sequences of Rap1a and Rap1b. Rap1a and Rap1b share 95% sequence identity. Differences in amino acid sequence are higlighted in yellow. Green indicates Cysteine of the CAAX sequence.

1.3.3.1 Integrins and their ligands

Chemokines act through G-protein coupled receptors and are important for T cell integrin activation. They were first suspected to be responsible for integrin activation after the observation that the G-protein signalling inhibitor blocked leukocyte adhesion to the endothelium (Bargatze and Butcher, 1993). Chemokines induce clustering of specific integrins on the leukocyte surface and more importantly, stimulate a conformational change in integrins which increases their affinity for ligands expressed on the endothelium (Neeson et al., 2000).

Integrins are transmembrane adhesion receptors composed of an α and β subunit. In humans there are 18 α and β subunits that can assemble into 24 distinct receptors, that preferentially bind specific extracellular matrix (ECM) proteins (Arnaout et al., 2007). Each integrin consists of a large extracellular domain, a transmembrane domain and a short cytoplasmic domain. The N-terminus of the α and β subunits forms a globular head contain the ligand-binding domain. Integrins can take 3 conformational states: an inactive state, with low affinity for their ligand, an active state with high affinity and a ligand-occupied state.

For leukocyte adhesion to the endothelium, the integrins LFA-1 (αLβ2) and VLA-4 (α4β1) play a major role. Their main ligands on the endothelium are the intercellular adhesion molecule (ICAM-1) for LFA-1 and the vascular cell adhesion molecule (VCAM-1) for VLA-4. LFA-1 also binds junctional adhesion molecule-A (JAM-A), contributing to T cell and neutrophil transendothelial migration (TEM) and LFA-1-mediated arrest of T cells (Ostermann et al., 2002). ICAM-1 and VCAM-1 are basally expressed in resting endothelial cells, and ICAM-1 and VCAM-1 expression is induced by stimulation with proinflammatory cytokines such as IL-1 and TNF-α (Barreiro et al., 2002). VCAM-1 and ICAM-1 appear to play different roles during adhesion and TEM. Adhesion of T cells to activated endothelial cells was markedly inhibited by blocking antibodies to VCAM-1, but not by blocking antibodies to ICAM-1. ICAM-1 instead had a predominant role in TEM even when T cell adhesion to the endothelium was not mediated by ICAM-1 (Oppenheimer-Marks et al., 1991).

Leukocytes and platelets express various types of integrins and defects in integrin expression or activation in immune cells result in immunodeficiency or autoimmune diseases. An α4 integrin antagonist has been used for treatment of multiple sclerosis as it reduces the adhesion and migration of lymphocytes and monocytes into the parenchyma reducing brain lesions (Gottlieb et al., 2004; Miller et al., 2003).

In resting T lymphocytes, integrins are evenly distributed on the cell surface in an inactive state but they can be rapidly activated by diverse cellular agonists. The activation of integrins induces a conformational change in the extracellular domains leading to an increase in affinity for ligand binding (Stewart and Hogg, 1996). Integrin-ligand interactions are dependent of divalent cations, that can enhance or suppress the ligand binding activity. The α subunit I domain contains a unique metal binding site specific for Mg^{2+} and Mn^{2+}, and the conserved I-like domain of the β subunit contains a similar cation binding motif. Mg^{2+} and Mn^{2+} can induce conformational changes in many integrins that correlate with an increase in the affinity state. The stimulation of integrin with Mg^{2+} requires chelation of the divalent cation Ca^{2+} (Leitinger et al., 2000).

Chemokine or TCR stimulate inside-out signalling to activate integrins. As mentioned above, in the inactive state the ligand-binding site is bent and close to the cell membrane and the cytoplasmic tails are close together. The binding of talin to

the tail of the β subunit can generate a conformational change outside with an intermediate ligand affinity. Once the cytoplasmic α and β tails are sufficiently separated and the extracellular parts stand up the high-affinity conformation is reached (Zhang and Wang, 2012). The change in integrin conformation is important to arrest rolling leukocytes on blood vessels, as integrins can then bind the endothelial ligands, undergoing an additional allosteric rearraengment of the ligand-binding domain to induce the anchorage of integrins to the actin cytoskeleton. This process might be mediated by the actin binding sites of talin (Alon and Shulman, 2011). There are two talins, talin1 and talin2. Suppression of talin1 by RNAi inhibits VLA-4 and LFA-1 mediated arrest of lymphocytes on endothelial ligands (Manevich et al., 2007; Shamri et al., 2005). The binding of talin to the β subunit of integrins can be enhanced by phosphatidylinositol (4,5)-bisphosphate. The association of talin is not always enough to anchor integrins to the actin cytoskeleton. The β subunit needs a second co-activating signal by kindlin proteins (Figure1.15). In murine leukocytes binding of β1 and β2 integrin requires the presence of both talin1 and the hematopoietic-specific kindlin-3 (Malinin et al., 2009; Moser et al., 2009).

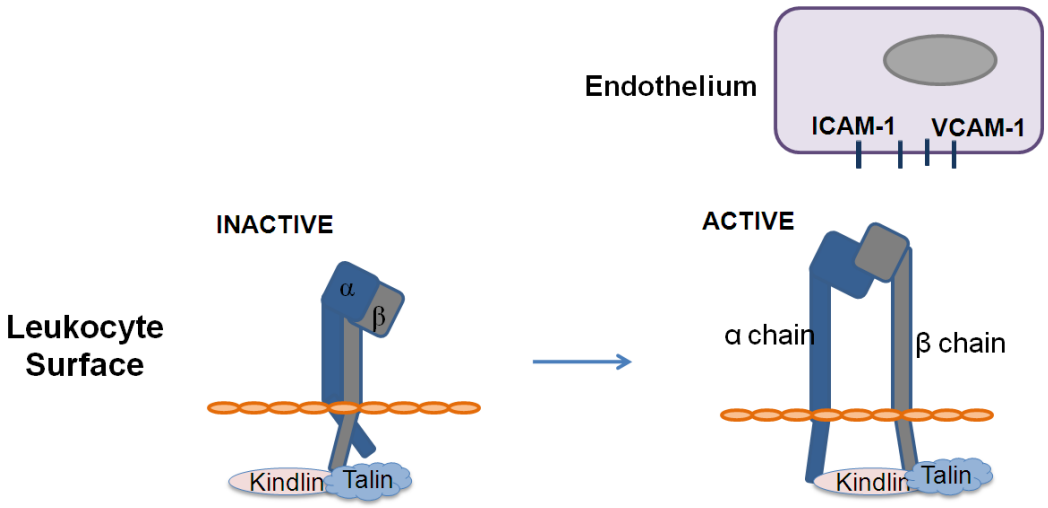

Figure 1.15 Integrin activation. Talin and kindlin bind the cytoplasmic tail of β integrin leading to changes in the conformation from an inactive state to active state. Active integrin can then bind VCAM-1 or ICAM-1 expressed on the endothelium.

Several Rho GTPases have been reported to be involved in integrin activation, including RhoA, Rac1 and Rap1. RhoA activation stimulated β1 and β2 integrin-mediated adhesion in murine thymocytes. In vivo RhoA depletion was found to impair adhesion to VCAM-1, but this process was suggested to be downstream of Rap1 and Rac1 (Vielkind et al., 2005). A constitutively active Rac mutant induced spreading of Jurkat cells and their adhesion to fibronectin in an integin-dependent manner. Cell adhesion mediated by active Rac was not due to changes in the expression or affinity state of integrins but to cell spreading (D'Souza-Schorey et al., 1998). Rap1 has been well characterized as a protein involved in inside-out integrin activation, although the different contribution of the two isoforms Rap1a and Rap1b is not yet well understood. Rap1 regulates all integrins connected to the actin cytoskeleton (β1, β2 and β3) and was shown to control both integrin activation and integrin clustering depending on the integrin and the cell type (Bos, 2005).

1.3.4 Rho GTPases

There are 20 Rho GTPases in humans (Figure 1.6). Rho GTPases are implicated in the regulation of several cellular process and functions including cytoskeleton rearrangements, cell movement, vesicles trafficking and cell cycle progression. Most Rho GTPases are 20-28 kDa. Rho GTPase expression varies across tissues and is regulated by multiple stimuli. They exert their function by interaction with downstream targets such as protein kinases, phospholipases and actin nucleators (Heasman and Ridley, 2008).

To date 83 RhoGEFs have been identified (Sanz-Moreno et al., 2008). Different GEFs can activate one or more Rho GTPases coordinating the Rho GTPases with different downstream effectors (Garcia-Mata and Burridge, 2007). GEFs are classified into two families: the Dbl family and the DOCK family. The Dbl proteins contain a Dbl-homology (DH) domain, which is responsible for the catalytic activity, and an adjacent PH domain. Some PH domains mediate GEF membrane localization as they can bind phospholipids promoting their localization to the plasma membrane (Rossman et al., 2005). The DOCK family lacks the DH domain and contains two DOCK homology regions (DHR1 and 2) that promote guanine nucleotide exchange (Cote and Vuori, 2007). GEFs and GAPs contain protein or lipid interaction domains

important for localization or for the formation of protein complexes. Extracellular signals regulate GEFs and GAPs by inducing postranslational modifications which affect activity and localization allowing protein complex formation. There are more than 70 RhoGAPs in humans (Bos et al., 2007).

The atypical members of the Rho GTPase family do not act as molecular switches and do not cycle between a GTP-bound and a GDP-bound form. Rnd, RhoH and RhoBTB proteins lack GTPase activity, hence they are constitutively bound to GTP (Aspenstrom et al., 2007). The atypical Rho GTPases RhoU and RhoV have a high intrinsic GDP/GTP exchange rate and are therefore mainly in an active form (Shutes et al., 2004).

1.3.4.1 RhoU

RhoU belongs to the Cdc42 subfamily which also includes RhoV, RhoQ and RhoJ (Ellenbroek and Collard, 2007). RhoU shares 57% of the amino acid sequence identity with Cdc42.

RhoU is also known as Wrch1, and its gene is located on the human chromosome 1q42. RhoU was first isolated and cloned as a Wnt-inducible gene (Tao et al., 2001). Wnt-1 signalling is important for the development of organisms from nematodes to mammals (Cadigan and Nusse, 1997), but Wnt-1 was also identified as an oncogene implicated in tumorigenesis (Peifer and Polakis, 2000). The role of Wnt-1 signalling in development and tumorigenesis is mediated by its target genes. Wnt-1 through RhoU is able to induce transformation of mouse mammary epithelial cells (Tao et al., 2001).

RhoU possesses a unique N-terminal 46 amino acid sequence extension containing several PxxP SH3-binding motifs (Figure 1.16).

RhoU has a CAAX motif at the C terminus (CCFV). Despite this, RhoU does not undergo isoprenylation but is modified by palmitate (see section 1.3.1). Its localization is not affected by inhibitors of protein prenylation but by inhibitors of protein palmitoylation (Berzat et al., 2005). In fibroblasts, RhoU localizes to plasma membrane and endosomes (Tao et al., 2001).

RhoU has not so far been studied in T cells. RhoU overexpression was shown to induce morphological changes, cytoskeletal reorganization and cell proliferation in

fibroblasts. Like Cdc42, RhoU induces filopodium formation and stress fibre dissolution in NIH3T3 fibroblasts (Tao et al., 2001). In HeLa cells, RhoU strongly localized to focal adhesions, and RhoU downregulation incresead focal adhesions formation and inhibited cell migration (Chuang et al., 2007).

RhoU is able to activate p21 serine/threonine kinase (PAK), one of the most studied effectors of Rho GTPases (Tao et al., 2001). N-terminal deletion of RhoU enhances its ability to bind PAK1 (Shutes et al., 2004). NCK2 was also identified as a binding partner of RhoU. The PxxP-rich domain at the N-terminus of RhoU binds the second and third SH3 domains of NCK2 (Saras et al., 2004). The N-terminus of RhoU also associates with the adaptor protein Grb2, which increases RhoU activity (Shutes et al., 2004). Interestingly, after epidermal growth factor (EGF) stimulation, RhoU colocalizes with the EGF receptor on endosomes in a Grb2-dependent manner in pancreatic cancer cells (Zhang et al., 2011).

RhoU also binds the nonreceptor tyrosine kinase Pyk2. The interaction requires RhoU to be in a GTP-bound form and also required the N-terminal proline-rich extension. The interaction requires the presence and activity of Src and has a role in filopodium formation in fibroblasts (Ruusala and Aspenstrom, 2008). In H1299 non-small cell lung cancer cells RhoU relocates to the plasma membrane upon serum stimulation. Serum stimulation induces Src-mediated tyrosine phosphorylation of RhoU at Tyr254 residue. This phosphorylation decreases GTPase activity and the ability of RhoU to interact with downstream effectors (Alan et al., 2010).

RhoU was also shown to bind to Par6 in epithelial cells. Par6 is a scaffolding protein important in establishing epithelial cell polarity and in regulating tight junction (TJ) formation. Their interaction was shown to affect epithelial cell TJ assembly and actin organization (Brady et al., 2009).

Recently, ARHGAP30 has been identified to interact with RhoU. ARHGAP30 is closely related to the Cdc42-specific RhoGAP CdGAP. RhoU was found to bind ARHGAP30 and CdGAP in co-immunoprecipitation assays in fibroblasts. Overexpression of ARHGAP30 phenocopied RhoU in inducing filopodium formation and stress fibre disassembly, suggesting a role downstream of RhoU (Naji et al., 2011) (Figure 1.17).

1.3.4.2 RhoV

The RhoV gene is located on the human chromosome 15q15 which is a fragile site in the human genome. RhoV shares 55.4% of total amino acid identity with RhoU and 43.5% with Cdc42. RhoV is higly expressed in gastric, pancreatic and cervical cancer (Katoh, 2002). RhoV is also moderately overxpressed in pro-myelocytic leukaemia, Burkitt's lymphoma and colorectal cancer (Katoh, 2002). Like RhoU, RhoV is able to activate PAKs and contains a unique N and C-terminal extension (Aronheim et al., 1998; Weisz Hubsman et al., 2007) (Figure 1.16). Overexpression of RhoV induces the induction of lamellipodia possibly through interaction with Pak2 (Aronheim et al., 1998).

RhoV lacks a CAAX motif, and undergoes palmitoylation for membrane targeting. Immunofluorescence analysis of NIH3T3 fibroblasts overexpressing GFP-RhoV showed that RhoV localizes to the plasma membrane and endosomes. Moreover NIH3T3 cells overexpressing RhoV showed transforming activity which requires an intact C-terminus. Deletion of the N-terminal extension enhanced its transforming activity, suggesting a negative regulatory role of this domain (Chenette et al., 2006). In PC12 cells, RhoV expression induces apoptosis and activation of JNK signalling via both death receptor-mediated and mitochondrial apoptotic pathways as determined by caspase-8 and caspase-9 activation. This suggests a possible role of RhoV in regulating PC12 apoptotic activity in a JNK-dependent manner (Shepelev et al., 2011) (Figure 1.17).

Figure 1.16 Amino acid sequences of Cdc42, RhoV and RhoU. The amino acid sequence of Cdc42 was aligned with those of RhoU and RhoV. The proline residues in the N-terminal domain of RhoU are underlined. Amino acids required for RhoU and RhoV membrane targeting are denoted by orange boxes. The yellow box indicates RhoU phosphorylation site. The red boxes indicates palmitoylation site of RhoU and RhoV. Asterisks indicate Cdc42 CAAX box.

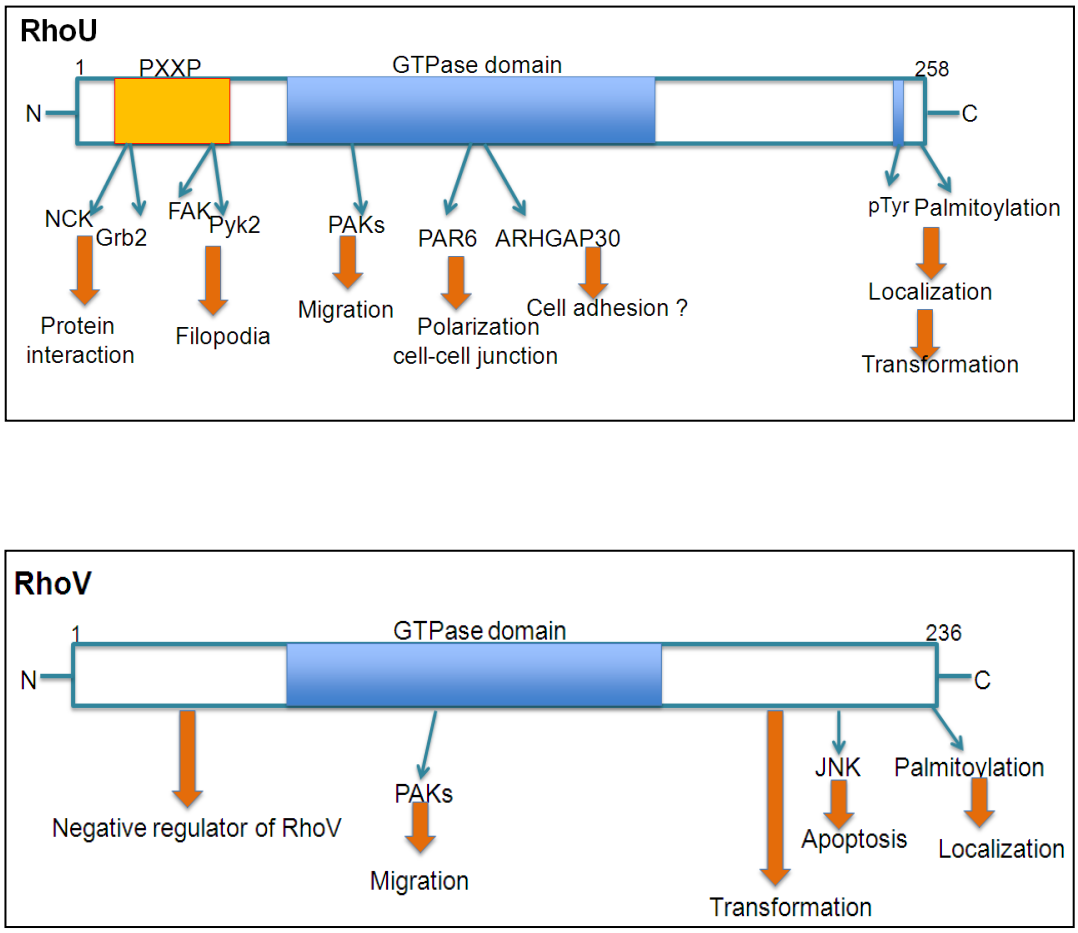

Figure 1.17 Domain structure of RhoU and RhoV. RhoU and RhoV consist of 258 and 236 amino acids respectively. The C- terminus of both proteins is palmitoylated. The phosphorylation site at the C-terminus of RhoU is indicated. The N-terminal domain of RhoU is proline-rich. Downstream partners of RhoU and RhoV and their function are indicated.

1.4 Rap and Rho GTPases and T lymphocyte migration

Mature T lymphocytes circulate in the blood stream as non-adherent cells. It has been estimated that under normal conditions T lymphocytes spend less then 30 minutes in the blood circulation, repeatedly visiting secondary lymphoid organs. This traffic is fundamental for a good immune surveillance. To reach secondary lymphoid organs, T lymphocytes need to cross the vascular endothelium. Once in the lymph nodes, T cells scan the area searching for APCs. The immunological synapse between the T lymphocytes and APCs triggers a signalling cascade that eventually induces the activation and proliferation of the T lymphocytes. After activation T lymphocytes enter in the blood stream and transmigrate through the blood vessels to reach the inflamed or infected area (Rougerie and Delon, 2012). Rho GTPases mediate this process by controlling each step of transendothelial migration: adhesion and protrusion of lamellipodia, polarization and chemotaxis (Rougerie and Delon, 2012).

1.4.1 Rap and Rho GTPases in adhesion

In resting T cells, integrins are in an inactive conformation. This conformation is maintained by the atypical Rho GTPase RhoH. Downregulation of RhoH in Jurkat and primary human T cells causes an increase of αLβ2/LFA1-dependent adhesion onto ICAM-1 (Cherry et al., 2004). Recently Cdc42 was also described as a negative regulator of LFA-1 activation (Bolomini-Vittori et al., 2009). Rap1 is a major and well established regulator of integrin activation as described above.

Rac1 also plays a role in integrin activation during chemotaxis. Rac1 was shown to increase spreading of Jurkat cells in a β1-dependent manner (D'Souza-Schorey et al., 1998). In addition stimulation with the chemokine CXCL12 promotes α4β1-dependent integrin activation through Rac1 in human T cells (Garcia-Bernal et al., 2005). Interestingly, Rac1 and Rac2 deficient T cells have a defect in adhesion to ICAM-1, suggesting that Rac1 and Rac2 participate in β2 as well as β1-mediated adhesion. Moreover, only depletion of both Rac1and Rac2 induces this striking defect, suggesting a possible redundant function of these two GTPases (Faroudi et al., 2010; Rougerie and Delon, 2012; Vielkind et al., 2005). However, in

macrophages Rac1 and Rac2 were showed to have distinct roles. Macrophages lacking Rac2 had a reduction in podosomes while lack of Rac1 altered cell shape and reduced membrane ruffling (Zhang et al., 2012).

RhoA has important functions in T cell development in the thymus (Corre et al., 2001). RhoA activation is sufficient to promote β1 and β2 integrin-mediated adhesion in murine thymocyte. Loss of RhoA function impaired thymocytes to adhere and to migrate on VCAM-1 and prevented integrin activation induced by the GTPases Rac-1 and Rap1a in vivo. This suggests a role of RhoA in regulating cell adhesion and migration during T cell development (Vielkind et al., 2005).

1.4.2 Rho GTPases and cell migration

Chemokine stimulation is important for T cell polarization and this is a fundamental step for T cell migration. During polarization, T cells acquire a motile morphology with a broad leading edge at the front called the lamellipodium, where the chemokine receptor and activated αLβ2 integrin (LFA-1) are localized, and a uropod at the back where ezrin-radixin-moesin proteins (ERM), ICAM-1/3 and CD44 are distributed (Gerard et al., 2007).

T cell polarization and migration require the re-organization of the actin cytoskeleton, a process regulated mainly by the classical Rho GTPases Rac, Rho and Cdc42. The cytoskeleton undergoes dynamic changes depending on what is required in a particular situation. Monomeric G-actin can polymerize into filaments (F-actin). G-actin binds ATP in a complex with Mg^{2+}. ATP binding stabilizes the actin monomer promoting polymerization (Le Clainche and Carlier, 2008). The new actin filaments initiate from an actin nucleus that can accept actin monomers. During actin polymerisation, actin monomers are added either free or in complex with the actin binding protein profilin to the barbed ends of pre-existing filaments. The polymerization is terminated by capping proteins such as Gelsolin or Eps8 (Mathisen et al., 2013). The spontaneous assembly of monomers into actin filaments is a slow and an unfavourable process. It is enhanced by actin nucleators such as the Arp2/3 complex or proteins of the formin family. The Arp2/3 complex comprises of Arp2 and Arp3 proteins and together with 5 actin-related proteins (ARPC). The Arp2/3 complex binds pre-existing filaments. Its activation is mediated by nucleation

promoting factors (NPFs) such as WAVE and WASP (Park et al., 2007). The formin family is divided in different subclasses: Diaphanous (mDia), formin-related proteins in leukocytes (FRLs), dishevelled-associated activators of morphogenesis (DAAMs), formin homology domain proteins (FHODs), formins (FMNs), delphilin and inverted formins (INFs). Formins nucleate non-branching actin filaments and remain bound inhibiting the apability of capping proteins to block polymerisation. Formins nucleate linear actin filaments and they have been proposed to mediate filopodium formation (Campellone and Welch, 2010; Faix and Grosse, 2006). Depolymerisation of F-actin is mediated by ADF/Cofilin proteins that bind preferentially to ADP-actin, promoting the release of actin monomers. Profilin promotes the exchange of ADP for TP on G-actin monomers, to start a new cycle of polymerisation (Kiuchi et al., 2007).

The lamellipodium contains a branching network of actin filaments. The main regulators of lamellipodium formation are Rac1 and Rac2 (Ridley et al., 1992). Rac GTPases regulates actin polymerization through the WAVE complex, consisting of WAVE, PIR121/Sra-1, Nap125, HSPC300 and Abl interactor (Abi). Rac binds to PIR121/Sra-1. In response to stimuli, WAVE can signal to the Arp2/3 complex inducing actin polymerization (Rougerie and Delon, 2012).

Several GEFs play a role in T cell migration by activating Rac1. Among these, DOCK2 is particularly important in T cells. Knockout of DOCK2 blocks Rac activation and consequently cell migration (Garcia-Bernal et al., 2006). Rac is not the only Rho GTPase to induce actin polymerization. Cdc42 can also activate WASP and N-WASP leading to actin nucleation by the Arp2/3 complex (Harris and Tepass, 2010). Cdc42 is also able to induce filopodium formation via mDia formins, which is not important to generate force but is instead important for chemotaxis in T cells (Rougerie and Delon, 2012).

RhoA has recently been shown to play a role at the leading edge of crawling and transmigrating T cells. Active RhoA was found at the front of CCRF-CEM cells during TEM and its activity correlates with both retraction and protrusion (Heasman et al., 2010).

The accumulation of F-actin at the front of cells is, together with the contraction of the uropod, important to generate the force to move forward. The uropod generates a contractile force through myosin II interaction with actin bundles (Rougerie and Delon, 2012). RhoA is a major player in the T cell uropod, because it is a regulator

on myosin II activity. Rho isoforms induce myosin light chain (MLC) phosphorylation and inhibit MLC phosphatase via their downstream targets ROCK1 and ROCK2 (Kaibuchi et al., 1999; Takesono et al., 2010).

The RhoA/ROCK/myosinII axis was also shown to be important in the maintenance of migratory polarity by controlling actomyosin contractility and microtubule stability (Heasman et al., 2010). In polarized T cells the microtubule organizing centre (MTOC) localizes at the back of the cell, behind the nucleus, along with ROCK. Treatment of T cells with nocodazole depolymerizes microtubules, increasing RhoA activity and inducing loss of migratory polarity (Takesono et al., 2010). Moreover, RhoA depletion in CCRF-CEM T-ALL cells leads to loss of migratory polarity (Heasman et al., 2010). Active RhoA localizes at the back of T cells where it is associated with ROCK-mediated contraction (Heasman et al., 2010) (Figure 1.18).

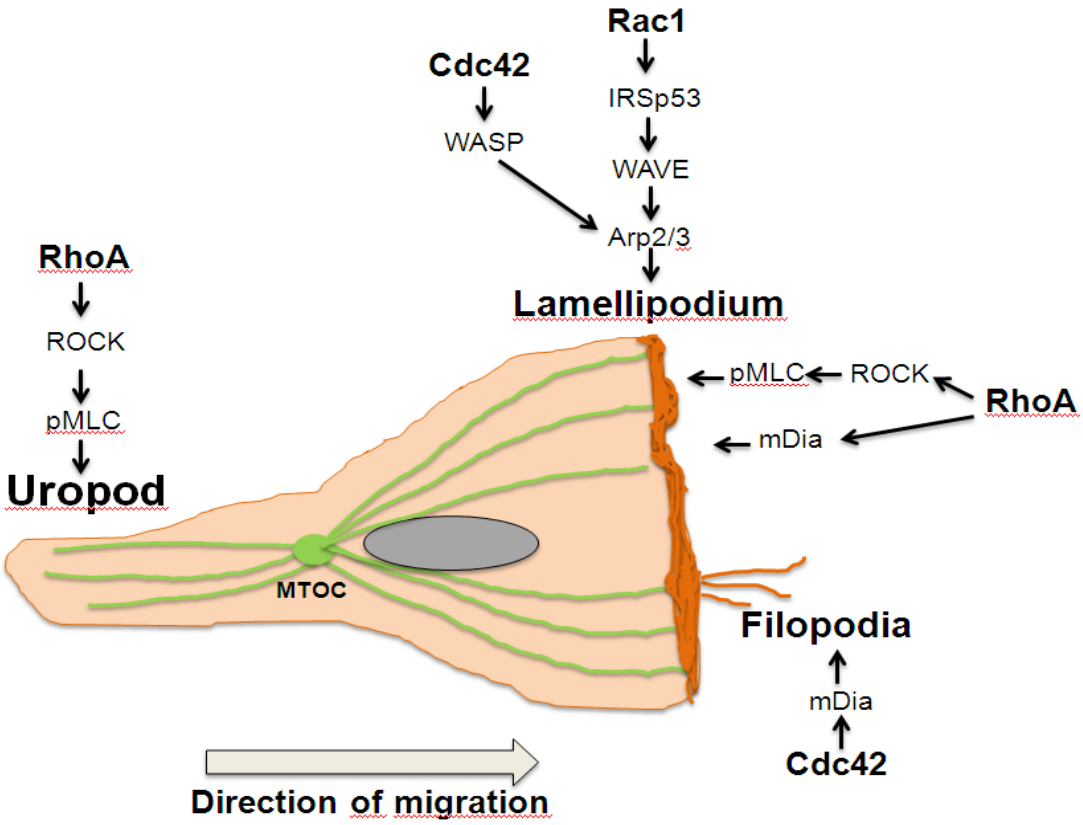

Figure 1.18 Signalling in T cell migration. In polarized T cells the microtubule organizing centre localizes behind the nucleus. Rac1 activates the WAVE complex, leading to Arp2/3-mediated actin polymerisation at the lamellipodium. Cdc42 induces filopodia via the formin mDia2. RhoA activation at the rear of the cell controls uropod contractility through ROCK inhibtion of MLC phosphatase and subsequent MLC phosphorylation. Cdc42 contributes to membrane extension via WASP which activate the Arp2/3 complex. RhoA is also proposed to be active at the front of the cell to induce actin polymerization through mDia and membrane retraction via ROCK.

Polarity proteins mediate migratory polarity in T cells. These proteins are conserved during evolution and they induce the polarized distribution of multiprotein complexes. The most well characterized polarity complexes are Par, Crumbs and

Scribble modules. During migratory polarization these complexes can cooperate to induce polarity or antagonize each other to achieve cell asymmetry.

The Crumbs complex was identified in *Drosophila melanoganster* and consists of Crumbs, Protein associated with Lin seven 1 (Pals1) and Pals1-associated tight junction protein (PATJ). The Scribble complex consists of Scibble, Discs large (Dlg) and Lethal giant larvae (Lgl) (Ellenbroek et al., 2012). Components of the Par, Scribble and Crumbs complexes localize asymmetrically in migrating polarized T cells. The scribble protein complex localizes in the uropod and downregulation of Scribble impairs T cell polarization (Iden and Collard, 2008). Immunological synapses between T-cells and APC involves a polarized and adhesive contact between the T cell and APC. Dlg and Scribble proteins are important during immunological synapse formation as they redistribute from the uropod to the immunological synapse to colocalize with Par3 and the TCR (Ludford-Menting et al., 2005). Cdc42 not surprisingly has a role in T cell polarization. It was found to prevent the formation of a lamellipodium in the uropod avoiding "two headed" cells, hence preserving polarity (Ratner et al., 2003). The Par polarity complex is formed by Cdc42, Par3, Par6 and the atypical PKCs (aPKCι and aPKCζ). The activation of the complex at the front of the cell leads to the binding of adenomatous polyposis coli protein, a tubulin binding protein at the plus-ends of microtubules. The binding of adenomatous polyposis coli protein to the plus ends of microtubules together with the association of Dlg helps to establish polarity (Jaffe and Hall, 2005). The Par complex controls T cell migratory polarity. Active Cdc42 at the leading edge binds the Par6/Par3/aPKC complex inducing binding to the T lymphoma invasion and metastasis 1 (Tiam1). Tiam1 is a GEF that activates Rac via Par3. Tiam1 is a downstream effector of active Rap1a and acts as a scaffolding protein bringing Par3 complex close to Rap1a and Rac1 by simultaneous binding to Par3 and Rap1a-GTP. This suggests that Rap1a recruts Tiam1 and the Par complex to the site of activation. Tiam1 can therefore couple Rap1a/Cdc42/Par-complex leading to the activation of Rac1 inducing actin polymerization at the front of the cell (Gerard et al., 2007).

1.4.3 Chemotaxis

The selective recruitment of different leukocyte populations into tissues is determined by the presence of chemokines on a tissue and the respective receptors on leukocytes. Chemokine and chemokine receptor expression varies on different leukocyte subtypes and across the vasculature. For example, CCR7 and CXCR5 are differentially expressed on lymphocytes and dendritic cells allowing these cells to change their homing capacity and traffic routes (Lipp and Muller, 2003; Mackay, 2001).

So far about 40 chemokines are known, and they are classified according to the configuration of cysteine residues at the N-terminus into four families: CC, CXC, C and CX_3C. They are small (8-14 kDa) molecules that regulate trafficking and host defence of leukocytes. They signal through the G protein-coupled receptors (GPCR) superfamily (Zlotnik and Yoshie, 2000). CXCL12 (also known as SDF-1) is produced by the bone marrow stromal and endothelial cells and is the ligand of the GPCR CXCR4. CXCLl2 has been shown to activate several signalling pathways in T cells, including PI3Ks, mitogen-activated protein kinase and protein kinase C. CXCL12 was also shown to induce Rac1 and Cdc42 activation and its effectors (Haddad et al., 2001).

Several studies indicate the important role of CXCR4 in leukaemic cell homing into the bone marrow. Treatment of primary human leukaemic cells with CXCR4 blocking antibodies decreased their homing into the bone marrow of mice which fail to develop mature T and B cells and consequently are immunodeficient (NOD/SCID). Administration of anti-human CXCR4 monoclonal antibodies to mice previously engrafted with primary human AML or ALL cells leads to a decrease in the levels of leukaemic cells (Tavor and Petit, 2010). Since the expression of a specific chemokine directs the homing of hematopoietic cells, chemokine receptor expression can be used to predict the possible metastatic site of a tumour. For example, at diagnosis, a 4-year old T-ALL patient had marked overexpression of the gut homing molecules chemokine receptor 9 (CCR9) and CD103. The relapse of leukaemia was subsequently confined to the gut. This suggests a role of chemokines in determining the location of relapse (Annels et al., 2004).

To reach a site of inflammation, leukocytes have to move significant distances where they encounter various chemoattractants. The ability of cells to sense external

molecules and to respond by directional migration is known as chemotaxis. Cells are also able to detect small changes in chemoattractant concentrations. During chemotaxis, T cells acquire a motile morphology as described above with a lamellipodium where the chemokine receptor and activated αLβ2 integrin (LFA-1) are localized, and a uropod at the back where ERM, ICAM-1/3 and CD44 are distributed (Gerard et al., 2007). The movement of leukocytes is controlled by internal and external signals, which activate signalling pathways resulting in cytoskeleton remodelling and cell movement.

One of the main signalling proteins activated upon chemotactic stimulus is the PI3K pathway (Welch et al., 2003). There are 3 classes of PI3K: type I (which is divided in two subclasses IA and IB), type II and type III. The type I PI3KA (PI3Kα, β and δ) are activated by tyrosine kinase receptors while PI3KB (PI3Kγ) is activated by G protein-coupled receptors. Their activation leads to the accumulation of phosphatidylinositol 3,4,5-trisphosphate on the plasma membrane recruiting phosphatidylinositol 3,4,5-trisphosphate-binding proteins that drive further signals. The type II and III differ from the type I structurally and are involved respectively in clathrin and endosomal regulation (Giambra et al., 2012).

The migration speed is affected by PI3K inhibitors, emphasizing a role of PI3Ks in chemotaxis (Stephens et al., 2002). PI3Ks have been shown to stabilize protrusion of the leading edge, facilitating accumulation of downstream effectors in this region (Stephens et al., 2008). Receptor activation of heterotrimeric G proteins is important for chemotaxis. In particular, Gβγ components of G proteins have been shown to be essential for chemotaxis signalling (Firtel and Chung, 2000). The dissociation of heterotrimeric G proteins activates PI3Kγ (Stephens et al., 2002). Phosphatidylinositol (3,4,5)-triphosphate can activate Rac. Rac can also stimulate PI3K activation, creating a positive-feedback loop at the front of the cells (Welch et al., 2003). PI3K was also shown to activate Cdc42, which is not involved in feedback loop but constrains the leading edge where phosphatidylinositol (3,4,5)-triphosphate accumulates, thereby maintaining a persistent direction during chemotaxis (Etienne-Manneville, 2004).

1.4.4 Leukocyte transendothelial migration

TEM and localization of leukocytes is an essential requirement for the immune system to clear pathogens. This process is active and tightly regulated and involves multiple molecules on the leukocyte and endothelium surface (Figure 1.20).

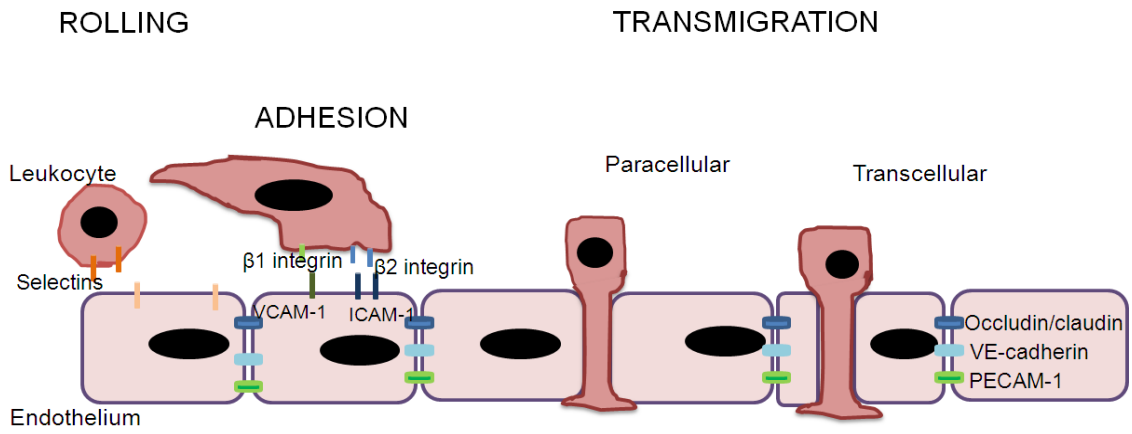

Figure 1.20 Schematic rappresentation of leukocyte transendothelial migration. Rolling is the first step of transendothelial migration. It is mediated by selectins and PSGL-1. Subsequently the leukocyte firmly adheres to the endothelium by binding of active β1 and β2 integrins to VCAM-1 and ICAM-1 expressed on the endothelium surface. Leukocytes can then transmigrate either through endothelial junctions (paracellular route) or through transcellular pores of an endothelial cell (transcellular route).

1.4.4.1 Endothelium: the blood vessel wall

The endothelium consists of a monolayer of cells that acts as a barrier for the passage of cells and macromolecules from the blood to tissues. On the other hand the endothelium needs to function as an entry point for the lymphocytes and leukocytes to reach the targeted tissue or organ. In the endothelium, cell-cell junctions are classified into adherens junctions (AJ) and TJ. AJ are important for the initiation of cell-cell contact and maintenance of junctions. They are also important for inhibition

of endothelial cell growth and angiogenesis. TJ have a major role in permeability controlling the passage of solutes and ions (Bazzoni and Dejana, 2004). Different molecules characterize these two types of junctions, forming homophilic interactions. Adhesion molecules are anchored to the actin cytoskeleton by adaptor molecules. These adaptor molecules also transmit signals to the cell interior to modulate gene expression and cell behaviour (Matter and Balda, 2003)

The main transmembrane protein of endothelial AJ is vascular endothelial cadherin (VE-cadherin). Optimal cell-cell adhesion by VE-cadherin requires the binding of the C-terminal intracellular domain to catenins. The intracellular portion of VE-cadherin binds p120, β and γ-catenin (Vestweber, 2008). The nectin-afadin complex colocalizes with cadherins at AJ. Nectin is an immunoglobulin-like adhesion molecule linked to the actin cytoskeleton via the afadin protein. The nectin-afadin complex seems to be important for TJ formation as well as it associates with TJ proteins (Takahashi et al., 1999). The major trans-membrane components of TJs are claudins and occludins. Among these, claudin-5 was shown to be an endothelial cell-specific TJ protein (Morita et al., 1999). Occludin also contributes to TJ stabilization and optimal barrier function. For example downregulation of occludin induces an increase in endothelial permeability (Cummins, 2012). The transmembrane junctional adhesion molecule (JAM) proteins are associated with TJs and regulate tight junction assembly and endothelial permeability (Ebnet et al., 2004). The cytoplasmic TJ components zona occludens-1 and 2 (ZO-1 and ZO-2) act as scaffolding proteins between transmembrane and cytoplasmic proteins and ZO-1 has been proposed to act as a link between AJs and TJs (Hartsock and Nelson, 2008) (Figure 1.19).

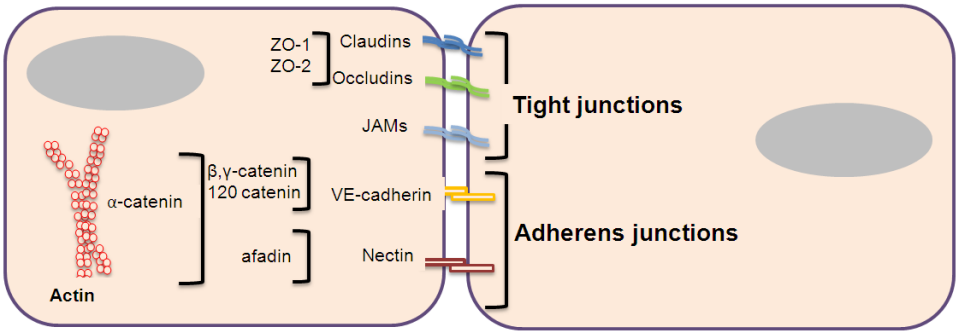

Figure 1.19 Endothelial cell-cell adhesion. Cell-cell adhesion is regulated by tight and adherens junctions. The transmembrane proteins of the adherens junctions are linked via catenin proteins to the actin cytoskeleton.

1.4.4.2 Rolling and adhesion

It is well established that leukocyte TEM involves sequential events, starting with the rolling of the leukocyte on blood vessel walls (Cernuda-Morollon and Ridley, 2006). This process is mediated by transmembrane glycoproteins known as selectins. The selectins are L-selectins, expressed on leukocytes, and E- and P-selectins expressed on endothelial cells which interact with P-selectin glycoprotein ligand1 (PSGL1) and other glycosylated ligands. They regulate the capture and rolling of the leukocyte on the endothelium (Laubli and Borsig, 2010).

One of the key events for the initiation of this process is the activation of the endothelium by proinflammatory cytokines such as tumour necrosis factorα (TNFα), thrombin, and IL-1. TNFα stimulation induces the expression of E-selectin on the endothelium (Puri et al., 2005). P-selectin is stored in granules that fuse with the plasma membrane when platelets and endothelial cells are activated (Zarbock et al., 2011). The extracellular domain of all selectins is a C-type lectin domain followed by an epidermal growth factor-like domain. The cytoplasmic tail of L-selectin is composed of 17 amino acids in humans and has been reported to bind α-actinin, calmodulin and members of the ERM family (Ivetic and Ridley, 2004). Most L-selectin ligands posses a tetrasaccharide sial Lewis x (sLeX) structure. For a higher

affinity binding, L-selectin often contains sulphated sugar moieties or sulphated tyrosyl residues that are important for leukocyte homing. Leukocyte activation leads to the cleavage of the membrane-proximal region of L-selectin resulting in the shedding of the extracellular domain (Wedepohl et al., 2012).

PSGL-1 is expressed on almost all leukocytes and on certain endothelial cells and it is functional only when it is glycosytated. One role of PSGL-1 is to promote leukocyte-leukocyte interaction facilitating the recruitment of other leukocytes to the site of inflammation including those that do not express ligands for E or P-selectin. E-selectin also can bind glycosylated CD44 and the E-selectin ligand 1 (ESL1).

Leukocyte rolling requires rapid formation and breaking of selectin binding to their ligands, and this process occurs under blood flow conditions. It has been demonstrated that rolling cells detach from the endothelium when the flow is stopped. This is a characteristic of selectins, as L and P-selectin require shear stress to act (Ley et al., 2007).

Leukocyte rolling can also be mediated by integrins. T cell lines, T cells and neutrophils, have been shown to roll on vascular cell-adhesion molecule 1 (VCAM1) by engaging of VLA4/α4β1 on their surface. VLA4 was also shown to mediate lymphocyte rolling in venules of the central nervous system (Alon et al., 1995). β2 integrins were suggested to mediate rolling of mouse neutrophils on ICAM-1, and human lymphocytes were shown to enhance rolling when ICAM-1 was co-expressed with L-selectin ligands on endothelial cells (Kadono et al., 2002; Singbartl et al., 2001).

The rolling of leukocytes on the blood wall allows the cells to slow down and to detect chemokines on the endothelium surface. Chemokines activate leukocyte integrins receptor promoting adhesion to ICAM-1 and VCAM-1 expressed on the endothelium surface (see sections 1.3.3.1 and 1.4.1) (Huo et al., 2003).

1.4.4.4 Transendothelial migration

The transmigration of leukocytes through the endothelium can occur through a paracellular or transcellular route. In the paracellular route the leukocyte migrates between endothelial cells, whereas in the transcellular route the leukocyte migrates

through an endothelial cell (Cernuda-Morollon et al., 2010; Johnson-Leger et al., 2000).

1.4.4.4.1 Paracellular TEM

This mechanism can be very rapid and involves the transient opening of the endothelial junctions allowing the leukocyte passage. The binding of leukocytes to the endothelium induces cytoskeleton rearrangements in the endothelial cells via ROCK and MLC phosphorylation. The clustering of ICAM-1 or VCAM-1 induced by leukocyte binding induces an increase in RhoA activity and in stress fibres. This leads to an increase in cell contractility and endothelial permeability. RhoA might be activated via the ERM family. ERM could bind RhoGDI facilitating RhoA activation (Millan and Ridley, 2005).

Reactive oxygen species (ROS) production upon Rac1 activation in endothelial cells has also been reported to be important for TEM, as preteatment with oxygen-radical scavengers inhibits TEM (van Wetering et al., 2002). Moreover ICAM-1 mediated signalling during neutrophil adhesion activates ROS production in endothelial cells, leading to cytoskeletal remodeling important for TEM (Wang and Doerschuk, 2000).

Several molecules expressed at the endothelium junction facilitate TEM. These molecules include PECAM-1, VE-cadherin, CD99 and JAMs and ESAM. PECAM-1 and JAM proteins are members of the Ig superfamily. VE-cadherin, as previously described, is a member of the cadherin family, and CD99 is a unique molecule (Muller, 2003). During extravasation VE-cadherin transiently disperses from the junctions to allow the passage of the leukocyte (Shaw et al., 2001). PECAM-1 is expressed on both leukocytes and on endothelial cells. In endothelial cells, it localizes to cell-cell junctions and on structures know as the lateral border recycling compartment (LBCR). The homophilic interaction between the N-terminal domain of PECAM-1 expressed on endothelium and leukocytes is important for transmigration. During transmigration, PECAM recycles from the LBCR and concentrates around the migrating leukocyte (Mamdouh et al., 2008; Mamdouh et al., 2003). Although PECAM-1 is required for transmigration, blocking antibody against PECAM-1 is not able to inhibit leukocyte migration completely, suggesting that other players are important for this process. PECAM-1 knockout mice have no difference in TEM of monocytes and neutrophils, although neutrophils get trapped

between the endothelium and the basement membrane (Bogen et al., 1994; Muller et al., 1993). CD99 is expressed on the leukocyte surface and at endothelial cell-cell adhesions and like PECAM-1, facilitates leukocyte TEM in a homophilic manner. Blocking of CD99 on the leukocyte or endothelium inhibits monocyte TEM, and blocking both CD99 and PECAM-1 gives an additive effect abolishing TEM almost completely (Schenkel et al., 2002). JAMs have been reported to be involved in inflammation and to facilitate TEM of leukocytes. JAM-A was shown to bind the leukocyte integrin LFA-1 in a heterophilic manner involving the membrane proximal domain of JAM-A. JAM-A also mediates homophilic binding between leukocytes and endothelial cells (Ostermann et al., 2002). JAM-B has not been demonstrated to be involved in TEM. JAM-C is highly expressed on endothelial venules and HUVECs. Antibodies against JAM-C block migration of polymorphonuclear leukocytes across HUVECs in response to CXCL12 in vitro (Johnson-Leger et al., 2002). ESAM is JAM-related protein expressed on endothelial cells and on activated platelets (Petri and Bixel, 2006). It was shown to mediate migration of neutrophils through the vessel wall by influencing endothelial cell contacts. Extravasation is reduced in ESAM knockout mice (Wegmann et al., 2006).

In summary, several endothelial cell surface and adhesion molecules localize at endothelial cell contacts. These molecules have been found to participate in leukocyte TEM.

1.4.4.4.2 Transcellular TEM

The paracellular route is not the only mechanism by which leukocytes can cross the endothelial barrier. In the early 1960s, morphological studies of leukocyte TEM revealed that some leukocytes could extravasate without disrupting endothelial junctions. Leukocytes can in fact pass through a membrane pore of an endothelial cell and this was observed in vitro and in vivo (Carman and Springer, 2004; Phillipson et al., 2008).

The mechanism of transcellular migration involves subcellular membranous structures such as caveolae, fenestrae and vesiculo-vacuolar organelles that promote the passage of liquid and macromolecules through the endothelial cells (Wittchen, 2009). Fenestrae are specialized plasma membrane microdomains where the apical and basal plasma membranes fuse to form a circular pore. These domains are

frequent in specialized vascular beds that require high permeability such as endocrine organs. Tumours can also have a fenestrated endothelium (Roberts and Palade, 1997). Caveolar localization is determined by F-actin and caveolin-1 distribution. ICAM-1 was shown to translocate to F-actin and caveolin-1-rich regions where it was transcytosed to the basal plasma membrane via caveolae. T-lymphocytes were shown to extend pseudopodia into endothelial cells in caveolin and F-actin-rich regions, inducing the translocation of ICAM-1 and caveolin-1 the endothelial basal membrane, membrane fusion and transcellular passage of the T-lymphocyte (Millan et al., 2006).

Lymphocytes use "invasive podosomes" to explore the endothelial surface and form transcellular pores in a process mediated by Src kinase and WASP. Treatment of lymphocyes with Src inhibitors reduced podosome formation. The inhibition of podosomes selectively blockes transcelluar migration (Carman et al., 2007).

Interstingly, another group showed that Mac-1 (CD11b/CD18) deficient leukocytes, which are not able to crawl on the endothelium surface preferentially, use the trascellular route to cross the endothelium (Phillipson et al., 2006; Wittchen, 2009).

1.5 Aims of the project

The migration and infiltration of T-ALL cells into tissues is correlated with a poor prognosis (Aifantis et al., 2008). Leukaemic cells need to adhere and transmigrate from the blood vessels in order to infiltrate and accumulate into tissues. Rap and Rho GTPase are masters of T lymphocyte migration, and they are known to contribute to cancer progression by regulating cancer cell proliferation and invasion, but their role in T-ALL is far from being elucidated.

1. The first aim of my project was to investigate whether the lack of GTPase prenylation caused by the compund statin could affect T-ALL cell adhesion and migration. The main objective was to identify which GTPases are involved in the adhesion and migration of T-ALL cells.
2. Several Rho GTPase genes were found to be dysregulated in T-ALL patient samples. These genes include the atypical GTPase RhoU. The dysregulation of RhoU was found to be correlated with aberrant Notch1 signalling. RhoU was identified as a target gene of Notch1. The second aim of my project was to characterize the function of RhoU and Notch1 in T-ALL cell adhesion and migration. This was achieved by using different Notch1- mutated T-ALL cell lines.
3. The third aim of my project was to further characterize the function of RhoU in T-ALL cell transendothelial migration, in parallel with its close relative RhoV. Interestingly, RhoV was also found to be upregulated in T-ALL patients. Using an overexpression approach, the localization and distribution of RhoU and RhoV was also investigated in T-ALL cells. Furthermore the interaction partners of RhoU were investigated.

2

Statins inhibit T-acute lymphoblastic leukaemia cell adhesion and migration through Rap1b

Elvira Infante[*,†], Sarah J. Heasman[*] and Anne J. Ridley[*]

[*]Randall Division of Cell and Molecular Biophysics, King's College London, New Hunt's House, Guy's Campus, London SE1 1UL, UK
[†]National Institute for Health Research (NIHR), Biomedical Research Centre, Guy's and St Thomas' NHS and King's College London, London, UK.

Journal of Leukocyte Biology
Received August 5, 2010;
Revised November 24, 2010;
Accepted December 19, 2010.
DOI: 10.1189/jlb.0810441

AUTHORSHIP
E.I. designed and carried out experiments and wrote the manuscript; S.J.H. designed experiments and established conditions for studying CCRF-CEM, T-lymphoblast adhesion, and TEM; and A.J.R. planned experiments and wrote the manuscript.

2.1 Abstract

Statins are known to inhibit signaling of Ras superfamily GTPases and reduce T-cell adhesion to ICAM-1. Here we address the hypothesis that statins affect T-cell adhesion and migration by modulating the function of specific GTPases. Statins inhibit the synthesis of mevalonic acid, which is required for farnesyl and geranylgeranyl isoprenoid synthesis. Ras superfamily GTPases are post-translationally isoprenylated to facilitate their anchorage to membranes, where they function to stimulate signal transduction processes. We demonstrate that 1 μM statin inhibits the adhesion, migration, and chemotaxis of the T-acute lymphoblastic leukemia (T-ALL) cell line CCRF-CEM, and transendothelial migration of CCRF-CEM and PEER T-ALL cells, but higher statin concentrations are needed to inhibit adhesion of primary T cells. Similar effects are observed following treatment with a geranylgeranyl transferase inhibitor (GGTI-298) or RNAi-mediated knockdown of Rap1b but not Rap1a, Rac1, Rac2, RhoA or Cdc42. Statins also alter Rap1 activity and Rap1b localization. Rap1 levels are higher in primary T cells than T-ALL cells, which could explain their reduced sensitivity to statins. These results demonstrate for the first time that the closely related Rap1a and Rap1b isoforms have different functions, and suggest that statins or Rap1b depletion could be used to reduce tissue invasion in T-ALL.

2.2 Introduction

Statins are widely used to lower cholesterol levels in patients, thereby reducing risk of cardiovascular disease. In particular in patients with heart failure statins are beneficial due to their effects on inflammation, oxidative stress and vascular tone (Tang and Francis, 2010; Zeiser et al., 2009). These drugs have been reported to have anti-inflammatory properties (Dinarello, 2010; Liao and Laufs, 2005) and their possible role in cancer prevention has also attracted attention (Gauthaman et al., 2009; Kuoppala et al., 2008).

Statins acts by competitive inhibition of 3-hydroxy-3 methylglutaryl coenzyme A (HMG-CoA) reductase, resulting in a decrease in mevalonic acid synthesis. Mevalonic acid is an upstream substrate in the formation of cholesterol and also of the farnesyl and geranylgeranyl isoprenoids. These isoprenoids are post-translationally added to a carboxy terminal cysteine of CAAX motifs on proteins such as small Ras-superfamily GTPases, and facilitate anchorage of these proteins in membranes, where they signal to downstream effectors (Greenwood et al., 2006). By inhibiting synthesis of isoprenoids, statins therefore reduce the localization of Ras-superfamily proteins to membranes. A beneficial effect of statins has been reported in colorectal and melanoma cancer prevention, and the inhibition of Ras/Rho GTPase prenylation, leading to their mislocalization, could contribute to the cancer prevention property of statins (Demierre et al., 2005).

Ras and Rho family GTPases are signal transduction proteins involved in cell proliferation, cell survival, cytoskeletal reorganization, membrane trafficking and motility. These proteins are normally activated by guanine nucleotide exchange factors (GEFs) that promote the switching from an inactive GDP to an active GTP state, and inactivated by GTPase activating proteins (GAPs) which enhance the intrinsic GTPase activity of the proteins. Some Rho GTPases are also regulated by GDP dissociation inhibitors (GDIs) that bind to prenyl groups and thereby inhibit membrane localization (Schmidt and Hall, 2002). Statins have been shown to increase the level of RhoA-GTP yet inhibit its signaling to downstream targets such as ROCKs (Cordle et al., 2005; Rattan, 2010; Wang et al., 2008).

T-ALL is a hemotological cancer of T lymphocytes (Real and Ferrando, 2009), for which poor prognosis has often been shown to correlate with the migration and accumulation of leukemia cells in the tissues (Uchiyama et al., 1995). In order to

transmigrate from the blood to tissues, leukocytes interact with and adhere to the endothelial cells lining the blood vessels. This involves the activation of integrins such as LFA-1, which is expressed on the leukocyte surface and binds to endothelial cell adhesion molecule ICAM-1 (Liu et al., 2004). Chemokines and cytokines can activate the Ras GTPase Rap1 which induces integrin activation through inside-out signaling (Wittchen et al., 2005).

Here we demonstrate that low concentrations of statins inhibit LFA-1 activation on T-ALL cells and consequently reduce adhesion to ICAM-1 and transendothelial migration of T-ALL cells, but do not affect migration of primary T cells. Downregulation of Rap1b but not Rap1a induces similar effects on T-ALL cells, implying that the response to statins is primarily due to inhibition of Rap1b-mediated activation of LFA-1.

2.3 Materials and Methods

2.3.1 Cell culture and drug treatment

CCRF-CEM (ATCC, LGL Promochem, Middlesex, UK), PEER, Jurkat and SUPT1 (kind gift of Prof. Asim Khwaja) cells were maintained in RPMI-1640 containing 2 mM glutamine and supplemented with 10% fetal calf serum, 1 mM sodium pyruvate, 10 mM Hepes, penicillin (100 U/ml) and streptomycin (100 µg/ml). Cells were used between passage 1 and 10. T-lymphoblasts were derived from human peripheral blood mononuclear cells. Cells were cultured in RPMI-1640 supplemented with 10% human AB serum, penicillin (100 U/ml) and streptomycin (100 µg/ml) and stimulated with 8 µg/ml phytohaemagglutinin for 48 h. Cells were subsequently maintained in medium containing 10 U/ml of interleukin-2 (Roche, Mannheim, Germany), and used between passage 4 and 10. Where indicated, T-ALL cells and T-lymphoblasts were treated for 16 h with 1 µM simvastatin or lovastatin (Calbiochem, Nottingham, UK), 250 µM mevalonolactone (mevalonic acid; Sigma-Aldrich, Dorset, UK), 10 µM FFI (Enzo, Exeter, UK) or GGTI-298 (Calbiochem). Cell viability was determined with 0.4% Trypan blue solution. Human umbilical vein endothelial cells (HUVECs) (Biowhittaker, Wokingham, UK) were cultured in flasks coated with 10 µg/ml fibronectin (FN; Sigma-Aldrich) in EBM-2 medium supplemented with 2% fetal calf serum and endothelial cell growth supplements (Lonza Biologics, Slough, UK). Cells were used between passage 1 and 4.

2.3.2 Transfection

CCRF-CEM cells (5 x 10^5) were transfected by nucleofection (Amaxa Biosystems Nucleofection System, Lonza Biologics) with 20 µg plasmid DNA (see 4.2.2.6, 4.2.2.7 and 4.2.2.8) or 1.2 µM siRNA (Dharmacon, Colorado, USA) in 100 µl of Nucleofection reagent (kit C, Lonza Biologics). siRNA sequences were Rap1b-1: GAACAACUGUGCAUUCUUA; Rap1b-2: CAAUGAUUCUUGUUGGUAA; Rap1a-1: CAAUAAAUGUGACCUGGAA; Rap1a-2: GCGAGUAGUUGGCAAAGAG; Rac1-1: AGACGGAGCUGUAGGUAAA; Rac1-2: UAAGGAGAUUGGUGCUGUA; Rac2-1: CAGCCAAUGUGAUGGUGGA; Rac2-2: ACAAGGACACCAUCGGAGAA; Cdc42-1: GAUUACGACCGCUGAGUUA; Cdc42-2: GAUGACCCCUCUACUAUUG; RhoA-1: AUGGAAAGCAGGUAGAGUU; RhoA-2:

CGACAGCCCUGAUAGUUUA. siControl was from Thermo Fisher Scientific (D-001810-02-20, Lafayette, USA). Cells were used for experiments 48-72 h after siRNA transfection or 24 h after DNA plasmid transfection. pMT2-HA-Rap1b was a kind gift of Prof Johannes Bos.

2.3.3 Adhesion assays

Ninety-six-well plates were coated overnight with 5 µg/ml ICAM-1 (R&D Systems, Abingdon, UK) or 10 µg/ml FN, then blocked in 1% BSA in PBS for 30 min. Treated cells were centrifuged at 240 g for 4 min and resuspended in PBS at 10^6 cells/ml. Cells were then incubated at 37°C for 15 min with 2 µM Cell Tracker CMFDA (Invitrogen, Paisley, UK). Samples were resuspended in warm media and 10^5 cells/well (each sample in triplicate) were incubated at 37°C for 30 min. After washing with PBS, the plate was read on a Fusion-αFP plate reader (PerkinElmer, Cambridge, UK) at 485 nm excitation and 525-535 nm emission. Alternatively, images of CMFDA-labeled cells were acquired using Metamorph software (MDS Analytical Technologies, Wokingham, UK), on a Nikon Eclipse TE2000 microscope with a 4x objective. Cell numbers were determined using Volocity software (PerkinElmer, Cambridge, UK).

2.3.4 Chemotaxis assay and transendothelial migration

Transwell filters (Costar) were coated with 5 µg/ml ICAM-1. $2x10^5$ T cells were added in the top chamber and 600 µl of medium containing 30 ng/ml CXCL12 (R&D Systems) was added to the bottom chamber. Cells in the lower chamber were counted after 1 using a Casy Counter (Roche Innovatis, Bielefeld, Germany).
HUVECs were grown to confluency on FN-coated 5-µm transwell filters and then stimulated with 10 ng/ml TNF-α (R&D Systems, Abingdon, UK) for 16 h. After washing, $2x10^5$ T cells were added onto the HUVECs in the top chamber and 600 µl of medium containing 30 ng/ml CXCL12 was added to the bottom chamber. Cells in the lower chamber were counted after 1h or 2 h using a Casy Counter.

2.3.5 Timelapse microscopy

HUVECs were grown to confluency on FN-coated coverslips and stimulated with TNF-α for 16 h. Cells were incubated for 8 min with 30 ng/ml CXCL12 then washed and incubated for 1 h at 37°C. CCRF-CEM cells ($0.75x10^5$) in 500 µl of CEM media

were added to the HUVECs and time lapse images were acquired every minute for 1 h using Metamorph software on a Nikon Eclipse TE2000 microscope with a 20x objective. Cells were tracked and migration speed (μm/min) determined using ImageJ analysis software.

2.3.6 Flow cytometry

To measure total surface LFA-1, CCRF-CEM cells ($2x10^5$) were incubated for 30 min at 4°C with 1:100 CD11a antibody (BD Bioscience, Oxford, UK) or 1:50 IgG2a as an isotype control (Serotec, Kidlington, UK). To measure surface levels of active LFA-1, cells were incubated for 15 min at 37°C with 200 μM $MnCl_2$ (Hogg et al., 2002), then for 30 min at 37°C with 1:100 mAb24 (kind gift of Prof Nancy Hogg). Cells were incubated with Alexa Fluor 488-labelled anti-mouse antibody (Invitrogen) then analysed on a Becton Dickinson FACS Calibur machine using the FlowJo program.

2.3.7 Immunofluorescence

CCRF-CEM cells ($5x10^5$) were transfected with 20 μg pMT2-HA-Rap1b (see 4.2.2.6, 4.2.2.7 and 4.2.2.8). After 24 h, cells were treated with 1 μM simvastatin for 16 h and cytospun onto coverslips by centrifugation at 300g for 5 min. HUVECs ($1.5x10^5$) were seeded onto FN-coated coverslips and treated for 16 h with 1 μM simvastatin. Samples were fixed with 4% paraformaldehyde, permeabilized with 0.1% Triton-X100, then incubated for 1 h with 1:200 mouse anti-HA antibody (Santa Cruz, California, USA) or 1:200 anti-mouse VE-cadherin antibody (BD Biosciences, Oxford, UK) followed by 1:500 Alexa Fluor 488 anti-mouse antibody (Invitrogen). Coverslips were mounted onto slides using anti-fade mounting medium (Dako, Ely, UK).

2.3.8 GTPase activity assays

GST-RalGDS-RBD, GST-PAK-PBD and GST-Rhotekin-RBD were transformed in BL21 *E.coli* and plated on a LB agar plate containing 100 μg/ml ampicillin. A colony was inoculated in 100 ml of LB/ampicillin and grown overnight at 37°C. The following day the cultures were diluted 1:20 into fresh medium and grown to an optical density of 0.7 (600 nm). 0.3 mM IPTG was then added to induce protein

expression and the bacteria were incubated for 2 h at 30°C. Bacterial pellets were collected by centrifugation for 15 min at 1500 g and the pellets stored at -40°C.
Bacterial pellets were resuspended in STE buffer (10 mM Tris pH 8.0, 150 mM NaCl, 1 mM EDTA) and lysed by the addition of 100 µg/ml lysozyme for 20 min on ice. After, 5 mM DTT, 1% Tween-20 and 0.03% SDS were added, the lysates were mixed and then centrifuged at 14000 g for 20 min and the supernatant collected. The supernatants were then incubated with the glutatione sepharose beads (GE Healthcare) at 4°C for 2 h, and the bead-bound proteins washed three times and used in the pull-down assays. CCRF-CEM cells (10^6/pulldown) were lysed in 400 µl of pull-down buffer (25 mM Hepes pH7.5, 150 mM NaCl, 1% NP-40, 10 mM $MgCl_2$, 1 mM EDTA, 25 mM NaF, 1 mM Na_3VaO_4, 10 µg/ml aprotinin, 100 µM PMSF and 10% glycerol). 40 µl of the lysate was retained to determine total GTPase levels. The remaining lysate was incubated with the protein-bound beads on a rotor for 1 h at 4°C. The beads were washed 3 times in pull-down buffer, boiled in Laemmli sample buffer and used for western blotting.

2.3.9 Western blot analysis

Cells were lysed in 1% SDS followed by addition of 1% Triton X-100, 25 mM NaF, 1 mM Na_3VO_4 and 10 mg/ml aprotinin, then incubated for 10 min on ice and clarified by centrifugation. Cleared lysates were boiled for 5 min in 4X sample buffer (0.25 M Tris-HCl pH 6.8, 8% SDS (w/v), 40% glycerol (w/v), 10% β–mercaptoethanol (w/v), 0.2% Bromophenol blue (w/v)). Lysates were separated on 4-12% Bis-Tris polyacrylamide gels (Invitrogen) or on a 12.5% poly-acrilamide gel then transferred to nitrocellulose membrane (Millipore, Watford, UK). Membranes were incubated in blocking buffer (5% non-fat dried milk in TBS containing 0.1% Tween-20) for 1 h at room temperature and then incubated for 1 h with 1:1000 dilutions of the following antibodies diluted in blocking buffer: Rap1b (36E1), Rap1a/Rap1b (26B4), RhoA (67B9), or Cdc42 (11A11) (Cell Signaling Technology, Massachusetts, USA), Rap1a (C-17) (Santa Cruz), Rac1 (23A8) or Rac2 07-604 (Millipore). Membranes were then incubated with horseradish-peroxidase-conjugated anti-mouse, anti-rabbit or anti-goat antibodies (GE Healthcare, Chalfont St Giles, UK). Antibodies were visualized using the ECL detection system (GE Healthcare).

2.4 Results

2.4.1 Statins inhibit adhesion and chemotaxis of T-ALL cell lines but not of primary T-lymphoblasts

To investigate the effect of statin treatment on T-ALL cell adhesion, we first performed an adhesion assay on ICAM-1. ICAM-1 is expressed on the endothelial cell surface and is fundamental in mediating adhesion between the endothelium and leukocytes (Vestweber, 2007). We observed a 50% reduction in the binding of CCRF-CEM cells to ICAM-1 following treatment with 1 μM simvastatin or lovastatin (Figure 2.1A). Addition of 250 μM mevalonic acid rescued the statin-induced inhibition of adhesion (Figure 2.1A). This indicates that statins are acting by inhibiting HMG-CoA reductase, rather than binding directly to the β2 integrin (LFA-1) L-site and thereby inhibiting adhesion to ICAM-1 (Kallen et al., 1999; Weitz-Schmidt et al., 2001). We also observed a significant decrease in Jurkat cell adhesion to FN that was rescued by mevalonic acid (Figure 2.1B). As T cells bind FN mostly through the β1 integrin (Hauzenberger et al., 1994), this effect cannot be attributed to statin binding to β2 integrin. The effect of statins on adhesion was not due to changes in T-ALL cell viability (Supplementary Figures 2.1A and B).

Surprisingly, 1 μM simvastatin or lovastatin did not reduce the adhesion of primary T-lymphoblasts, but some inhibition was observed at 10 μM statins (Figure 2.1C). This was not due to a difference in adhesion to ICAM-1 between primary T-lymphoblasts and CCRF-CEM cells (supplementary Figure 2.1C).

Similarly, 1 μM statin treatment did not affect T-lymphoblast chemotaxis towards CXCL12 (SDF-1), whereas it inhibited chemotaxis of CCRF-CEM cells (Figures 2.1D and E). The reduction in CCRF-CEM cell chemotaxis was also rescued by mevalonic acid (Figure 2.1E), while mevalonic acid by itself had no effect on chemotaxis (supplementary Figure 2.1D). Together, these results indicate that statins inhibit adhesion and migration of T cells and that T-lymphoblasts are less sensitive to statins than CCRF-CEM or Jurkat T-ALL cell.

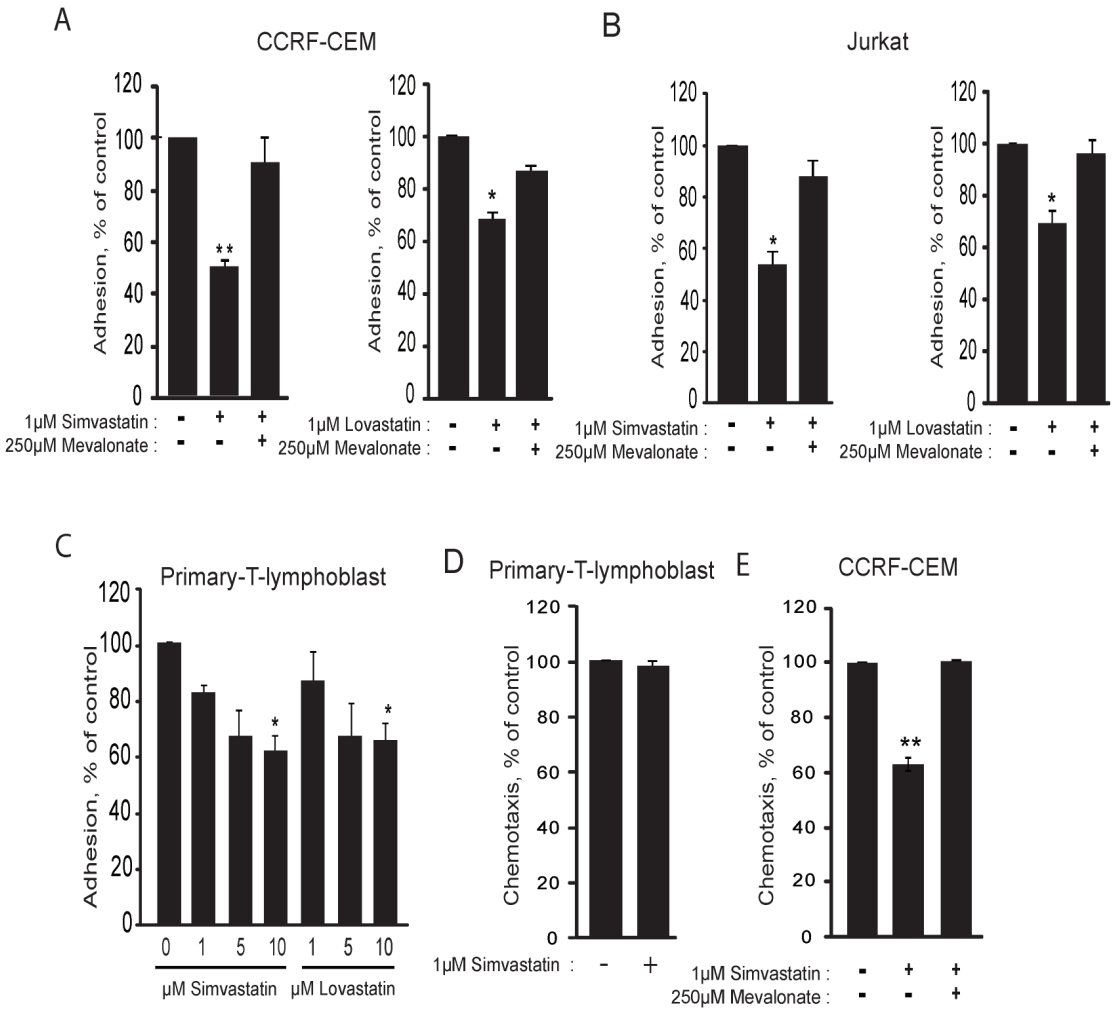

Figure 2.1. Statins inhibit adhesion and chemotaxis of T-ALL cell lines but not of primary T-lymphoblasts. CCRF-CEM (A) and Jurkat (B) cells were treated for 16 h with 1 μM simvastatin or lovastatin alone or in combination with 250 μM mevalonate. The cells were then labeled with Cell Tracker CMFDA, added to wells coated with ICAM-1 (A) or FN (B) and adhesion determined after 30 min. Primary T-lymphoblasts (C) were treated with 1, 5, or 10 μM simvastatin or lovastatin. Cells were labeled with Cell Tracker CMFDA and adhesion to ICAM-1-coated wells determined after 30 min. (D,E) T-lymphoblasts (D) or CCRF-CEM cells (E) were treated for 16 h with 1 μM simvastatin and 250 μM mevalonic acid where indicated. Cells were then added to ICAM-1-coated transwells containing 30 ng/ml SDF-1 in the lower chamber. Cells in the lower chamber were counted after 1 h. Data shown are the mean of 3 independent experiments ± SEM. * $p<0.05$, **$p<0.01$; 2-way-paired t-test. *Experiments performed by Elvira Infante.*

2.4.2 Statins dysregulate Rap1, Rac1 and RhoA activity in CCRF-CEM cells

Given the effect of statin treatment on CCRF-CEM and Jurkat cell adhesion and the known effect of statins in inhibiting protein prenylation, we investigated whether they altered the activity of GTPases. In particular, we focused on Rap1, Rac1 and RhoA as these GTPases have been implicated in integrin-mediated adhesion (Hattori and Minato, 2003; Takaishi et al., 1997; Vielkind et al., 2005).

Incubation of CCRF-CEM cells for 16 h with simvastatin increased the level of GTP-bound Rap1 (Figure 2.2A and B). This was prevented by co-treatment with mevalonic acid (Figure 2.2A). Statin treatment induced a shift in the mobility of Rap1 on SDS-PAGE, reflecting the reduced prenylation (Supplementary Figure 2.2A). Statins have been reported to increase levels of RhoA-GTP and Rac1-GTP in THP-1 cells (Cordle et al., 2005), and we also observed an increase in active Rac1 and RhoA in CCRF-CEM cells (Figure 2.2A, B and C). This increase in GTP-loading could be due to mislocalization of unprenylated proteins, for example leading to reduced interaction with GAPs. This hypothesis is supported by the observation that treatment with the geranylgeranyl transferase inhibitor (GGTI) GGTI-298, which prevents prenylation of Rap1, Rac1 and RhoA (Roberts et al., 2008; Wennerberg et al., 2005), also resulted in higher levels of GTP-bound Rap1, Rac1 and RhoA (Figure 2.2E-H). Rap1, Rac1 and RhoA are post-translationally geranylgeranylated at the C-terminus, whereas some other Rho and Ras family proteins are farnesylated (Roberts et al., 2008; Wennerberg et al., 2005). Consistent with this, no changes in GTP-loading of Rap1 was observed following incubation with 10 μM FFI, which inhibits farnesyltransferases (Figure 2.2I).

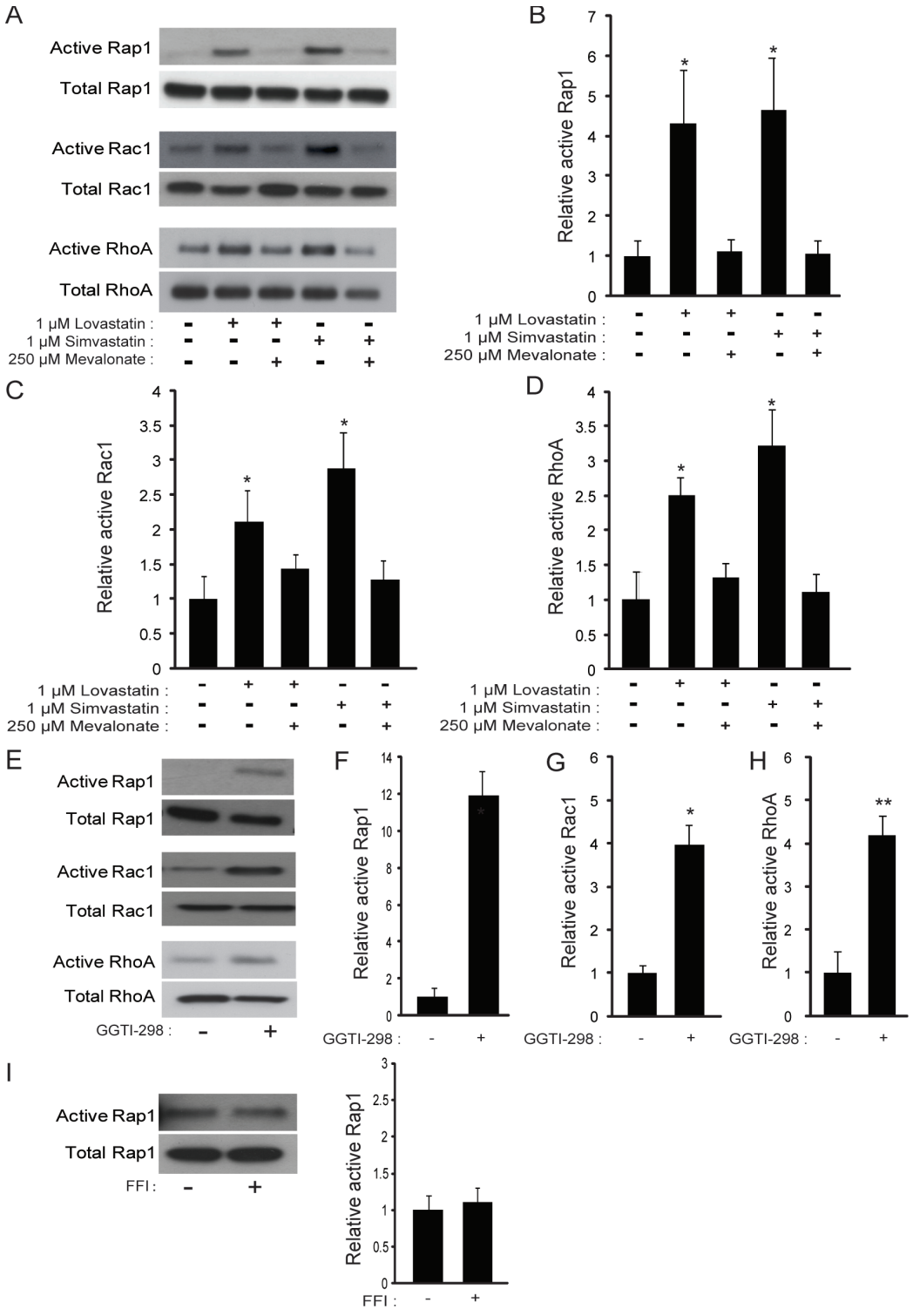

Figure 2.2. Statins and GGTI increase Rap1, Rac1 and RhoA activity in CCRF-CEM cells. CCRF-CEM cells were treated for 16 h with 1 µM lovastatin or simvastatin alone or in combination with 250 µM mevalonic acid (A-D), or with 10 µM GGI-298 (E-H) or FFI (I). Cell lysates was incubated with GST-RalGDS (Rap1), GST-PAK-PBD (Rac1) or GST-Rhotekin-RBD (RhoA) beads then analysed by western blotting with the indicated antibodies. The relative levels of active Rap1

(B, F, I), Rac1 (C and G) and RhoA (D and H) were quantified using ImageJ. Data shown are the mean of 3 independent experiments ± SEM. *p<0.05, **p<0.01; 2-way-paired t-test. *Experiments performed by Elvira Infante.*

2.4.3 Low concentrations of statins do not dysregulate Rap1 activity in primary T-lymphoblasts

As we had observed that statins at 1 μM did not affect the adhesion or chemotaxis of primary T-lymphoblasts (Figure 2.1C, D), we next investigated the effect of statins on Rap1 activity in these cells. Treatment of T-lymphoblasts with 1 μM simvastatin did not affect Rap1 activity (Figure 2.3A). However, 10 μM simvastatin did increase Rap1 activity significantly in T-lymphoblasts, and induced a further increase in Rap1 activity in CCRF-CEM cells above that induced by 1 μM simvastatin (Figure 2.3B-D). This analysis also showed that the total level of Rap1 was much lower in CCRF-CEM cells than in T-lymphoblasts. Similarly, Rap1 levels were lower in a panel of T-ALL cell lines compared to primary T-lymphoblasts (Figure 2.3E). These results suggest that the higher expression level of Rap1 protein in T-lymphoblasts could be responsible for their reduced sensitivity to statins.

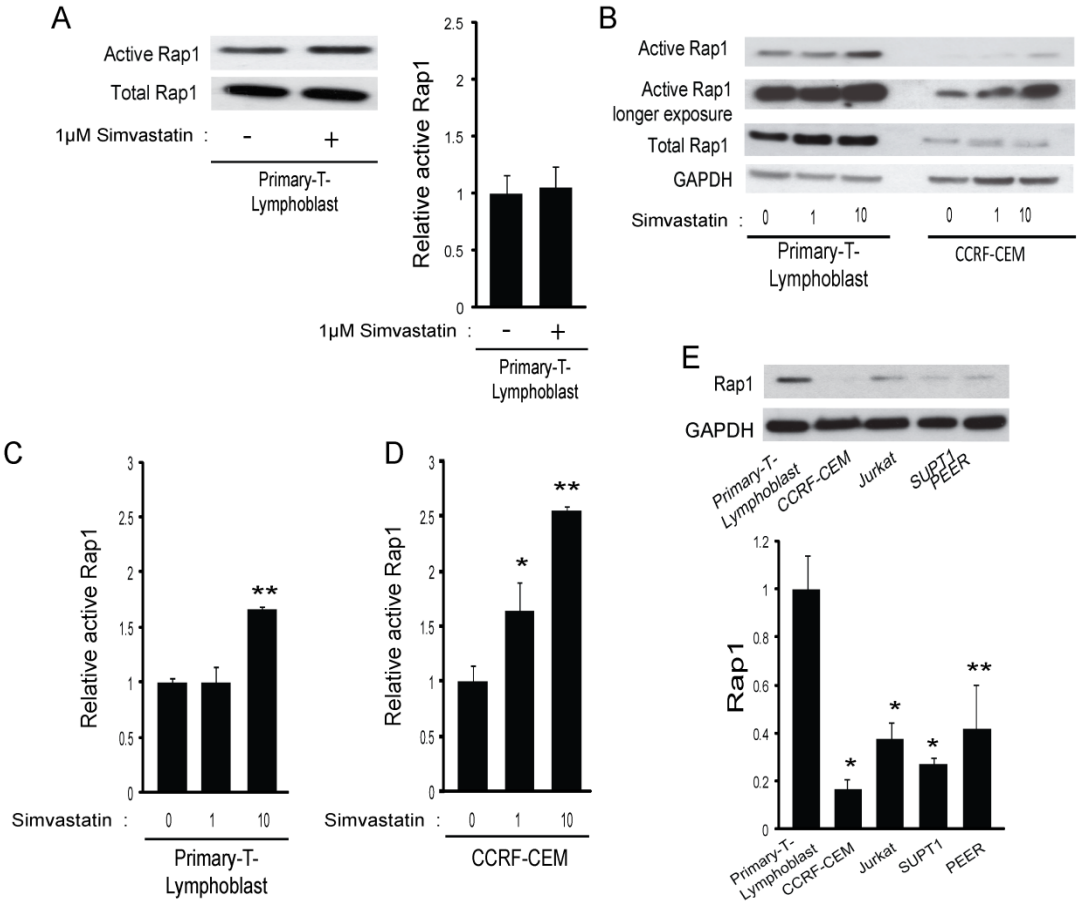

Figure 2.3. Primary T-lymphoblasts are less sensitive to statins and have higher Rap1 levels than T-ALL cells . Primary T-lymphoblasts (A-C) and CCRF-CEM cells (B, C) were treated for 16 h with the indicated concentrations of simvastatin. Cell lysates were incubated with GST-RalGDS beads then analysed by western blotting with Rap1 antibody. Relative levels of active Rap1 were quantified using ImageJ (A, C, D). (E)Total Rap1 expression in primary-T-lymphoblasts and T-ALL cell lines CCRF-CEM, Jurkat, SUPT-1 and PEER was analyzed by western blotting and relative levels quantified using ImageJ. Data shown are the mean of 3 independent experiments ± SEM. * $p<0.05$, **$p<0.01$; 2-way-paired t-test. *Experiments performed by Elvira Infante.*

2.4.4 Rap1b is required for T-ALL cell adhesion and migration

To investigate the importance of prenylation for adhesion, we treated CCRF-CEM cells with 10 μM GGTI-298 or FFI. There was a significant reduction of adhesion to ICAM-1 when cells are treated with GGTI-298 compared to untreated or FFI-treated samples (Figures 2.4A and B). To determine whether GTPases implicated in integrin-mediated adhesion affected T-ALL cell adhesion to ICAM-1, we used siRNA to knockdown the expression of the two Rap1 isoforms (Rap1a and Rap1b) (Figure 2.4C), RhoA, Rac1, Rac2 and Cdc42 in CCRF-CEM cells (Figure 2.4H). Rap1b but not Rap1a depletion strongly reduced adhesion to ICAM-1 (Figures 2.4D and E). Interestingly, knockdown of Rap1a led to reduced adhesion to FN suggesting that this isoform is involved in β1 but not ß2/LFA-1 activation (Figure 2.4F). Knockdown of Rac1, Rac2, Cdc42 and RhoA did not affect adhesion (Figure 2.4G). Interestingly, Rap1a and Rap1b levels were higher in T-lymphoblasts than in CCRF-CEM and Jurkat cells (Supplementary Figure 2.1C), indicating that both Rap1a and Rap1b contribute to the increase in total Rap1 observed (Figure 2.3E).

As statins can affect the localization of GTPases through inhibiting prenylation, we examined the effect of simvastatin on Rap1b localization in CCRF-CEM cells. Rap1 has previously been shown to be activated by the chemokine CXCL12 (Wittchen et al., 2005). Simvastatin treatment altered the localization of Rap1b and induced its accumulation on multiple punctate structures in the cytoplasm in CXCL12-stimulated cells (Figure 2.4I). These might be endosomes, similar to the localization of Rap1a prior to translocation and activation at the plasma membrane (Bivona et al., 2004; Mor et al., 2009).

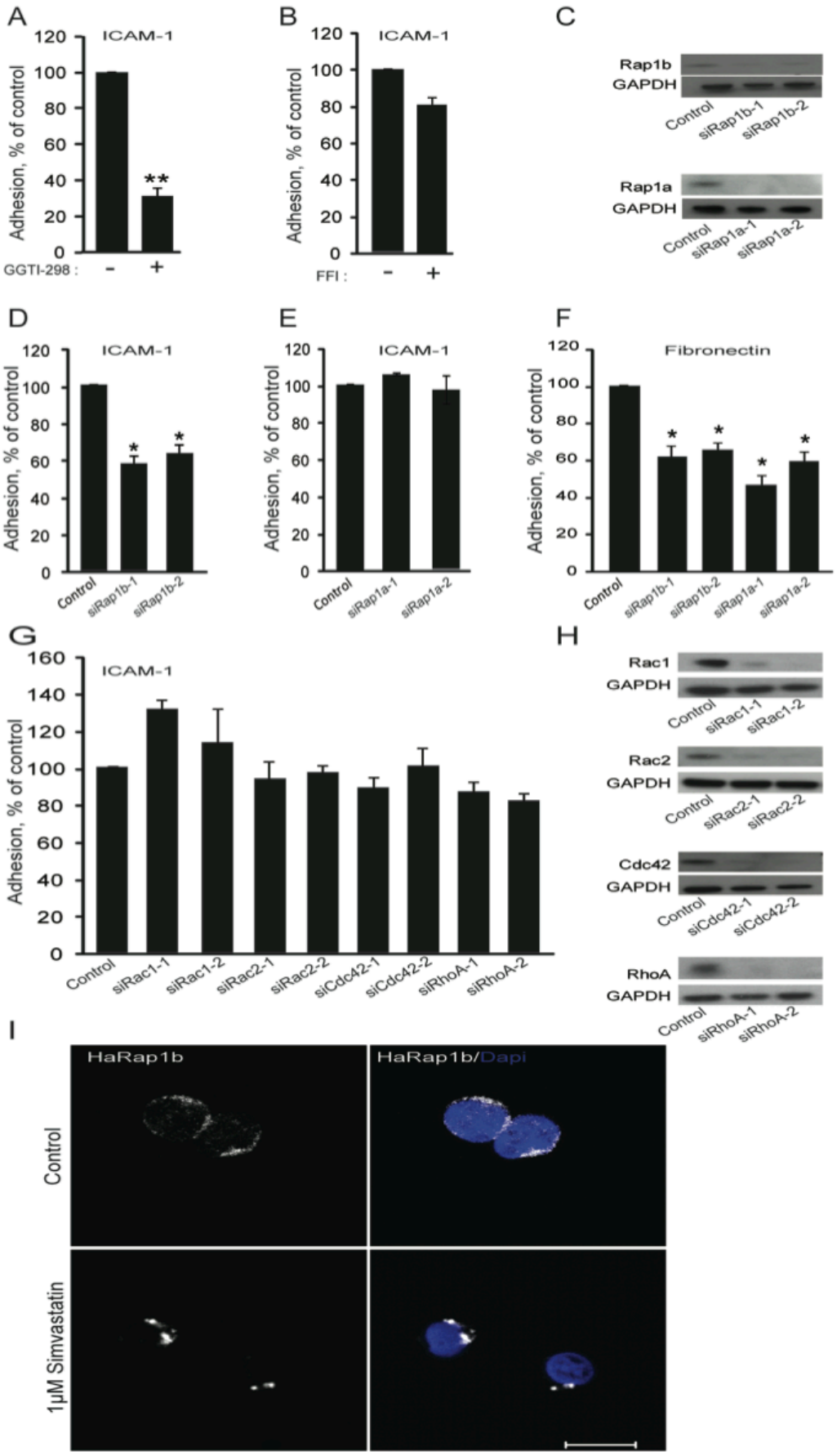
A
ICAM-1
Adhesion, % of control
120
100
80
60
40
20
0
**
GGTI-298 : - +
B
ICAM-1
Adhesion, % of control
FFI : - +
C
Rap1b
GAPDH
Control
siRap1b-1
siRap1b-2
Rap1a
GAPDH
Control
siRap1a-1
siRap1a-2
D
ICAM-1
Adhesion, % of control
Control
siRap1b-1
siRap1b-2
E
ICAM-1
Adhesion, % of control
Control
siRap1a-1
siRap1a-2
F
Fibronectin
Adhesion, % of control
Control
siRap1b-1
siRap1b-2
siRap1a-1
siRap1a-2
G
ICAM-1
Adhesion, % of control
160
140
120
100
80
60
40
20
0
Control
siRac1-1
siRac1-2
siRac2-1
siRac2-2
siCdc42-1
siCdc42-2
siRhoA-1
siRhoA-2
H
Rac1
GAPDH
Control
siRac1-1
siRac1-2
Rac2
GAPDH
Control
siRac2-1
siRac2-2
Cdc42
GAPDH
Control
siCdc42-1
siCdc42-2
RhoA
GAPDH
Control
siRhoA-1
siRhoA-2
I
HaRap1b
HaRap1b/Dapi
Control
1μM Simvastatin

Figure 2.4. Rap1b depletion leads to reduced adhesion of CCRF-CEM clls. CCRF-CEM cells were treated for 16 h with 10 μM GGI-298 (A) or FFI (B). Cells were then labeled with Cell Tracker CMFDA, plated on ICAM-1 and adhesion measured after 30 min. CCRF-CEM cells were transfected with siRNAs targeting Rap1b, Rap1a (C-F), Rac1, Rac2, Cdc42 or RhoA (G, H). (C, H) Levels of each protein were analysed by western blotting. GAPDH was used as a loading control. Blots shown are representative of 3 independent experiments. (D-G) Adhesion assays were performed on ICAM-1 or fibronectin as indicated. *$p<0.05$, **$p<0.01$; 2-way-paired t-test. (I) CCRF-CEM cells were transfected with a plasmid encoding pMT2-HA-Rap1b. After 24 h, cells were treated for 16 h with 1 μM simvastatin then incubated with 1 ng/ml CXCL12 for 30 min. Subsequently, samples were cytospun for 5 min at 300g onto coverslips. After fixation and permeabilization, samples were stained with an anti-HA antibody and with DAPI to stain nuclei and imaged by confocal microscopy. Bar, 10 μm. *Experiments performed by Elvira Infante.*

2.4.5 Statins and Rap1b regulate integrin activity

We next investigated if statins, GGTI or Rap1b depletion affected adhesion by inducing changes in the surface expression and/or activation of integrins. LFA-1 is normally expressed on the leukocyte surface in an inactive form but it can be activated by addition of Mn^{2+} (Hogg et al., 2002). No significant changes were observed in the cell surface expression of LFA-1 subunit CD11a (αL) following statin or GGTI treatment (Figure 2.5A) or knockdown of Rap1a or Rap1b (Figure 2.5B). To investigate LFA-1 activation, we used the mAb24 antibody which recognizes the active form of LFA-1 (Dransfield and Hogg, 1989; Lu et al., 2001). Both statins and GGTI-298 but not FFI inhibited LFA-1 activation (Figures 2.5C and D). Similarly, knockdown of Rap1b but not Rap1a reduced LFA-1 activation (Figure 2.5E). These results indicate that the statin-induced inhibition of adhesion to ICAM-1 is due at least in part to reduced Rap1b prenylation and hence, decreased activation of the integrin LFA-1.

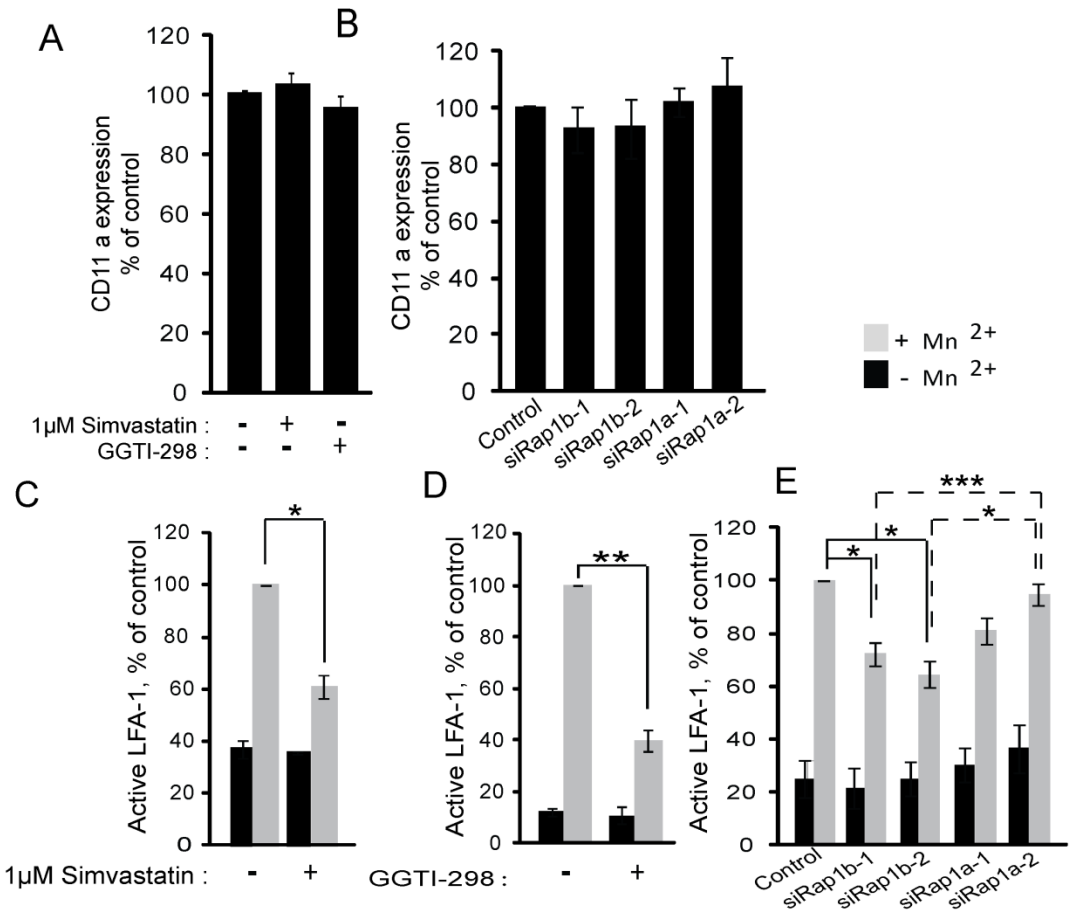

Figure 2.5. Statins, GGTI and Rap1b regulate LFA-1 integrin activity. CCRF-CEM cells were treated for 16 h with 1 μM simvastatin (A and C) or 10 μM GGTI-298 (A and D), or transfected with siRNAs targeting Rap1b or Rap1a (B and E). Cells were then stained for αL integrin (CD11a) (A and B), or were incubated for 15 min with 200 μM $MnCl_2$ (Mn^{2+}) then stained for active LFA-1 with mab24 (C-E). Cells were analysed by flow cytometry. Data show the mean of 3 experiments ± SEM. *, $p<0.05$, **$p<0.01$; 2-way-paired t-test. *Experiments performed by Elvira Infante.*

2.4.6 Statin treatment and Rap1b downregulation inhibits transendothelial migration of T-ALL cells

Transendothelial migration (TEM) of leukocytes is a crucial step during inflammation and immune responses, and requires LFA-1 adhesion to endothelial ICAM-1 (Newton et al., 2009). We found that statin treatment significantly decreased the TEM of CCRF-CEM and PEER T-ALL cells, but not primary T-lymphoblasts (Figure 2.6A). Consistent with a specific involvement of Rap1b in LFA-1 activation, Rap1b but not Rap1a depletion reduced TEM of CCRF-CEM cells (Figures 2.6B and C). Treatment of endothelial cells for 16 h with1 μM simvastatin did not disrupt endothelial cell-cell junctions or the endothelial monolayer (Supplementary Figure 2.2E), indicating that at this concentration statins are unlikely to alter endothelial integrity.

Time-lapse movies were performed in order to visualize the effect of statins on T-ALL cell morphology and migration on endothelial cells. Most control CCRF-CEM cells had a polarized migratory morphology, with a lamellipodium at the front and uropod at the back (Sanchez-Madrid and Serrador, 2009), and migrated across the endothelial monolayer (Figure 2.6D, top panels). Cells treated with 1 μM simvastatin had a more rounded phenotype and were not polarized (Figure 2.6D, middle panels). Some statin-treated cells transiently extended protrusions in different directions but without forming a stable lamellipodium or uropod (Figures 2.6D and E). These effects were reversed by co-incubation with mevalonic acid (Figure 2.6D, lower panels). Tracking of statin-treated cells showed that they had a reduced migration speed on the endothelial surface compared to controls (Figure 2.6F). These data indicate that statins reduce TEM both by reducing adhesion of T-ALL cells to ICAM-1 and inhibiting their migration on endothelial cells.

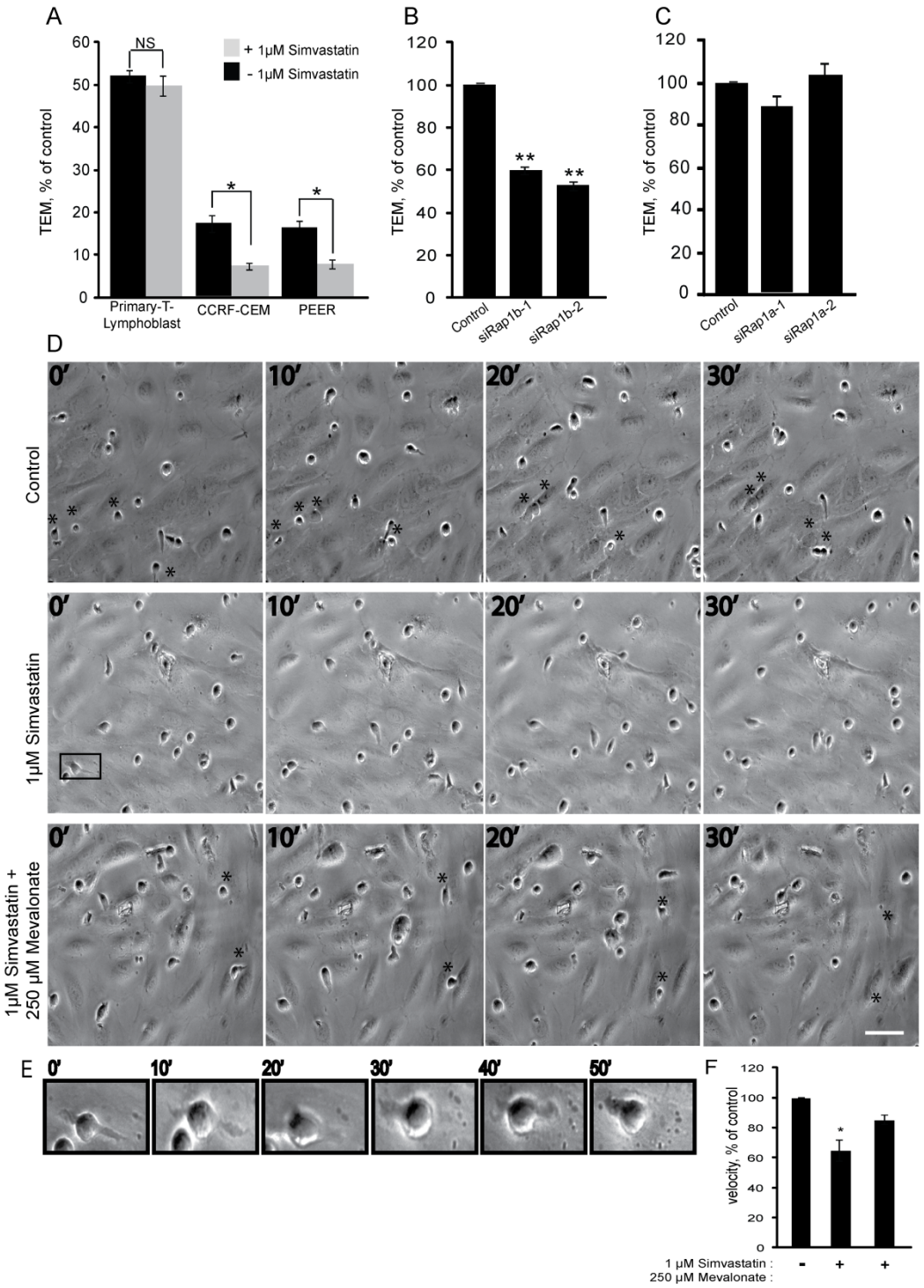

Figure 2.6. Statin treatment and Rap1b downregulation reduce transendothelial migration of T-ALL cells. Primary T-lymphoblasts, CCRF-CEM cells and PEER cells were treated for 16 h with 1 μM simvastatin (A) or transfected with siRNAs targeting Rap1a or Rap1b (B and C) then added to confluent HUVECs on transwell filters. After 1 h (primary-T-lymphoblasts) or 2 h (CCRF-CEM and PEER), cells that had transmigrated through the HUVECs towards SDF-1 in the lower chamber were counted. Data shown are mean of 3 independent experiments ± SEM. *p<0.05,

**p<0.01; 2-way-paired t-test. (D) CCRF-CEM cells treated with 1 μM simvastatin with or without 250 μM mevalonic acid for 16 h were added to HUVECs and imaged by timelapse microscopy. Images show cells at 0, 10, 20 and 30 min; asterisks (top panels) indicate examples of CCRF-CEM cells undergoing transendothelial migration. Bar, 50 μm. (E) Zoom of a representative cell treated with 1 μM simvastatin (boxed region in D), showing extension of protrusions in different directions. (F) Relative velocity of CCRF-CEM cells on HUVECs, compared to control. Data are from 3 independent experiments ± SEM. *p<0.05; 2-way-paired t-test. *Experiments performed by Elvira Infante.*

2.5 Discussion

A critical step in T-ALL progression is the accumulation of leukaemic cells in the tissues, which requires adhesion to and transmigration through the endothelium. Here we demonstrate that both statins and a geranylgeranyl transferase inhibitor reduce of T-ALL cell adhesion, LFA-1 integrin activation, migration and TEM, indicating that the effects of statins are due to reduced protein prenylation rather than cholesterol depletion. Our results suggest these responses are predominantly due to inhibition of Rap1b, since depletion of Rap1b but not its closely related isoform Rap1a has similar effects to statins on T-ALL cell adhesion and migration.

The relative contributions of the two Rap1 isoforms, Rap1a and Rap1b, to integrin activation have not been investigated previously. Studies with Rap1a- and Rap1b-null mice indicate that each isoform affects integrin-mediated leukocyte adhesion, although the two isoforms have not been compared directly. For example, primary hematopoietic cells isolated from Rap1a-null mice have reduced adhesion to FN but just a slight decrease of adhesion to ICAM-1 (Duchniewicz et al., 2006), while B cells from Rap1b-null mice have reduced ICAM-1 adhesion and chemotaxis (Chu et al., 2008).

Rap1 stimulates integrin activation through its target Riam, which in turn regulates talin interaction with integrins (Banno and Ginsberg, 2008; Frische and Zwartkruis, 2010). In addition, in T cells the Rap1 target RAPL interacts with and regulates the spatial distribution of LFA-1 (Katagiri et al., 2003; Mor et al., 2007). Rap1a and Rap1b differ by only 8 amino acids, most of which are close to the C-terminus (Lee et al., 2009; Raaijmakers and Bos, 2009). Our results indicate that Rap1b is specifically required for T-ALL cell adhesion to ICAM-1 whereas both isoforms contribute to adhesion to FN. This suggests that the interacting partners and/or localization of Rap1a and Rap1b could be different.

It is interesting that Rac1, Rac2 and RhoA were not required for T-ALL adhesion to ICAM-1, since there is evidence that they and/or specific RhoGEFs regulate ICAM-1 adhesion in response to chemokines or B/T cell receptor engagement (Tybulewicz and Henderson, 2009). The signal transduction pathways leading from Rac and Rho to integrin activation are not clear, in contrast to the well-characterized mechanisms linking Rap1 to integrins. It is thus possible that Rho GTPase involvement in adhesion is indirect and due to their effects on cytoskeletal dynamics. However,

depletion of Rac and Rho proteins clearly affects T-cell behavior: we have recently shown that RhoA and Rac2 are required in CCRF-CEM cells for transendothelial migration, and that RhoA depletion dramatically alters T-cell morphology and reduces migration on endothelial cells (Heasman et al., 2010).

The increase in GTP-bound Rap1 and Rho GTPases in statin- and GGTI-treated cells is presumably due to altered localization of the unprenylated proteins. Since GTP levels are higher than GDP levels in cells, we predict that GTPase proteins are initially loaded with GTP when they are synthesized. If GTPases are unable to be prenylated and hence are mislocalized then it is unlikely they will encounter GAPs and thus they will remain GTP-loaded (Spilker and Kreutz, 2010). However, they also will not interact efficiently with their downstream targets when unprenylated and thus their downstream signaling will be inhibited, despite being GTP-loaded (Satoh et al., 2001; Wang et al., 2008).

Simvastatin and lovastatin are often used at 10 μM or higher concentrations in experiments in vitro (Schiefelbein et al., 2008; Zhang et al., 2008), although they can increase RhoA-GTP levels at 1 μM (Cordle et al., 2005). Plasma levels of lovastatin were reported to be between 200-250 nM, 6 h after administration of 160 or 200 mg of lovastatin to human acute myeloid leukaemia (AML) patients (Lewis et al., 2005). Thus statin levels of 1 μM could be present at earlier timepoints, but 10 μM is likely to be much higher than most leukaemia cells in the blood would be exposed to for any significant time in vivo. Statins at 10 μM have been reported to reduce AML cell viability in vitro (Sassano et al., 2007), but in our experiments 1 μM statin did not affect the viability of primary T-lymphoblasts or T-ALL cells. Furthermore, 1 μM statin did not affect T-lymphoblast adhesion to ICAM-1 or migration but did inhibit T-ALL responses, suggesting that it may be possible to inhibit T-ALL recruitment to tissues selectively without affecting primary T cells. Interestingly, we found that the active form of Rap1 and the levels of Rap1a and Rap1b protein are higher in primary T-lymphoblasts than CCRF-CEM and Jurkat cells, and that Rap1 was only activated by 10 μM statin but not 1 μM statin in T-lymphoblasts. This might explain why statins are less effective at inhibiting primary T-lymphoblast adhesion to ICAM-1.

In conclusion, our data indicate that Rap1b is the main Rap1 isoform required for adhesion to ICAM-1, chemotaxis and TEM of T-ALL cell lines. Our results suggest that statins, GGTIs or other inhibitors of Rap1b signalling could be potential therapies to reduce invasion and metastasis in T-ALL.

2.6 Supplementary materials

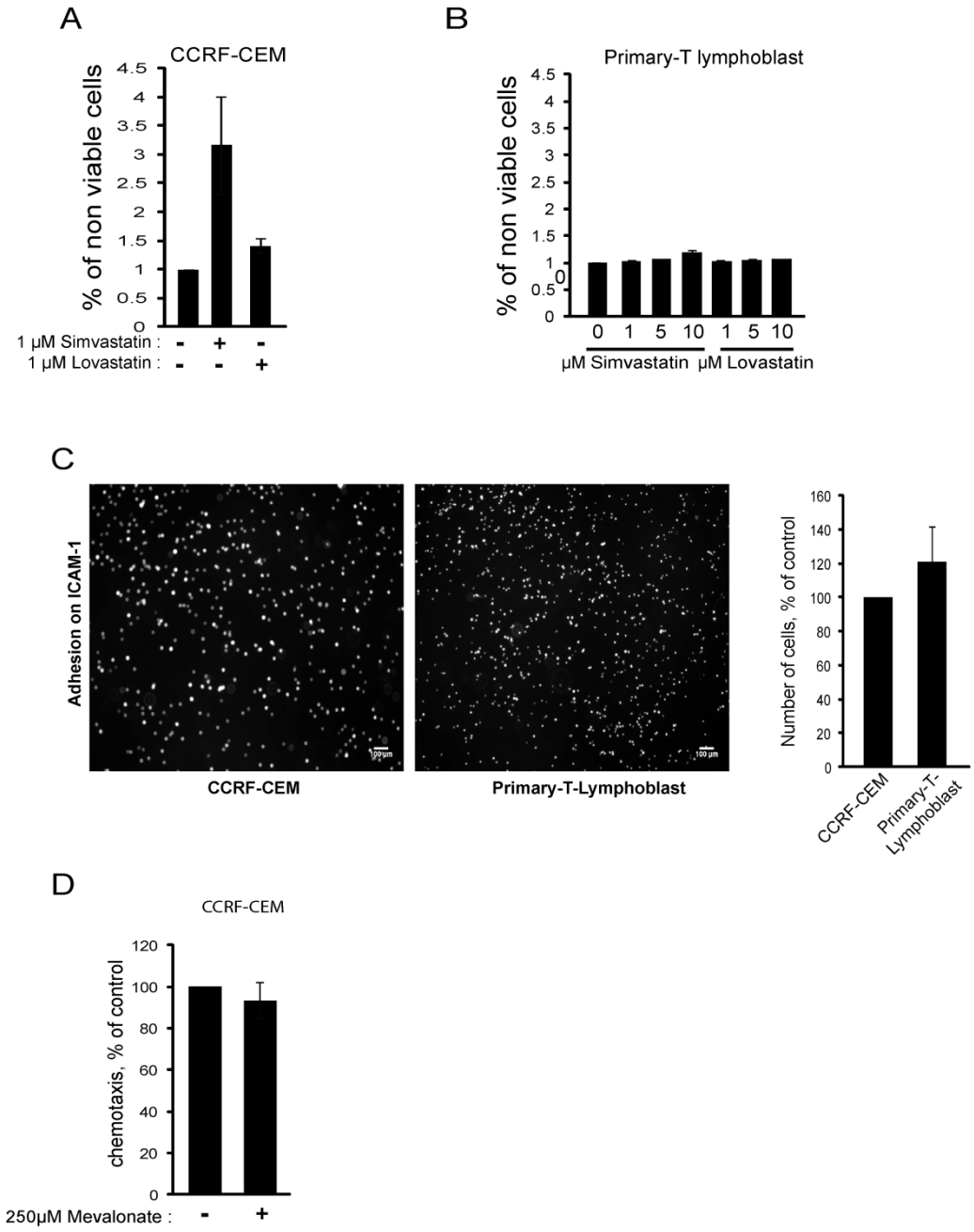

Supplementary Figure 1.1. CCRF-CEM cells (A) or primary-T-lymphobasts (B) were treated for 16 h with the indicated concentrations of simvastatin or lovastatin. Cell viability was determined with Trypan blue. (C) CCRF-CEM cells and primary T-lymphoblasts were labeled with Cell Tracker CMFDA and added to ICAM-1-coated wells for 30 min. Adherent cells were counted from images acquired by epifluorescence microscopy. Bars, 100 µm. (D) CCRF-CEM cells were treated with 250 µM mevalonic acid for 16 h. Cells were then added to ICAM-1-coated transwells containing 30 ng/ml SDF-1 in the lower chamber. Cells in the lower chamber were counted after 1 h. *Experiments performed by Elvira Infante.*

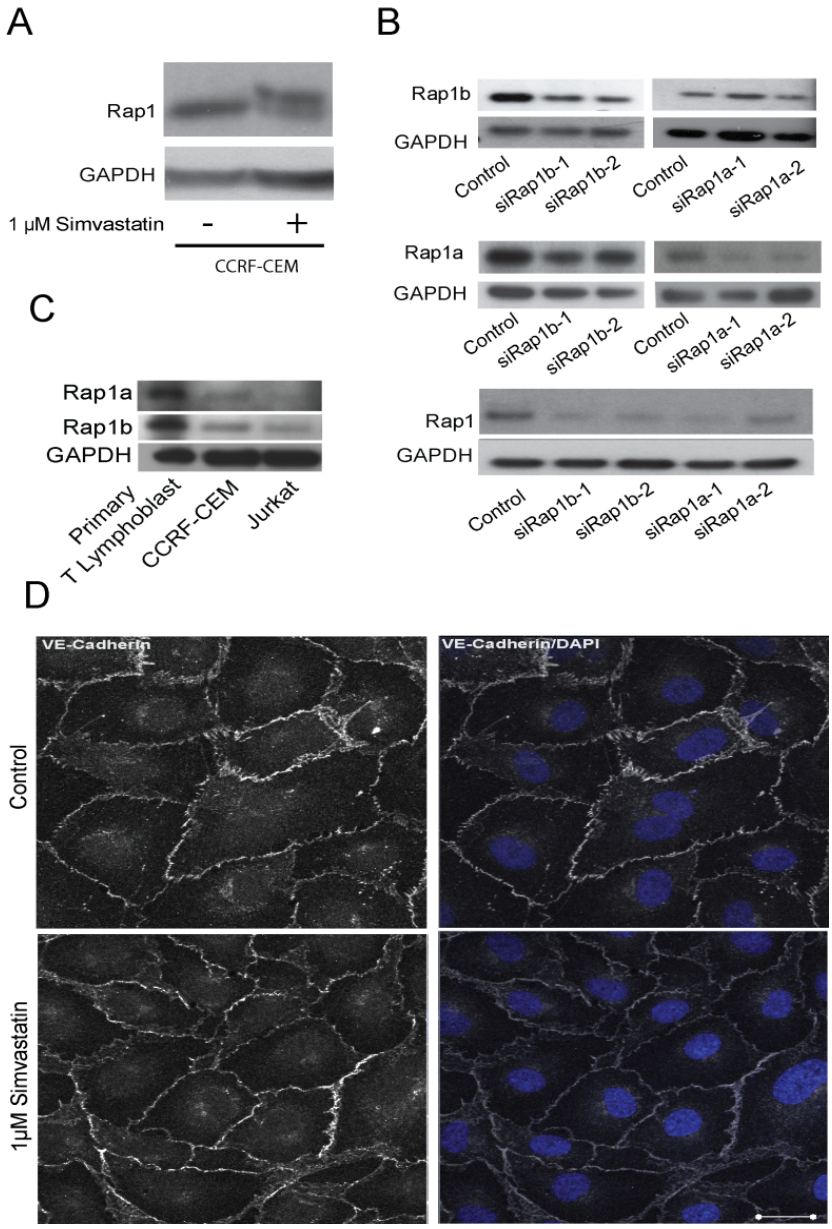

Supplementary Figure 1.2. (A) CCRF-CEM cells were treated for 16 h with 1 μM simvastatin. Cell lysates were separated on a 12.5% polyacrylamide gel and analysed by western blotting using Rap1 antibody. (B) CCRF-CEM cells were transfected with the indicated siRNAs. After 72 h, cell lysates were prepared and western blotted with antibodies to Rap1a, Rap1b or total Rap1 (lower panel: antibody recognizes Rap1a and Rap1b). (C) Rap1a and Rap1b expression in T-lymphoblasts, CCRF-CEM and Jurkat cell lysates was analysed by western blotting. GAPDH was used as a loading control. Blots shown are representative of 3 independent experiments. (D) HUVECs were treated for 16 h with 1 μM simvastatin. Cells were stained with anti-VE-cadherin antibody and DAPI to stain nuclei and analysed by confocal microscopy. Bar, 20 μm. *Experiments performed by Elvira Infante.*

3

Analysis of Rho GTPase expression in T-ALL identifies RhoU as a target for Notch involved in T-ALL cell migration

Parag J. Bhavsar[1,*] Elvira Infante[1,2,*], Asim Khwaja[3] and Anne J. Ridley[1]

[1]Randall Division of Cell and Molecular Biophysics, King's College London, New Hunt's House, Guy's Campus, London SE1 1UL, UK
[2]National Institute for Health Research (NIHR), Biomedical Research Centre, Guy's and St Thomas' NHS and King's College London, London, UK
[3]UCL Cancer Institute, University College London, London, UK
[*]These authors contributed equally to this work.

Oncogene

Received 14 August 2011;
Revised 6 January 2012;
Accepted 6 January 2012
DOI: 10.1038/onc.2012.42

AUTHORSHIP

P.J.B and E.I. prepared figures and wrote the manuscript. A.K. provided cell lines and edited the manuscript. A.J.R. planned experiments and wrote the manuscript

3.1 Abstract

NOTCH1 is frequently mutated in T-cell acute lymphoblastic leukaemia (T-ALL), and can stimulate T-ALL cell survival and proliferation. Here we explore the hypothesis that Notch1 also alters T-ALL cell migration. Rho GTPases are well-known to regulate cell adhesion and migration. We have analysed the expression levels of Rho GTPases in primary T-ALL samples compared to normal T cells by quantitative PCR. We found that 5 of the 20 human Rho genes are highly and consistently upregulated in T-ALL, and 3 further Rho genes are expressed in T-ALL but not detectably in normal T cells. Of these, *RHOU* expression is highly correlated with the expression of the Notch1 target *DELTEX-1*. Inhibition of Notch1 signalling with a γ-secretase inhibitor (GSI) or Notch1 RNAi reduces RhoU expression in T-ALL cells, whereas constitutively active Notch1 increased RhoU expression. In addition, Notch1 or RhoU depletion, or GSI treatment, inhibits T-ALL cell adhesion, migration and chemotaxis. These results indicate that NOTCH1 mutation stimulates T-ALL cell migration through RhoU upregulation which could contribute to the leukaemia cell dissemination.

3.2 Introduction

T-cell acute lymphoblastic leukaemia (T-ALL) is a common cancer in children. T-ALL patients usually present with large numbers of leukaemic blasts with an immature T-cell phenotype in the bone marrow and peripheral blood. Although current ALL treatment protocols have success rate of around 70 to 80% five-year event-free survival in children, T-ALL is associated with a poorer prognosis than B-ALL (Pieters and Carroll, 2010). Leukaemic blasts can infiltrate numerous tissues, with the central nervous system (CNS) being a frequent site of metastasis (Aifantis et al., 2008; Crazzolara et al., 2001). CNS relapse in T-ALL requires more aggressive treatment regimens that can lead to secondary malignancies or neurocognitive disorders(Bhojwani et al., 2009). A better understanding of the genes involved in the pathogenesis of T-ALL could allow the development of T-ALL therapies that have fewer negative effects on long-term patient health.

Among the genetic alterations that are associated with the development of T-ALL, mutation of the NOTCH1 oncogene is one of the most common, being present in over 50% of cases (van Grotel et al., 2008; Weng et al., 2004). Notch1 is required for T lineage commitment and regulates T cell maturation in the thymus (Hayday and Pennington, 2007; Vicente et al., 2010). Notch1 recognises ligands of the Delta and Serrate/Jagged families expressed in the thymic stroma. Ligand binding induces two sequential proteolytic cleavage events. The first cleaves a large portion of the ectodomain, exposing a site recognised by the intramembrane γ-secretase proteolytic complex (GS). Cleavage by GS releases the Notch1 intracellular domain (NICD), which enters the nucleus where it associates with the DNA-binding protein CSL (CBF1/Su(H)/Lag1) and other proteins to regulate transcription of a wide range of genes, including *DELTEX-1* and *HES1* (Aster et al., 2011). NOTCH1 mutations found in T-ALL commonly lead to constitutive Notch1 signalling via ligand-independent NICD production, or enhanced NICD half-life (Ferrando, 2009). Constitutive Notch1 signalling promotes leukaemic cell survival and proliferation. Notch1 also regulates expression of the chemokine receptor CCR7, which contributes to CNS metastasis in T-ALL (Buonamici et al., 2009), but whether Notch1 signalling affects other genes that regulate cell motility has not been investigated.

Rho family GTPases control haematopoietic cell morphology, migration and adhesion as well as cell proliferation and differentiation (Tybulewicz and Henderson, 2009; Van Hennik and Hordijk, 2005). Most Rho GTPases are active when bound to GTP, and inactivated when the bound GTP is hydrolysed to GDP. Signalling through Rho GTPases is therefore controlled by regulatory proteins that modulate GTP binding and hydrolysis, including guanine nucleotide exchange factors (GEFs) and GTPase-activating proteins (GAPs). Twenty Rho family members have been identified in humans, several of which have atypical properties (Boureux et al., 2007). Rnd1, Rnd2, Rnd3 and RhoH have amino acid substitutions that prevent GTPase catalytic activity, and therefore only exist in a GTP-bound state. RhoBTB1 and RhoBTB2 are much larger than other Rho GTPases, and appear not to bind or hydrolyse GTP (Aspenstrom et al., 2007; Chang et al., 2006). RhoU and RhoV are also considered atypical because they have high intrinsic GDP/GTP exchange rates and therefore are likely to be predominantly in the GTP-bound state (Aspenstrom et al., 2007). Rho proteins act through their downstream effectors to regulate cytoskeletal and adhesion dynamics, and thereby contribute to cell migration. Altered expression of Rho genes or activation of Rho proteins has been reported in a variety of cancer types, and the *RhoH* gene is mutated in some lymphomas (Ellenbroek and Collard, 2007; Vega and Ridley, 2008). Rho proteins contribute to the enhanced migration and invasion of cancer cells (Parri and Chiarugi, 2010; Symons and Segall, 2009; Vega and Ridley, 2008).

In this study, we have investigated the hypothesis that the pathogenesis of T-ALL involves the altered expression of Rho family genes. We have investigated the mRNA expression of human Rho genes in primary T-ALL leukaemic blast samples and compared it to the expression in normal peripheral blood T cells. We have found that several Rho genes have significantly increased expression in T-ALL, and in particular shown that RhoU expression is regulated by Notch1 signalling.

3.3 Materials & Methods

3.3.1 T-ALL patient samples and normal T-lymphocyte isolation

The primary childhood leukaemia samples used in this study were provided by the Leukaemia and Lymphoma Research Childhood Leukaemia Cell Bank (UK), in accordance with the requirements of the Childhood Cancer and Leukaemia Group (CCLG) and the Cell Bank Steering Committee. Frozen samples (mononuclear bone marrow cells or peripheral blood) obtained from 30 T-ALL patients at diagnosis were used. T-ALL samples are generally accepted to be more than 90% leukaemic blasts. T-lymphocytes were isolated from buffy coats of 5 healthy blood donors. Mononuclear cells were separated by density gradient according to the manufacturer's protocol (Lymphoprep, Axis-Shield). Cells were then treated with 0.5% phytohaemagglutinin (Sigma-Aldrich, Dorset, UK) in RPMI medium (Invitrogen, Paisley, UK) containing 10% foetal calf serum for 48 h, followed by culture for 10 days in 10 U/ml human IL-2 (Roche Diagnostics, Burgess Hill, UK). The T-lymphocyte populations obtained were >90% pure, defined by CD4+ or CD8+ single positive populations measured by flow cytometry with anti-CD4 and anti-CD8 antibodies (BD Bioscences, Oxford, UK).

3.3.2 Cell culture and GSI treatment

CCRF-CEM cells were purchased from ATCC (LGL Promochem, Middlesex, UK). PEER, SUPT1, MOLT16 and LOUCY T-ALL cell lines (see Figure 1.5) were from the German Collection of Microorganisms and Cell Cultures (DSMZ, Braunschweig, Germany). Cell lines were cultured in Dulbeco's RPMI containing 2 mM glutamine and supplemented with 10% fetal calf serum, 1 mM sodium pyruvate, 10 mM Hepes, penicillin (100 U/ml) and streptomycin (100 μg/ml). COS7 cells were grown in DMEM containing 10% fetal calf serum, penicillin (100 U/ml) and streptomycin (100 μg/ml). GSI (Compound E, Calbiochem, Nottingham, UK) was solubilised in dimethylsulphoxide (DMSO). Cell lines were resuspended in medium containing 100 nM GSI or an equal volume of DMSO and cultured for the indicated times. For 7 day treatments, cells were re-treated at a lower cell density in fresh GSI-containing medium after 3 or 4 days.

3.3.3 Transfection

CCRF-CEM cells (5 x 10^5) were transfected by nucleofection (Amaxa Biosystems Nucleofection System) with 1.2 µM siRNA (Sigma-Aldrich) in 100 µl of Nucleofection reagent (kit C, Lonza Biologics, Slough, UK). siRNA sequences were RhoU-1: CAGAGAAGAUGUCAAAGUC; RhoU-2: AAGCAGGACUCCAGAUAAAUU; Notch1-1: GAACGGGGCUAACAAAGAU; Notch1-2: GCAAGGACCACUUCAGCGA. siControl was from Thermo Fisher Scientific (D-001810-02-20, Lafayette, USA). Cells were used for experiments 48 to 72 h after siRNA transfection.

pcDNA3 encoding HIS-tagged Notch1 intracellular domain (NICD) or vector alone (see 4.2.2.6, 4.2.2.7 and 4.2.2.8) was transfected into COS7 cells by electroporation. Cells were detached from the plate and washed twice in electroporation buffer (10 mM KCl, 10 mM K_2PO_4/$KHPO_4$ pH 7.6, 25 mM Hepes pH 7.6, 2 mM $MgCl_2$, 0.5% Ficoll 400). After resuspending in 250 µl of electroporation buffer cells were mixed with 5 µg DNA in a 0.4 cm electroporation cuvette and left on ice for 10 min. Samples were then electroporated at 250 V, 975 µF and left again on ice for 5 min and at room temperature for other 5 min. Cells were finally plated in 10 cm dish and incubated for 24 h at 37°C. After 48 h, cells were solubilised in protein sample buffer, and protein expression was analysed by immunoblotting.

3.3.4 Sample preparation and real-time SYBR-Green PCR

RNA from T-ALL samples and control T-lymphocytes was extracted by the Trizol method (Invitrogen), and treated with DNase (RNase-free, Ambion) to remove genomic DNA. RNA concentration was determined, and purity was checked by measuring the A260/A280 ratio. cDNA was prepared from identical amounts of RNA template with Superscript VILO cDNA synthesis kit (Invitrogen).

Relative mRNA expression of Rho genes was determined by real-time polymerase chain reaction (RT-PCR) assays, using SYBR-Green detection chemistry (PCR mastermix from Primer Design, Southampton, UK) and the ABI Prism 7000 Sequence Detection System (Applied Biosystems). Primers used for each gene are shown in Supplementary Table 1. Wherever possible, primers were designed either

across different exons or across exon-exon boundaries to avoid detection of genomic sequences. Each gene assay was validated for amplification efficiency between 90 and 110% by serial template dilutions, and for specificity by melting curve analysis and agarose gel electrophoresis. The expression analysis for each gene was carried out in a 96 well format, comparing all 5 control samples to batches of 6 or 7 T-ALL samples, and for each sample assaying a Rho gene in parallel with GAPDH as a reference. CT values of controls could therefore be used to correct for plate-to-plate variations (see 4.2.2.10, 4.2.2.11 and 4.2.2.12).

3.3.5 Statistical analyses

For T-ALL-associated expression changes, mean CT values for each sample were first normalised to GAPDH CT values (expressed as dCT). Differential gene expression between control and T-ALL samples was determined by the Mann-Whitney *U* test for medians of dCT values. For clustering analyses, the comparative CT method (Schmittgen and Livak, 2008) (using the average CT of the controls) was used to determine relative fold expression changes for Rho genes in each T-ALL sample. Cluster analysis software (Cluster 3.0) (de Hoon et al., 2004) and Java Treeview (Saldanha, 2004) were used to generate a heat-map of the fold changes as well as carry out unsupervised hierarchical clustering of genes and T-ALL samples. Complete linkage clustering algorithm was applied, using Pearson correlation as the similarity metric. Characteristics of grouped or clustered T-ALL patients were compared by Mann-Whitney *U* test for medians or the Fisher's Exact test for associations, in two-tailed tests and considered significant if $P < 0.05$. Statistical tests were carried out using Graphpad Prism 5 software.

3.3.6 Immunoblotting

Cells were lysed directly in 4X sample buffer (see 2.3.9) and immediately heated to at least 90°C for 10 min. Proteins were resolved by polyacrylamide gel electrophoresis, transferred to PVDF membrane, and detected by immunoblotting. The following antibodies were used: Cleaved Notch1 intracellular domain (Val1744,

Cell Signaling, Hitchin, UK), RhoU (Wrch1 ab80315, Abcam, Cambridge, UK), ß-tubulin (Sigma-Aldrich), HIS-tag (Cell Signaling), GAPDH and Rac2 (Millipore).

3.3.7 Immunofluorescence

Glass coverslips were coated with 10 µg/ml fibronectin at 4°C overnight and blocked in 2.5% BSA in phosphate-buffered saline (PBS) for 1 h. $2x10^5$ cells were added to each coverslip and incubated at 37°C with 1ng/ml of CXCL12 (R&D Systems, Abingdon, UK) for 30 min. Subsequently, samples were fixed with 4% paraformaldehyde and permeabilized in 0.1% Triton-X-100. Following 2 washes in PBS cells were incubated with Alexa Fluor 546 phalloidin (A22283, Invitrogen) and FITC-labeled anti-α-tubulin antibody (Sigma) for 1 h. Coverslips were mounted onto glass slides using Dako (Ely, UK) anti-fade mounting medium. Images were acquired using a Zeiss LSM500 confocal microscope (Zeiss). F-actin content was measured using ImageJ software. Each experimental condition was done with triplicate coverslips, counting 100 cells on each. Data was pooled from three independent experiments. Polarized cells were defined as having F-actin localized to one side of the cell, defined as the leading edge, and the microtubule organizing center (MTOC) localized at the other side of the nucleus with respect to the leading edge. Elongated tails on cells were defined as a narrow protrusion at the opposite side to the leading edge, at least the length of the cell body.

3.3.8 Time-lapse microscopy

The siRNA-transfected or DMSO/GSI-treated CCRF-CEM cells were counted (Innovatis CASY cell counter, Roche Applied Bioscience, Burgess Hill, UK), and 2×10^5 were added to each well of a fibronectin-coated 8-well culture slides (BD Falcon, Oxford, UK). After 30 min, wells were washed three times with complete culture medium to remove loosely attached and non-viable cells, and then stimulated with 1 ng/ml of CXCL12. Bright field phase-contrast images were collected every minute for 1 h on a Nikon Eclipse TE2000 microscope with a charge-coupled

device camera (ORCA, Hamamatsu Photonics, Welwyn Garden City, UK) using Metamorph software (Cairn Research, Faversham, UK). Cells were tracked, and velocities and distance migrated calculated using ImageJ.

3.3.9 Adhesion assay

The 96-well plates were coated overnight at 4°C with 10 μg/ml fibronectin. Cells were resuspended in PBS at 10^6 cells per ml and incubated at 37 °C for 15 min with 2 μM CellTracker Green CMFDA (Invitrogen). Cells were then resuspended in warm media and 105 cells per well (each sample in triplicate) were incubated at 37°C for 30 min. After washes with PBS, the plate was read on a Fusion-αFP plate reader (PerkinElmer, Cambridge, UK) at 485 nm excitation and 525–535 nm emission.

3.3.10 Flow cytometry

T-ALL cells (2×10^5) were centrifuged and washed with PBS. Cells were fixed at room temperature for 10 min with 4% paraformaldehyde and permeabilized with 0.1% Triton X-100. Samples were then incubated with 0.2 μg/ml Alexa 488-labelled phalloidin and analysed on a Becton Dickinson FACS Calibur machine (Oxford, UK) using FlowJo program (Ashland, OR, USA).

3.4 Results

3.4.1 Atypical Rho genes are upregulated in T-ALL

To study Rho GTPase involvement in the pathogenesis of T-ALL we investigated Rho gene expression in 30 primary T-ALL blast samples compared to mature T cells from 5 healthy blood donors. Expression of each Rho gene mRNA was determined by quantitative PCR, using *glyceraldehyde-3-phosphate dehydrogenase* (GAPDH) as a reference gene (Suppl Fig. 3.1). Rho mRNA expression for each T-ALL sample was quantified relative to the mean of the control samples (Fig. 3.1A, Table 1). To determine which of the genes were differentially expressed to a statistically significant degree, a Mann-Whitney test was applied (Table 1), considering the median to be the best representation of the data, which in many cases were skewed and not normally distributed (Fig. 3.1A). Five Rho genes were significantly upregulated in the T-ALL samples: *RHOH, RHOBTB1, RHOA, RHOB* and *RHOU*. *RHOA* and *RHOH* were very consistently increased in nearly all the T-ALL samples although the median fold upregulation was quite small. The magnitude of *RHOBTB1*, *RHOB* and *RHOU* upregulation was much higher, but with more variation across the T-ALL samples (Fig. 3.1A, Table 1). Three genes were not detectable in normal T cell samples but were detected in more than 30% of T-ALL samples: *RHOV*, *RND2* and *RND3*. We therefore could not determine the fold expression differences relative to normal T cells for these genes, however the variation in expression with T-ALL samples was analysed (Fig. 3.1B). *RHOD* was not expressed in normal T-cell or T-ALL samples, and preliminary analysis indicated that *RHOJ* is also not expressed (data not shown), in agreement with our published data on normal T cells and the CCRF-CEM T-ALL cell line (Heasman et al., 2010). Interestingly, 5 of the 8 differentially expressed Rho genes (*RHOBTB1*, *RHOU*, *RHOV*, *RND2* and *RND3*) belonged to the atypical sub-class (Aspenstrom et al., 2007), which was therefore over-represented among the altered genes.

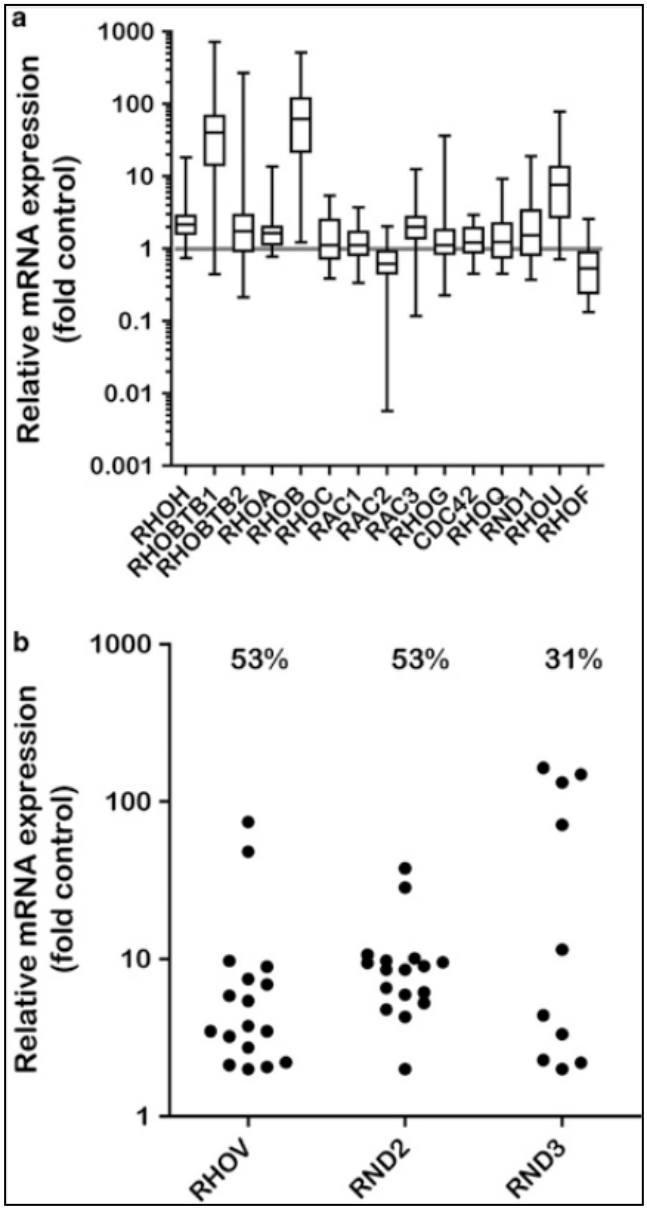

Figure 3.1 Rho mRNA expression in T-ALL. (A) RNA was extracted from 30 T-ALL blast samples and normal T lymphocytes from 5 peripheral blood samples of healthy donors. mRNA expression of each Rho gene was measured by quantitative PCR, using GAPDH expression as a reference. Rho gene expression in each T-ALL sample was determined relative to the mean expression of the normal control samples using the comparative Ct method. Data are expressed as fold expression relative to control on a logarithmic scale. (B) mRNA expression of Rho genes not detected in normal T lymphocytes. The T-ALL sample with the lowest detected mRNA expression was assigned a relative expression level of 2. Other values are shown relative to this sample. Values above each column indicate the percentage of T-ALL samples that detectably expressed each gene. *Experiments performed by Dr Parag Bhavsar*

Gene	P-value	Test summary
RHOF	0.079	NS
RHOH	0.002	**
RND1	0.113	NS
RHOBTB1	0.003	**
RHOBTB2	0.218	NS
RHOA	0.008	**
RHOB	0.001	***
RHOC	0.437	NS
RAC1	0.522	NS
RAC2	0.044	*
RAC3	0.012	*
RHOG	0.579	NS
CDC42	0.340	NS
RHOQ	0.579	NS
RHOU	0.003	**

Table 1. Rho mRNA expression in T-ALL relative to healthy controls. RNA was extracted from 30 T-ALL blast samples and normal T lymphoblasts from 5 peripheral blood samples of healthy donors. mRNA expression of each Rho gene was measured by quantitative PCR (qPCR) using glyceraldehyde 3-phosphate dehydrogenase (GAPDH) as a reference gene. GAPDH-normalized Rho expression values (dCT) were used to compare expression levels between normal and T-ALL populations using a two-tailed Mann–Whitney U-test of medians. *P<0.05, **P<0.01 and ***P<0.001. *Analysis performed by Dr Parag Bhavsar.*

3.4.2 Rho gene expression patterns cluster T-ALL patients in two groups

T-ALL samples were grouped according to similarity of Rho expression (fold expression relative to controls) using clustering algorithms. The expression values were visualized in a heat-map, with a dendrogram showing the resulting clusters of T-ALL samples (Fig. 3.2). This analysis resulted in the resolution of two major clusters of T-ALL patients (denoted clusters A and B). The upregulation of *RHOH*, *RHOBTB1*, *RHOA*, *RHOB* and *RHOU* was similar in both clusters, as expected due to the consistency of the changes in these 5 genes across all samples. The distinction between the two groups reflected the expression of genes that showed variable expression across the T-ALL samples. Cluster A was enriched in samples where the expression of several Rho genes was lower than normal controls, including *RAC1*, *RHOC*, *CDC42* and *RHOQ*, whereas cluster B had a greater incidence of higher-than-normal expression of these genes. The two Rho expression profile clusters might reflect different patient characteristics. They did not show a significant association with available patient information on age at diagnosis, white blood cell count (WBC), CNS disease and relapse incidence, but it is likely that a higher number of T-ALL samples would be required for this analysis.

In addition to the cluster analysis, the expression of each Rho gene was independently tested for association with patient information. Interestingly, the expression of *RHOQ*, *RND1* and *RHOB* was significantly correlated with WBC count (Table 2). As described above, *RHOB* is highly upregulated in the T-ALL samples. Although *RHOQ* and *RND1* expression in T-ALL was not different overall from normal controls (Fig. 3.1), this suggests that *RHOQ* and *RND1* expression are increased in a subset of patients with higher WBC. The WBC count could correlate with differences in the migratory properties of leukaemic cells.

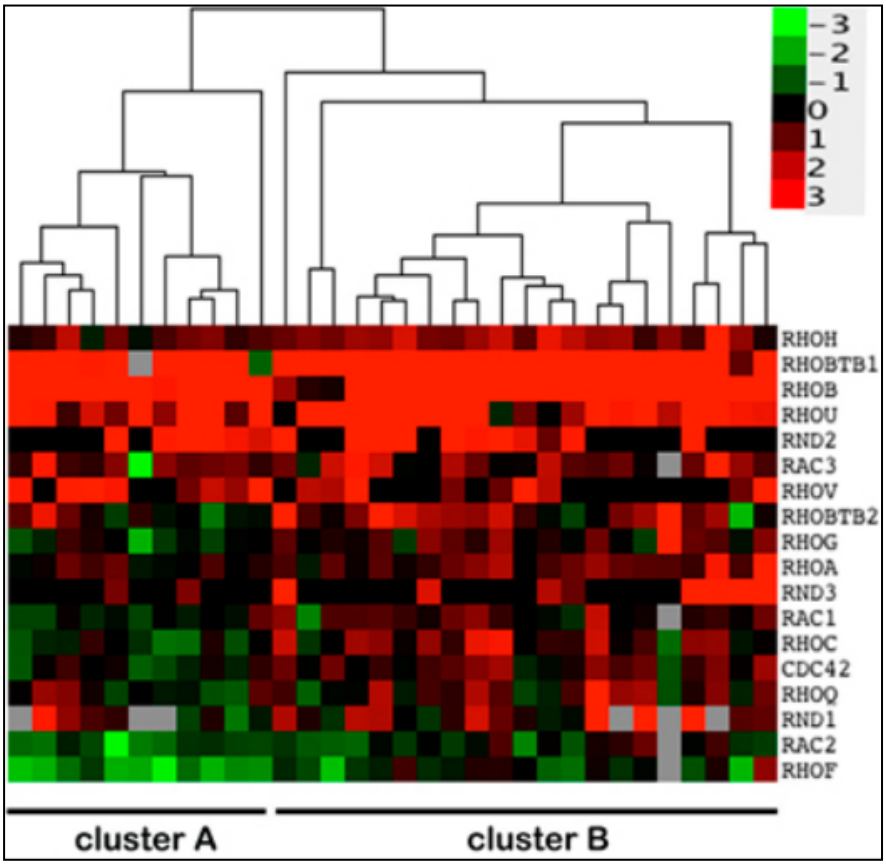

Figure 3.2 Association of Rho expression and T-ALL disease characteristics. Relative expression data for T-ALL samples were log2 transformed and an unsupervised hierarchical clustering algorithm applied (see Materials and methods). The legend indicates the magnitude and direction of expression changes relative to control T-lymphocyte samples. *Analysis performed by Dr Parag Bhavsar.*

Gene	Pearson's r	P-value	Test summary
RHOH	0.14	0.440	NS
RHOBTB1	−0.15	0.433	NS
RHOBTB2	0.11	0.551	NS
RHOA	0.04	0.838	NS
RHOC	0.25	0.172	NS
RAC1	0.24	0.195	NS
RAC2	0.33	0.069	NS
RAC3	0.25	0.178	NS
RHOG	−0.15	0.424	NS
CDC42	0.24	0.186	NS
RHOQ	0.50	0.004	**
RND1	0.40	0.050	*
RHOU	−0.02	0.912	NS
RHOF	0.16	0.405	NS
RHOB	0.48	0.006	**

Table 2. Association between relative Rho expression in T-ALL and WBC.
The fold expression values for each Rho gene were tested for correlation with WBC at diagnosis, using Pearson's correlation statistic, r. The r values can range from 1, indicating perfect correlation, to −1, indicating perfect inverse correlation. *P<0.05, **P<0.01. *Analysis performed by Dr Parag Bhavsar.*

3.4.3 *RHOU* expression correlates with Notch1 signalling in T-ALL

The *NOTCH1* gene is mutated in over 50% of T-ALL cases, leading to dysregulated Notch1 signalling (Aster et al., 2011). Mutations in other genes such as *FBXW7*, a ubiquitin ligase involved in Notch1 turnover, also contribute to constitutive Notch1 signalling in T-ALL (O'Neil et al., 2007). We therefore investigated whether the Rho gene alterations we observed in the T-ALL samples were linked to aberrant Notch1 signalling.

We used the mRNA expression levels of the Notch1 target gene *DELTEX1* as a read-out of constitutive Notch1 signalling and screened the T-ALL samples using quantitative PCR (Fig. 3.3A).

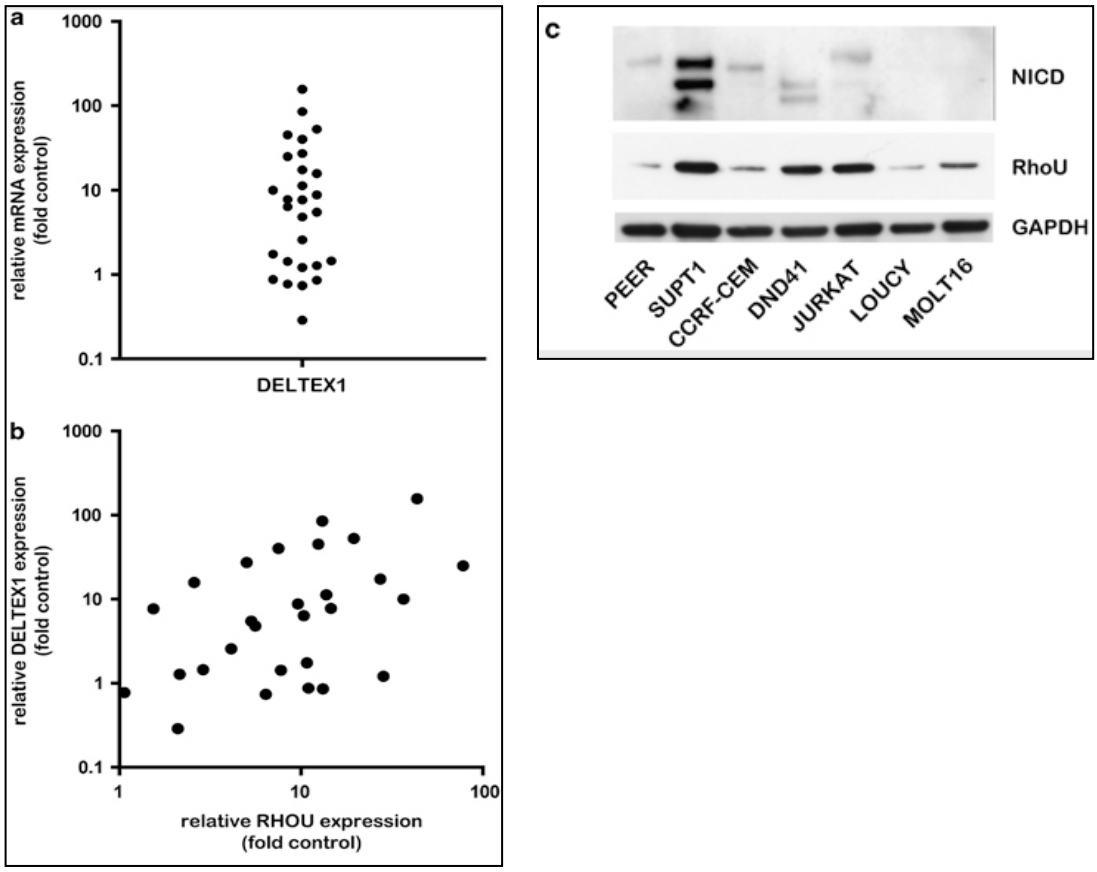

Figure 3.3 Association of RhoU expression with Notch1 signalling in T-ALL patients and cell lines. (A) *DELTEX-1* mRNA expression in T-ALL and control samples was analysed by quantitative PCR using GAPDH expression as a reference. *DELTEX-1* mRNA expression in each T-ALL sample was determined relative to the mean expression of the normal control samples using the comparative Ct method. Data are expressed as fold expression relative to controls on a logarithmic scale. (B) Scatter plot of *RHOU* and *DELTEX-1* expression in T-ALL samples. (C) Cells from a panel of T-ALL-derived cell lines in growth phase were lysed and then analysed for RhoU protein expression and cleaved Notch1 intracellular domain levels by immunoblotting. A representative blot from three independent experiments is shown *Experiments in A and B were performed by Dr Parag Bhavsar. Experiments in C were performed by Elvira Infante*

DELTEX1 transcript levels were at least two-fold higher than control T cells in 68% of samples, indicating increased Notch1 signalling. This could be due to NOTCH1 mutations or other mutations that affect Notch1 signalling.

We determined whether the relative expression levels of any of the Rho genes correlated with the expression of *DELTEX1* using a Spearman Rank test (Table 3). *RHOU* (Fig. 3.3B) and *RAC2* mRNA levels were found to be significantly associated with *DELTEX1* in T-ALL samples. Since we had identified *RHOU* as upregulated in T-ALL, we decided to investigate the relationship between *RHOU* and Notch1 signalling further.

A number of T-lymphoblastic cell lines have been derived from T-ALL patients. Several have mutations that lead to constitutive Notch1 signalling, whereas others have normal ligand-dependent Notch signaling (O'Neil et al., 2007). We used a panel of T-ALL cell lines to investigate whether there was an association between Notch1 signalling status and RhoU protein expression. In accordance with published data, we detected cleaved Notch1 in PEER, SUPT1, CCRF-CEM, DND41 and Jurkat lines but not in LOUCY and MOLT16 lines, which do not have Notch1 mutations (Fig. 3.3C) (O'Neil et al., 2007). The different sizes of NICD detected in the cell lines reflect different sites of mutation in Notch1 and/or FBW7, a ubiquitin ligase involved in Notch1 degradation (O'Neil et al., 2007). RhoU protein was expressed in all the cell lines, indicating that RhoU expression is not strictly dependent on oncogenic Notch1 activation. However, it was highest in SUPT1, DND41 and JURKAT cells, which have cleaved Notch1.

Gene	*Spearman's r*	*P-value*	*Test summary*
RHOH	0.02	0.925	NS
RHOBTB1	0.20	0.324	NS
RHOBTB2	0.30	0.122	NS
RHOA	0.26	0.175	NS
RHOC	0.21	0.287	NS
RAC1	0.24	0.220	NS
RAC2	0.46	0.014	*
RAC3	0.00	0.980	NS
RHOG	0.29	0.137	NS
CDC42	0.34	0.073	NS
RHOQ	0.29	0.137	NS
RND1	0.25	0.260	NS
RHOU	0.45	0.016	*
RHOF	0.27	0.163	NS
RHOV	−0.31	0.111	NS
RND2	−0.15	0.443	NS
RND3	0.10	0.605	NS

Table 3. Association between relative Rho gene expression and DELTEX-1 levels in T-ALL. DELTEX-1 mRNA expression was analysed by quantitative PCR, and glyceraldehyde 3-phosphate dehydrogenase (GAPDH)-normalized dCT values were used to test for correlation between Rho gene and DELTEX-1 expression using Spearman's rank correlation test. *P<0.05. *Analysis performed by Dr Parag Bhavsar.*

3.4.4 RhoU expression is regulated by Notch1 signalling

To determine if RhoU expression is influenced by Notch1 signalling, we first utilized the γ-secretase inhibitor (GSI) compound E to block the generation of NICD (Palomero et al., 2006; Palomero et al., 2007). T-ALL cell lines with activating Notch1 mutations (CCRF-CEM, SUPT1 and PEER) and lines with wild-type Notch1 (LOUCY and MOLT16) were treated with GSI or DMSO (vehicle control) for three and seven days to allow time for gene expression changes to occur. *RHOU* mRNA levels in response to the treatment were determined by qPCR (Fig. 3.4A). *DELTEX1* mRNA levels were quantified to confirm Notch1 signalling inhibition, and *CDC42* mRNA was used as an additional control since its expression was not correlated with *DELTEX1* (Table 3). As expected, GSI treatment led to a dramatic reduction in the levels of *DELTEX1* mRNA in all three NOTCH1 mutant lines. GSI treatment resulted in a reduction of *RHOU* mRNA in these T-ALL lines, whereas *CDC42* was unaffected (Fig. 3.4A). In contrast, in the NOTCH1 wild-type lines, *RHOU* expression was unaffected by GSI treatment. We could not detect *DELTEX1* mRNA well enough for quantification in LOUCY and MOLT16 lines, consistent with the absence of constitutive Notch1 signalling (Fig. 3.4A).

We next analyzed the dependence of RhoU protein expression on Notch1 signalling. GSI treatment resulted in a reduction of NICD levels at three and seven days of treatment in the three NOTCH1 mutant lines, showing that the GSI treatment was inhibiting Notch1 cleavage. There was a progressive reduction in RhoU protein with GSI treatment in these lines (Fig. 3.4B), whereas Rac2 levels were not affected (Suppl Fig. 3.2A). In contrast, RhoU protein levels in the lines with wild-type NOTCH1 (LOUCY, MOLT16) were unaffected by GSI treatment. As expected, NICD was not detected in these lines (Fig. 3.4B).

γ-secretase cleaves a number of proteins in addition to Notch1 (Wolfe, 2009), and thus we tested whether the effects of GSI on RhoU were also observed with direct Notch1 inhibition. Two different Notch1 siRNAs strongly reduced RhoU protein levels in CCRF-CEM cells (Fig. 3.4C). To determine whether Notch1 signalling alone could induce RhoU expression, the NICD was expressed in COS7 cells. NICD expression led to an increase in RhoU protein levels (Fig. 3.4D). Together, these data show that Notch1 signalling positively regulates the expression of RhoU.

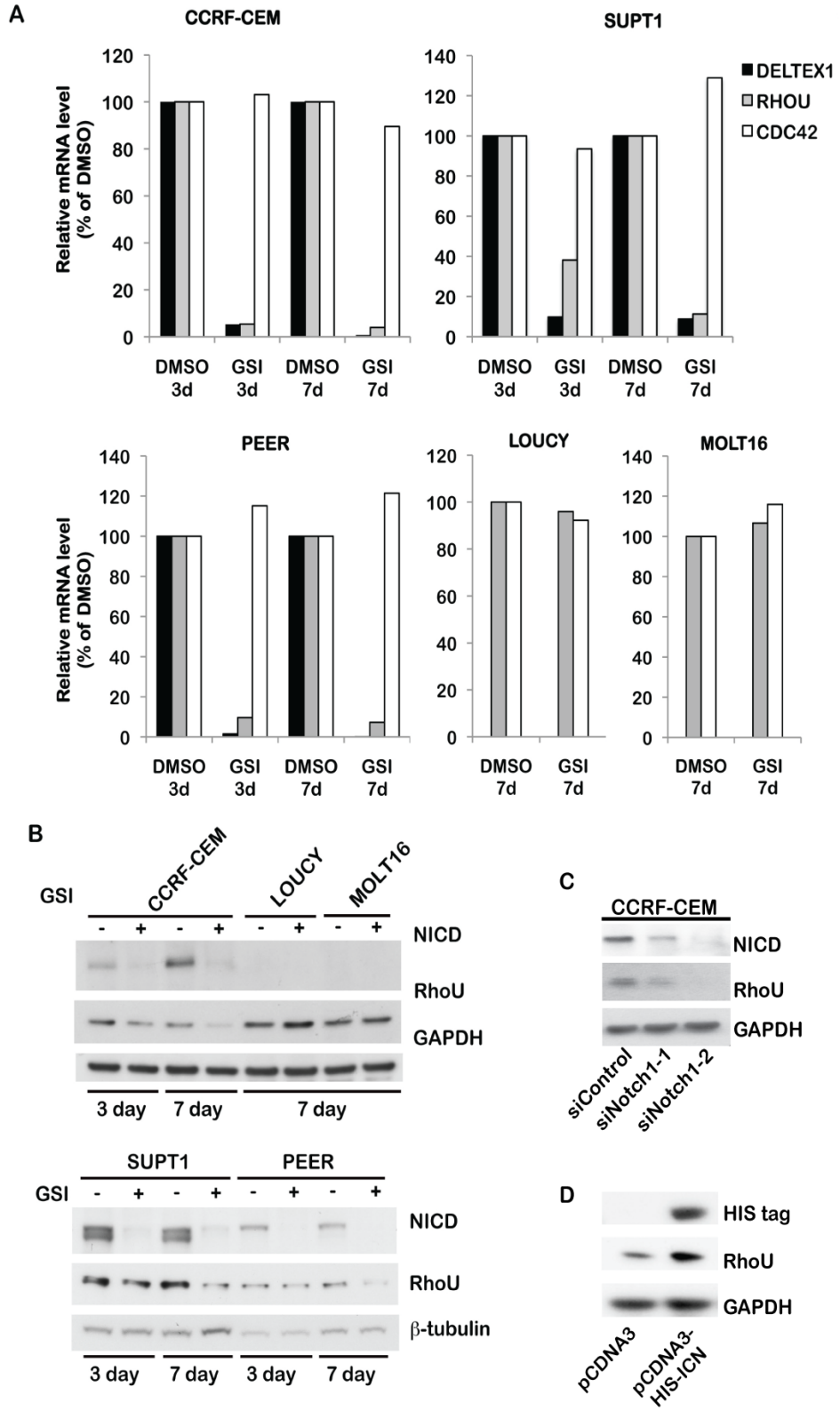

Figure 3.4 Notch1 regulates RhoU expression. (A) T-ALL cell lines were treated with GSI or DMSO (vehicle) for 3 days (3d) or 7 days (7d). RNA was extracted and

analysed by quantitative PCR to determine relative mRNA expression levels of *DELTEX-1*, *RHOU* and *CD CDC42*, with *GAPDH* as a reference. Fold expression changes were determined relative to expression in DMSO-treated cells using the comparative Ct method. (B) Cells treated as in (A) were lysed and protein levels of the cleaved NICD and RhoU were determined by immunoblotting. Blots were probed for GAPDH or β-tubulin as loading controls. Representative data from three independent experiments are shown. (C) CCRF-CEM cells were transfected with control siRNA or two different siRNAs (1, 2) targeting Notch1. Cells were lysed after 72 h and analysed by immunoblotting for levels of NICD, RhoU, and GADPH as a loading control. (D) A construct encoding His-tagged NICD was transfected into Cos7 cells. After 48 h, cells were solubilized in protein sample buffer and His-tag and RhoU were detected by immunoblotting. GADPH was used as a loading control. A representative blot from three independent experiments is shown. *Experiments in A, B were performed by Dr Parag Bhavsar (CCRF-CEM) and Elvira Infante (SUPT-1, PEER, LOUCY and MOLT16). Experiments in C and D were performed by Elvira Infante.*

3.4.5 RhoU regulates T-ALL cell polarization, migration and adhesion

Since Rho GTPases are well known to regulate cell migration (Heasman and Ridley, 2008), we investigated whether RhoU affected the migration of T-ALL cells. We chose CCRF-CEM cells since they have mutated *NOTCH1*, and are well characterized for their migration behaviour (Heasman et al., 2010; Infante et al., 2011; Takesono et al., 2010). RhoU expression was downregulated in CCRF-CEM cells by transfection with two different siRNAs (Suppl Fig. 3.2B). RhoU-depleted cells had a rounder morphology and migrated more slowly on fibronectin than control siRNA-transfected cells (Fig. 3.5A, B). Similarly, GSI-treated cells and Notch1-depleted cells were more rounded and migrated more slowly than control cells (Fig. 3.5A, B). RhoU- and Notch1-depleted cells and GSI-treated cells also showed reduced total migration distance over 1 h (Fig. 3.5C) and RhoU and GSI affected chemotaxis towards CXCL12 in transwells (Fig. 3.5D).

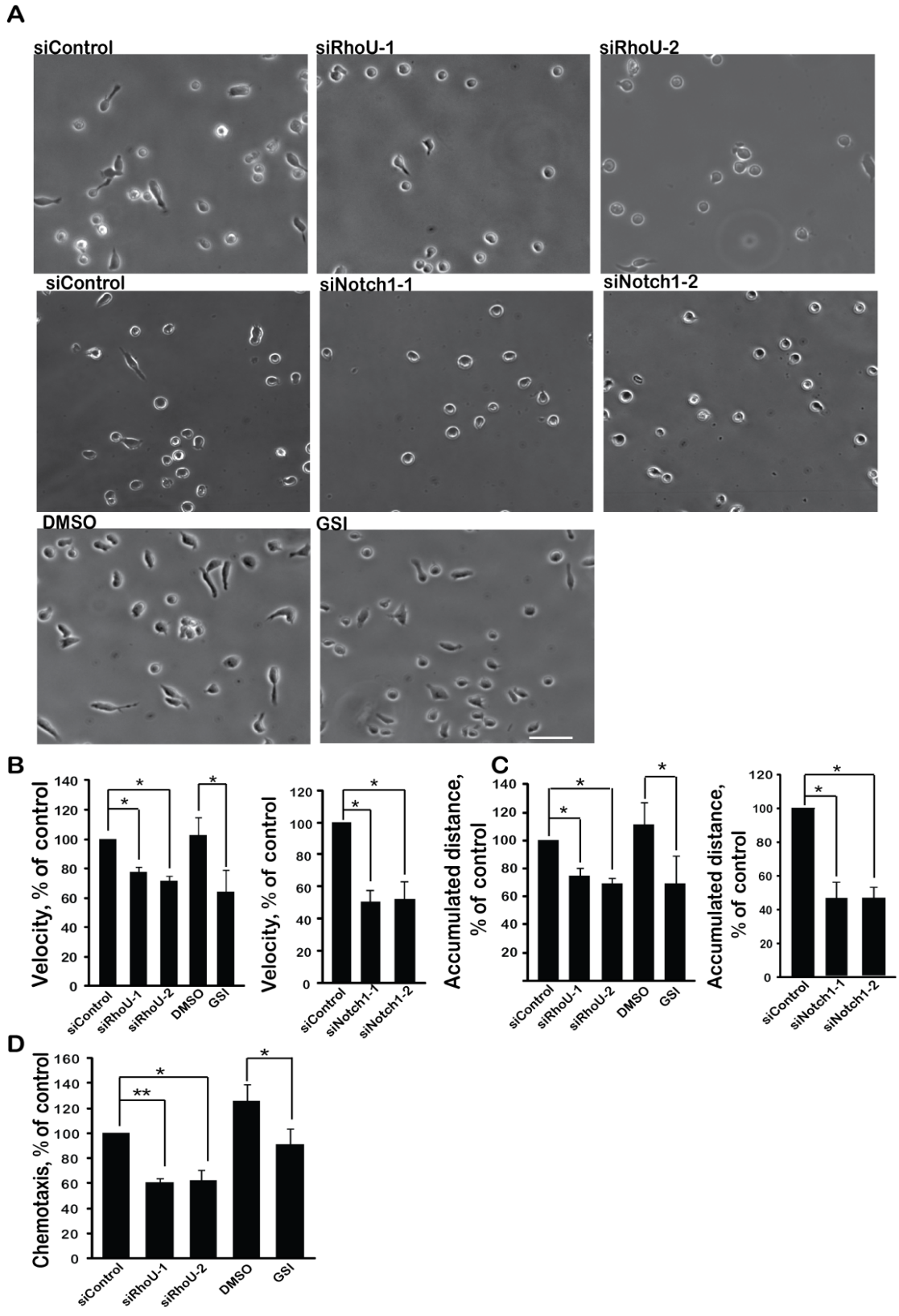

Figure 3.5 RhoU regulates T-ALL cell morphology and migration. CCRF-CEM cells were transfected with control siRNA, two different siRNAs (1, 2) targeting RhoU or Notch1 or treated for 7 days with 100 nM GSI or DMSO (vehicle). (A)

Cells were added onto fibronectin-coated wells and stimulated with 1 ng/ml CXCL12 for 30 min. Phase-contrast time-lapse images were collected every 1 min for 1 h. Images shown are at 0 min. Scale bar, 50 μm. Representative of three independent experiments. Relative velocity (B) and accumulated distance (C) was determined by tracking 60 cells in each of three independent experiments. (D) Cells were added to fibronectin-coated transwells containing 30 ng/ml CXC12 in the lower chamber. Cells that had migrated into the bottom of the well were counted after 1 h using a Casy Counter. Data shown are mean of three independent experiments±s.e.m. *P<0.05, **P<0.01; two-tailed paired t-test. *Experiments performed by Elvira Infante.*

The rounded phenotype of RhoU-depleted and Notch1-inhibited cells suggested they might have an adhesion defect. Indeed, depletion of RhoU or Notch1 or treatment with GSI reduced adhesion CCRF-CEM cells to fibronectin (Fig. 3.6, Suppl Fig. 3.2C).

Similarly, RhoU depletion reduced adhesion of two other T-ALL cell lines, JURKAT and PEER (Fig. 3.6A, Suppl Fig. 3.2B), indicating that the effect of RhoU is not cell type-specific.

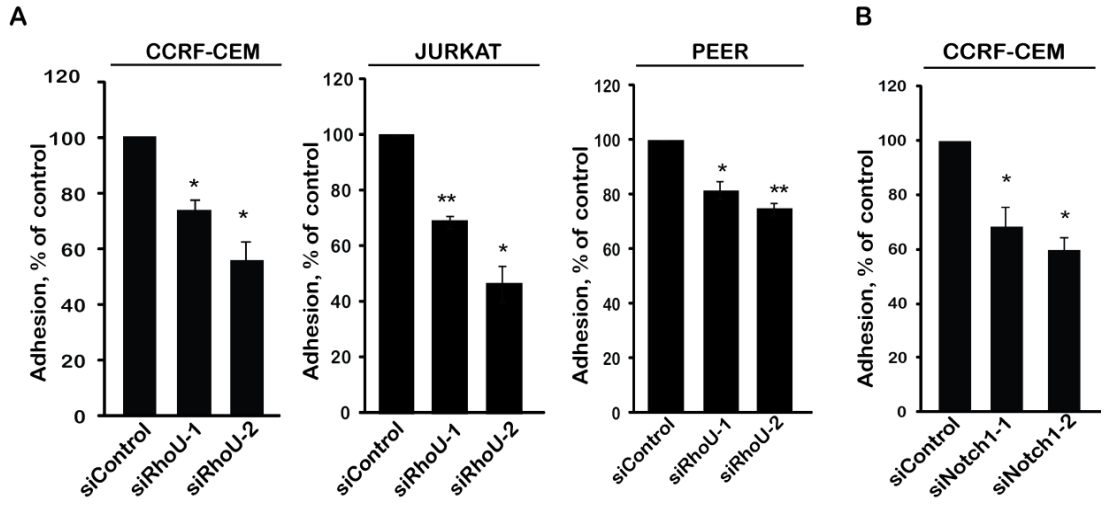

Figure 3.6 RhoU and Notch1 regulate T-ALL cell adhesion. CCRF-CEM, JURKAT or PEER cells were transfected with control siRNA or two different siRNAs (1, 2) targeting RhoU or Notch1, as indicated. After 72 h, cells were labelled with CellTracker dye CMFDA and incubated on fibronectin-coated wells. Adhesion was determined after 30 min. Data shown are the mean of three independent experiments±s.e.m. *P<0.05, **P<0.01; two-tailed paired t-test. *Experiments performed by Elvira Infante*

Next we investigated whether RhoU depletion or Notch1 inhibition altered migratory polarity by staining for F-actin and microtubules (Takesono et al., 2010). RhoU or Notch1-depleted cells and GSI-treated cells still had a single F-actin-rich lamellipodium at the front and the microtubule-organising center was behind the nucleus, but there was a strong reduction in the number of cells with tails compared to control cells (Fig. 3.7A-D). Interestingly, the total level of F-actin in RhoU-depleted or GSI-treated cells was increased (Fig. 3.7E), and the level of F-actin in lamellipodia also increased (Fig. 3.7F). RhoU depletion therefore affects T-ALL cell morphology and migration, and these effects can be reproduced by GSI-mediated inhibition of Notch1 signalling.

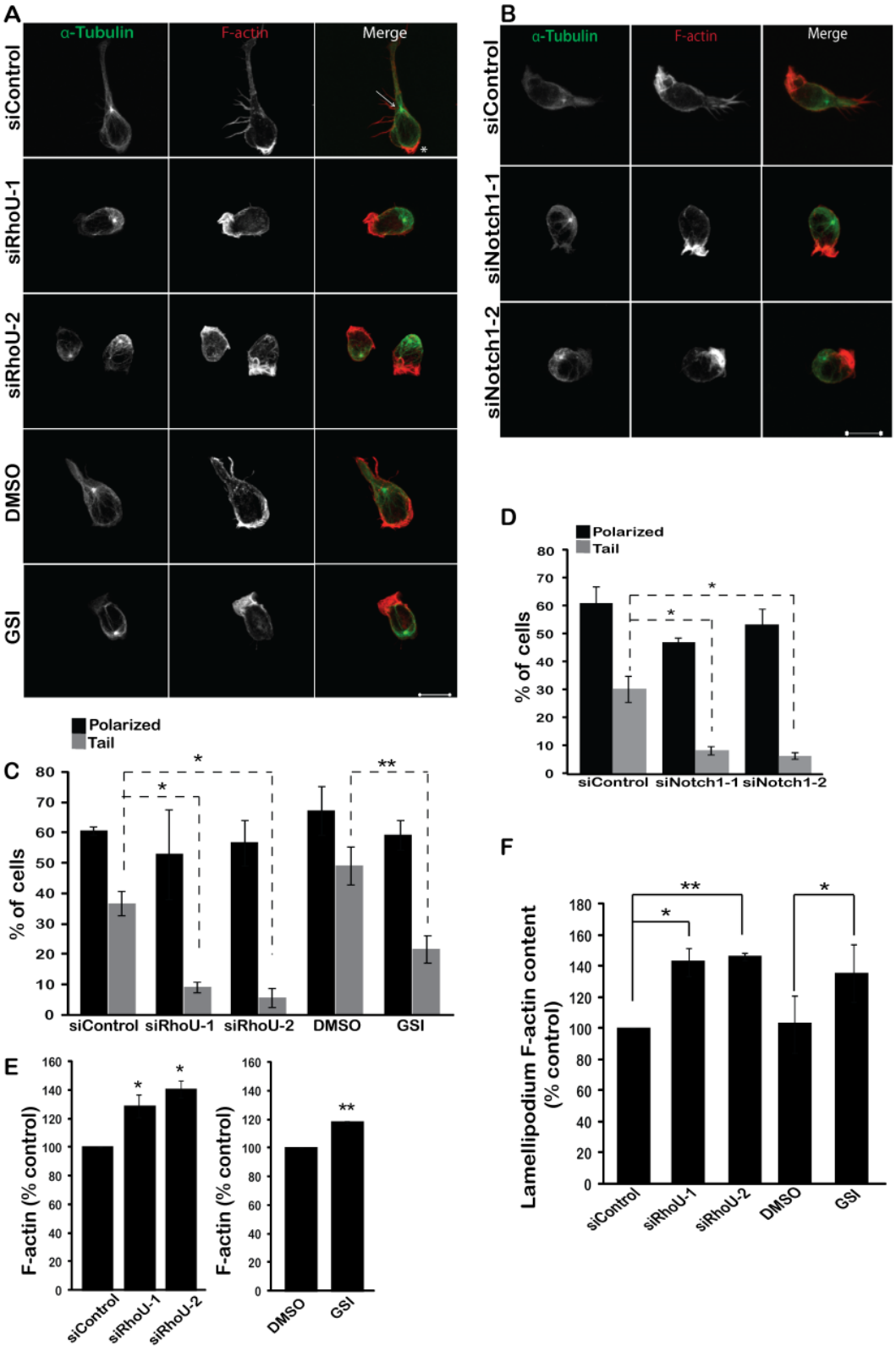

Figure 3.7 RhoU regulates polarity. CCRF-CEM cells were transfected with control siRNA, two different siRNAs targeting RhoU or Notch1 (1, 2) or treated for 7 days with 100 nM GSI or DMSO (vehicle). (A, B) Cells were plated onto fibronectin-coated wells and stimulated for 30 min with 1 ng/ml CXCL12. Samples

were then fixed and stained for F-actin and α-tubulin and imaged by confocal microscopy. Arrow indicates microtubule-organizing centre (MTOC); * indicates high F-actin staining in the lamellipodium. Scale bar, 10 μm. (C, D) The percent of polarized cells and cells with tails was quantified as described in the Materials and methods, by counting 100 cells in each of 3 independent experiments. (E) Cells were fixed, permeabilized and incubated with Alexa Fluor 488-labelled phalloidin and analysed by flow cytometry. (F) F-actin level at the leading edge was quantified using ImageJ software. Data shown are the mean of three independent experiments±s.e.m. *P<0.05, **P<0.01; two-tailed paired t-test. *Experiments performed by Elvira Infante*

3.5 Discussion

The pathophysiology of T-ALL suggests a significant deregulation of cell migration and tissue infiltration. Large numbers of T-ALL cells accumulate in the peripheral blood and tissues, with frequent metastasis to the CNS. We show that 8 of the 20 human Rho GTPases are upregulated in T-ALL compared to normal T cells. We find that expression of the atypical Rho family member RHOU is regulated by Notch1 and demonstrate that RhoU is required for optimal adhesion, migration and transendothelial migration of T-ALL cells. This indicates that RhoU could contribute to T-ALL progression in NOTCH1 mutant T-ALL patients.

RhoU and RhoV form a subfamily of Rho GTPases that have a high intrinsic guanine nucleotide exchange activity and are thus believed to be predominantly GTP-bound (Aspenstrom et al., 2007). RhoU (also known as Wrch1) and RhoV (also known as Chp) have been implicated in migration in several cell types but have not previously been studied in leukocytes. For example, they have been shown to stimulate lamellipodial or filopodial extension and/or an increase in integrin-based focal adhesions (Aronheim et al., 1998; Aspenstrom et al., 2004; Chuang et al., 2007). In osteoclasts, RhoU is found in podosomes and influences integrin signaling (Brazier et al., 2009), and RhoU is required for neural crest cell migration in vivo (Fort et al., 2011). Our data also indicate that RhoU is involved in regulating T-ALL cell adhesion. RhoU-depleted T-ALL cells had a more rounded phenotype and lacked uropods/tails. RhoU depletion also resulted in reduced migration and CXCL12-stimulated chemotaxis. Loss of the uropod and reduced migration are consistent with a decrease in cell adhesion. So far it is not clear how RhoU or RhoV affect cell adhesion, although RhoV was shown to bind to and cause the degradation of the Rac/Cdc42 effector PAK1, which is implicated in focal adhesion turnover (Arias-Romero and Chernoff, 2008; Weisz Hubsman et al., 2007). The increased expression of RhoU and RhoV in T-ALL samples compared to normal T cells could therefore affect their attachment in the bone marrow and thymus, as well as entry into and out of the peripheral circulation and tissues.

The increased expression of Rho GTPases that we observe in T-ALL samples is likely to reflect gene expression changes due to T-ALL genetic alterations (Aifantis et al., 2008; Ferrando et al., 2002). Indeed, we show that *RHOU* expression is regulated by Notch1. *RHOU* was also among the most downregulated genes in two

T-ALL cell lines treated with SAHM1, a new type of Notch inhibitor that prevents formation of the active NICD/CSL transcription factor complex (Downward, 2003). Importantly, similar morphological and migratory phenotypes were induced in T-ALL cells by RhoU depletion and by inhibiting Notch1 activation with GSI treatment, indicating that *RHOU* is the predominant target of Notch1 involved in regulating cell migration. Interestingly, *RHOU* was initially identified as a Wnt-regulated gene (Tao et al., 2001), and Wnt signaling plays an important role in T cell development (Weerkamp et al., 2006). In the future it will be important to test whether other T-ALL-associated transcription factors affect the expression of Rho GTPases upregulated in T-ALL.

In addition to *RHOU* and *RHOV*, we found that 4 other atypical Rho GTPases are upregulated in T-ALL: *RHOH, RHOBTB1, RND2* and *RND3*. RHOH is mutated through chromosomal translocations or somatic hypermutation in a number of B-cell-derived leukaemias and lymphomas, but has not previously been implicated in T-cell-derived leukemias (Fueller and Kubatzky, 2008). However, it does regulate T-cell receptor signaling and T-cell migration (Tybulewicz and Henderson, 2009; Wang et al., 2010), and could thereby affect T-ALL progression. So far little is known about RhoBTB1 in cancer. It has been proposed as a candidate tumour suppressor in head and neck cancer, but the mechanistic basis for this function is unknown (Berthold et al., 2008a). There is no evidence as yet that RhoBTB1 is involved in cytoskeletal regulation (Aspenstrom et al., 2004); instead, the RhoBTB proteins have been implicated in cullin3-based ubiquitination as well as transcription regulation via BTB domain-dependent interactions (Aspenstrom et al., 2004; Berthold et al., 2008b). It will therefore be important to determine how RhoBTB1 contributes to T-ALL. In contrast to RhoBTB1, Rnd2 and Rnd3 affect the actin cytoskeleton and affect cell migration in a variety of cultured cell lines (Aspenstrom et al., 2004; Riou et al., 2010), although their function has not so far been studied in lymphocytes.

RHOB was consistently highly upregulated in T-ALL, whereas the fold-increase in *RHOA* expression was less. *RHOA* overexpression has been reported in a variety of tumor types, including colon, breast, testicular germ cell and head and neck squamous cell carcinomas (Gomez del Pulgar et al., 2005). On the other hand, RhoB, which is involved in actin organization and membrane receptor trafficking (Ridley, 2006), has been primarily reported as a tumor suppressor based on expression

analysis in solid tumors, although how it acts is not completely understood (Huang and Prendergast, 2006; Vega and Ridley, 2008). *RHOB* expression is rapidly induced in response to a variety of stimuli including growth factor stimulation and genotoxic stress (Huang and Prendergast, 2006), and thus it is possible that a specific stimulus in T-ALL cells induces high *RHOB* levels.

In addition to our results on Rho GTPases, some T-ALL-related gene expression analysis studies have identified other potential regulators of cell migration. For example, the tetraspanin TALLA-1 (tetraspanin-7) is a target of the transcription factor TAL1 (Ono et al., 1997), which is frequently overexpressed in T-ALL (Graux et al., 2006). Several tetraspanins affect integrin-mediated processes such as adhesion, migration and invasion, but the function of TALLA-1 is not known (Yanez-Mo et al., 2009). TAL1 target genes identified by chromatin immunoprecipitation included some regulators of the cytoskeleton (Palomero et al., 2006). Overexpression of NICD altered the expression of chemokines, cell adhesion molecules and metalloproteases (Buonamici et al., 2009). In particular, the chemokine receptor CCR7 was upregulated and caused targeting of leukaemic blast cells to the brain endothelium. Together with our data, these results indicate that genes regulating cell adhesion, migration and invasion are modulated in T-ALL and could contribute to disease pathophysiology.

3.6 Supplementary figures

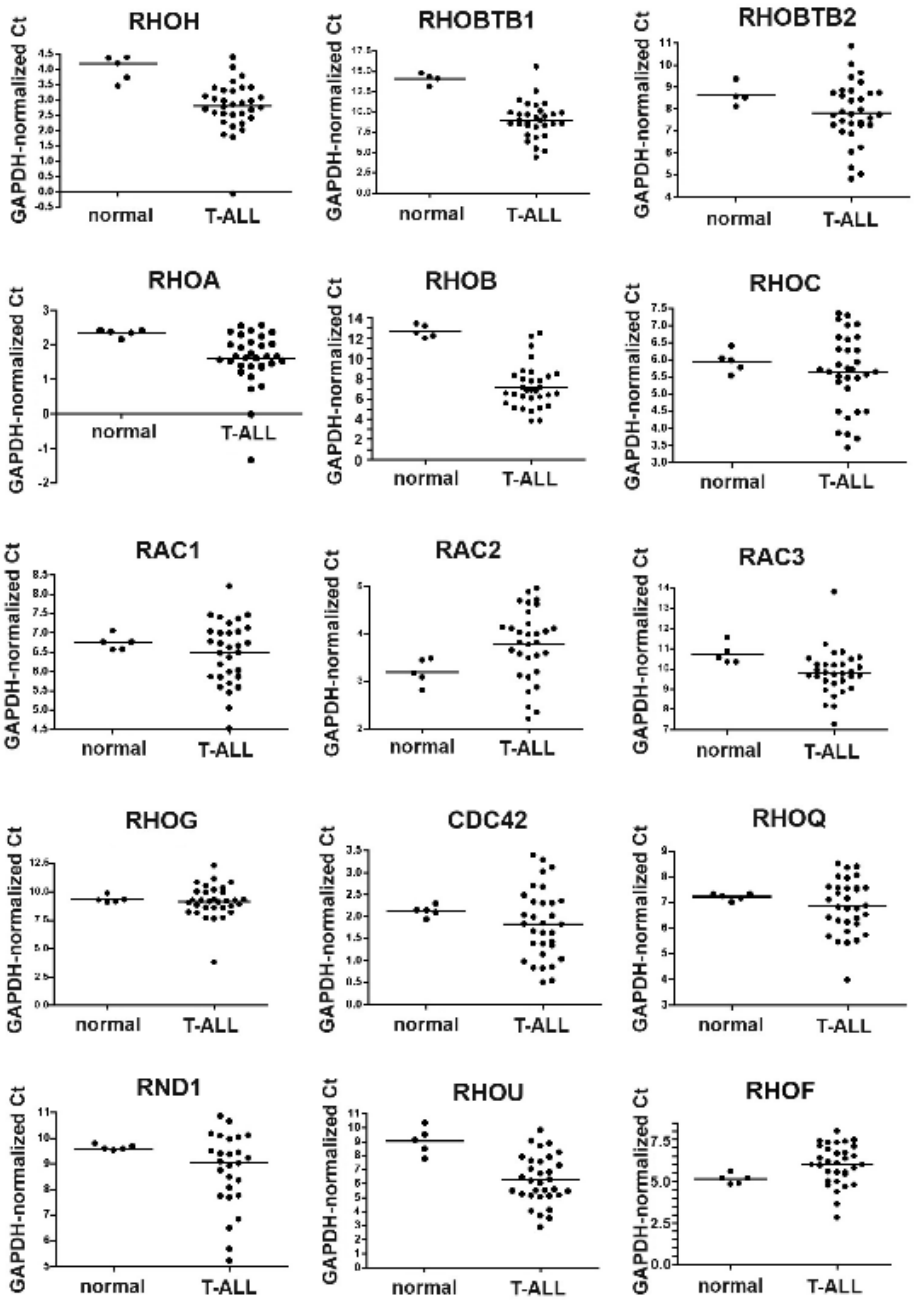

Supplementary Figure 3.1. Range of Rho GTPase expression in control T cells and T-ALL samples. RNA was extracted from 30 T-ALL blast samples and normal T-lymphocytes from 5 peripheral blood samples of healthy donors. mRNA expression of each Rho gene was measured by quantitative PCR, using GAPDH expression as a reference. The C_T value for each Rho gene is shown relative to the C_T value for GADPH in each sample.*Experiments were performed by Dr Parag Bhavsar.*

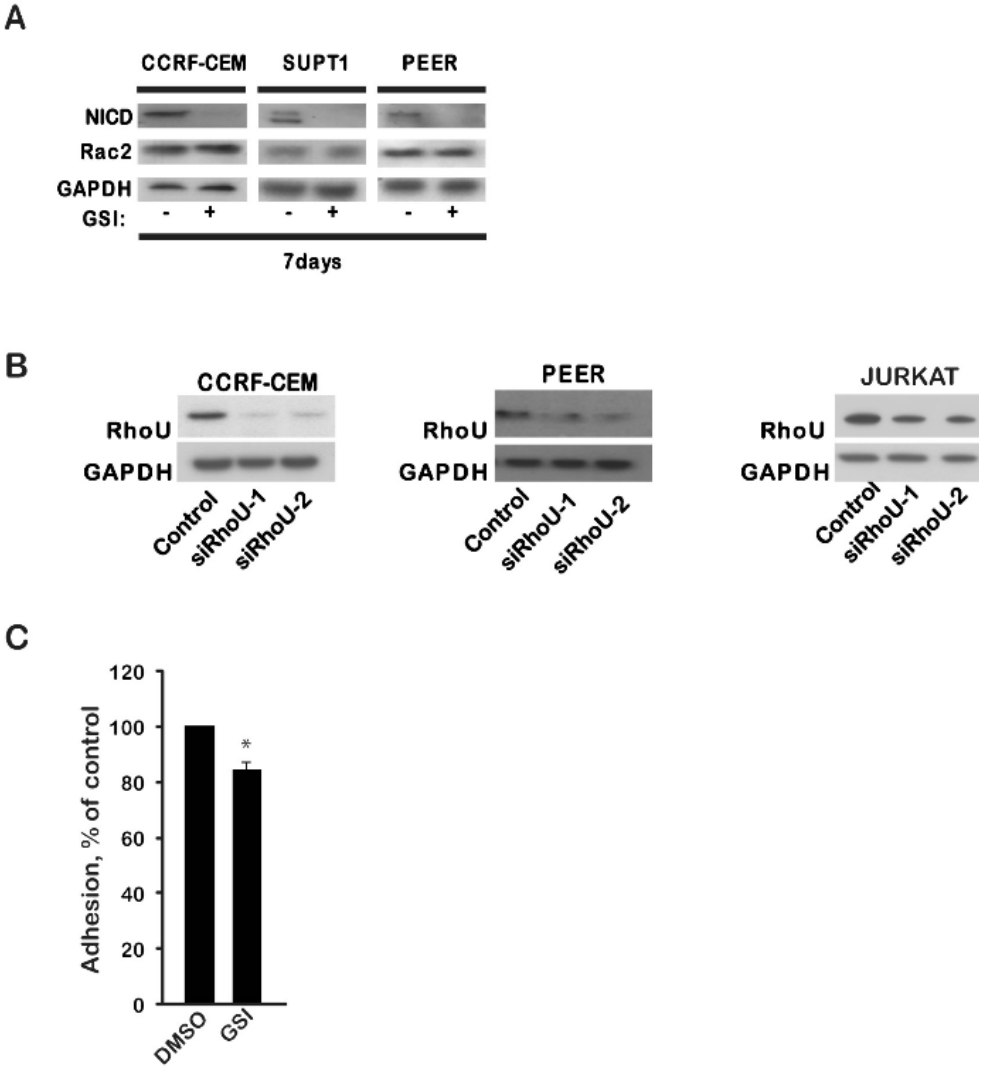

Supplementary Figure 3.2. RhoU depletion in T-ALL and effects of γ-secretase inhibition on protein expression and cell adhesion. (A) CCRF-CEM, SUPT1 and PEER cells were treated with 100 nM GSI or DMSO (vehicle) for 7 days. Cleaved Notch1 intracellular domain and Rac2 were detected by western blotting. (B) CCRF-CEM, JURKAT and PEER cells were transfected with control siRNA and two different siRNAs (1, 2) targeting RhoU. The level of RhoU was determined 3 days after transfection by immunoblotting. GADPH was used as a loading control. (C) CCRF-CEM cells were treated with 100 nM GSI or DMSO for 7 days. Cells were then labelled with cell tracker dye CMFDA and incubated on fibronectin-coated wells. Adhesion was determined after 30 min. Data shown are the mean of 3 independent experiments ± SEM. *p <0.05, **p <0.01; two-tailed paired *t*-test. *Experiments were performed by Elvira Infante.*

4

Roles of RhoU and RhoV in T-ALL cell adhesion and migration

4.1 Introduction

RhoU and RhoV belong to the Cdc42 subfamily. They are atypical GTPases with high intrinsic guanine nucleotide exchange, and are therefore likely to be constitutively GTP-bound in cells (Chenette et al., 2005; Saras et al., 2004). In contrast to most Rho GTPases, both RhoU and RhoV have an N-terminal and C-terminal extension that distinguishes them from the classical Rho GTPases. In particular the N-terminal extension is proline-rich and is likely to bind SH3 domain containing proteins. RhoU has been demonstrated to bind via its proline-rich domain to NCK2 (Saras et al., 2004). They do not have a functional CAAX box and instead are targeted to membranes by palmitoylation (Aronheim et al., 1998; Saras et al., 2004). RhoU and RhoV protein sequences share 55% identity. They have both been reported to be involved in the formation of filopodia and migration of several cell types (Aronheim et al., 1998; Fort et al., 2011). Like Cdc42, RhoU and RhoV were shown to activate PAK (Weisz Hubsman et al., 2007) (Saras et al., 2004; Tao et al., 2001). Interestingly, RhoV is not expressed in normal T cells but is overexpressed in a subset of T-ALL patients samples (Bhavsar et al., 2012).

In the previous chapter, RhoU was shown to regulate T-ALL cell migration. Knockdown of RhoU by siRNA transfection affected the morphology of CCRF-CEM cells, inducing a round phenotype and a decrease in tail formation. RhoU depletion also inhibited the adhesion of several T-ALL cell lines to fibronectin. These results suggested RhoU might contribute to tissue infiltration in T-ALL by affecting adhesion. The role of RhoV in T-ALL cells has never been investigated before. In this chapter the roles of RhoU and RhoV in T-ALL cells were investigated in parallel using Jurkat cells, as this cell line was shown to express both RhoU and RhoV. The localization, distribution and interaction of these proteins was also investigated.

4.2 Materials and Methods

Chemicals were all purchased from Sigma-Aldrich (Dorset, UK) unless otherwise stated.

4.2.1 Cell biology

4.2.1.1 Cell culture

T-ALL cell lines (CCRF-CEM, PEER, SUPT-1 and Jurkat) were maintained in RPMI-1640 (containing 2 mM glutamine) (Invitrogen, Paisley, UK) supplemented with 10% fetal calf serum (FCS) (Biosera, East Sussex UK), 1 mM sodium pyruvate, 10 mM Hepes, Penicillin (100 U/ml) and Streptomycin (10 µg/ml) (Invitrogen). Once cells reached a density of 2 x 10^6 cells/ml, they were diluted to a concentration between 2 and 5 x 10^5 cells/ml.

Human umbilical vein endothelial cells (HUVECs) were grown in EBM-2 medium with growth factors (EGM-2) containing 2% FCS (Lonza, Slough, UK). Prior to seeding the cells, flasks were coated 10 µg/ml fibronectin (FN) (Sigma-Aldrich) for 1 hour at 37°C. For passaging, cells were washed with PBS (without Ca^{2+}/Mg^{2+}) (Invitrogen) and incubated with 1 ml trypsin-EDTA (Invitrogen) at 37°C until all cells detached. The cells were then diluted in fresh culture medium. Cells were used until passage five.

COS7 cells were grown in DMEM medium (Invitrogen) containing 10% FCS, Penicillin (100 U/ml) and Streptomycin (10 µg/ml). For passaging, cells were washed with PBS (without Ca^{2+}/Mg^{2+}) and incubated with 1 ml trypsin-EDTA at 37°C until all cells detached. Cells were then diluted in fresh culture medium.

4.2.1.2 Transfection of siRNAs

Jurkat cells were diluted to a density of 5 x 10^5 cells/ml. After 24 h, cells were mixed with 1.2 µM siRNA in 100 µl Nucleofection reagent kit C (Lonza) and transferred to an electroporation cuvette. Cells were then nucleofected with an Amaxa Nucleofector apparatus, using programme X-001 according to the manufacturer's instructions (Lonza). siRNA sequences were RhoV-1: GAGGGACGAUGUCAACGUA; RhoV-2 GAAGAAACUGAAUGCCAAA; RhoV-3: GUAUUUGACUCGGCUAUUC; RhoV-4:

GCUCAGCCUUGACGCAGAA. siControl was from Thermo Fisher Scientific (D-001810-02-20, Lafayette, USA). After transfection cells were transferred to 5 ml of warm medium and incubated for 48-72 h at 37°C.

4.2.1.3 Transfection of plasmids

Jurkat cells (10^7) were mixed with 30 µg plasmid in 250 µl of Opti-MEM (Gibco), transferred to a 0.4 cm electroporation cuvette and left at room temperature for 10 min. Samples were electroporated using a GenepulserII (Bio-Rad, Hertfordshire, UK) at 250 V, 975 µF and left again at room temperature for 10 min. Cells were then plated in 5 ml warm medium and incubated for 8-16 h at 37°C.

COS7 cells were detached from the plate and washed twice with electroporation buffer (10 mM KCl, 10 mM $K_2PO_4/KHPO_4$, pH 7.6, 25 mM Hepes, 2 mM $MgCl_2$ and 0.5% Ficoll 400). After resuspending in 250 µl of electroporation buffer, cells were mixed with 5 µg DNA in a 0.4 cm electroporation cuvette, left on ice for 5 min, then at room temperature for 5 min. Cells were finally plated in a 10 cm dish and incubated for 24 h at 37°C.

4.2.1.4 Adhesion assay on endothelial cells (manual counting)

Glass coverslips were incubated for 16 h with 10 µg/ml FN at 37°C. HUVECs were grown to confluency on coverslips and stimulated for 16 h with 10 ng/ml TNF-α (R&D systems, Abingdon, UK). Jurkat cells were then incubated at 37°C for 15 min with 2 µM Cell Tracker CMFDA (Invitrogen, Paisley, UK). Samples were resuspended in warm media, and 2 x 10^5 cells/well were seeded onto the HUVEC monolayer and incubated at 37°C for 15 min. After two washes to remove un-bound cells, samples were fixed with 4% paraformaldehyde for 10 min. Following two washes in PBS, cells were incubated with Alexa Fluor 546 phalloidin (Invitrogen) for 1 h to visualize F-actin. Coverslips were mounted onto glass slides using Dako anti-fade mounting medium (Dako, Ely, UK). Images were acquired using a Zeiss LSM510 confocal microscope using a Plan Fluor 20x objective and Zen software was used to analyse the data. Five random fields for each condition were acquired and the total number of cells per field was counted.

4.2.1.5 Adhesion assay on endothelial (plate reader)

Black 96 well plates (Costar, Corning, NY, USA) were coated for 1 h with 10 μg/ml FN at 37°C. HUVECs were grown to confluency in the wells and stimulated for 16 h with 10 ng/ml TNF-α. Jurkat cells were then incubated at 37°C for 15 min with 2 μM Cell Tracker CMFDA. Samples were resuspended in warm medium and 2 x 10^5 cells/well (each sample in triplicate) seeded onto the HUVECs monolayer. Cells were incubated at 37°C for 15 min. After 3 washes to remove un-bound cells, adhered cells were measured by detection of fluorescence using a plate reader (PerkinElmer, Cambridge, UK) at 485 nm excitation and 523-535 nm emission.

4.2.1.6 Transwell based transendothelial migration assay

HUVECs were grown to confluency on FN-coated (10 μg/ml) 5 μm pore transwell filters (Costar) and then stimulated with 10 ng/ml TNF-α for 16 h. After washing, 2.5 x 10^5 Jurkat cells in 200 μl medium were added onto the HUVECs monolayer in the top chamber, and 600 μl medium containing 30 ng/ml of CXCL-12 (R&D systems) was added to the bottom of the wells. After 3 h of incubation at 37°C, the cells that had transmigrated into the lower chamber were counted using a Casy cell counter.

4.2.1.7 Live imaging microscopy

Glass bottom dishes (MatTek, Ashland, MA, USA) were coated with 10 μg/ml FN at 4°C overnight and blocked with 2.5% bovine serum albumin in PBS for 1 h. Jurkat cells (10^6) were added to the dishes, and incubated at 37°C for 30 min. After two washes cells were stimulated with 1 ng/ml of CXCL12 in 1 ml of phenol red-free RPMI and images acquired every 10 sec for 10 min using a LSM510 confocal microscope with a Plan-Apochromat 63x/1.40 NAOil DIC M27 objective. Zen software was used to analyse the movies.
Vesicles (13 for each condition) were tracked and velocities calculated using ImageJ.

4.2.1.8 Immunofluorescence microscopy

Glass coverslips were coated with 10 μg/ml FN at 4°C overnight and blocked with 2.5% bovine serum albumin in PBS for 1 h. Jurkat cells (2.5 x 10^5) were added to each coverslip and incubated at 37°C with 1 ng/ml CXCL12 for 30 min. Subsequently, samples were fixed with 4% paraformaldehyde for 10 min and permeabilized in 0.1% Triton-X-100 for 4 min. Cells were then incubated with 1:200 dilution of anti-myc-epitope (sc-40, Santa Cruz Biotechnology, SA, USA) primary antibody for 1 h at room temperature, followed by incubation with Alexa Fluor-488, 546 or 647 anti-mouse IgG secondary antibody (Invitrogen) for 1 h at room temperature. Samples were, when indicated, incubated for 1 h at room temperature with Alexa Fluor-546 phalloidin to visualize F-actin. Coverslips were mounted onto glass slides using Dako anti-fade mounting medium and visualized under a LSM510 confocal microscope with a Plan-Apochromat 63x/1.40 NAOil DIC M27 objective and Zen software was used to analyse the data.

Protein co-localization was quantified using Zen software, which calculates an overlap coefficient. Overlap values range from 0 to 1. An overlap of 1 indicates perfect pixel co-localization (Hoebe et al., 2007).

4.2.1.9 Analysis of filopodia and cell spreading

Jurkat cells transfected with plasmids encoding pRK5-myc-RhoU or RhoV (kind gift of Pontus Aspenström (Saras et al., 2004)) were seeded onto FN-coated coverslips. Cells were then fixed and stained with anti-myc epitope antibody and Alexa Fluor-546 phalloidin. Filopodia and spread cells were quantified by scoring myc-RhoU or myc-RhoV positive cells compared to cells transfected with pRK5 empty vector.

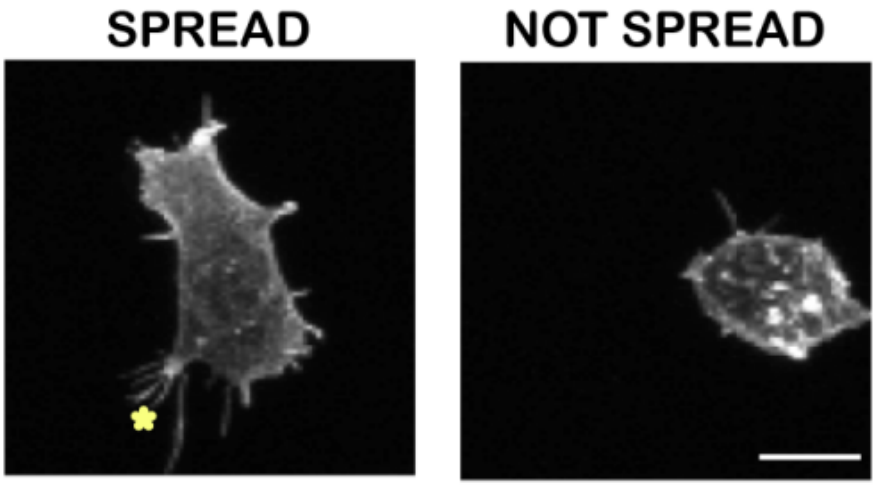

Figure 4.1 Example of filopodia and a spread cell. Jurkat cells were seeded onto FN-coated coverslips for 30 min. Cells were fixed and stained with Alexa Fluor-546 phalloidin. Left image shows a well spread cell. Star indicates filopodia protrusions. Right image shows a round and not spread cell (scale bar 10 μm).

4.2.2 Molecular Biology

4.2.2.1 Generation of GFP-RhoU, GFP-RhoV and Cherry-RhoU vector

RhoU and RhoV cDNAs were subcloned from a pRK5 to pEGFP-C1 vector (Clontech, Saint-Germain-en-Laye France). pEGFP-C1 was digested using BamHI and DraI, while pRK5-myc-RhoU or pRK5-myc-RhoV were digested using BamHI and PsiI. After purification on agarose gels, RhoU and RhoV were ligated into pEGFP-C1. *E. coli* were transformed with 5 μl of ligation and clones were verified by plasmid digestion using EcoRI (Figure 4.2).

RhoU from pEGFP-RhoU was subsequently subcloned in pmCherry-C1 (kind gift Dr Maddy Parsons). pEGFP-RhoU and pmCherry-C1 were digested with EcoRI. To avoid self-ligation, pmCherry-C1 was incubated with calf intestinal alkaline phosphate (CIP). Since this enzyme catalyzes the removal of 5' phosphate groups required by ligases, the plasmid DNA cannot self-ligate. After agarose gel purification, RhoU was ligated into pmCherry-C1 and *E. coli* transformed with 5 μl of ligaton. Clones were verified by plasmid digestion using EcoRI restriction enzyme (Figure 4.3).

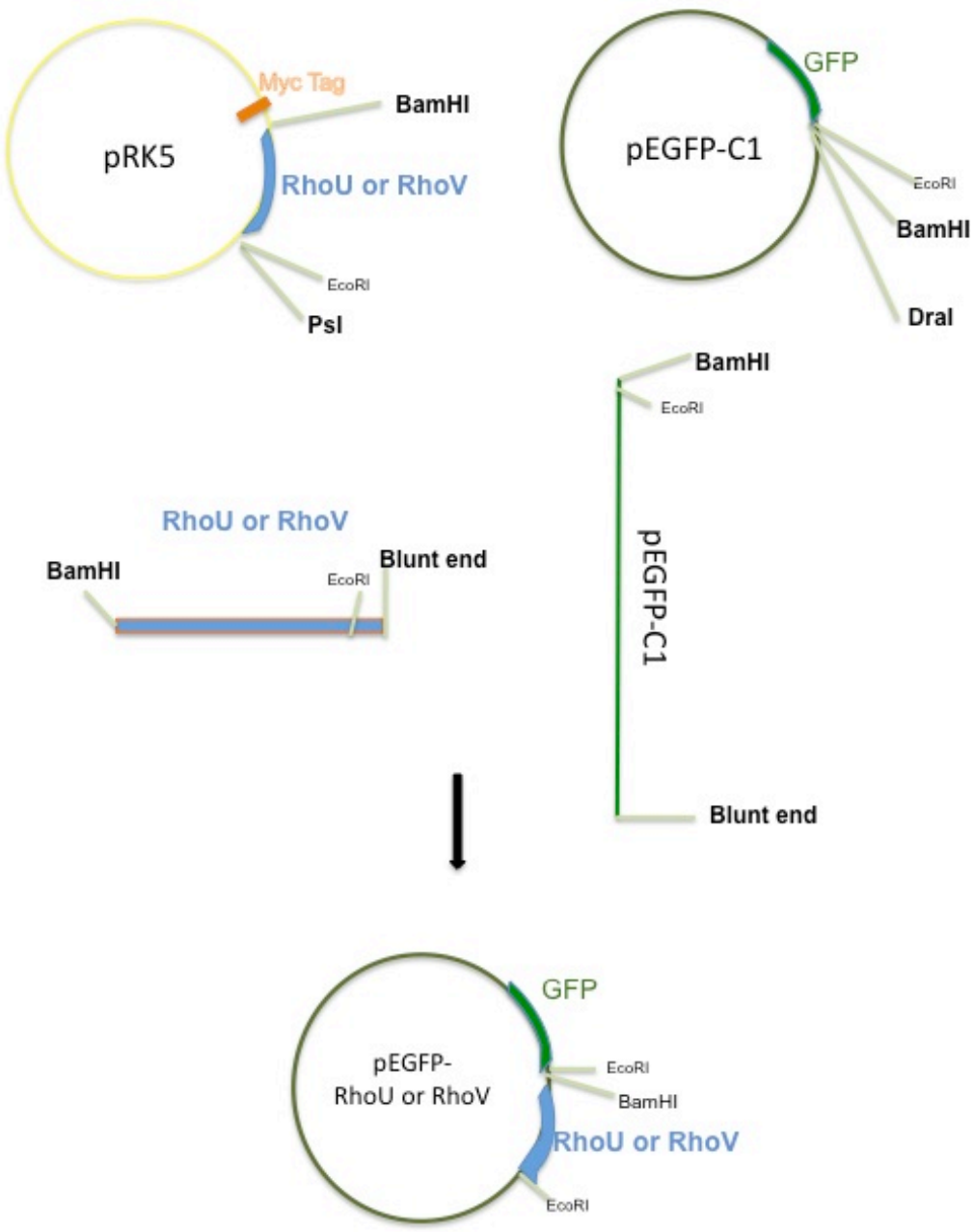

Figure 4.2 Schematic diagram of RhoU and RhoV subcloning into pEGFP-C1. pRK5-RhoU or RhoV were digested with BamHI and PsiI while pEGFP-C1 was digested with BamHI and DraI restriction enzymes. RhoU and RhoV cDNAs were ligated into pEGFP-C1 using T4 ligase.

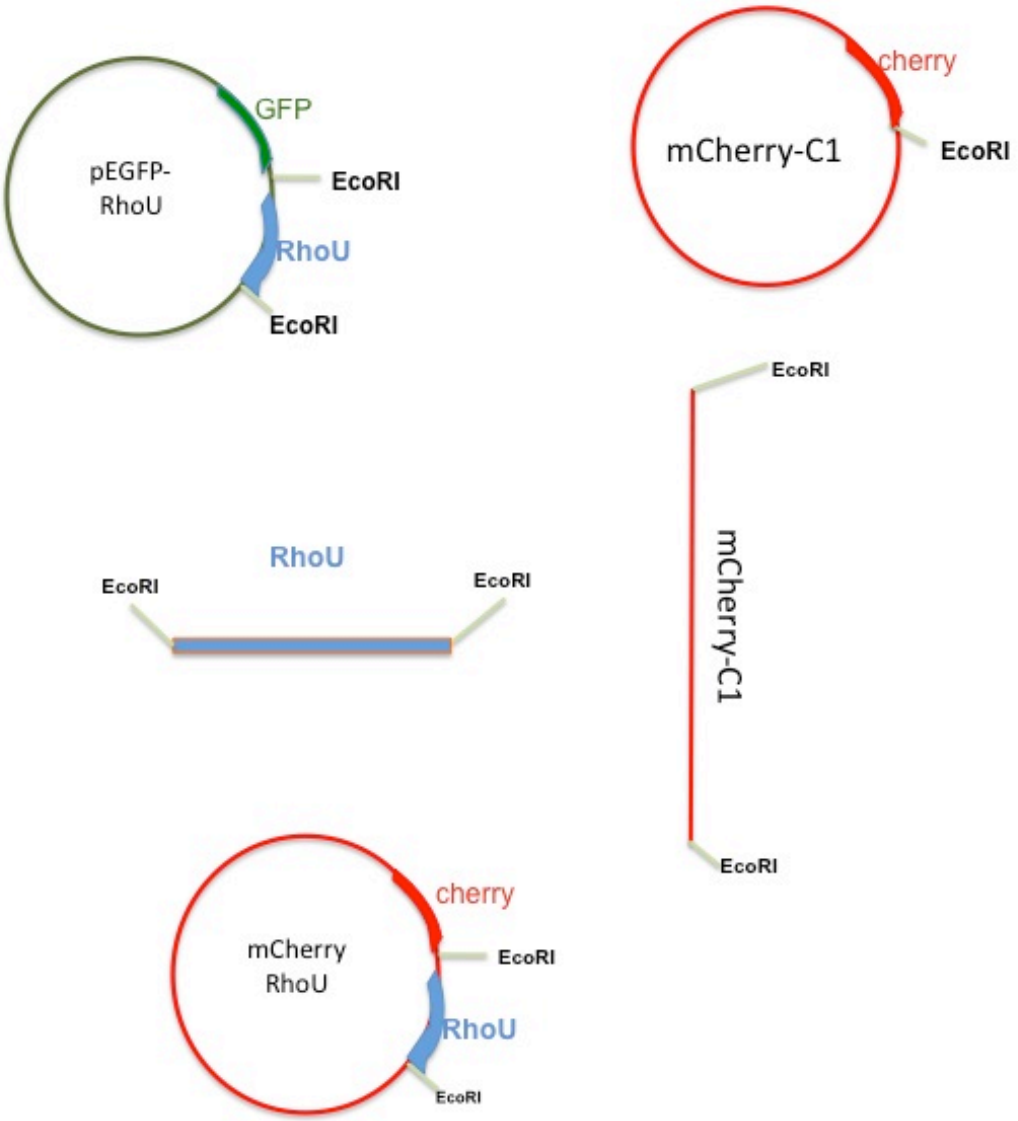

Figure 4.3 Schematic diagram of RhoU subcloning into a pmCherry-C1. pEGFP-RhoU and pmCherry-C1 were digested with EcoRI restriction enzyme. RhoU was ligated into pmCherry-C1 using T4 ligase.

4.2.2.2 Restriction enzyme digestion of DNA

Plasmid DNA (1μg) was digested with 10 units of the appropriate restriction enzyme (DraI, PsiI, BamHI and EcoRI) in the buffers recommended by the manufacturer (New England Biolabs, Hertfordshire, UK) for up to 2 h. To avoid self-ligation, destination vectors were incubated with 10 units of CIP (New England Biolabs) for 30 min at 37°C.

4.2.2.3 Agarose gel elctrophoresis

1% (w/v) agarose was dissolved in TAE buffer (40 mM Tris acetate, 1 mM EDTA and 11.4% (v/v) glacial acetic acid) using a microwave oven. Ethidium bromide (0.5 μg/μl) was added to the gel and, after complete polymerization, DNA samples separated by electrophoresis at 100 V in TAE buffer. DNA fragments were visualized on a UV-transilluminator.

4.2.2.4 Extraction of DNA from agarose gels

The DNA fragments of interest were excised under a UV-transilluminator using a sterile scalpel and weighed. DNA was then isolated using the QIAquick gel extraction kit (QIAGEN, West Sussex, UK) according to the manufacturer's instructions. Fragments were mixed with 3 volumes of buffer QG (composition not provided) per mg of gel and incubated at 50°C until the gel was completely dissolved. After addition of 1 volume of isopropanol, the sample was applied to a QIAquick spin column and centrifuged at 14000 g for 1 minute. The column was washed twice with PE (composition not provided) at 14000 g for 1 min and DNA eluted in 50 μl ddH_20 by centrifugation at 14000 g for 2 min.

4.2.2.5 DNA ligation

DNA fragments were ligated into the appropriate destination vector using 200 units T4 DNA ligase (New England Biology) in the supplied ligation buffer at 16°C for 16 h. A 3-fold excess volume of insert over destination vector was used. 5 μl of ligation was subsequently used for bacterial transformation.

4.2.2.6 Transformation of competent bacteria

Plasmid DNA (10 ng) or 5 µl of ligation were mixed with 100 µl of competent DH5α cells and incubated on ice for 30 min. The bacterial suspension was heat-pulsed for 45 sec at 42°C and placed again on ice for 2 min. 900 µl LB (without antibiotics) was then added to the bacteria and incubated at 37°C for 1 hour. Finally, 100 µl of the cells were plated onto a Luria broth (LB) agar plates containing 100 µg/ml ampicillin or 50 µg/ml kanamycin, as appropriate.

4.2.2.7 Purification of plasmid DNA from bacteria

For small-scale production of plasmid DNA, QIAprep Miniprep Kits were used. LB medium (2 ml) containing 100 µg/ml ampicillin or 50 µg/ml kanamycin was inoculated with a single colony from an agar plate and incubated overnight at 37°C. Bacteria were centrifuged at 3000 g for 15 min and the pellet resuspended in 250 µl Buffer A (50 mM glucose, 25 mM Tris-HCl, pH 8.0, 10 mM EDTA, 10 µg/ml RNase A). After mixing with 250 µl lysis buffer (200 mM NaOH, 1% SDS), 350 µl neutralization buffer (3 M potassium acetate and 2 M acetic acid) were added to the sample and cell debris and proteins removed by centrifugation at 14000 g for 10 min. The supernatant was then applied to a QIAprep spin column and centrifuged at 14000 g for 1 min. Columns was washed twice with 750 µl wash buffer (750 mM NaCl, 50 mM MOPS pH 7.0, 15% isopropanol (v/v)) and DNA eluted with 50 µl ddH_20 by centrifugation for 1 min at 14000 g.

For larger scale plasmid DNA purification, Qiagen EndoFree Maxiprep Kits were used. 100 ml of bacterial culture was pelleted at 3000 g for 15 min and resuspended, lysed and neutralized in 10 ml of buffers described for the miniprep protocol. Lysates were clarified using filter-syringes provided with the kit. Endotoxin removal buffer (1.5 ml) was added to the sample and incubated on ice for 30 min. In the meantime a column provided by the kit was equilibrated with the equilibration buffer (50 mM NaCl, 50 mM MOPS pH 7.0, 15% isopropanol (v/v), 15% Triton-X-100). The sample was then applied to the column and washed twice with wash buffer (1 M NaCl, 50 mM MOPS pH 7.0, 15% isopropanol (v/v)). The DNA was eluted with 15 ml of higher salt buffer (1.25 M NaCl, 50 mM Tris/HCl pH 8.5, 15% isopropanol (v/v) and then precipitated by adding 0.7 volumes isopropanol and centrifuged at

8000 g for 45 min. Pellets were washed with 5 ml 70% ethanol and resuspended in 200 µl ddH_20.

4.2.2.8 Determination of DNA and RNA concentration

DNA or RNA concentration was determined using a Nano-Drop spectrophotometer system (Thermo scientific, Hampshire, UK) at an optical density (OD) of 260 nm and 280 nm. The DNA concentration (ng/µl) was automatically calculated using the formula $_{conc}$DNA= OD260 x 50 µg/ml. The RNA concentration (ng/µl) was automatically calculated using the formula $_{conc}$RNA= OD260 x 40 µg/ml.

4.2.2.9 DNA sequencing

Purified plasmid DNA (1 µg) was sent to MWG (www.eurofinsdna.com) for DNA sequencing.

4.2.2.10 RNA isolation using Trizol

Suspension cells (5 x 10^6) were pelleted in a microcentrifuge tube and incubated for 5 min with 1 ml Trizol (Invitrogen) at room temperature. Chloroform (0.2 ml) was added to the sample and the tube was vigorously inverted 10 times. Samples were left at room temperature for 3 min and subsequently centrifugated at 14000 g for 15 min at 4°C. After centrifugation the upper phase of the samples was transferred into a new tube, mixed with 0.25 ml of isopropanol to precipitate the RNA and incubated on ice for 10 min. RNA was pelletted by centrifugation at 14000 g for 15 min at 4°C and the pellet air-dried for 10 min. Pellets were resuspended in 10 µl of RNase free H_2O (Ambion, Invitrogen, Paisley, UK).

In order to remove DNA contamination, the purified RNA was incubated with DNase1 buffer and 1 µl DNase enzyme (Ambion) for 30 min at 37°C. The DNase was inactivated following the addition of 5 µl DNase inactivation buffer beads for 2 min at 37°C. Samples were then centrifuged at 10000 g for 2 min and supernatants transferred to a new tube.

4.2.2.11 cDNA synthesis

Reverse transcription was performed using SuperScript-Vilo cDNA Synthesis Kit (Invitrogen). RNA (1 µg) was mixed with the VILO reaction mix and SuperScript Enzyme Mix according to the manufacturer's instructions. Samples were first incubated for 10 min at room temperature and subsequently incubated for 1 hour at 42°C. The reaction was terminated by 5 min at 85°C.

4.2.2.12 Real-time SYBR-green PCR

The relative mRNA level of RhoV was determined by qPCR using SYBR green detection chemistry (PCR mastermix from Primer Design, Southampton, UK). SYBR green is a fluorescent dye that binds double stranded DNA. Therefore, during the qPCR reaction the fluorescence increase proportionally with the amount of amplified DNA. The reaction was performed in an ABI Prism 7000 Sequence Detection System (Applied Biosystems). Primers for RhoV and GAPDH (for normalization) were designed and validated by Dr Parag Bhavsar as described in chapter 3. cDNA obtained from 1 µg RNA was diluted 1/65, and of this 3 µl were mixed with 3 µl of primers and 6 µl 2X SYBR green mix in a total reaction volume of 12 µl. The reaction was carried out with an initial 10 min denaturation at 95°C followed by 40 cycles of 10 sec at 95°C (denaturation) and 30 sec at 60°C (annealing and extension). To verify that just one product was amplified a dissociation step was added at the end of the reaction (one denaturation cycle at 95°C for 15 sec followed by 20 sec of amplification at 60°C). The data were analysed using the ABI7000 analysis software using the ΔΔCT method (Schmittgen and Livak, 2008).

$2^{-\Delta\Delta C_T}$ = [(CT gene of interest – CT internal control) *sampleA*- (CT gene of interest-CT internal control) *sampleB*)]

The CT values indicate the number of cycles after which the SYBR green fluorescent signal crosses a threshold level. In this calculation the fold difference of the expression of a gene between two samples is calculated.

4.2.3 Biochemistry

4.2.3.1 Immunoprecipitation

For immunoprecipitation of myc-epitope-tagged proteins, transfected COS7 cells were lysed into lysis buffer containing 1% Triton-X-100, 50 mM Tris HCl, 150 mM NaCl, 1 mM DTT, 25 mM NaF and complete EDTA-free protease inhibitor (Roche Applied Science, Burgess Hill, UK). Samples were centrifuged for 10 min at 14000 g. 40 μl of clarified samples was kept to determine total protein level, while the remaining lysate was incubated with 20 μl of anti-myc-agarose beads (Santa Cruz Biotechnology, Santa Cruz, CA, USA) at 4°C for 2 h on a rotating wheel. Beads were then washed five times in 1 ml lysis buffer and boiled in 4X sample buffer

4.2.3.2 Western blot analysis

Cells were lysed in 1% SDS, followed by addition of 1% Triton-X-100, 25 mM NaF, 1 mM Na_3VO_4 and 10 mg/ml aprotinin, then incubated on ice for 10 min. Lysates were clarified by centrifugation at 14000 g for 30 min. Cleared lysates were boiled for 5 min in 4X sample buffer and separated on a 4-12% Bis-Tris polyacrylamide gel at 150 V in NuPAGE MES running buffer (Invitrogen). Proteins were then transferred to a nitrocellulose membrane (GE Healthcare, Chalfont St Giles, UK) for immunblotting. Transfer was carried out for 90 min at 100 V in transfer buffer (25 mM Tris HCl pH 8.3, 192 mM glycine, 20% methanol). Membranes were then blocked in blocking buffer (5% nonfat dried milk in TBS (25 mM Tris HCl 7.6, 50 mM NaCl, 2.5 mM KCl)) for 1 hour at room temperature and incubated with 1:1000 dilutions of the following antibodies: c-myc (sc-789, Santa Cruz), GFP (FL, Santa Cruz), RhoU (Wrch-1 ab80315, Cambridge, UK) and GAPDH (Millipore, Watford, UK)) primary antibody either for 1 hour at room temperature or overnight at 4°C. Membranes were washed three times in TBS, containing 0.1% Tween-20, and incubated with HRP-conjugated anti-mouse, anti –rabbit or anti-goat antibody. After

3 washes, immunodetection was performed using an ECL detection kit (GE Healthcare) according to manufacture's instructions and signal detected by exposure to X-ray films.

4.3 Results

4.3.1 RhoV expression in T-ALL cell lines and siRNA transfection in Jurkat cells

The function of the atypical Rho GTPase RhoV is far from being fully understood. The RhoV gene is not expressed in primary-T-lymphoblasts but expressed in a subset of T-ALL patients samples (Figure 3.1). This raises questions concerning its possible role in the pathogenesis of T-ALL.

First, the expression of RhoV was analysed in different T-ALL cell lines and primary-T-lymphoblasts. As already mentioned, primary-T-lymphoblasts do not express RhoV and they were included as a negative control. RNA was purified from Jurkat, CCRF-CEM, PEER and SUPT1 T-ALL cell lines and primary T-lymphoblast cells. The expression of RhoV was then determined by quantitative PCR. Among the T-ALL cell lines Jurkat and Supt1 expressed the highest level of RhoV. Interestingly these cell lines also expressed the highest level of RhoU, as described in chapter 3 (see Figure 3.3.). CCRF-CEM and PEER cell lines had lower levels of RhoV and primary T-lymphoblasts had no detectable RhoV (Figure 4.4A). Jurkat cells were then selected for further studies of RhoV as this cell line was already well characterized and used for previous studies in the laboratory.

In order to study whether RhoV affected adhesion and migration, Jurkat cells were transfected with four different siRNAs targeting RhoV and an siRNA control. Cells were also nucleofected with nucleofection reagent only (Mock control). In the absence of a reliable antibody to detect endogenous RhoV protein, the efficiency of RhoV mRNA depletion was determined by qPCR. Two siRNAs siRhoV-1 and siRhoV-3 gave the strongest depletion of RhoV mRNA (Figure 4.4B and C).

A

	RhoV Ct
Jurkat	30
CCRF-CEM	34
SUPT-1	29
Peer	33
Primary-T-lymphoblast	Not detectable

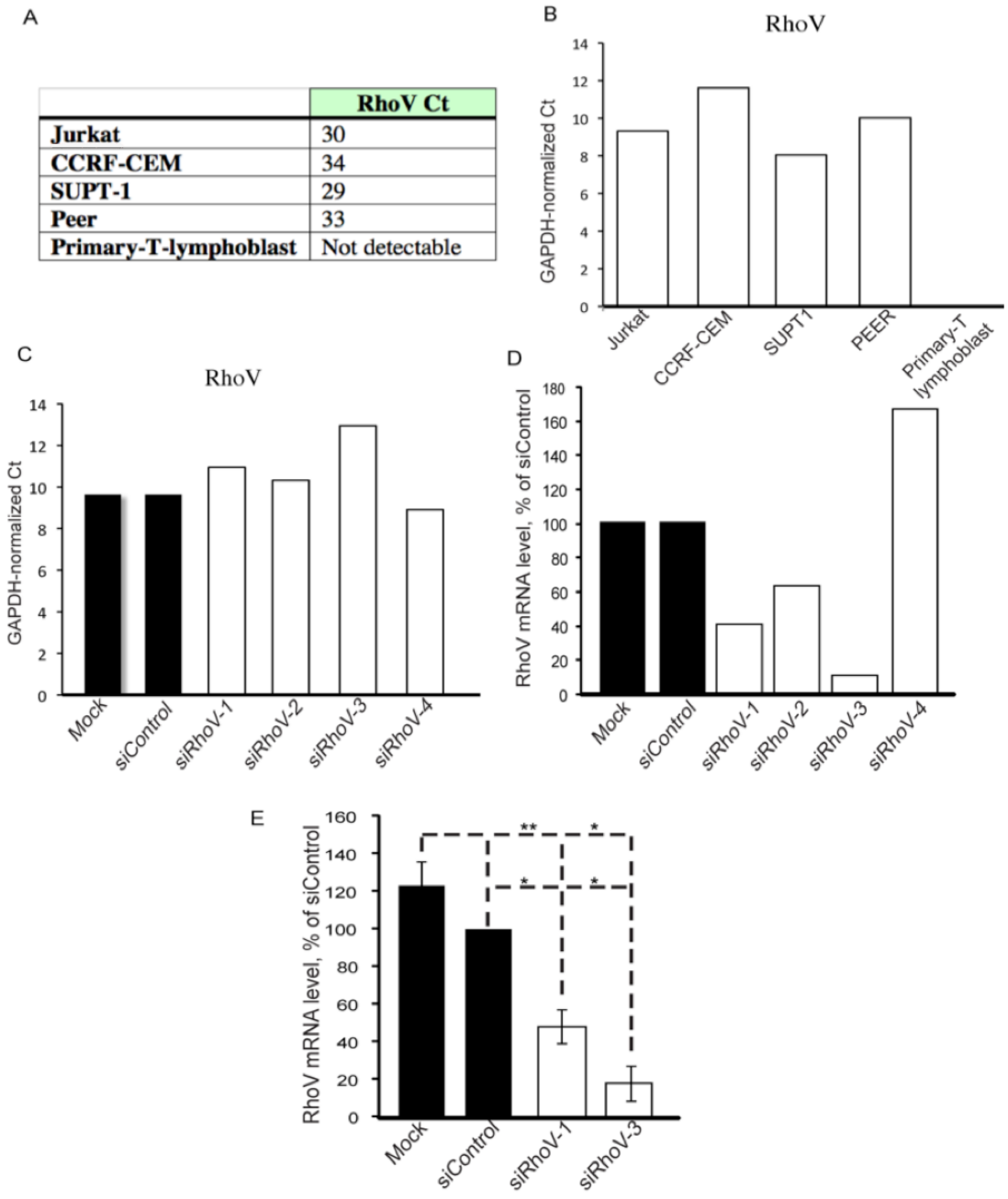

Figure 4.4 RhoV expression in T-ALL cell lines and RhoV siRNA knockdown. Total RNA was isolated from Jurkat, CCRF-CEM, PEER, SUPT1 and primary-T-lymphoblast cells (A and B) or Jurkat cells transfected with control siRNA or four (C and D) or two (E) different oligos for RhoV. mRNA was converted into cDNA and the amount of RhoV cDNA was determined by qPCR. Ct value of RhoV (A) is shown relative to Ct value for GAPDH (B and C). All values in D and E are represented as percentage of siControl. C and D represent data from one single experiment. Data shown in A, B and E are the mean of 3 independent experiments ± SEM. * $p<0.05$, **$p<0.01$; 2-way-paired t-test.

4.3.2 RhoU and RhoV depletion reduces adhesion of Jurkat cells to fibronectin and endothelial cells

T-ALL progression is characterized by T-ALL cell accumulation in lymph nodes, spleen and CNS (Kebriaei et al., 2002). Molecules involved in migration, adhesion and chemotaxis of T-ALL cells are likely to be important in the infiltration process. β1 integrin is widely expressed in mammalian cell types and is expressed in T-lymphocytes (Bauer et al., 2009; Zhang and Wang, 2012). Integrins are important for both rolling and adhesion of T cells on endothelial cells. It has been demonstrated that β1 integrin-deficient T cells are unable to infiltrate the CNS (Bauer et al., 2009). Fibronectin is a ligand for β1 integrin (Hauzenberger et al., 1994). In chapter 3 (see section 3.4.6) RhoU depletion, was shown to reduce adhesion of CCRF-CEM, Jurkat and Peer and Jurkat cells to fibronectin. It was therefore further investigated whether RhoU and RhoV could affect adhesion of Jurkat cells to fibronectin. A reduction of 50% in the binding of Jurkat cells to fibronectin was observed after depletion of RhoU and RhoV compared to Mock and siRNA control (Figure 4.5). This indicates that both proteins are important for adhesion of Jurkat cells to fibronectin. The physiological ligand of β1 integrin on endothelial cells is the VCAM-1 on endothelial cells. Upregulation of VCAM-1 is observed after stimulation of endothelial cells with TNF-α (Cernuda-Morollon and Ridley, 2006). To investigate the effect of RhoU and RhoV depletion on T cell adhesion to endothelial cells, HUVECs were used. Two different types of adhesion assay were carried out. The first assay was performed in order to visualize the effect of RhoU and RhoV knockdown on adhesion. In this assay HUVECs were grown on coverslips and adherent Jurkat cells were counted manually. Knockdown of both RhoU and RhoV with 2 single oligos significantly decreased the adhesion of Jurkat cells to HUVECs (Figure 4.6A and B). The second assay, similar to the adhesion assay on fibronectin described in chapter 2 and 3, was used to obtain an automated quantification of adhered cells. In these experiments, knockdown of RhoU and RhoV also reduced adhesion of Jurkat cells to the endothelial monolayer (Figure 4.6 C).

Taking together these results indicated that RhoU and RhoV regulate Jurkat cell adhesion to fibronectin and endothelial cells.

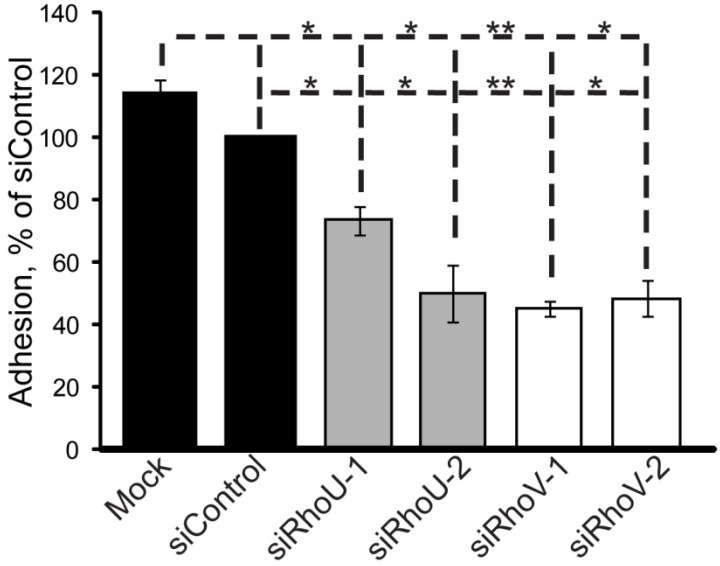

Figure 4.5 RhoU and RhoV depletion affect adhesion of Jurkat cells to fibronectin. Jurkat cells were transfected with transfection reagent alone (MOCK), control siRNA or two different siRNAs targeting RhoU or RhoV. After 72 h cells were labelled with Cell Tracker CMFDA and added to wells coated with FN. Adhesion was determined after 30 min. Data shown are the mean of 3 independent experiments ± SEM. * $p<0.05$, ** $p<0.01$; 2-way-paired t-test.

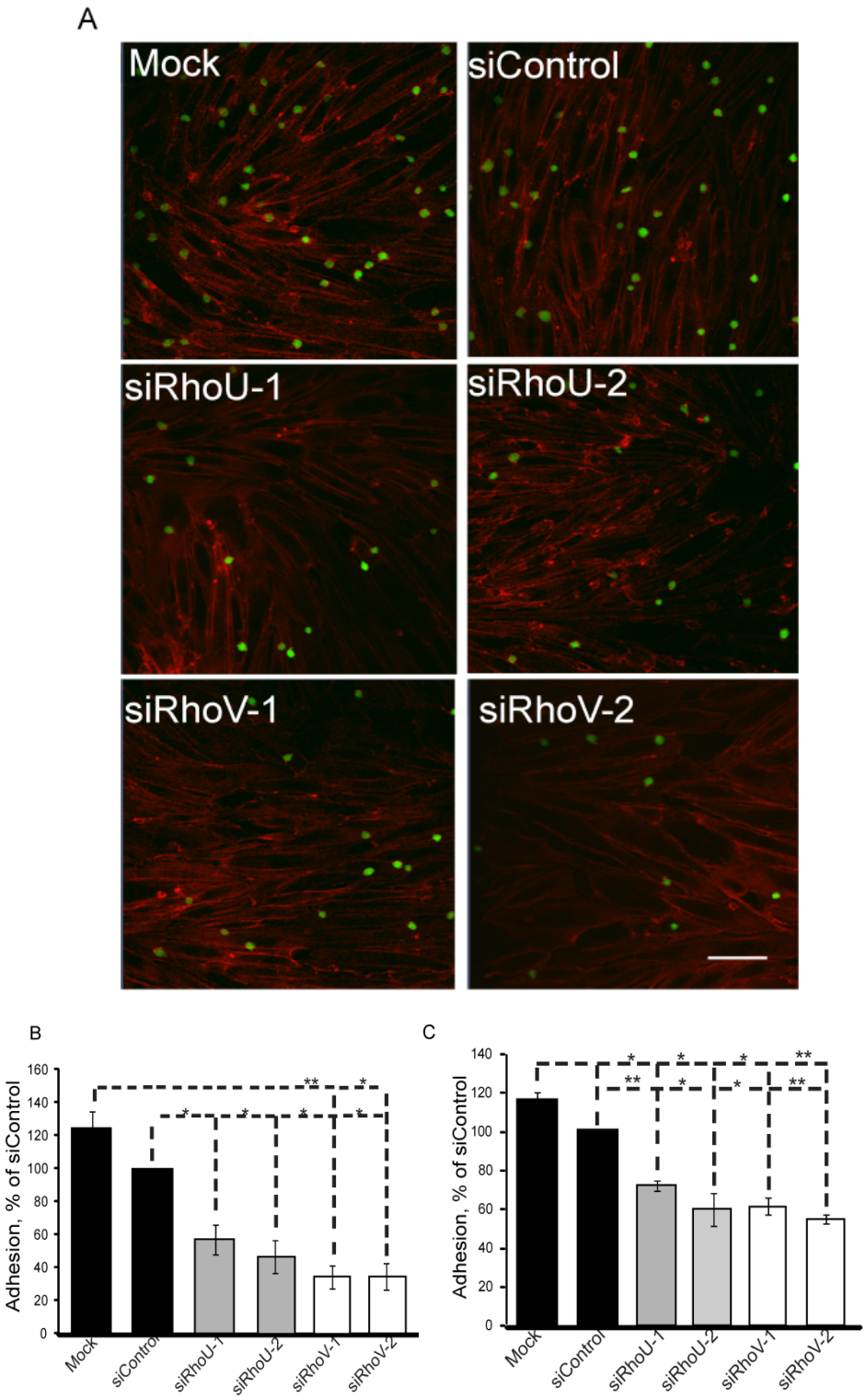

Figure 4. 6 RhoU and RhoV depletion affect adhesion of Jurkat cells to HUVECs. Jurkat cells were transfected with MOCK, control siRNAs or two different siRNA targeting RhoU or RhoV. After 72 h cells were labelled with Cell Tracker CMFDA and then added to a confluent HUVEC monolayer on coverslips (A and B) or to a confluent HUVEC monolayer on a 96 well plate. After 15 min samples were washed to remove un-bound Jurkat cells. Cells on coverslips were

fixed and stained for F-actin. Images were acquired by confocal microscopy. Five random fields for each condition were acquired and the total number of cells per field was counted. (A) Images are representative of 3 independent experiments. Scale bar, 50 μm. (B) Graph shows adhered cells as percentage of siControl. (C) Adhered cells were measured by detection of fluorescence on a plate reader. Data shown are the mean of 3 independent experiments ± SEM. * $p<0.05$, **$p<0.01$; 2-way-paired t-test.

4.3.3 RhoU and RhoV depletion reduces transendothelial migration

RhoU or RhoV knockdown decreases the adhesion of Jurkat cells to endothelial cells. Adhesion of leukaemia cells to the endothelium is an important step for transendothelial migration. T-ALL cells often migrate to and infiltrate lymph nodes and bone marrow where they proliferate. The bone marrow has been suggested as a site that allows neoplastic cells to evade chemotherapy and several adhesion molecules are involved in this process and affect patient outcome (Feng et al., 2010). In order to investigate whether RhoU and RhoV knockdown could affect transendothelial migration of Jurkat cells, HUVECs were allowed to grow on 0.5 μm transwell filters and stimulated with TNF-α. Jurkat cells were then seeded onto the HUVECs and the chemokine CXCL12 was added as a chemoattractant to the bottom (Figure 4.7). Both RhoU and RhoV depletion significantly impaired the transmigration of Jurkat cells.

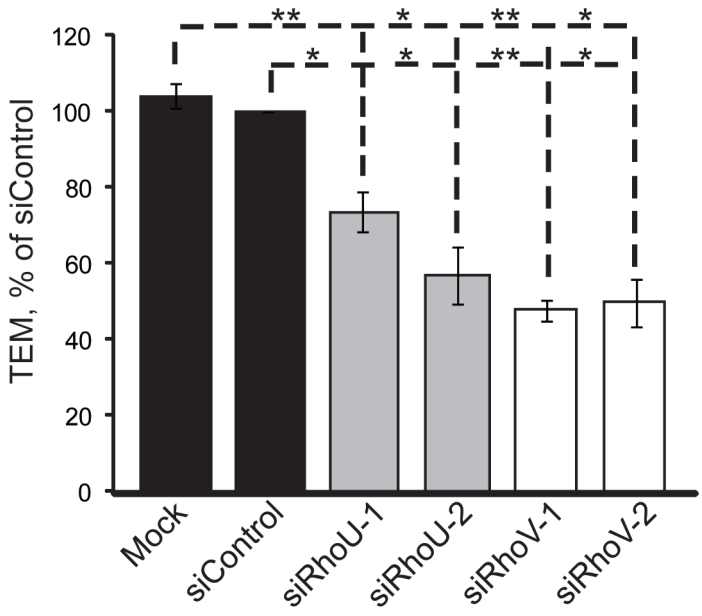

Figure 4.7 RhoU and RhoV down-regulation reduces TEM. Jurkat cells were transfected with siRNAs targeting RhoU, RhoV or siRNA controls and then added to confluent HUVECs on transwell filters. CXCL12 (30 ng/ml) was added to the bottom well. After 3 h, cells that had transmigrated through the HUVECs into the lower chamber were counted with a Casy counter.
Data shown are the mean of 3 independent experiments ± SEM. * $p<0.05$, **$p<0.01$; 2-way-paired t-test.

4.3.4 RhoU and RhoV induce morphological changes in Jurkat and SUPT1 cells.

To determine the effect of RhoU and RhoV overexpression on T-ALL cell lines, pRK5 empty vector (as a control), or vectors encoding Myc-RhoU and Myc-RhoV were transfected into Jurkat cells. After 24 h, cells were allowed to adhere to fibronectin. Cells were treated with CXCL12 to stimulate migration. RhoU and RhoV localized mainly on the plasma membrane and in punctate structures in the cytoplasm (Figure 4.8).

Expression of RhoU and RhoV increased the number of cells with filopodium-like protrusions compared to the control samples (Figure 4.8A and B). This has been already reported previously in fibroblasts (Aronheim et al., 1998; Saras et al., 2004).

Filopodia protrusions were also observed by timelapse confocal microscopy (see supplementary movies 12 and 13).

Expression of RhoU and RhoV induced an increase in cell spreading (Figure 4.8). Interestingly, in chapter 3 RhoU-depleted CCRF-CEM cells were shown to have a round, less spread phenotype and reduction in tail formation (see section 3.4.6). Similarly, RhoU and RhoV overexpression increased filopodium formation in SUPT1 cells, although this was not quantified (Figure 4.8C).

A

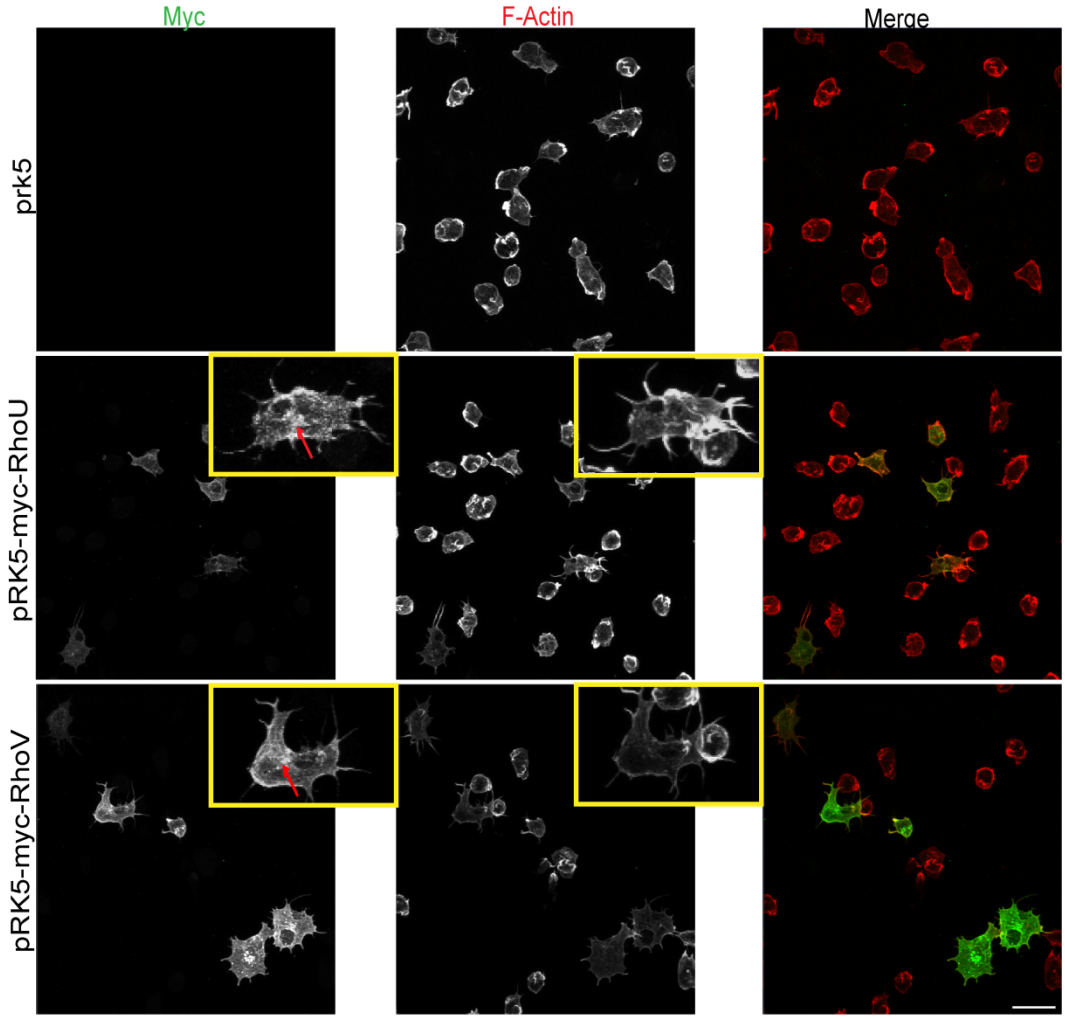
Myc
F-Actin
Merge
prk5
pRK5-myc-RhoU
pRK5-myc-RhoV

B

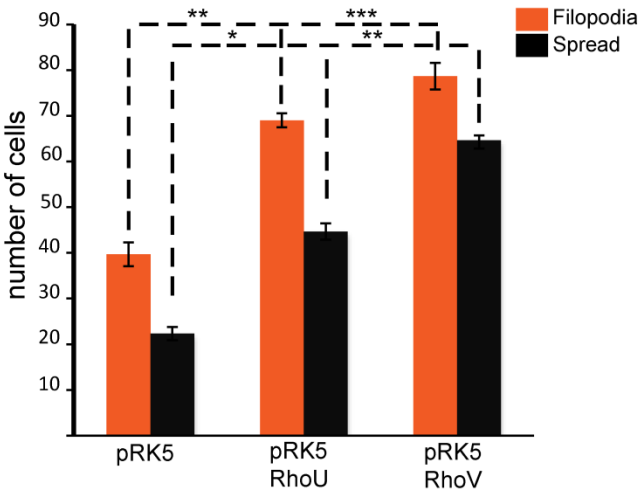
Filopodia
Spread
number of cells
90
80
70
60
50
40
30
20
10
**
*
***
**
pRK5
pRK5 RhoU
pRK5 RhoV

C

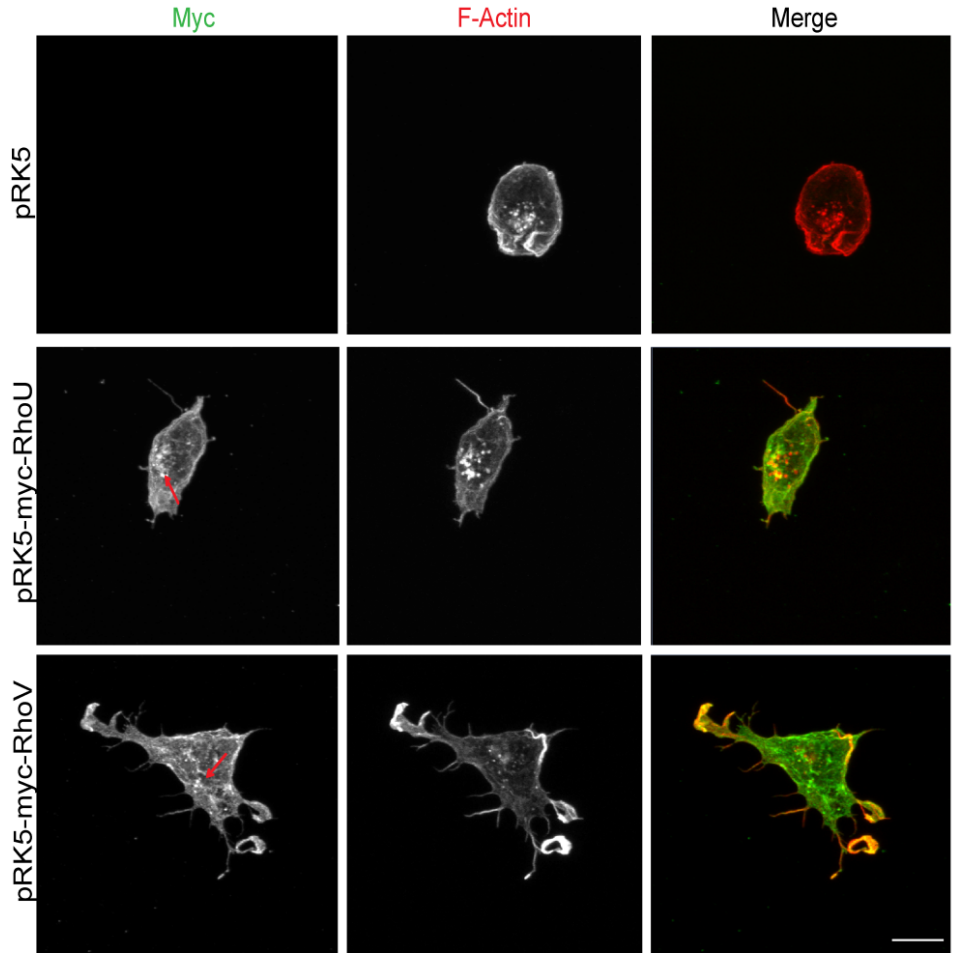

Figure 4.8 RhoU and RhoV overexpression induce cell spreading and filopodium formation. Jurkat (A) or SUPT1 (C) cells were transfected with pRK5 empty vector, pRK5-myc-RhoU and pRK5-myc-RhoV. After 24 h, cells were plated onto fibronectin-coated wells and stimulated with 1 ng/ml CXCL12 for 30 min. Samples were then fixed and stained for F-actin and myc-epitope and imaged by confocal microscopy. Arrows indicate punctate structures. Images show maximum intensity projection of 20 Z-stacks. Scale bar, 20 μm (A) or 10 μm (C). The percentage of Jurkat cells with filopodia formation and cell spreading was quantified by counting 100 myc-epitope positive cells in each of the pRK5-myc-RhoU and pRK5-myc-RhoV samples or 100 random cells in the pRK5 transfected cells in each of 3 independent experiments (B).

4.3.5 Dynamic analysis of RhoU and RhoV distribution

The distribution of RhoU and RhoV was followed by timelapse microscopy. GFP-RhoU or RhoV were expressed in Jurkat cells. RhoU strongly localized in vesicle-like structures and at the plasma membrane. These structures accumulated in the perinuclear area. Vesicles were often observed to traffic toward the lamellipodium and retract from the uropod during cell movement (Figure 49A, B and C). Vesicles were highly dynamic and trafficked to and from the plasma membrane (Figure 4.9D). GFP-RhoU showed a similar distribution during cell movement in CCRF-CEM cells (Figure 4.9F). Similar to GFP-RhoU, GFP-RhoV localized in vesicles in the perinuclear area (Figure 4.10). GFP was expressed as a control in both Jurkat and CCRF-CEM showing a uniform distribution in the entire cell (Figure 4.9E and G). To determine the speed of the vesicles 1 sec per frame movies were acquired. This acquisition allowed better visualization of the trafficking of the vesicles toward and from the plasma membrane (Figure 4.11).

It was really interesting to observe that RhoU and RhoV showed a similar dynamic distribution on vesicles and accumulation on membranes, suggesting they might co-localize. Indeed mCherryRhoU and GFP-RhoV co-localized strongly on vesicles and on the plasma membrane (Figure 4.12). An increase in the speed of the cells was observed when RhoU and RhoV were co-expressed although this has not been quantified so far (Supplementary Movies 22 and 23). It was not possible to perform 1 sec per frame movies of cells co-expressing mCherry-RhoU and GFP-RhoV due to photobleaching and phototoxicity problems. These are mainly induced by excited fluorophores, which produce ROS leading to loss of fluorescence signal and cell death (Hoebe et al., 2007).

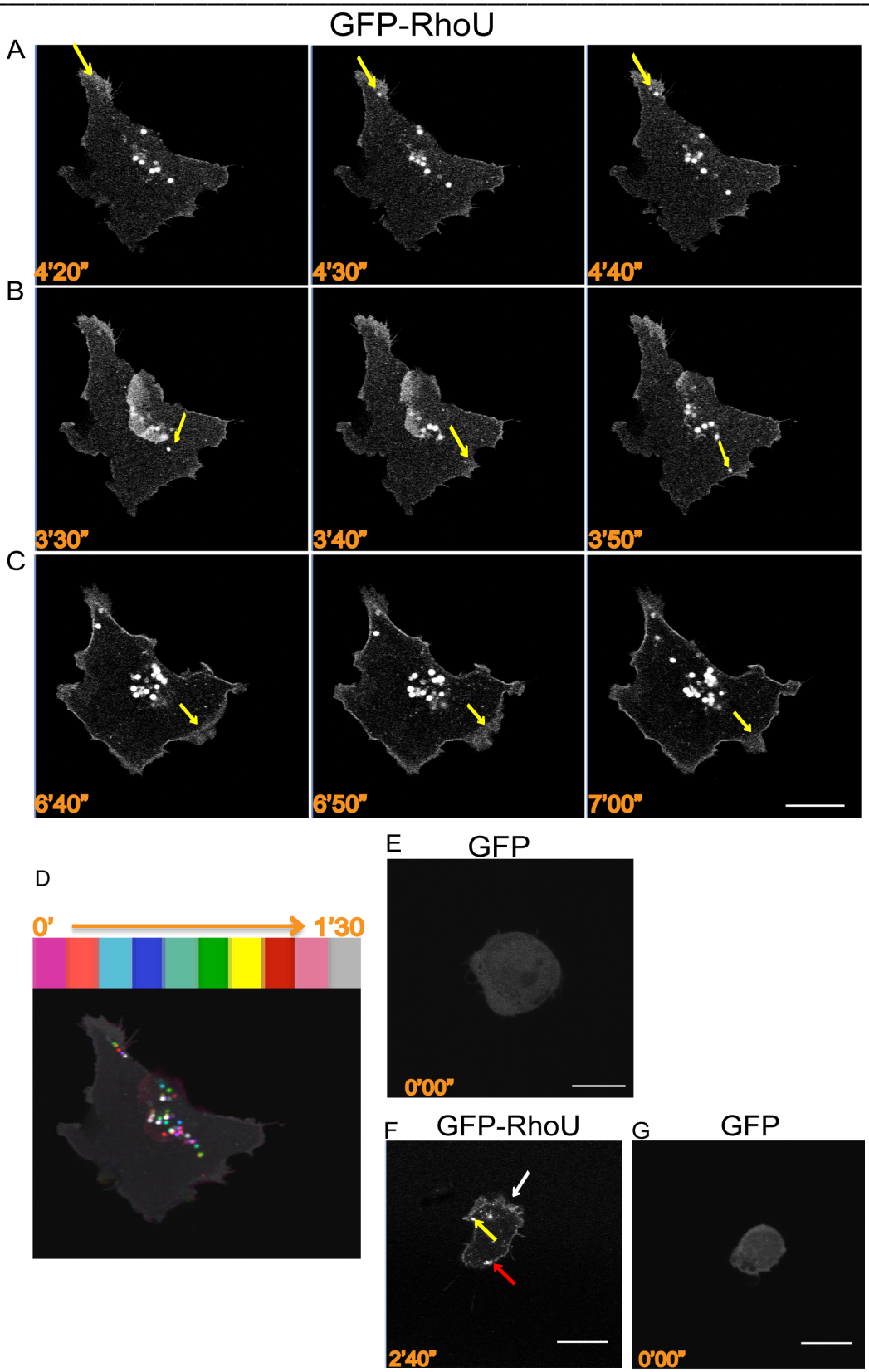

Figure 4.9 RhoU distribution in T-ALL cells. Jurkat or CCRF-CEM cells were transfected with pEGFP-C1 or pEGFP-RhoU plasmid. After 24 h cells were seeded

on fibronectin-coated glass wells and stimulated for 30 min with 1 ng/ml CXCL12. Cells were imaged by confocal microscopy acquiring images every 10 sec for 9 min. (A, B, C and D) Images show 3 frames of pEGFP-RhoU expressing Jurkat cells. (A) Arrows indicates RhoU accumulation at the uropod and vesicle formation during tail retraction. (B) Arrows indicate vesicle trafficking from the perinuclear area toward the plasma membrane. (C) Arrows indicate RhoU accumulation at the lamellipodium. (D) Image shows merging of 10 time frames. Each frame is represented with a different colour. (F) Image shows a frame of pEGFP-RhoU expressing CCRF-CEM cell. The red arrow indicates RhoU vesicles migration from the uropod. The yellow arrow indicates vesicles migrating toward the lamellipodium. The white arrow indicates RhoU accumulation at the lamellipodium. (E and G) Images show Jurkat (E) and CCRF-CEM (G) cell transfected with pEGFP-C1. Scale bars, 10 μm. Images are representative of three cells of three independent experiments.

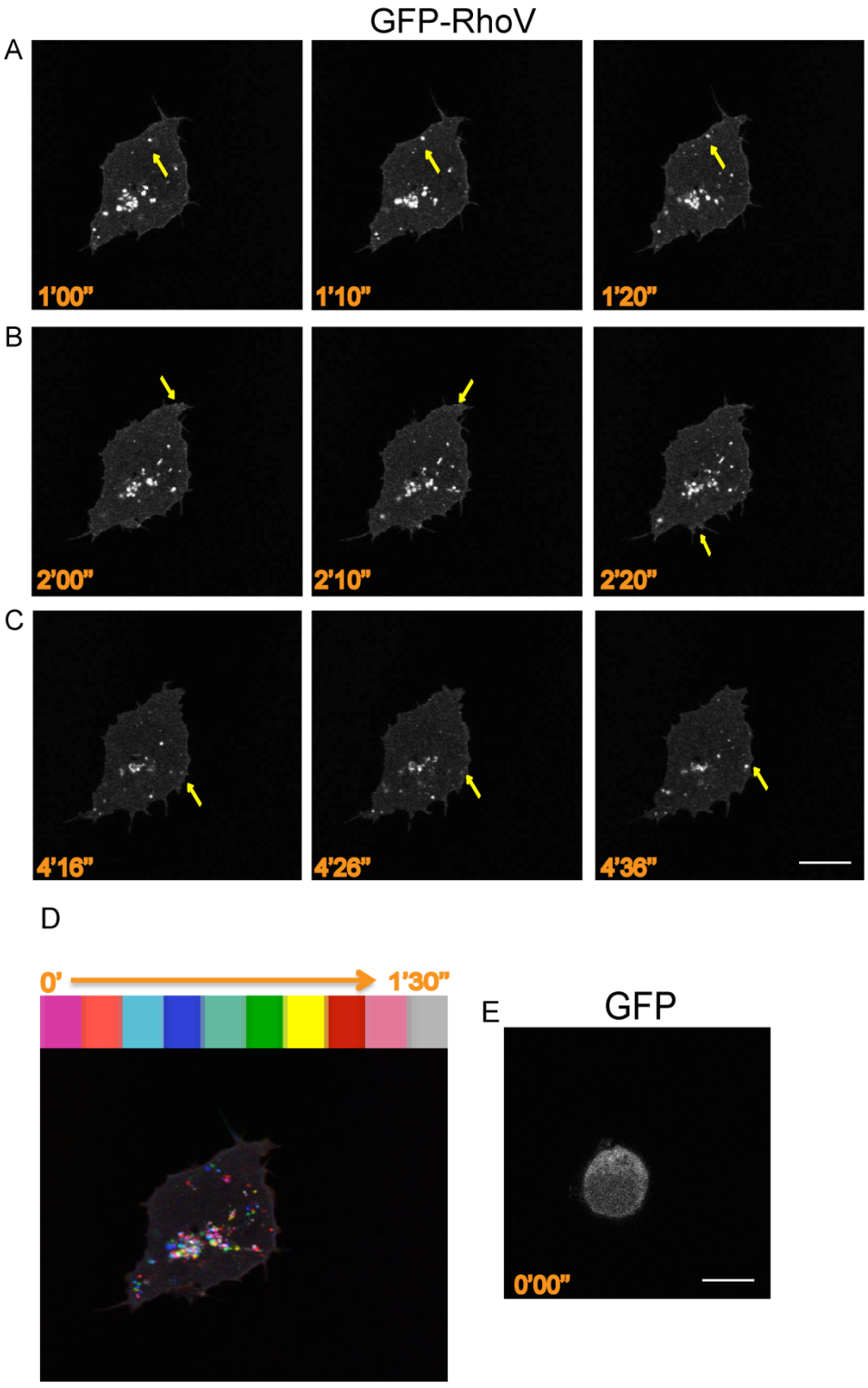

Figure 4.10. RhoV distribution in Jurkat cells. Jurkat cells were transfected with pEGFP-RhoV (A, B, C and D) and pEGFP-C1 (E) plasmid. After 24 h cells were seeded on fibronectin coated glass wells and stimulated for 30 min with 1 ng/ml

CXCL12. Cells were imaged by confocal microscopy acquiring images every 10 sec for 9 min. (A) Arrows indicate vesicle trafficking toward the plasma membrane. (B) Arrows indicate RhoV accumulation at the plasma membrane. (C) Arrows indicate vesicle trafficking from the plasma membrane. (D) Image shows merging of 10 time frames. Each frame is represented with a different colour. (E) Image shows Jurkat cell expressing GFP. Scale bar, 10 μm. Images are representative of three cells of three independent experiments.

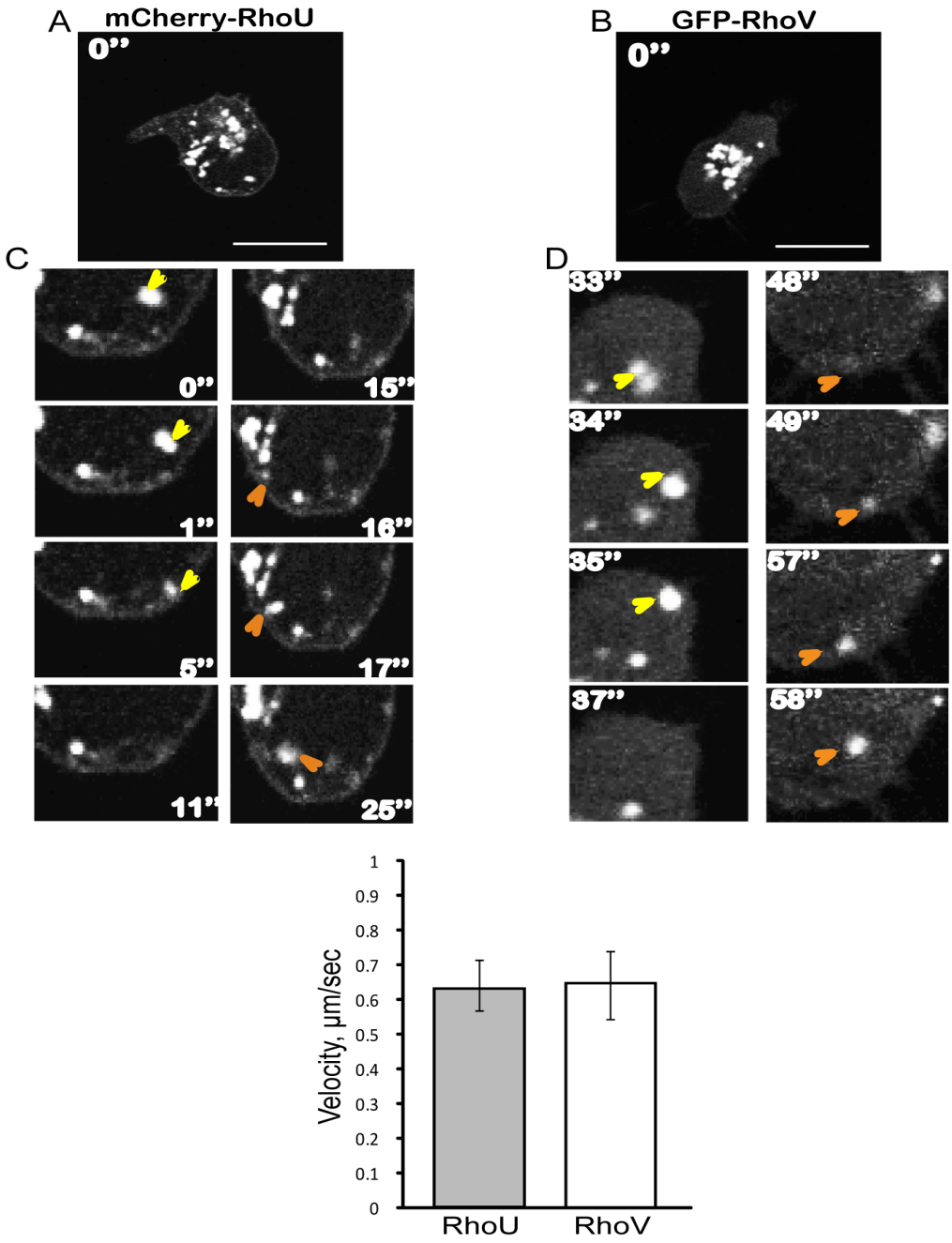

Figure 4.11 RhoU and RhoV distribution in Jurkat cells. Jurkat cells were transfected with pmCherry-RhoU (A, B and D) or pEGFP-RhoV (C and D) plasmid. After 24 h cells were seeded on fibronectin coated glass wells and stimulated for 30 min with 1 ng/ml CXCL12. Cells were imaged by confocal microscopes acquiring images every sec for 1 min. Images show Jurkat cell expressing pmCherry-RhoU (A) of pEGFP-RhoV (B). Zoom of pmCherry-RhoU (B) or pEGF-RhoV (D) showing migration of a vesicle toward (yellow arrows) or from the plasma membrane (orange arrows). (D) Mean of RhoU or RhoV vesicles speed. Relatively velocity was

determined by tracking 10 vesicles per condition of three independent experiments. Scale bar, 10 μm.

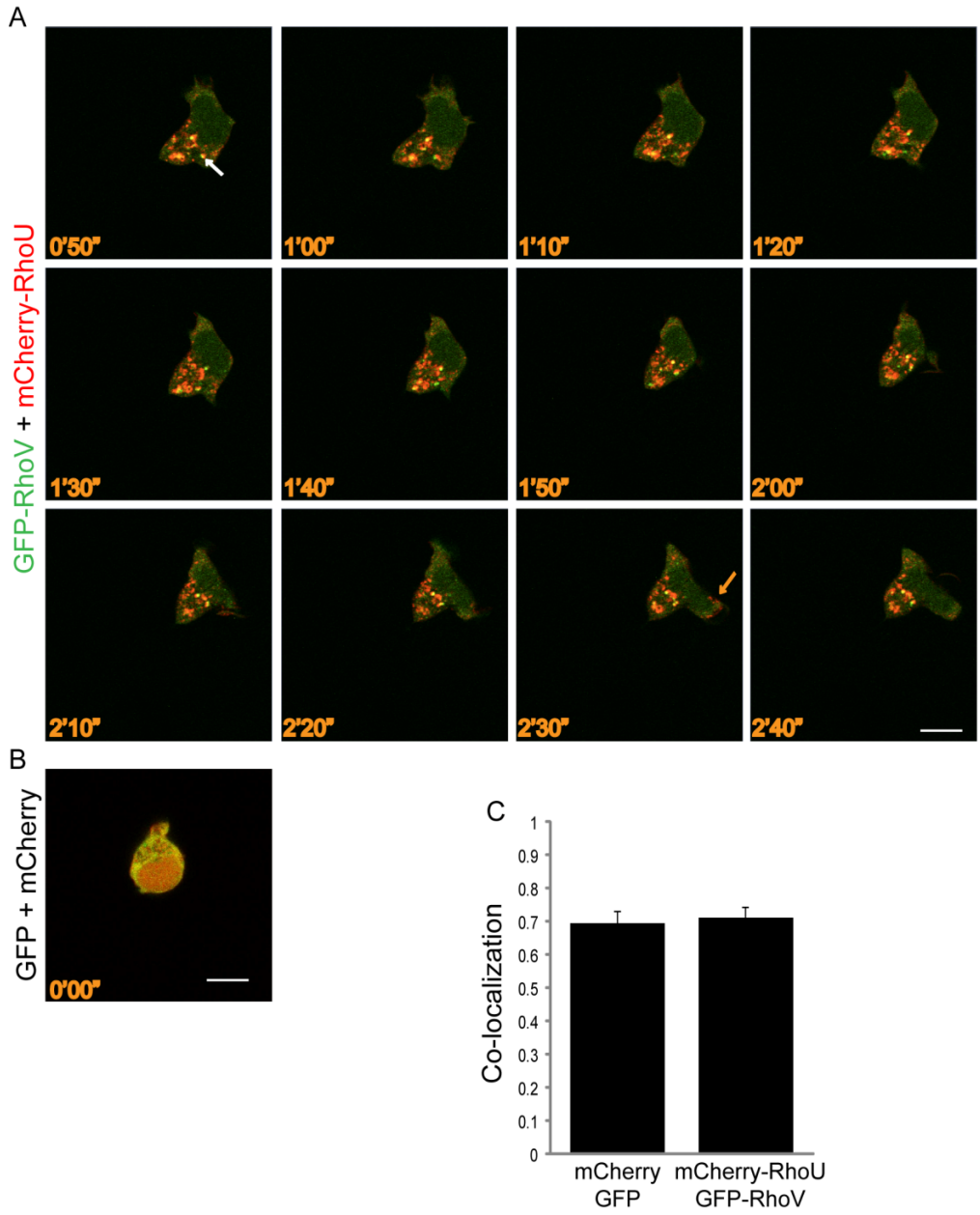

Figure 4.12 RhoU and RhoV co-localize. Jurkat cells were co-transfected with pEGFP-RhoV and pmCherry-RhoU or GFP and mCherry empty vector. After 24 h, cells were seeded onto FN-coated glass wells and stimulated for 30 min with 1 ng/ml CXCL12. Cells were imaged by confocal microscopy acquiring images every 10 sec for 10 min. (A) Images show 12 sequential frames of a Jurkat cell expressing GFP-RhoV and mCherry-RhoU. The white arrow indicates RhoU-RhoV co-localization in vesicles and the orange arrow accumulation in the front of the cell. (B) Images show Jurkat cell co-transfected with GFP and mCherry empty vector. Scale bars, 10 μm. Images are representative of three independent experiments. (C) Graph represents

co-localization of pEGFP-RhoV and pmCherry-RhoU using Zeiss Software. Mean of three frames of each cells of three independent experiments.

4.3.6 RhoU and RhoV localize in part on endosomes

RhoU and RhoV-containing vesicles accumulated in the perinuclear area around the MTOC as indicated by α-tubulin staining of myc-RhoU and myc-RhoV transfected cells (Figure 4.13). This distribution suggested an endosomal localization (Palfy et al., 2012). This was investigated using an antibody to an early-endosomal protein (EEA1). EEA1 interacts with early endosomes via binding to the membrane lipid phosphatidylinositol 3- phosphate and the active form of the small GTPase Rab5 (Callaghan et al., 1999). Unfortunately antibodies against RhoU and RhoV suitable for immunofluorescence experiments with endogenous RhoU and RhoV are not available. Therefore, immunofluorescence analysis was carried out on cells expressing exogenous RhoU and RhoV as described below.

mCherry-RhoU or GFP-RhoV showed a partial co-localization with EEA1 in Jurkat cells (Figure 4.14). The co-localization was also observed in cells co-expressing RhoU and RhoV (Figure 4.15). Cdc42 was reported to localize to the Golgi (Hehnly et al., 2010). It was therefore interesting to investigate if RhoU and RhoV localize to the Golgi. Jurkat cells expressing Myc-RhoU or Myc-RhoV were stained with GM130 antibody. This antibody is used as Golgi marker as it recognizes GM130 protein. This is a peripheral cytoplasmic protein part of the cis-Golgi matrix, and has a role in maintaining cis-Golgi structure (Nakamura et al., 1995). Myc-RhoU and Myc-RhoV did not co-localize with GM130 (Figure 4.16).

In summary, these results demonstrate that RhoU and RhoV partially co-localize on endosomes and the plasma membrane.

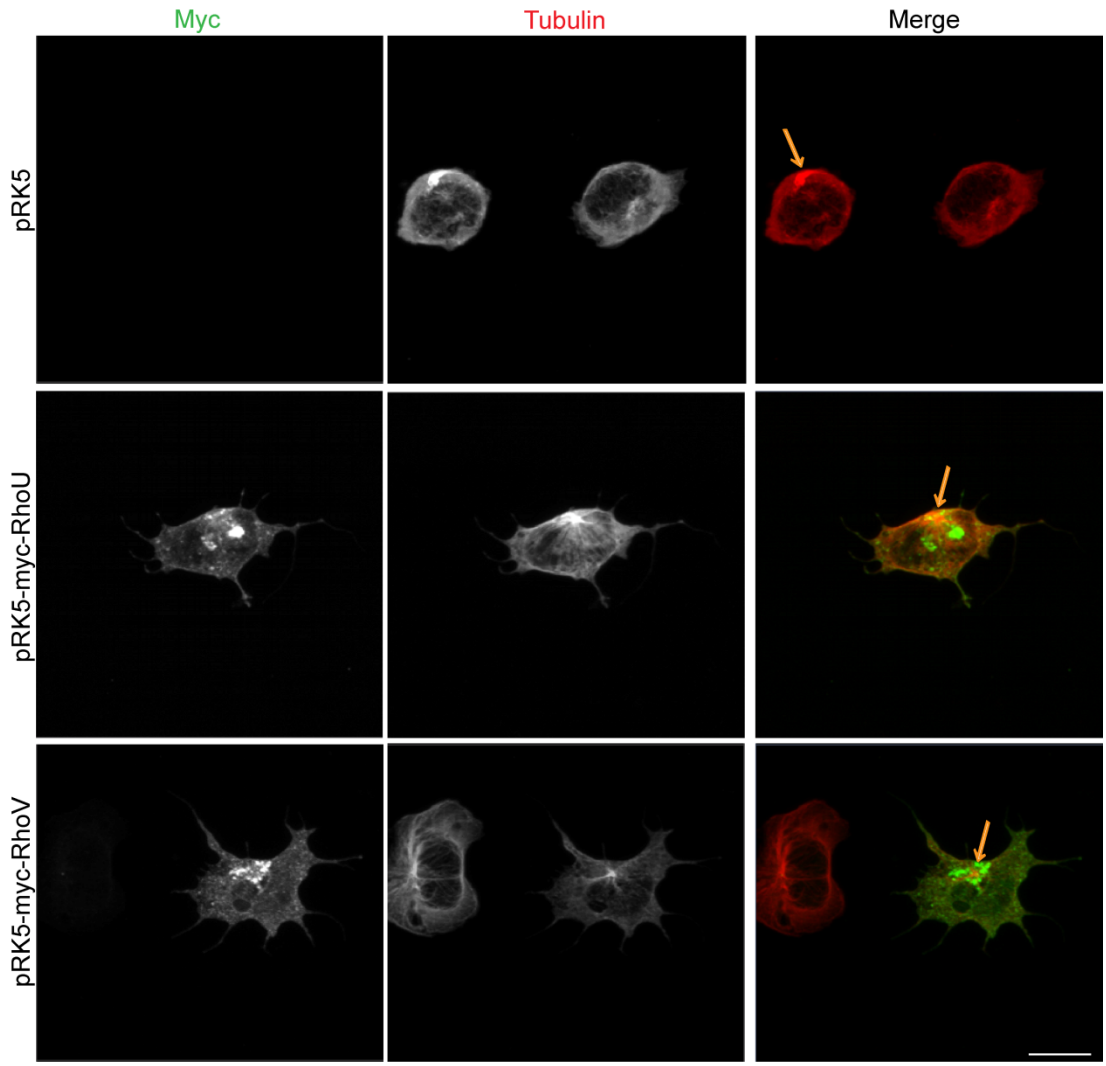

Figure 4.13 RhoU and RhoV-containing vesicles localize around the MTOC. Jurkat cells were transfected with pRK5, pRK5-myc-RhoU and pRK5-myc-RhoV. After 24 h cells were plated onto fibronectin-coated wells and stimulated with 1 ng/ml CXCL12. Samples were then fixed and stained for α-tubulin and myc-epitope, and imaged by confocal microscopy. Arrows indicate the MTOC. Scale bar, 10 μm. Images are representative of three independent experiments.

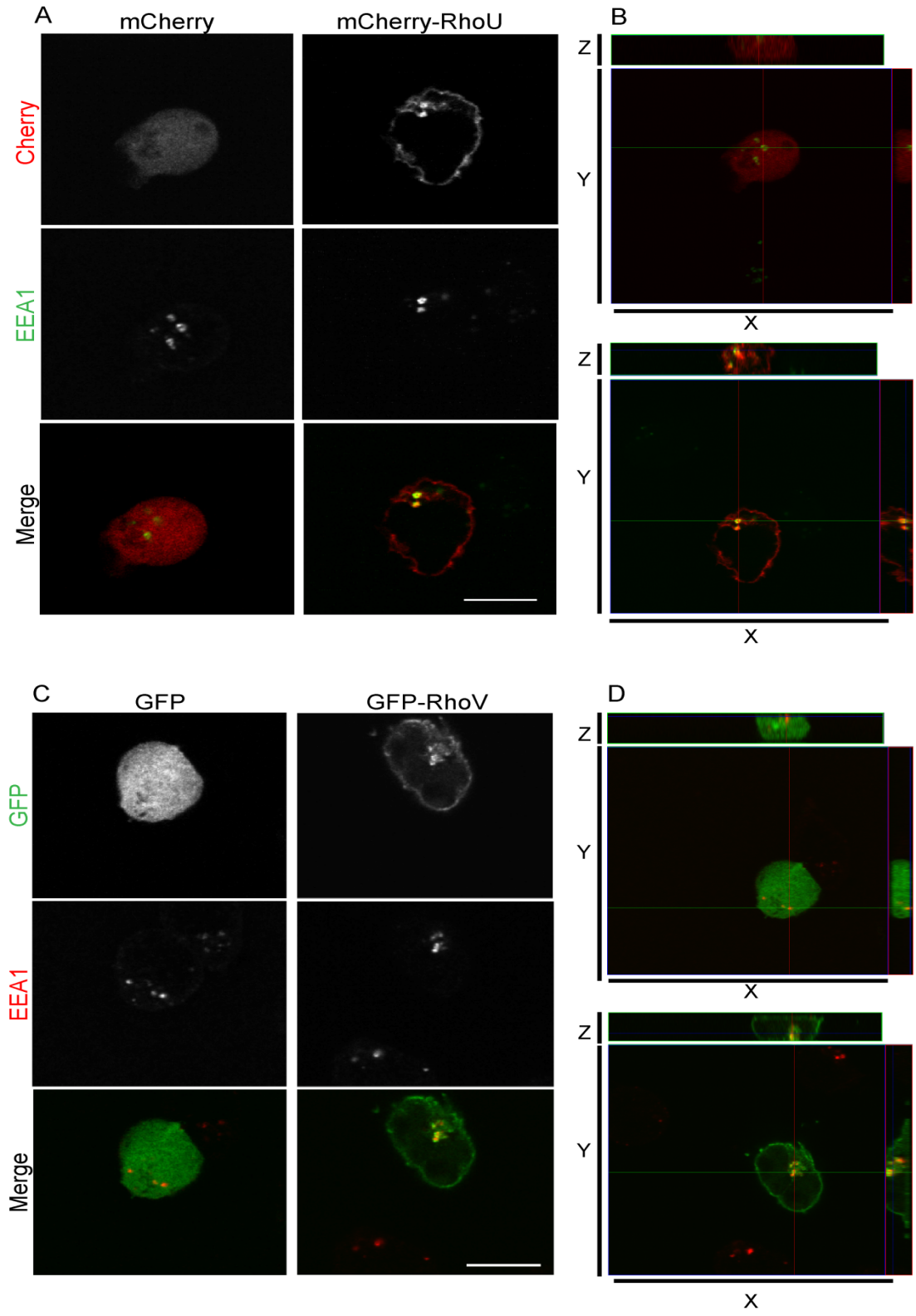

Figure 4.14 RhoU and RhoV localize on endosomes. Jurkat cells were transfected with pmCherry-C1, pmCherry-RhoU (A and B), pEGFP-C1 and pEGFP-RhoV (C and D). After 24 h cells were plated onto FN-coated wells and stimulated with 1 ng/ml CXCL12. Samples were then fixed and stained for EEA1 and imaged by confocal microscopy. Scale bars, 10 μm. Images (B and D) show ortho projections. Images are representative of three independent experiments.

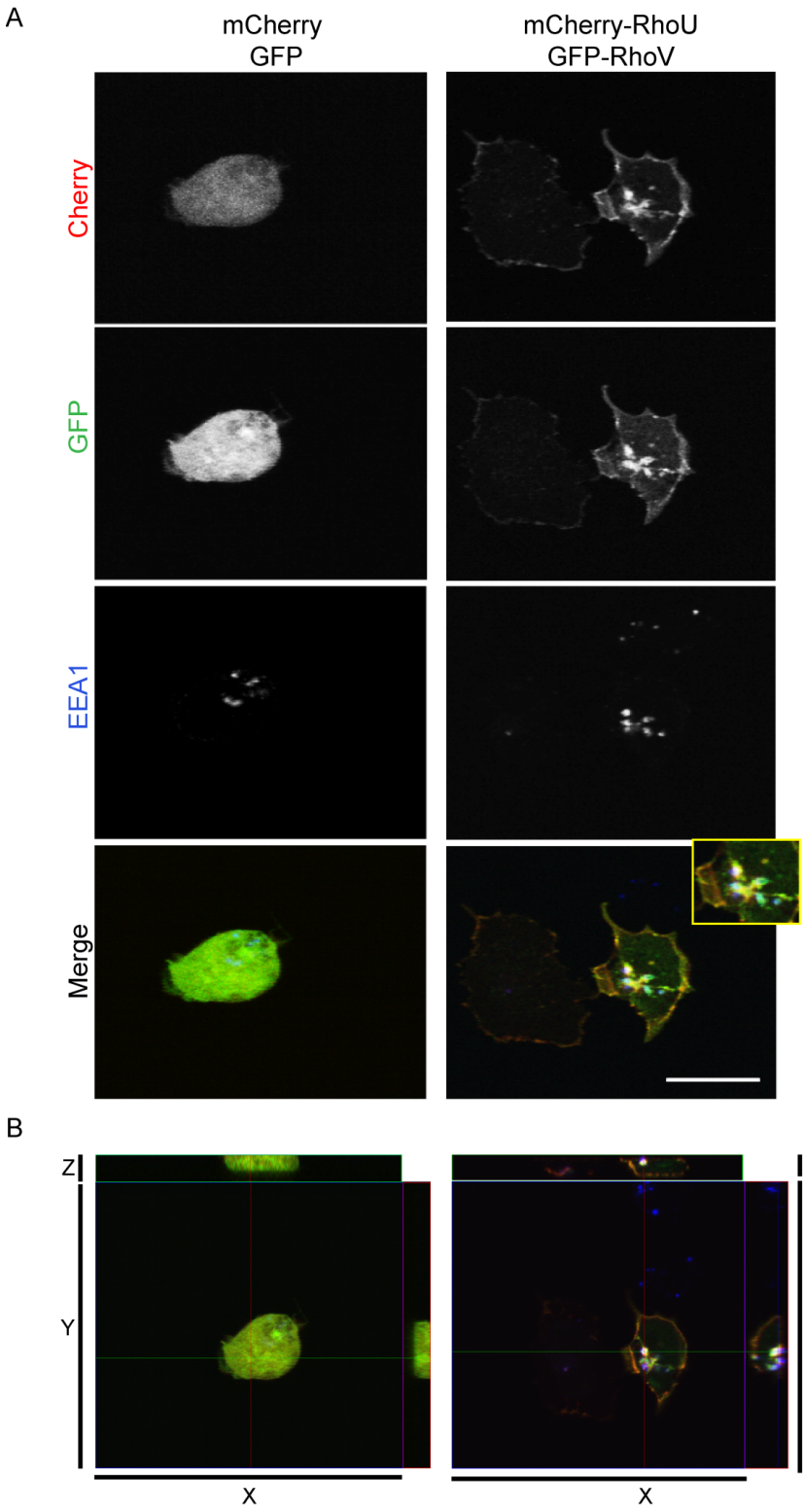

Figure 4.15 RhoU and RhoV co-localize on endosomes. Jurkat cells were co-transfected with plasmid encoding pEGFP-C1 and pmCherry-C1 (top panel), and vectors encoding pmCherry-RhoU and pEGFP-RhoV (bottom panel). After 24 h cells were plated onto fibronectin-coated wells and stimulated with 1 ng/ml CXCL12. Samples were then fixed and stained for EEA1 and imaged by confocal microscopy. Scale bar, 10 μm. Images (B) show ortho projections. Images are representative of three independent experiments.

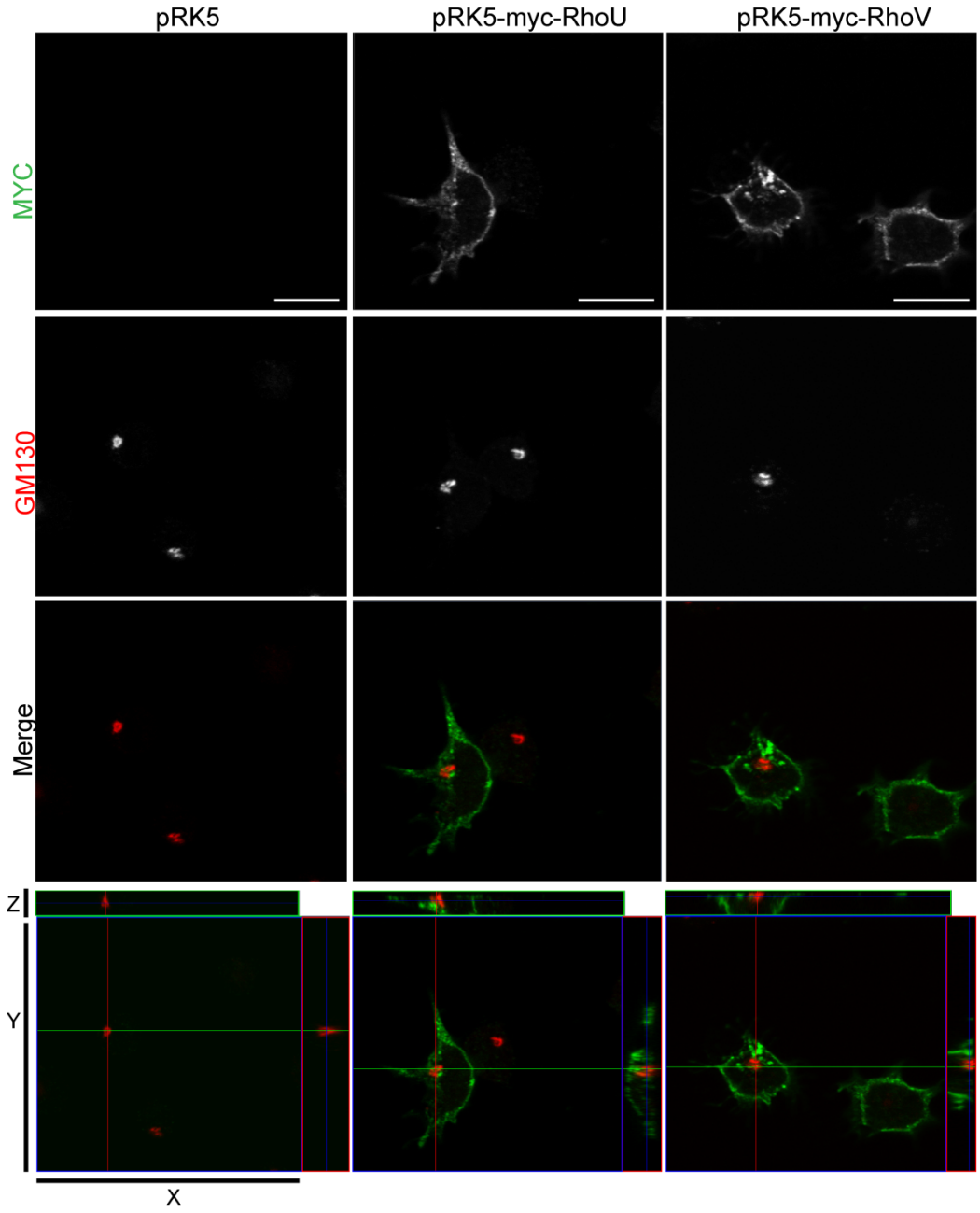

Figure 4.16 RhoU and RhoV do not localize to the Golgi. Jurkat cells were transfected with control pRK5, pRK5-myc-RhoU and pRK5-myc-RhoV. After 24 h cells were plated onto fibronectin-coated coverslips and stimulated with 1 ng/ml CXCL12. Samples were then fixed and stained for GM130 Golgi marker and myc and imaged by confocal microscopy. Scale bars, 10 μm. The bottom panels show ortho projections of the images. Images are representative of three independent experiments.

4.3.7 RhoU interacts with RhoV

Immunofluorescence analysis and live imaging movies of Jurkat cells showed a partially colocalization of RhoU and RhoV on endosomes and at the plasma membrane. To determine if an interaction occurs between RhoU and RhoV, Cos7 cells were cotransfected with plasmids encoding GFP-RhoV and Myc-RhoU. (Figure 4.17). GFP-RhoV was present in immunoprecipitates of myc-RhoU.

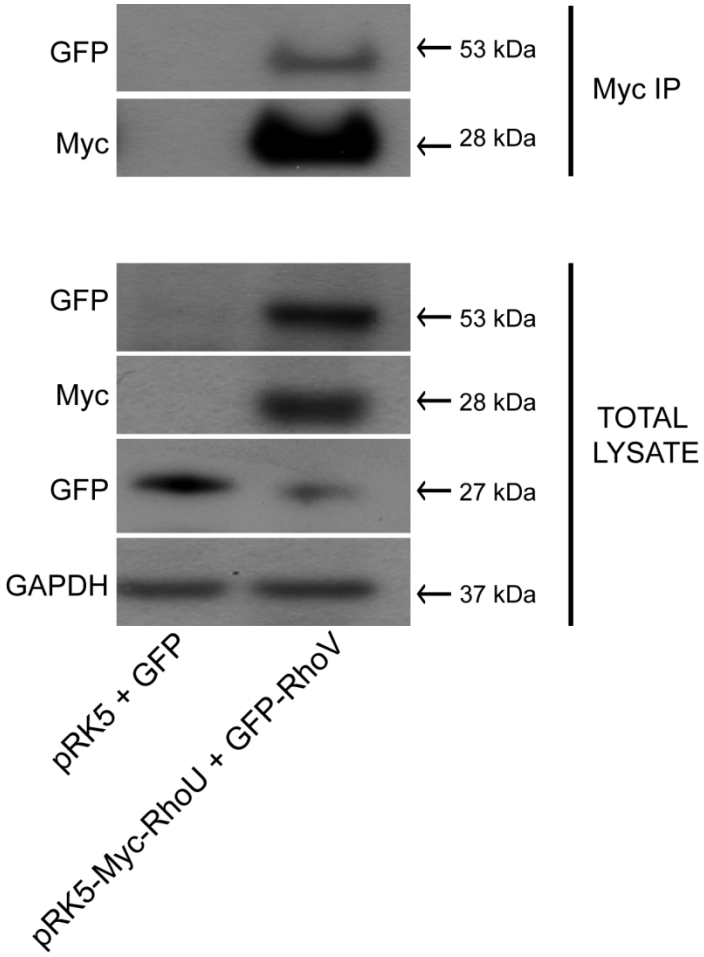

Figure 4. 17. Coimmunoprecipitation of RhoU and RhoV. Cos7 cells were transfected with pRK5-myc-RhoU and pEGFP-RhoV or empty vectors. After 24 h cells were lysed and cell lysates incubated with anti-myc-epitope agarose beads. GFP and GFP-RhoV proteins interacting with RhoU were detected by immunoblotting with antibody to GFP. GAPDH was used as a loading control. Image is representative of three independent experiments.

4.3.8 The N-terminus of RhoV is not required for RhoU binding

Unlike other Rho GTPases, RhoU has a prolin rich domain (Saras et al., 2004) that is likely to interact with SH3 domain containing proteins (see section 1.3.4.1 and 1.3.4.2). As the SH3 domain could act as an adaptor between two proteins, it was hypothesized that the interaction between RhoU and RhoV could occurred via the N-terminus of these proteins. To investigate the requirement of this domain, Cos7 cells were cotransfected with plasmid encoding GFP-RhoV lacking the N-terminal domain (ΔN-RhoV) or full length RhoV with Myc-RhoU plasmid (Figure 4.18). Wild type and ΔN-RhoV were both able to coprecipitate with RhoU suggesting that the interaction is not mediated through the N-terminal portion of RhoV.

```
RhoV    MPPRELSEAEPPPLRAPTPPPRRRSAPPELGIKCVLVGDGAVGKSSLIVSYTCNGYPARYRPTALDT 67
ΔNRhoV  MPPREL----------------------GIKCVLVGDGAVGKSSLIVSYTCNGYPARYRPTALDT 43

RhoV    FSVQVLVDGAPVRIELWDTAGQEDFDRLRSLCYPDTDVFLACFSVVQPSSFQNITEKWLPEIRTHNP 134
ΔNRhoV  FSVQVLVDGAPVRIELWDTAGQEDFDRLRSLCYPDTDVFLACFSVVQPSSFQNITEKWLPEIRTHNP 110

RhoV    QAPVLLVGTQADLRDDVNVLIQLDQGGREGPVPQPQAQGLAEKIRACCYLECSALTQKNLKEVFDSA 201
ΔNRhoV  QAPVLLVGTQADLRDDVNVLIQLDQGGREGPVPQPQAQGLAEKIRACCYLECSALTQKNLKEVFDSA 177

RhoV    ILSAIEHKARLEKKLNAKGVRTLSRCRWKKFFCFV 236
ΔNRhoV  ILSAIEHKARLEKKLNAKGVRTLSRCRWKKFFCFV 212
```

Figure 4.18 Sequence comparison between RhoV and ΔN-RhoV.

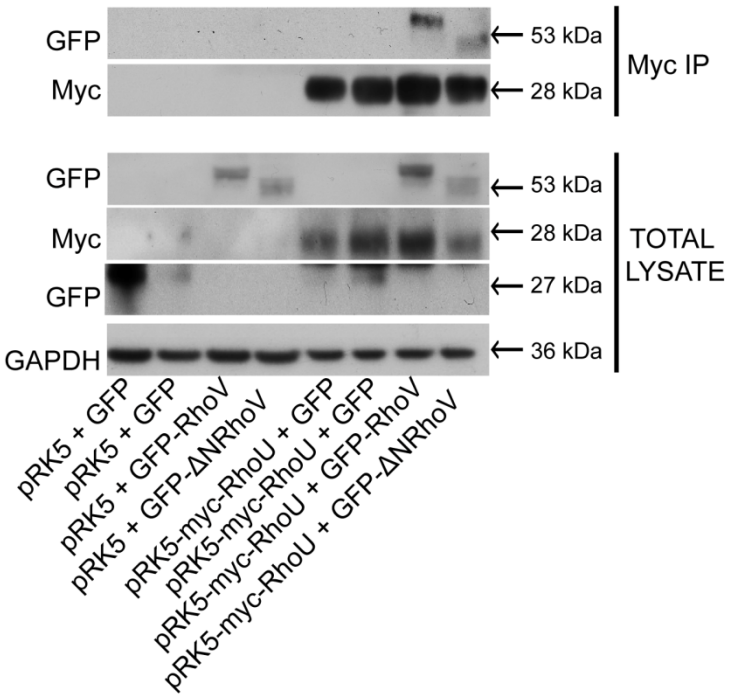

Figure 4.19 Coimmunoprecipitation of RhoU and ΔNRhoV. Cos7 cells were transfected with pRK5-mycRhoU and full length pEGFP-RhoV, CB6-GFP-ΔNRhoV or empty vectors. After 24 h, cells were lysed and incubated with anti-myc-epitope agarose beads. GFP and GFP-RhoV proteins interacting with RhoU were detected by immunoblotting with antibody to GFP. GAPDH was used as a loading control. Image is representative of three independent experiments.

.

4.3.9 FLIM analysis of Jurkat cells expressing cherry-RhoU and GFP-RhoV or GFP-ΔNRhoV

Immunofluorescence analysis and coimmunprecipitation experiments showed that RhoU and RhoV interact. This interaction was further analyzed. A widely used method to study protein-protein interactions in single cells (live or fixed) is Förster resonance energy transfer (FRET). FRET is a dipole-dipole coupling process where two proteins of interest are attached to two fluorophores (donor and acceptor) (Peter et al., 2005). Fluorophores have characteristic excitation and emission spectra. If these two molecules are close in proximity, the excitation of the donor fluorophores leads to a transfer of the energy to the acceptor, resulting in higher acceptor emission and quenching of the donor (Wouters et al., 2001). The absorption spectrum of the acceptor must overlap the spectrum of the fluorescence emission of the donor in order for the energy transfer to occur. Different pairs of fluorophores with overlapping emission can be used, including CFP/YFP, BFP/EGFP or GFP/mCherry (Morton and Parsons, 2011). The energy transfer can occur between fluorophores which are up to 11 nm apart (Sekar and Periasamy, 2003). In FLIM instead of fluorescence intensity, the fluorescence lifetime is measured. Fluorophores are not just characterized by an excitation and emission spectra but also by their lifetimes. The lifetime of a fluorophore refers to the average time it stays in its excitation state before emitting a photon. The fluorescence lifetime of a fluorophore is affected by FRET and in the presence of a suitable acceptor, the lifetime of the donor will decrease. This decrease in lifetime is measured by FLIM (Morton and Parsons, 2011).

In the experiments analysed by Dr Maddy Parsons, FLIM was used to measure fluorescence lifetime of GFP. The GFP lifetime of cells expressing “GFP-alone” was important to compare the difference in the GFP lifetime and the GFP lifetime in the presence of the acceptor (Morton and Parsons, 2011). FLIM analysis of Jurkat cells co-expressing RhoU and RhoV showed these proteins interact at the plasma membrane and partially in the cytoplasm. These results suggest that RhoU and RhoV are able to form heterodimers (Figure 4.20A and C).

To investigate whether RhoU and ΔNRhoV interact in T-ALL cells. Jurkat cells co-expressing mCherry-RhoU and GFP-ΔNRhoV were used. This was analysed by Dr Maddy Parsons in Jurkat cells cotransfected with cherry-RhoU and GFP-ΔNRhoV.

FLIM analysis of Jurkat showed that ΔNRhoV was still able to interact at the plasma membrane and in the cytoplasm with RhoU (Figure 4.20B and C).

Taking together these results demonstrate that RhoU interacts with RhoV and that this interaction occurs at the plasma membrane and in vesicles. RhoV lacking the N-terminus of proline-rich domain is still able to bind RhoU suggesting this domain is not required for their binding. It will be important to generate new mutants in order to determine which domains of RhoV and RhoU are critical for their interaction.

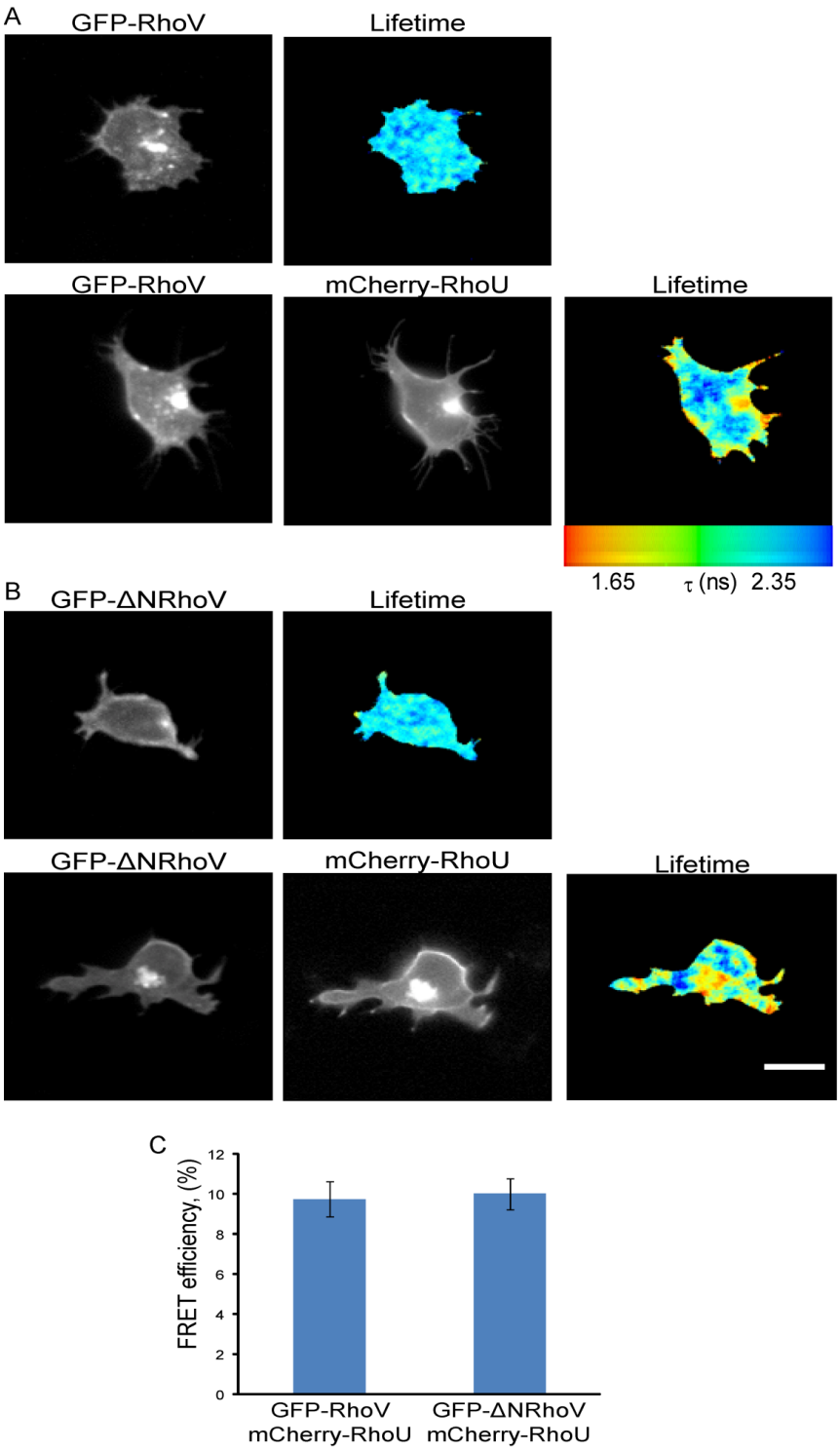

Figure 4.20 FLIM analysis of RhoU and RhoV interaction. Jurkat cells were transfected with plasmids encoding pEGFP-RhoV or co-transfected with pmCherry-RhoU and pEGFP-RhoV (A) or CB6-GFP-ΔNRhoV (B). After 8 h, cells were seeded on FN-coated glass bottom coverslips and stimulated with 1 ng/ml CXCL12. After 30 min cells were fixed and subjected to FRET analysis by FLIM. FRET is depicted using a pseudocolour scale (blue, normal lifetime, red FRET). Graph (C) represents FRET efficiency of 16 cells for each sample. Error bars indicate ± SEM.

4.3.10 RhoU and RhoV form homodimers

Since RhoU and RhoV heterodimerize, the possibility that they homodimerize was investigated. Cos7 cells were co-transfected with plasmids encoding GFP-RhoU and myc-RhoU, or cotransfected with GFP-RhoV and myc-RhoV. Immunoprecipitation analysis showed that myc-RhoU associates with GFP-RhoU and myc-RhoV with GFP-RhoV (Figure 4.21).

These results suggest that both RhoU and RhoV are able to form homodimers, although this could be an indirect interaction mediated by other proteins.

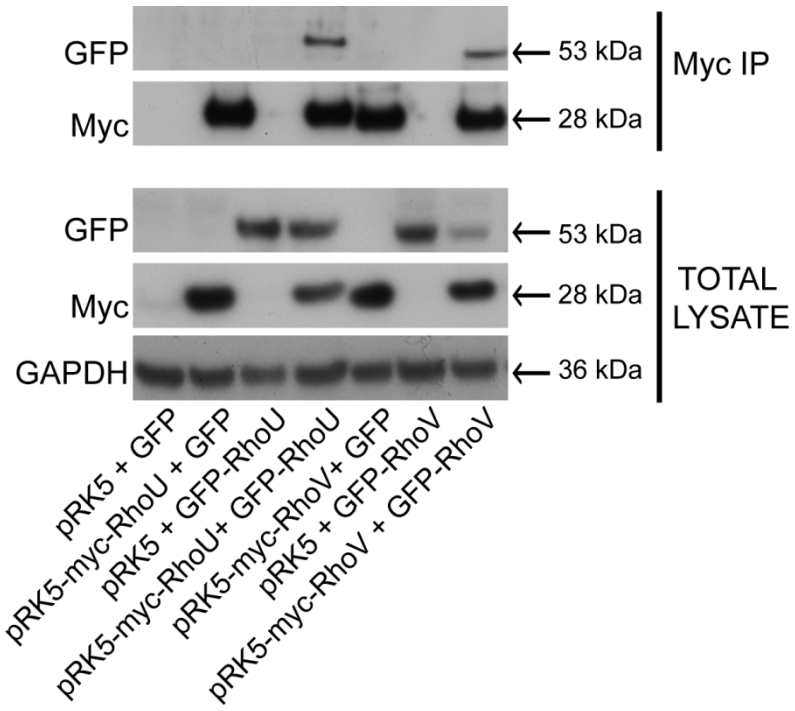

Figure 4.21 RhoU and RhoV homodimerize. Cos7 cells were cotransfected with pRK5-myc-RhoU and pEGFP-RhoU or pRK5-myc-RhoV and pEGFP-RhoV or empty vectors. After 24 h cells were lysed and incubated with myc-epitope agarose beads. GFP proteins interacting with RhoU or RhoV were detected by immunoblotting with antibody against GFP. Image is representative of two independent experiments.

4.3.11 RhoU interacts with Rac1, Rac2 and RhoV but not RhoA or Cdc42.

In the previous chapter, RhoU depletion was shown to affect the morphology and migration of T-ALL cell lines. It is possible that RhoU acts through RhoA, Cdc42,

Rac1 or Rac2, which are well-characterized for their roles in migration and cytoskeleton rearrangement (Rougerie and Delon, 2012). A possible interaction of RhoU with these GTPases has not been investigated before. Interestingly RhoU co-immunoprecipitated not only with RhoV but also with Rac1 and Rac2. However it did not co-immunoprecipitate with RhoA and Cdc42, demonstrating the specificity of these interactions (Figure 4. 22)

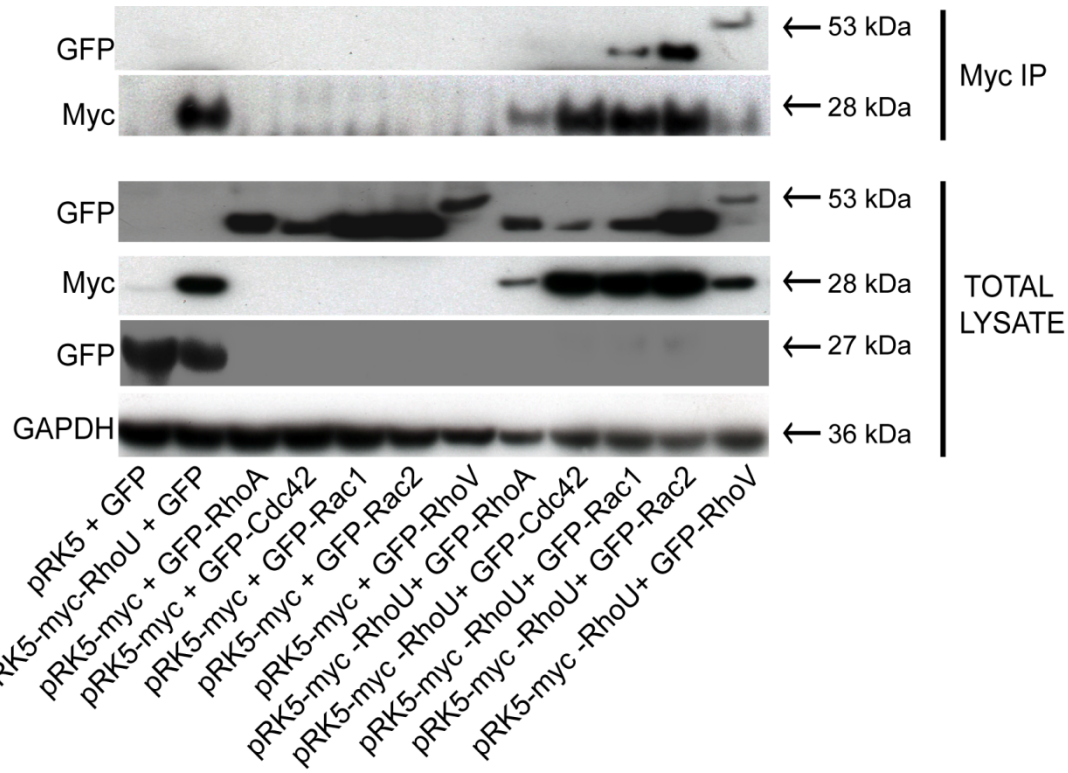

Figure 4.22 RhoU co-immunoprecipitates with Rac1, Rac2 and RhoV. Cos7 cells were transfected with pRK5-mycRhoU and CB6-GFP-RhoA, CB6-GFP-Cdc42, CB6-GFP-Rac1, pEGFP-Rac2 or pEGFP-RhoV or empty vectors. After 24 h cells were lysed and incubated with myc-epitope agarose beads. GFP proteins interacting with RhoU were detected by immunoblotting with antibody against GFP. Image is representative of three independent experiments.

4.3.12 RhoU but not Rac1 and RhoV interact with NCK1

NCK1 and NCK2 are adaptor proteins containing three SH3 domains and one SH2 domain. NCK1 protein has been shown to interact with a proline-rich region of R-Ras (Wang et al., 2000) and to interact with proteins involved in cytoskeleton regulation. It was demonstrated that RhoU binds NCK2 and that the N-terminus of RhoU mediates this interaction (Saras et al., 2004). Moreover Rac1 associates with the adapter protein Crk via a proline-rich region in its C-terminus (van Hennik et al., 2003). It was therefore hypothesized that a bridge between RhoU and Rac could be mediated by NCK1. This was investigated by coimmunoprecipitation analysis. Cos7 cells were cotransfected with GFP plasmids encoding for RhoU, RhoV or Rac1, and Myc-NCK1 (kind gift of Matthias Krause) and cell lysate incubated with Myc-beads. Preliminary western blot results confirmed that RhoU interacted with NCK1, but not Rac1 and RhoV (Figure 4.23). As NCK1 appears not to be an adaptor protein for Rac1 or RhoV, it is unlikely to link RhoU to these two Rho GTPases.

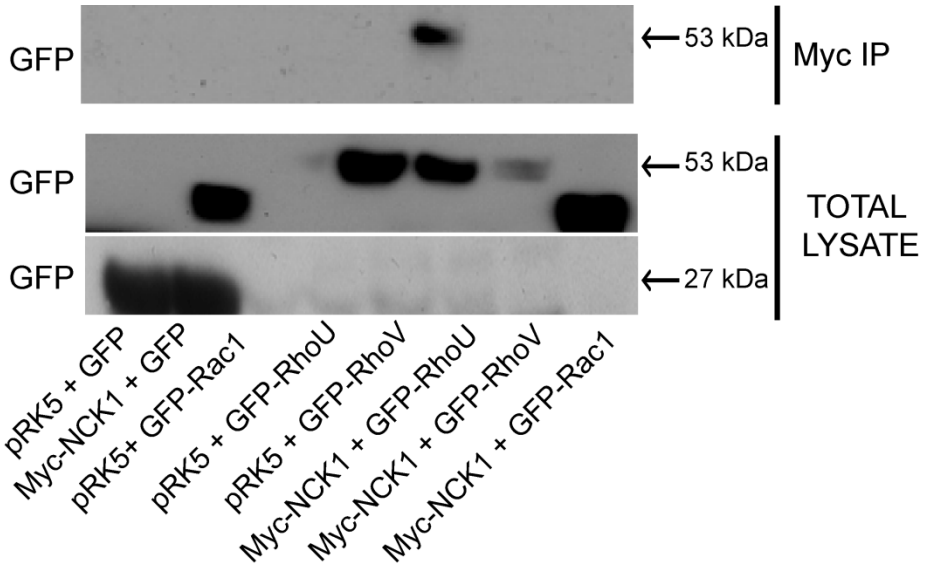

Figure 4.23 NCK1 co-immunoprecipitates with RhoU but not Rac1 or RhoV. Cos7 cells were cotransfected with pEBB-myc-NCK1 and pEGFP-RhoU, pEGFP-RhoV or CB6-GFP-Rac1. After 24 h cells were lysate and incubated with myc-epitope agarose beads. GFP proteins interacting with RhoU were detected by immunoblotting with antibody to GFP. Image of one single experiment.

4.3.13 RhoV regulates RhoU levels

siRNA depletion of RhoV induces a similar functional effect to RhoU depletion cells. RhoU and RhoV are both important for adhesion to fibronectin and endothelial cells. Moreover a reduction in transendothelial migration has been observed when these proteins are knocked down. It was therefore tested whether RhoV was able to affect RhoU expression levels. Western blotting analysis of RhoV-depleted cells with two single oligos showed a decrease in the protein expression of RhoU compared to Mock or siControl (Figure 4.24A and B). It was not possible to investigate if RhoU knockdown affects RhoV level due to a lack of a specific antibody. To determine whether RhoV was directly able to induce RhoU expression, GFP-RhoV was expressed in COS7 cells. RhoV expression leads to an increase in RhoU protein level (Figure 4.24C and D). Taking together, these results showed that RhoV signaling could regulate the expression of RhoU.

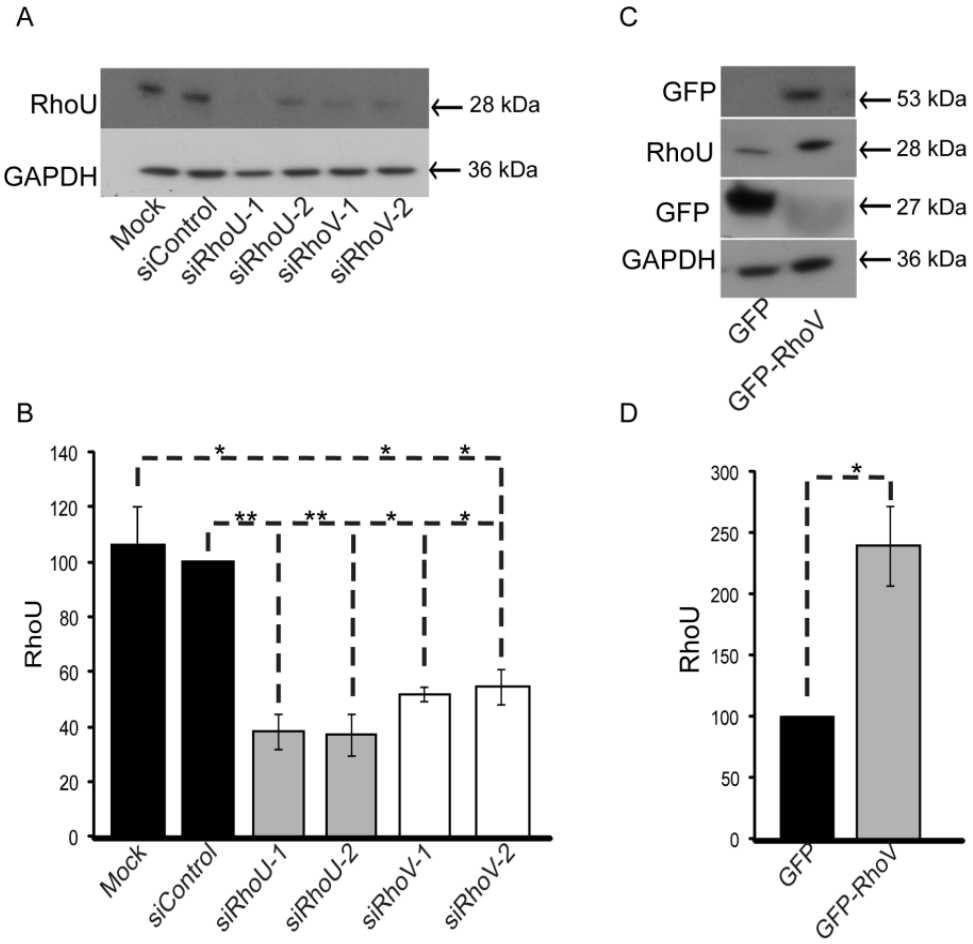

Figure 4.24 RhoV regulates RhoU expression. (A and B) Jurkat cells were transfected with transfection reagent alone (MOCK), control siRNA or two different siRNAs targeting RhoU and RhoV. Cells were lysed after 72 h and analysed by immunoblotting using the indicated antibodies. (B) Relative RhoU levels were quantified using ImageJ. (C and D) Cos7 cells were transfected with vectors encoding for GFP or GFP-RhoV. After 24 h cells were lysed and analysed by immunoblotting using the indicated antibodies. (D) Relative RhoU levels were quantified using ImageJ. Data shown are the mean of 3 independent experiments ± SEM. * $p<0.05$, **$p<0.01$; 2-way-paired t-test. GAPDH was used as a loading control.

4.4 Discussion

The aim of the research described in this chapter was to investigate the role of RhoU and RhoV in T-ALL cell adhesion and migration. It was demonstrated that both RhoU and RhoV depletion reduced Jurkat cell adhesion to fibronectin and endothelial cells and decreased transendothelial migration. RhoU and RhoV localized on endosomes and the plasma membrane. RhoU and RhoV were found to interact and to form hetero- and homodimers. Intriguingly, RhoV was demonstrated to modulate RhoU protein expression.

RhoU and RhoV were in vesicular structures and on the plasma membrane. Timelapse movies revealed that these vesicles traffic to and from the plasma membrane. RhoU and RhoV could be involved in vesicular trafficking of proteins to the plasma membrane, or they might play a role at the plasma membrane and be transported there by vesicles. RhoU and RhoV were also found to co-localize on these vesicles, suggesting they might cooperate to regulate membrane trafficking. The vesicles were found to be endosomes, a well-characterized cell compartment that provides a spatio-temporal regulation of cell signalling. Several Rho GTPases are involved in membrane trafficking (Segev, 2011). Rac1 and RhoA are involved in the uptake of extracellular material through pinocytosis and phagocytosis (Castellano et al., 2000; Leung et al., 1999). Cdc42 was demonstrated to control antigen internalization in dendritic cells (DC). Immature DCs actively internalize antigen, while in mature DCs endocytocis is strongly reduced as these cells mainly present the antigen to T cells. The reduction in endocytosis was demonstrated to reflect dowregulation of Cdc42 activaty (Garrett et al., 2000).

Generally, endocytosed molecules, including receptors, are first delivered to early endosomes which therefore provide spatial regulation of signalling (Vignjevic et al., 2006). Different mechanisms of internalization have been identified. The best characterized is clathrin-dependent endocytosis, which involves the assembly of different proteins including clathrin to form a clathrin-coated pit (CCP) on the cytplasmic face of the plasma membrane. The CCP facilitates the accumulation of the molecules that needed to be internalized. CCP then invaginate and form vesicles inside the cell (Yamashiro et al., 1998). The Rho GTPases RhoA and Rac1 were reported to inhibit CCP-dependent internalization of the transferrin receptors (Ellis and Mellor, 2000). Rho GTPases are also involved in clathrin-independent

internalization. These endocytic pathways are driven by actin polymerization and include phagocytosis, caveolar-mediated uptake and pinocytosis.

Ative Rac1 has been observed in early endosomes. These compartments were suggested to be important in regulating Rac1 distribution towards specific area of the cells in order to promote membrane ruffling (Miaczynska and Bar-Sagi, 2010). Rac1 co-localize at the plasma membrane and on endosomes with ADP-ribosylation factor 6 (ARF6). Rac1 recycling from endosomes to the cell surface appears to be facilitated by ARF6 (D'Souza-Schorey and Chavrier, 2006; Radhakrishna et al., 1999). Inhibition of ARF6-dependent membrane trafficking alters also the trafficking of Cdc42-positive vesicles and consequently cell polarity (Osmani et al., 2010).

Interestingly, RhoJ and RhoQ, which belong to the Cdc42 subfamily, were reported to control membrane trafficking. Like RhoU and RhoV, RhoJ was shown to localize on the plasma membrane and endosomes. Depletion of RhoJ disrupted internalization of transferrin receptor and was shown to be necessary for transport of endocytosed receptors to the early endosome (de Toledo et al., 2003). In adipocytes RhoQ was reported to regulate the insulin-dependent transfer of the glucose transporter GLUT4 from storage compartment to the plasma membrane (Chiang et al., 2001). This involved actin cytosketon rearrangements induced by RhoQ activation through N-WASP (Jiang et al., 2002). RhoB localizes to endocytic vesicles and regulates trafficking of EGF receptor by retarding the progress of the receptor to lysosomes for degradation (Ellis and Mellor, 2000; Kress et al., 2007). EGF receptor was also demonstrated to colocalize with RhoU on endosomes in a Grb2-dependent manner contributing to cell migration (Zhang et al., 2011). This supports the hypothesis that RhoU is involved in intracellular and receptor trafficking. It would be interesting to test whether RhoV is involved in transferring receptor or EGF receptor internalization.

In the previous chapter (see Figure 3.6) it was shown that downregulation of RhoU by siRNA reduced CCRF-CEM, Jurkat and PEER cell adhesion to fibronectin. In this chapter, it was demonstrated that both RhoU and RhoV knockdown strongly inhibit adhesion of Jurkat cells to fibronectin and endothelial cells. Interestingly, RhoU and RhoV reduced adhesion of prostate cancer cells (PC3) to the endothelium (Dr Nicolas Reymond, personal communication). In agreement with these results, cranial neural crest cells were shown to adhere poorly to fibronectin when depleted of RhoU and had a rounded morphology (Fort et al., 2011). This suggests that the

role of RhoU in adhesion is not just restricted to T-ALL cells. In the previous chapter (see Figure 3.7), RhoU-depleted cells had a rounded morphology and a defect in uropod/tail formation. Loss of the tail is consistent with a defect in adhesion. The mechanism by which RhoU and RhoV inhibit adhesion still remains to be clarified. RhoU has been shown to regulate focal adhesion dynamics in HeLa cells (Chuang et al., 2007). It is possible that RhoU and/or RhoV control integrins. Jurkat cells preferentially bind to fibronectin, a ligand of β1 integrin. No significant changes were observed in total β1 integrin expression levels in RhoU and RhoV-depleted cells (data not shown). Since RhoU and RhoV were found to traffic between the plasma membrane and cytoplasm it is possible they control the localization and clustering of β1 integrin. Integrins are trafficked by the endosomal pathway, and this trafficking is important for the polarized distribution of integrins (Caswell et al., 2009). Endosomes have been found to mediate the redistribution of integrins during cytokinesis (Pellinen et al., 2008). Moreover, it has been hypothesized that a polarized endocytic cycle is required to return integrins from the rear of a migrating cell toward its front (Bretscher, 1996), although there is no yet evidence for this. To investigate a possible role of RhoU and RhoV in β1 integrin localization immunofluorescence analysis would need to be performed.

RhoU and RhoV are targeted to the membrane by palmtoylation, and this protein modification allows proteins to move to and from membranes (Navarro-Lerida et al., 2012). It was interesting to observe that RhoU and RhoV vesicles traffic to and from the plasma membrane as this suggests a recycling mechanism. It would be therefore important to test if they traffic to perinuclear recycling compartments before returning to the plasma membrane through a mechanism requiring Rab11 or ARF6. Rab11 and ARF6 proteins controll traffic through the recycling endosome (Caswell et al., 2009). As RhoU and RhoV vesicles were observed to migrate from the rear of the cells during cell migration, one possible scenario could be that RhoU and/or RhoV control recycling of integrins from the tail of the cell.

A decrease in cell spread area upon RhoU siRNA knockdown has also been observed in HeLaS3 cells (Chuang et al., 2007). Here, overexpression of RhoU or RhoV increased cell spreading and filopodium formation. Filopodia are finger-like protrusion of the plasma membrane. They are formed of 10 or more parallel bundles of actin filaments. The filaments are crosslinked by fascin1. Fascin1 localizes along

the entire length of filopodia and fascin1 depletion leads to a reduction in the number of filopodia and migration (Vignjevic et al., 2006; Vignjevic et al., 2007; Yamashiro et al., 1998). The main function of filopodia is to sense the extracellular environment, and they are linked to enhancement of directed migration as the key components of filopodia promote cell motility. They contribute to angiogenesis, chemotaxis and adhesion (Eilken and Adams, 2010; Zhang et al., 2004) and an increase in filopodia is considered a characteristic of invasive cancer cells (Arjonen et al., 2011; Mattila and Lappalainen, 2008; Schafer et al., 2009). During cell spreading, integrins accumulate in filopodia in an active state, creating sticky fingers at the front of the cell, promoting cell adhesion and migration (Galbraith et al., 2007). Therefore filopodium formation and cell spreading induced by RhoU and RhoV could contribute to their roles in adhesion and migration. It would be interesting to investigate the localization of active β1 integrins on RhoU and RhoV expressing cells to analyze whether they accumulate in the filopodia induced by RhoU and RhoV.

Given the effect of RhoU and RhoV on adhesion to extracellular matrix and endothelial cells, it was important to investigate if these proteins were affecting transendothelial migration. Interestingly, RhoU and RhoV depletion inhibited Jurkat cells transmigration. siRNA depletion of RhoU was also shown to reduce transendothelial migration of CCRF-CEM cells (Heasman et al., 2010). The effect on transendothelial migration might be due to the role of RhoU and RhoV adhesion of Jurkat cells to the endothelium.

It is well established in the literature that Rho GTPases cooperate or antagonize each other to control many biological processes. One example of cross-talk between Rho GTPases is between the Rnd proteins and RhoA where Rnd1 and 3 inhibit RhoA activity and consequently cell contractility (Chardin, 2006; Guilluy et al., 2011). Hence, Rho GTPase interaction is important for cellular functions, but a direct interaction between two Rho GTPases has never been observed before.

It was surprising to observe that RhoU and RhoV interact, and this interaction occur at the plasma membrane and in vesicles. These observations suggest these two Rho GTPases can act together to regulate membrane trafficking and their cooperation could be therefore fundamental for their functions. Dimerization is an important property of proteins, which is often involved in signalling regulation. Dimerization

can enhance protein specificity, can facilitate the orientation and proximity of two molecules, or increase their surface of interaction with other proteins or DNA (Klemm et al., 1998). In yeast the Rsr1 GTPase has been shown to form homodimers and heterodimers with Cdc42 in a spatio-temporal controlled manner important for cell polarity. The C-terminal polybasic region of Rsr1 mediates the dimerization (Kang et al., 2010). In this chapter, it was demonstrated that both RhoU and RhoV are able to form homodimers. It would be interesting to determine which domain of these proteins is important for their inteaction with itself. This could be mediated as for Rsr1 and Cdc42 by their polybasic region at the C-terminus.

Homodimerization of some proteins facilitates or promotes their interaction with other proteins. For example it has been demonstrated that the homodimerization of ROCK-1 is required for Rnd3/RhoE binding (Garg et al., 2008).

It is possible that part of the phenotypic effects observed upon RhoV knockdown are due to its effect on RhoU protein levels. It was already proposed that RhoU could have a similar function to RhoV, controlling in a similar manner cell adhesion and migration of cranial neural crest cells. Moreover, it was demonstrated that RhoV depletion affects the induction of neural crest markers. This phenotype was rescued by RhoU expression (Guemar et al., 2007). The mechanism by which RhoV regulates RhoU expression still remains to be clarified. It would be critical to test whether RhoU depletion is also able to affect RhoV protein level. This was not analysed here due to the lack of a suitable antibody to detect endogenous RhoV. Moreover, it is interesting to observe that the expression pattern of RhoV in the T-ALL cells analysed (see Figure 4.4A) is similar to that of RhoU (see Figure 3.3). SUPT1 and Jurkat cells, express the highest levels of RhoU and RhoV. This might be explained by the modulation of RhoU expression mediated by RhoV.

Given that RhoV depletion induces a decrease in RhoU protein, it possible that the binding of these two proteins protects RhoU from proteosomal degradation. Proteosome inhibitors could be used upon RhoV siRNA knockdown to test whether they could prevent the reduction in RhoU levels.

Interestingly, RhoU was found to interact with Rac1 by co-immunoprecipitation. The main characterized function of Rac1 is to induce formation of lamellipodia. Depletion of RhoU in cranial neural crest cells inhibited lamellipodia formation (Fort et al., 2011) and Rac1 and RhoU interaction could mediate this effect. In NIH3T3 cells, RhoU overexpression induced loss of lamellipodia. Rac was proposed to be

downstream of this defect as stimulation with PDGFP-BB an activator of Rac was able to rescue the lack in lamellipodia (Saras et al., 2004). A lack of lamellipodia upon RhoU overexpression was never observed in T-ALL cells, and thus this effect is restricted to fibroblasts. This does not rule out the possibility that the interaction between Rac1 and RhoU also occurs in fibroblast. Rac1 endocytosis is important for its activation and recycling to the plasma membrane, where Rac1 induces lamellipodia (Palamidessi et al., 2008).

Since RhoU localizes to endosomes, it could control Rac1 traffic to the plasma membrane. The control of Rac1 trafficking toward the plasma membrane would be therefore important for Rac1 function. Rac1 depletion reduced transendothelial migration of T-ALL cells (Heasman et al., 2010). The regulation of Rac1 trafficking by RhoU could contribute to a correct localization of Rac1 to the lamellipodium where it drives migration and transendothelial migration.

NCK1 is an SH2/SH3 domain-containing adapter protein and is implicated in actin cytoskeleton rearrangement and cell migration (Buday et al., 2002). The proline-rich domain at the N-terminus of RhoU interacts with the middle and C-terminal SH3 domains of NCK2 (Saras et al., 2004). Although Rac1 also has a proline-rich domain at the C-terminus (van Hennik et al., 2003), NCK1 did not interact with Rac1 and thus is unlikely to link Rac1 to RhoU (or RhoV).

RhoU and RhoV were shown to interact with PAK1 (Saras et al., 2004; Weisz Hubsman et al., 2007). It is well established that PAKs are activated by Rac and Cdc42 and that they are important regulators of cell migration and invasion. PAKs are overexpressed and/or hyperactivated in several human tumours and PAK-targeted therapeutics are being developed (Dummler et al., 2009). It can be speculated that RhoU and RhoV control migration through activation of PAK1 (Saras et al., 2004; Weisz Hubsman et al., 2007). In this case, it could be possible that RhoU and/or RhoV dimerization is required for their binding to PAK1. It was demonstrated that the N-terminus of RhoV is not required for the binding with RhoU by co-immunoprecipitation experiments and FRET/FLIM. Their interaction could be mediated by their polybasic regions at their C-terminus. In that case, homodimerization could act as a negative regulator of RhoU and RhoV interaction, as they might compete for the same domain.

As the effects of RhoU and RhoV co-expression on migration have not been determined, it is not possible to exclude that these two proteins negatively regulate

each other. They could compete for their binding to Rac1. It is also possible that RhoU, RhoV and Rac1 form a proteins complex that regulates migration through PAK1. RhoV was also demonstrated to interact with Rac1 (data not shown) and to interact with RhoU. One possible scenario is that RhoU and RhoV hetero/homodimerization mediates the binding of Rac1 to PAK1. It is also possible that RhoU and RhoV dimerization controls PAK1 activity. There is no evidence that PAK1 localizes on endosomes but it was found on pinocytic vesicles in SWISS-3T3 cells, similar to Rac1 (Dharmawardhane et al., 1997).

Here, RhoU was also shown to interact with Rac2. Rac1 and Rac2 share 92% of identity and most of their effectors (Heasman and Ridley, 2008) (Figure 4.25).

```
Rac1 MQAIKCVVVGDGAVGKTCLLISYTTNAFPGEYIPTVFDNYSANVMVDGKPVNLGLWDTAGQEDYDRLRP-69
Rac2 MQAIKCVVVGDGAVGKTCLLISYTTNAFPGEYIPTVFDNYSANVMVDSKPVNLGLWDTAGQEDYDRLRP-69

Rac1 LSYPQTDVFLICFSLVSPASFENVRAKWYPEVRHHCPNTPIILVGTKLDLRDDKDTIEKLKEKKLTPIT-138
Rac2 LSYPQTDVFLICFSLVSPASYENVRAKWFPEVRHHCPSTPIILVGTKLDLRDDKDTIEKLKEKKLAPIT-138

Rac1 YPQGLAMAKEIGAVKYLECSALTQRGLKTVFDEAIRAVLCPPPVKKRKRKCLLL-192
Rac2 YPQGLALAKEIDSVKYLECSALTQRGLKTVFDEAIRAVLCPQPTRQQKRACSLL-192
```

Figure 4.25. Sequence alignment between Rac1 and Rac2. Rac1 and Rac2 share 92% of identity. Highlighted in green are the residues of Rac2 that differ from Rac1.

Rac1 and Rac2 are both important for the production of superoxidase in phagocytic cells. The high similarity suggests redundancy between these two Racs. It has been proposed that the main difference between Rac1 and Rac2 lies in their pattern of expression. Rac2 is highly expressed in haematopoietic tissues (Shirsat et al., 1990) and in human neutrophils Rac is the main isoform. The redundant function might be the reason why they both interact with RhoU. Interesting, in macrophages was showed that Rac1 and Rac2 have distinct roles. Macrophages lacking Rac2 had reduction in podosomes while lack of Rac1 altered cell shape and reduced membrane ruffling (Zhang et al., 2012). It is therefore possible that Rac1 and Rac2 have distinct roles in T-ALL cells.

A main characteristic of T-ALL is the extent of tumour cell dissemination between the bone marrow and peripheral blood. In T-ALL patients, the T lymphoblasts comprise more than 25% of the bone marrow cells. Patients have also a high number of circulating T-lymphoblasts (Feng et al., 2010) (Goldberg et al., 2003). Poor T-ALL prognosis is related to the infiltration of different tissues, in particular CNS. In order to infiltrate tissues leukaemic cells need to extravasate from the blood stream through the endothelium. Here, RhoU and RhoV depletion inhibited Jurkat cells adhesion to the endothelium and transendothelial migration. These proteins were also found to be up-regulated in T-ALL (Chapter 2). It is therefore possible that the increase in RhoU and RhoV expression in the patients could contribute to T-ALL progression.

5

Concluding remarks

In T-ALL, leukaemia cells can migrate and infiltrate multiple tissues, including the central nervous system, and this correlates with poor prognosis. Therefore the identification of genes involved in the migration of leukaemic cells is fundamental to understand this process and ultimately to design therapies for T-ALL patients. Ras superfamily proteins are already known to contribute to cancer formation and progression. Ras mutations have been found in 30% of all human tumours (Bos, 1989) while GTPases activity is increased in several tumours (Vega and Ridley, 2008). Most GTPases are post-translationally prenylated by farnesyl or geranylgeranyl isoprenoids which facilitates their anchorage in membranes and is important for Rap/Rho GTPase signalling.

In the first results chapter of this thesis, the effect of statin and GGTI on T-ALL cell adhesion and migration was described. Statins prevent prenylation of GTPases. These cholesterol lowering drugs were previously reported to have anticancer properties since they were shown to induce apoptosis in acute myeloid leukaemic and neuroblastoma cells (Dimitroulakos et al., 1999). These properties were attributed to the suppression of GTPase prenylation leading to a reduction in downstream signals essential for cell cycle progression (Gauthaman et al., 2009). Randomized controlled trials for preventing cardiovascular disease indicated that statins had benefits for reducing colorectal cancer and melanoma (Demierre et al., 2005). Atorvastatin was shown to decrease the metastatic potential in melanoma cells causing disruption of stress fibres a process mediated by Rho inhibition. Similarly, as a result of Rho inhibition statins were shown to reduce the invasive potential of breast carcinoma cells (Gauthaman et al., 2009).

Statins exhibit potent antileukaemic properties *in vitro*. For example, atorvastatin and fluvastatin were found to be inducers of cell differentiation and apoptosis of the NB4 acute promyelocytic leukemia cell line. These effects were correlated with engagement of the c-Jun kinase pathway (Sassano et al., 2007).

Results presented in this thesis demonstrated that treatment of T-ALL cells with 1 μM statin inhibits adhesion, chemotaxis and TEM. Higher statin concentrations were

needed to inhibit adhesion of primary T-lymphoblasts. Moreover siRNA depletion of Rap1b phenocopied statin effects. Rap1 levels are higher in primary T cells than T-ALL cells which could explain their reduced sensitivity to statins (Figure 5.1). This suggests that statin, GGTI and inhibitors of Rap1b could be used to prevent T-ALL cell invasion.

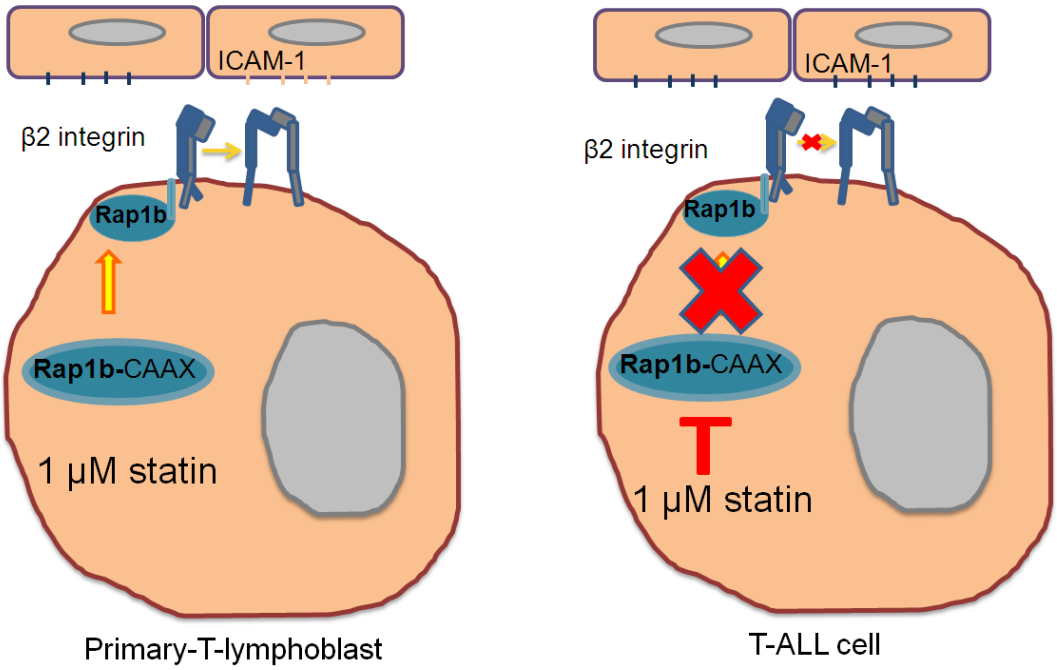

Figure 5.1 Schematic mechanism of action of statins in primary-T-lymphoblast and in T-ALL cell adhesion. Treatment of primary-T-lymphoblasts with 1 μM statin does not affect prenylation of Rap1b. This GTPase can still localize properly on the plasma membrane where it promotes β2-integrin activation. Active β2-integrin can bind to ICAM-1 expressed on the endothelium surface, leading to firm adhesion between T cell and the endothelium. Treatment of T-ALL cells with 1 μM statin inhibits Rap1b prenylation and consequently its localization on membranes. The mislocalization of Rap1b causes a decrease in the activation of β2-integrin affecting adhesion of T-ALL cells to the endothelium.

Given these promising *in vitro* results, it would be interesting to study the effect of statins, GGTI and Rap1b inhibitors in T-ALL using an *in vivo* model. The studies of statins in animals include a colorectal cancer mouse-model and breast cancer mouse

models. In the colorectal cancer mouse model, it was consistently found that statins reduced tumour incidence by 30–67% (Demierre et al., 2005). Lovastatin reduced tumour formation and metastatic dissemination to the lung from established mammary tumours of a mouse model (Alonso et al., 1998).
The LMO2 T-ALL mice express LMO2 selectively in T cells leading to the development of T-ALL. These mice would be a good model to study the effect of statins on T-ALL cells *in vivo* (McCormack et al., 2010). The LMO2 T-ALL mice could be also crossed with Rap1b knockout mice to study the role of Rap1b on T-ALL cells *in vivo* (Chrzanowska-Wodnicka et al., 2005).

In the LMO2 T-ALL mouse model the Notch1 oncogene is spontaneously mutated in approximately 50% of mice with T-ALL. In the second results chapter of this thesis, RhoU was described as a target gene of Notch1 in T-ALL. RhoU was demonstrated to be important for T-ALL cell adhesion to fibronectin and also for chemotaxis and migration possibly through its role in adhesion. It was also shown that Notch1 siRNA depletion induced a decrease in the adhesion and migration of T-ALL cell lines, suggesting that Notch1 could affect migration of T-ALL cells through RhoU. The LMO2 T-ALL mouse model could therefore be used to investigate whether the expression of RhoU is related to aberrant Notch1 signaling *in vivo*. The model could be also used to perform functional analysis on cell adhesion and migration in order to understand whether Notch1 signaling could affect T-ALL cell adhesion and migration through RhoU *in vivo*.

In the last results chapter of this thesis, it was demonstrated that expression of RhoU and its closest relative RhoV in T-ALL cell lines induces cell spreading and filopodium formation. RhoU and RhoV siRNA depletion were found to inhibit Jurkat cell adhesion on fibronectin and endothelial cells and to reduce TEM. It would be important to perform adhesion assays on endothelial cells and TEM assays using another T-ALL cell line as these experiments were performed only in Jurkat cells.
Unexpected, RhoU and RhoV were found to form homo- and heterodimers. However, in yeast the Rsr1/Bud1GTPase was shown to interact with itself, and Cdc42 and Ras molecules were found to exist as oligomers (Kang et al., 2010; Santos et al., 1988). It is therefore possible that other GTPases can form dimers.

Intriguingly, RhoV was shown to modulate RhoU protein expression. In the absence of a reliable antibody to detect endogenous RhoV, it was not possible to investigate whether RhoU is able to modulate RhoV protein expression. Therefore this possibility cannot be excluded.

As mentioned in the results chapter, it would be critical to perform rescue experiments to determine whether RhoU could rescue the effect of RhoV depletion and vivecersa. RhoU could be overexpressed in a RhoV knockdown background to analyse whether adhesion and TEM could be rescued in a T-ALL cell line such as Jurkat cells.

RhoU and RhoV were demonstrated to co-localize on endosomes and on the plasma membrane suggesting they could be involved in membrane trafficking. How RhoU and RhoV regulate T-ALL cell adhesion still remains to be clarified. It would be important to analyse whether RhoU and RhoV could modulate the trafficking or activation of integrins.

It can be also speculated that RhoU and RhoV could modulate adhesion through Rap1b. Rap1 proteins are well known regulators of integrins activation, and in the second chapter of this thesis, Rap1b was demonstrated to be important for adhesion of T-ALL cells to both fibronectin and ICAM-1, whereas Rap1a was shown to mainly mediate adhesion to fibronectin. Rap1 proteins localize on endosomes and the plasma membrane (Hattori and Minato, 2003). Given the possible role of RhoU and RhoV in membrane trafficking it is possible that RhoU and RhoV control the trafficking of Rap1b. A possible interaction between Rap1b and RhoU/RhoV could be investigated by co-immunoprecipitation analysis. It could be therefore informative to analyze the localization of Rap1b in the context of RhoU/RhoV depleted cells, to understand whether this could cause a mislocalization of Rap1b protein.

RhoU was shown to interact with Rac1 and Rac2 by co-immunoprecipitation experiments. The best characterized function of Rac1 is to promote lamellipodium formation (Rougerie and Delon, 2012). Rac1 and Rac2 depletion were shown to inhibit TEM of CCRF-CEM cells (Heasman et al., 2010). It would be interesting to perform FLIM/FRET experiments to further characterize the interaction of RhoU, and possibly RhoV, with Rac1 and Rac2. It is possible that RhoU regulates the trafficking of Rac1 and Rac2 to the plasma membrane where they drive migration and TEM. RhoV was also shown to interact with Rac1 by co-immunoprecipitation

analysis (data not shown). It would therefore be useful to analyze the localization of endogenous Rac1 and Rac2 in RhoU/RhoV depleted cells to determine whether they regulate the localization or Rac1 and Rac2. RhoU and RhoV share PAK1 as a downstream effector with Rac1 (Heasman and Ridley, 2008; Saras et al., 2004; Weisz Hubsman et al., 2007). The PAK proteins play important roles in cytoskeletal organisation, cellular morphogenesis and survival, and several PAKs have been implicated in cancer (Crawford et al., 2012). Expression of RhoU and RhoV activates PAK1 (Aronheim et al., 1998; Rougerie and Delon, 2012; Saras et al., 2004) and PAK1 could mediate the effect of RhoU and RhoV on T-ALL cell migration. It would therefore be interesting to perform migration assays in which siRNA depletion of RhoU and/or RhoV are used in the context of cells overexpressing a constitutively active form of PAK1, to investigate whether this could rescue the effect of RhoU and RhoV in migration. PAK inhibitors are still quite rare, and few exhibit 'drug-like' properties, however it is expected that other PAK inhibitors will be developed in the future (Crawford et al., 2012). These inhibitors could be used to analyse their effect on T-ALL cell migration *in vitro.* Finally, the LMO2 T-ALL mouse model described above could be used as a tool to develop and test new therapies to target the signalling pathway of RhoU and RhoV GTPases. In fact the implication of these proteins in leukaemia raises the question of whether inhibitors can be designed to target RhoU and RhoV. For example, inhibitors of RhoU/RhoV could be designed to prevent the interaction with Rac1/Rac2 and/or PAK1, which could be tested for effects on cell migration.

In conclusion the three chapters of this thesis indicate for the first time that Rap1b, RhoU and RhoV are crucial players in the adhesion and migration properties of T-ALL cells. The understanding of the intricate signalling pathways regulated by Rap1b, RhoU and RhoV will be important to design therapeutic drugs.
The following figure represents a hypothetical model of Rap1b, RhoU and RhoV function in T-ALL cell adhesion and migration (Figure 5.2).

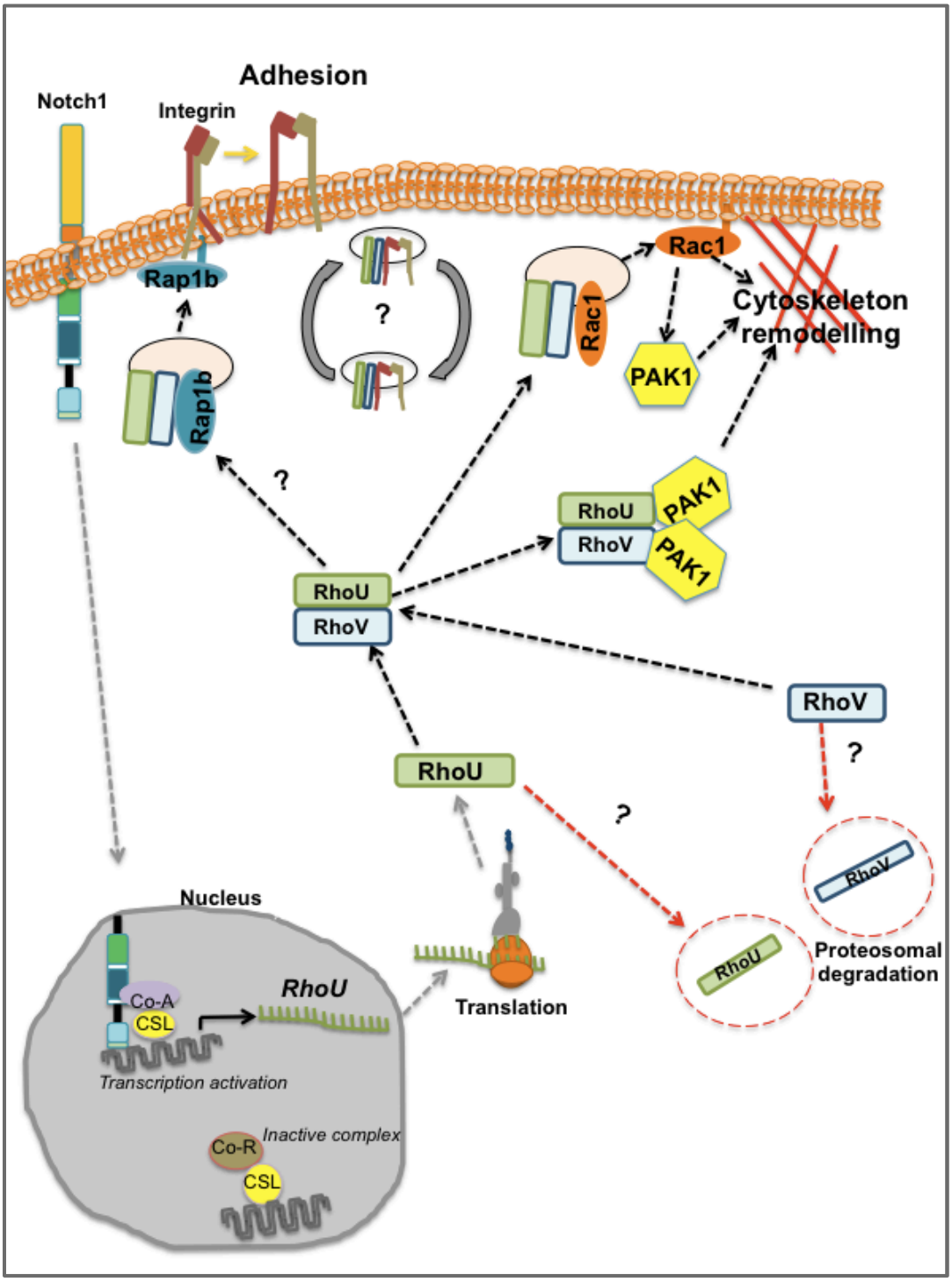

Figure 5.2 Hypothetical model for the control of adhesion and migration by Rap1b, RhoU and RhoV in T-ALL. Aberrant Notch1 signalling in T-ALL induces an increase in the transcription of its target gene RhoU. In the cytoplasm RhoU can form heterodimers with RhoV. These two proteins interact in vesicles that traffic toward the plasma membrane. In vesicles, RhoU and RhoV could form a complex with Rap1b promoting its localization on the plasma membrane. The localization on the plasma membrane of Rap1b leads to the activation of β1 and/or β2 integrin, promoting cell adhesion. Integrins are trafficked by the endosomal pathway a

process that could be mediated by the RhoU/RhoV complex. RhoU and RhoV heterodimers could also interact on vesicle with Rac1 promoting its localization on the plasma membrane, where it induces actin polymerization and lamellipodium formation important for cell migration. Dimerization could prevent these proteins from proteosomal degradation. RhoU and RhoV dimerization could enhance their binding to their downstream effector PAK1. The binding could promote the transition of PAK1 to an active conformation that exposes key residues to undergo autophosphorylation. Rac1 also binds and activate PAK1. Activation of PAK1 or other PAKs induces cytoskeleton rearrangement promoting cell migration.

References

Acuto, O., and F. Michel. 2003. CD28-mediated co-stimulation: a quantitative support for TCR signalling. *Nat Rev Immunol*. 3:939-951.

Aifantis, I., E. Raetz, and S. Buonamici. 2008. Molecular pathogenesis of T-cell leukaemia and lymphoma. *Nat Rev Immunol*. 8:380-390.

Alan, J.K., A.C. Berzat, B.J. Dewar, L.M. Graves, and A.D. Cox. 2010. Regulation of the Rho family small GTPase Wrch-1/RhoU by C-terminal tyrosine phosphorylation requires Src. *Mol Cell Biol*. 30:4324-4338.

Allman, D., F.G. Karnell, J.A. Punt, S. Bakkour, L. Xu, P. Myung, G.A. Koretzky, J.C. Pui, J.C. Aster, and W.S. Pear. 2001. Separation of Notch1 promoted lineage commitment and expansion/transformation in developing T cells. *J Exp Med*. 194:99-106.

Alon, R., P.D. Kassner, M.W. Carr, E.B. Finger, M.E. Hemler, and T.A. Springer. 1995. The integrin VLA-4 supports tethering and rolling in flow on VCAM-1. *J Cell Biol*. 128:1243-1253.

Alon, R., and Z. Shulman. 2011. Chemokine triggered integrin activation and actin remodeling events guiding lymphocyte migration across vascular barriers. *Exp Cell Res*. 317:632-641.

Alonso, D.F., H.G. Farina, G. Skilton, M.R. Gabri, M.S. De Lorenzo, and D.E. Gomez. 1998. Reduction of mouse mammary tumor formation and metastasis by lovastatin, an inhibitor of the mevalonate pathway of cholesterol synthesis. *Breast Cancer Res Treat*. 50:83-93.

Altschuler, D.L., and F. Ribeiro-Neto. 1998. Mitogenic and oncogenic properties of the small G protein Rap1b. *Proc Natl Acad Sci U S A*. 95:7475-7479.

Annels, N.E., A.J. Willemze, V.H. van der Velden, C.M. Faaij, E. van Wering, D.M. Sie-Go, R.M. Egeler, M.J. van Tol, and T. Revesz. 2004. Possible link between unique chemokine and homing receptor expression at diagnosis and relapse location in a patient with childhood T-ALL. *Blood*. 103:2806-2808.

Aplan, P.D., C.A. Jones, D.S. Chervinsky, X. Zhao, M. Ellsworth, C. Wu, E.A. McGuire, and K.W. Gross. 1997. An scl gene product lacking the transactivation domain induces bony abnormalities and cooperates with LMO1 to generate T-cell malignancies in transgenic mice. *EMBO J*. 16:2408-2419.

Arias-Romero, L.E., and J. Chernoff. 2008. A tale of two Paks. *Biol Cell*. 100:97-108.

Arjonen, A., R. Kaukonen, and J. Ivaska. 2011. Filopodia and adhesion in cancer cell motility. *Cell Adh Migr*. 5:421-430.

Arnaout, M.A., S.L. Goodman, and J.P. Xiong. 2007. Structure and mechanics of integrin-based cell adhesion. *Curr Opin Cell Biol*. 19:495-507.

Aronheim, A., Y.C. Broder, A. Cohen, A. Fritsch, B. Belisle, and A. Abo. 1998. Chp, a homologue of the GTPase Cdc42Hs, activates the JNK pathway and is implicated in reorganizing the actin cytoskeleton. *Curr Biol*. 8:1125-1128.

Aspenstrom, P., A. Fransson, and J. Saras. 2004. Rho GTPases have diverse effects on the organization of the actin filament system. *Biochem J*. 377:327-337.

Aspenstrom, P., A. Ruusala, and D. Pacholsky. 2007. Taking Rho GTPases to the next level: the cellular functions of atypical Rho GTPases. *Exp Cell Res*. 313:3673-3679.

Aster, J.C., S.C. Blacklow, and W.S. Pear. 2011. Notch signalling in T-cell lymphoblastic leukaemia/lymphoma and other haematological malignancies. *J Pathol*. 223:262-273.

Baines, A.T., D. Xu, and C.J. Der. 2011. Inhibition of Ras for cancer treatment: the search continues. *Future Med Chem*. 3:1787-1808.

Banno, A., and M.H. Ginsberg. 2008. Integrin activation. *Biochem Soc Trans*. 36:229-234.

Bargatze, R.F., and E.C. Butcher. 1993. Rapid G protein-regulated activation event involved in lymphocyte binding to high endothelial venules. *J Exp Med*. 178:367-372.

Barreiro, O., M. Yanez-Mo, J.M. Serrador, M.C. Montoya, M. Vicente-Manzanares, R. Tejedor, H. Furthmayr, and F. Sanchez-Madrid. 2002. Dynamic interaction of VCAM-1 and ICAM-1 with moesin and ezrin in a novel endothelial docking structure for adherent leukocytes. *J Cell Biol*. 157:1233-1245.

Bauer, M., C. Brakebusch, C. Coisne, M. Sixt, H. Wekerle, B. Engelhardt, and R. Fassler. 2009. Beta1 integrins differentially control extravasation of inflammatory cell subsets into the CNS during autoimmunity. *Proc Natl Acad Sci U S A*. 106:1920-1925.

Baumgarth, N. 2000. A two-phase model of B-cell activation. *Immunol Rev*. 176:171-180.

Bazzoni, G., and E. Dejana. 2004. Endothelial cell-to-cell junctions: molecular organization and role in vascular homeostasis. *Physiol Rev*. 84:869-901.

Bellavia, D., A.F. Campese, A. Vacca, A. Gulino, and I. Screpanti. 2003. Notch3, another Notch in T cell development. *Semin Immunol*. 15:107-112.

Berndt, N., A.D. Hamilton, and S.M. Sebti. 2011. Targeting protein prenylation for cancer therapy. *Nat Rev Cancer*. 11:775-791.

Berthold, J., K. Schenkova, S. Ramos, Y. Miura, M. Furukawa, P. Aspenstrom, and F. Rivero. 2008a. Characterization of RhoBTB-dependent Cul3 ubiquitin ligase complexes--evidence for an autoregulatory mechanism. *Exp Cell Res*. 314:3453-3465.

Berthold, J., K. Schenkova, and F. Rivero. 2008b. Rho GTPases of the RhoBTB subfamily and tumorigenesis. *Acta Pharmacol Sin*. 29:285-295.

Berzat, A.C., J.E. Buss, E.J. Chenette, C.A. Weinbaum, A. Shutes, C.J. Der, A. Minden, and A.D. Cox. 2005. Transforming activity of the Rho family GTPase, Wrch-1, a Wnt-regulated Cdc42 homolog, is dependent on a novel carboxyl-terminal palmitoylation motif. *J Biol Chem*. 280:33055-33065.

Bhavsar, P.J., E. Infante, A. Khwaja, and A.J. Ridley. 2012. Analysis of Rho GTPase expression in T-ALL identifies RhoU as a target for Notch involved in T-ALL cell migration. *Oncogene*.

Bhojwani, D., S.C. Howard, and C.H. Pui. 2009. High-risk childhood acute lymphoblastic leukemia. *Clin Lymphoma Myeloma*. 9 Suppl 3:S222-230.

Bivona, T.G., H.H. Wiener, I.M. Ahearn, J. Silletti, V.K. Chiu, and M.R. Philips. 2004. Rap1 up-regulation and activation on plasma membrane regulates T cell adhesion. *J Cell Biol*. 164:461-470.

Bjorkman, P.J. 1997. MHC restriction in three dimensions: a view of T cell receptor/ligand interactions. *Cell*. 89:167-170.

Boettner, B., and L. Van Aelst. 2009. Control of cell adhesion dynamics by Rap1 signaling. *Curr Opin Cell Biol*. 21:684-693.

Bogen, S., J. Pak, M. Garifallou, X. Deng, and W.A. Muller. 1994. Monoclonal antibody to murine PECAM-1 (CD31) blocks acute inflammation in vivo. *J Exp Med*. 179:1059-1064.

Bolomini-Vittori, M., A. Montresor, C. Giagulli, D. Staunton, B. Rossi, M. Martinello, G. Constantin, and C. Laudanna. 2009. Regulation of conformer-specific activation of the integrin LFA-1 by a chemokine-triggered Rho signaling module. *Nat Immunol*. 10:185-194.

Bos, J.L. 1989. ras oncogenes in human cancer: a review. *Cancer Res*. 49:4682-4689.

Bos, J.L. 2005. Linking Rap to cell adhesion. *Curr Opin Cell Biol*. 17:123-128.

Bos, J.L., H. Rehmann, and A. Wittinghofer. 2007. GEFs and GAPs: critical elements in the control of small G proteins. *Cell*. 129:865-877.

Boureux, A., E. Vignal, S. Faure, and P. Fort. 2007. Evolution of the Rho family of ras-like GTPases in eukaryotes. *Mol Biol Evol*. 24:203-216.

Brady, D.C., J.K. Alan, J.P. Madigan, A.S. Fanning, and A.D. Cox. 2009. The transforming Rho family GTPase Wrch-1 disrupts epithelial cell tight junctions and epithelial morphogenesis. *Mol Cell Biol*. 29:1035-1049.

Brazier, H., G. Pawlak, V. Vives, and A. Blangy. 2009. The Rho GTPase Wrch1 regulates osteoclast precursor adhesion and migration. *Int J Biochem Cell Biol*. 41:1391-1401.

Bretscher, M.S. 1996. Moving membrane up to the front of migrating cells. *Cell*. 85:465-467.

Brown, L., J.T. Cheng, Q. Chen, M.J. Siciliano, W. Crist, G. Buchanan, and R. Baer. 1990. Site-specific recombination of the tal-1 gene is a common occurrence in human T cell leukemia. *EMBO J*. 9:3343-3351.

Buday, L., L. Wunderlich, and P. Tamas. 2002. The Nck family of adapter proteins: regulators of actin cytoskeleton. *Cell Signal*. 14:723-731.

Buonamici, S., T. Trimarchi, M.G. Ruocco, L. Reavie, S. Cathelin, B.G. Mar, A. Klinakis, Y. Lukyanov, J.C. Tseng, F. Sen, E. Gehrie, M. Li, E. Newcomb, J. Zavadil, D. Meruelo, M. Lipp, S. Ibrahim, A. Efstratiadis, D. Zagzag, J.S. Bromberg, M.L. Dustin, and I. Aifantis. 2009. CCR7 signalling as an essential regulator of CNS infiltration in T-cell leukaemia. *Nature*. 459:1000-1004.

Burger, R., T.E. Hansen-Hagge, H.G. Drexler, and M. Gramatzki. 1999. Heterogeneity of T-acute lymphoblastic leukemia (T-ALL) cell lines: suggestion for classification by immunophenotype and T-cell receptor studies. *Leuk Res*. 23:19-27.

Cadigan, K.M., and R. Nusse. 1997. Wnt signaling: a common theme in animal development. *Genes Dev*. 11:3286-3305.

Callaghan, J., A. Simonsen, J.M. Gaullier, B.H. Toh, and H. Stenmark. 1999. The endosome fusion regulator early-endosomal autoantigen 1 (EEA1) is a dimer. *Biochem J*. 338 (Pt 2):539-543.

Campellone, K.G., and M.D. Welch. 2010. A nucleator arms race: cellular control of actin assembly. *Nat Rev Mol Cell Biol*. 11:237-251.

Campese, A.F., D. Bellavia, A. Gulino, and I. Screpanti. 2003. Notch signalling at the crossroads of T cell development and leukemogenesis. *Semin Cell Dev Biol*. 14:151-157.

Carman, C.V., P.T. Sage, T.E. Sciuto, M.A. de la Fuente, R.S. Geha, H.D. Ochs, H.F. Dvorak, A.M. Dvorak, and T.A. Springer. 2007. Transcellular diapedesis is initiated by invasive podosomes. *Immunity*. 26:784-797.

Carman, C.V., and T.A. Springer. 2004. A transmigratory cup in leukocyte diapedesis both through individual vascular endothelial cells and between them. *J Cell Biol*. 167:377-388.

Castellano, F., P. Montcourrier, and P. Chavrier. 2000. Membrane recruitment of Rac1 triggers phagocytosis. *J Cell Sci*. 113 (Pt 17):2955-2961.

Caswell, P.T., S. Vadrevu, and J.C. Norman. 2009. Integrins: masters and slaves of endocytic transport. *Nat Rev Mol Cell Biol*. 10:843-853.

Cernuda-Morollon, E., S. Gharbi, and J. Millan. 2010. Discriminating between the paracellular and transcellular routes of diapedesis. *Methods Mol Biol*. 616:69-82.

Cernuda-Morollon, E., and A.J. Ridley. 2006. Rho GTPases and leukocyte adhesion receptor expression and function in endothelial cells. *Circ Res*. 98:757-767.

Chang, F.K., N. Sato, N. Kobayashi-Simorowski, T. Yoshihara, J.L. Meth, and M. Hamaguchi. 2006. DBC2 is essential for transporting vesicular stomatitis virus glycoprotein. *J Mol Biol*. 364:302-308.

Chaplin, D.D. 2006. 1. Overview of the human immune response. *J Allergy Clin Immunol*. 117:S430-435.

Chaplin, D.D. 2010. Overview of the immune response. *J Allergy Clin Immunol*. 125:S3-23.

Chardin, P. 2006. Function and regulation of Rnd proteins. *Nat Rev Mol Cell Biol*. 7:54-62.

Chenette, E.J., A. Abo, and C.J. Der. 2005. Critical and distinct roles of amino- and carboxyl-terminal sequences in regulation of the biological activity of the Chp atypical Rho GTPase. *J Biol Chem*. 280:13784-13792.

Chenette, E.J., N.Y. Mitin, and C.J. Der. 2006. Multiple sequence elements facilitate Chp Rho GTPase subcellular location, membrane association, and transforming activity. *Mol Biol Cell*. 17:3108-3121.

Cherry, L.K., X. Li, P. Schwab, B. Lim, and L.B. Klickstein. 2004. RhoH is required to maintain the integrin LFA-1 in a nonadhesive state on lymphocytes. *Nat Immunol*. 5:961-967.

Chiang, S.H., C.A. Baumann, M. Kanzaki, D.C. Thurmond, R.T. Watson, C.L. Neudauer, I.G. Macara, J.E. Pessin, and A.R. Saltiel. 2001. Insulin-stimulated GLUT4 translocation requires the CAP-dependent activation of TC10. *Nature*. 410:944-948.

Chrzanowska-Wodnicka, M., S.S. Smyth, S.M. Schoenwaelder, T.H. Fischer, and G.C. White, 2nd. 2005. Rap1b is required for normal platelet function and hemostasis in mice. *J Clin Invest*. 115:680-687.

Chu, H., A. Awasthi, G.C. White, 2nd, M. Chrzanowska-Wodnicka, and S. Malarkannan. 2008. Rap1b regulates B cell development, homing, and T cell-dependent humoral immunity. *J Immunol*. 181:3373-3383.

Chuang, Y.Y., A. Valster, S.J. Coniglio, J.M. Backer, and M. Symons. 2007. The atypical Rho family GTPase Wrch-1 regulates focal adhesion formation and cell migration. *J Cell Sci*. 120:1927-1934.

Cordle, A., J. Koenigsknecht-Talboo, B. Wilkinson, A. Limpert, and G. Landreth. 2005. Mechanisms of statin-mediated inhibition of small G-protein function. *J Biol Chem*. 280:34202-34209.

Corre, I., M. Gomez, S. Vielkind, and D.A. Cantrell. 2001. Analysis of thymocyte development reveals that the GTPase RhoA is a positive regulator of T cell receptor responses in vivo. *J Exp Med*. 194:903-914.

Cote, J.F., and K. Vuori. 2007. GEF what? Dock180 and related proteins help Rac to polarize cells in new ways. *Trends Cell Biol*. 17:383-393.

Crawford, J.J., K.P. Hoeflich, and J. Rudolph. 2012. p21-Activated kinase inhibitors: a patent review. *Expert Opin Ther Pat*. 22:293-310.

Crazzolara, R., A. Kreczy, G. Mann, A. Heitger, G. Eibl, F.M. Fink, R. Mohle, and B. Meister. 2001. High expression of the chemokine receptor CXCR4 predicts extramedullary organ infiltration in childhood acute lymphoblastic leukaemia. *Br J Haematol*. 115:545-553.

Cummins, P.M. 2012. Occludin: one protein, many forms. *Mol Cell Biol*. 32:242-250.

D'Souza, B., A. Miyamoto, and G. Weinmaster. 2008. The many facets of Notch ligands. *Oncogene*. 27:5148-5167.

D'Souza-Schorey, C., B. Boettner, and L. Van Aelst. 1998. Rac regulates integrin-mediated spreading and increased adhesion of T lymphocytes. *Mol Cell Biol*. 18:3936-3946.

D'Souza-Schorey, C., and P. Chavrier. 2006. ARF proteins: roles in membrane traffic and beyond. *Nat Rev Mol Cell Biol*. 7:347-358.

de Hoon, M.J., S. Imoto, J. Nolan, and S. Miyano. 2004. Open source clustering software. *Bioinformatics*. 20:1453-1454.

de Toledo, M., F. Senic-Matuglia, J. Salamero, G. Uze, F. Comunale, P. Fort, and A. Blangy. 2003. The GTP/GDP cycling of rho GTPase TCL is an essential regulator of the early endocytic pathway. *Mol Biol Cell*. 14:4846-4856.

Deftos, M.L., and M.J. Bevan. 2000. Notch signaling in T cell development. *Curr Opin Immunol*. 12:166-172.

Demarest, R.M., F. Ratti, and A.J. Capobianco. 2008. It's T-ALL about Notch. *Oncogene*. 27:5082-5091.

Demierre, M.F., P.D. Higgins, S.B. Gruber, E. Hawk, and S.M. Lippman. 2005. Statins and cancer prevention. *Nat Rev Cancer*. 5:930-942.

Dharmawardhane, S., L.C. Sanders, S.S. Martin, R.H. Daniels, and G.M. Bokoch. 1997. Localization of p21-activated kinase 1 (PAK1) to pinocytic vesicles and cortical actin structures in stimulated cells. *J Cell Biol*. 138:1265-1278.

Dimitroulakos, J., D. Nohynek, K.L. Backway, D.W. Hedley, H. Yeger, M.H. Freedman, M.D. Minden, and L.Z. Penn. 1999. Increased sensitivity of acute myeloid leukemias to lovastatin-induced apoptosis: A potential therapeutic approach. *Blood*. 93:1308-1318.

Dinarello, C.A. 2010. Anti-inflammatory Agents: Present and Future. *Cell*. 140:935-950.

Downward, J. 2003. Targeting RAS signalling pathways in cancer therapy. *Nat Rev Cancer*. 3:11-22.

Dransfield, I., and N. Hogg. 1989. Regulated expression of Mg2+ binding epitope on leukocyte integrin alpha subunits. *EMBO J*. 8:3759-3765.

Duchniewicz, M., T. Zemojtel, M. Kolanczyk, S. Grossmann, J.S. Scheele, and F.J. Zwartkruis. 2006. Rap1A-deficient T and B cells show impaired integrin-mediated cell adhesion. *Mol Cell Biol*. 26:643-653.

Dudley, D.D., H.C. Wang, and X.H. Sun. 2009. Hes1 potentiates T cell lymphomagenesis by up-regulating a subset of notch target genes. *PLoS One*. 4:e6678.

Dummler, B., K. Ohshiro, R. Kumar, and J. Field. 2009. Pak protein kinases and their role in cancer. *Cancer Metastasis Rev*. 28:51-63.

Dupuy, A.J., K. Morgan, F.C. von Lintig, H. Shen, H. Acar, D.E. Hasz, N.A. Jenkins, N.G. Copeland, G.R. Boss, and D.A. Largaespada. 2001. Activation of the Rap1 guanine nucleotide exchange gene, CalDAG-GEF I, in BXH-2 murine myeloid leukemia. *J Biol Chem*. 276:11804-11811.

Ebnet, K., A. Suzuki, S. Ohno, and D. Vestweber. 2004. Junctional adhesion molecules (JAMs): more molecules with dual functions? *J Cell Sci*. 117:19-29.

Eilken, H.M., and R.H. Adams. 2010. Dynamics of endothelial cell behavior in sprouting angiogenesis. *Curr Opin Cell Biol*. 22:617-625.

Ellenbroek, S.I., and J.G. Collard. 2007. Rho GTPases: functions and association with cancer. *Clin Exp Metastasis*. 24:657-672.

Ellenbroek, S.I., S. Iden, and J.G. Collard. 2012. Cell polarity proteins and cancer. *Semin Cancer Biol*. 22:208-215.

Ellis, S., and H. Mellor. 2000. Regulation of endocytic traffic by rho family GTPases. *Trends Cell Biol*. 10:85-88.

Etienne-Manneville, S. 2004. Cdc42--the centre of polarity. *J Cell Sci*. 117:1291-1300.

Faix, J., and R. Grosse. 2006. Staying in shape with formins. *Dev Cell*. 10:693-706.

Faroudi, M., M. Hons, A. Zachacz, C. Dumont, R. Lyck, J.V. Stein, and V.L. Tybulewicz. 2010. Critical roles for Rac GTPases in T-cell migration to and within lymph nodes. *Blood*. 116:5536-5547.

Feng, H., D.L. Stachura, R.M. White, A. Gutierrez, L. Zhang, T. Sanda, C.A. Jette, J.R. Testa, D.S. Neuberg, D.M. Langenau, J.L. Kutok, L.I. Zon, D. Traver, M.D. Fleming, J.P. Kanki, and A.T. Look. 2010. T-lymphoblastic lymphoma cells express high levels of BCL2, S1P1, and ICAM1, leading to a blockade of tumor cell intravasation. *Cancer Cell*. 18:353-366.

Ferrando, A.A. 2009. The role of NOTCH1 signaling in T-ALL. *Hematology Am Soc Hematol Educ Program*:353-361.

Ferrando, A.A., S. Herblot, T. Palomero, M. Hansen, T. Hoang, E.A. Fox, and A.T. Look. 2004. Biallelic transcriptional activation of oncogenic transcription factors in T-cell acute lymphoblastic leukemia. *Blood*. 103:1909-1911.

Ferrando, A.A., D.S. Neuberg, J. Staunton, M.L. Loh, C. Huard, S.C. Raimondi, F.G. Behm, C.H. Pui, J.R. Downing, D.G. Gilliland, E.S. Lander, T.R. Golub, and A.T. Look. 2002. Gene expression signatures define novel oncogenic pathways in T cell acute lymphoblastic leukemia. *Cancer Cell*. 1:75-87.

Firtel, R.A., and C.Y. Chung. 2000. The molecular genetics of chemotaxis: sensing and responding to chemoattractant gradients. *Bioessays*. 22:603-615.

Fort, P., L. Guemar, E. Vignal, N. Morin, C. Notarnicola, P. de Santa Barbara, and S. Faure. 2011. Activity of the RhoU/Wrch1 GTPase is critical for cranial neural crest cell migration. *Dev Biol*. 350:451-463.

Frische, E.W., and F.J. Zwartkruis. 2010. Rap1, a mercenary among the Ras-like GTPases. *Dev Biol*. 340:1-9.

Fuchs, D., C. Berges, G. Opelz, V. Daniel, and C. Naujokat. 2008. HMG-CoA reductase inhibitor simvastatin overcomes bortezomib-induced apoptosis resistance by disrupting a geranylgeranyl pyrophosphate-dependent survival pathway. *Biochem Biophys Res Commun*. 374:309-314.

Fueller, F., and K.F. Kubatzky. 2008. The small GTPase RhoH is an atypical regulator of haematopoietic cells. *Cell Commun Signal*. 6:6.

Galbraith, C.G., K.M. Yamada, and J.A. Galbraith. 2007. Polymerizing actin fibers position integrins primed to probe for adhesion sites. *Science*. 315:992-995.

Garcia-Bernal, D., E. Sotillo-Mallo, C. Nombela-Arrieta, R. Samaniego, Y. Fukui, J.V. Stein, and J. Teixido. 2006. DOCK2 is required for chemokine-promoted human T lymphocyte adhesion under shear stress mediated by the integrin alpha4beta1. *J Immunol*. 177:5215-5225.

Garcia-Bernal, D., N. Wright, E. Sotillo-Mallo, C. Nombela-Arrieta, J.V. Stein, X.R. Bustelo, and J. Teixido. 2005. Vav1 and Rac control chemokine-promoted T lymphocyte adhesion mediated by the integrin alpha4beta1. *Mol Biol Cell*. 16:3223-3235.

Garcia-Mata, R., and K. Burridge. 2007. Catching a GEF by its tail. *Trends Cell Biol*. 17:36-43.

Garg, R., K. Riento, N. Keep, J.D. Morris, and A.J. Ridley. 2008. N-terminus-mediated dimerization of ROCK-I is required for RhoE binding and actin reorganization. *Biochem J*. 411:407-414.

Garrett, W.S., L.M. Chen, R. Kroschewski, M. Ebersold, S. Turley, S. Trombetta, J.E. Galan, and I. Mellman. 2000. Developmental control of endocytosis in dendritic cells by Cdc42. *Cell*. 102:325-334.

Gauthaman, K., C.Y. Fong, and A. Bongso. 2009. Statins, stem cells, and cancer. *J Cell Biochem*. 106:975-983.

Gerard, A., A.E. Mertens, R.A. van der Kammen, and J.G. Collard. 2007. The Par polarity complex regulates Rap1- and chemokine-induced T cell polarization. *J Cell Biol*. 176:863-875.

Giambra, V., C.R. Jenkins, H. Wang, S.H. Lam, O.O. Shevchuk, O. Nemirovsky, C. Wai, S. Gusscott, M.Y. Chiang, J.C. Aster, R.K. Humphries, C. Eaves, and A.P. Weng. 2012. NOTCH1 promotes T cell leukemia-initiating activity by RUNX-mediated regulation of PKC-theta and reactive oxygen species. *Nat Med*. 18:1693-1698.

Giroux, S., A.L. Kaushik, C. Capron, A. Jalil, C. Kelaidi, F. Sablitzky, D. Dumenil, O. Albagli, and I. Godin. 2007. lyl-1 and tal-1/scl, two genes encoding closely related bHLH transcription factors, display highly overlapping expression patterns during cardiovascular and hematopoietic ontogeny. *Gene Expr Patterns*. 7:215-226.

Goldberg, J.M., L.B. Silverman, D.E. Levy, V.K. Dalton, R.D. Gelber, L. Lehmann, H.J. Cohen, S.E. Sallan, and B.L. Asselin. 2003. Childhood T-cell acute lymphoblastic leukemia: the Dana-Farber Cancer Institute acute lymphoblastic leukemia consortium experience. *J Clin Oncol*. 21:3616-3622.

Gomez del Pulgar, T., S.A. Benitah, P.F. Valeron, C. Espina, and J.C. Lacal. 2005. Rho GTPase expression in tumourigenesis: evidence for a significant link. *Bioessays*. 27:602-613.

Gottlieb, A.B., K.B. Gordon, M.G. Lebwohl, I. Caro, P.A. Walicke, N. Li, C.L. Leonardi, and G. Efalizumab Study. 2004. Extended efalizumab therapy sustains efficacy without increasing toxicity in patients with moderate to severe chronic plaque psoriasis. *J Drugs Dermatol*. 3:614-624.

Graux, C., J. Cools, L. Michaux, P. Vandenberghe, and A. Hagemeijer. 2006. Cytogenetics and molecular genetics of T-cell acute lymphoblastic leukemia: from thymocyte to lymphoblast. *Leukemia*. 20:1496-1510.

Greenwood, J., L. Steinman, and S.S. Zamvil. 2006. Statin therapy and autoimmune disease: from protein prenylation to immunomodulation. *Nat Rev Immunol*. 6:358-370.

Guemar, L., P. de Santa Barbara, E. Vignal, B. Maurel, P. Fort, and S. Faure. 2007. The small GTPase RhoV is an essential regulator of neural crest induction in Xenopus. *Dev Biol*. 310:113-128.

Guilluy, C., R. Garcia-Mata, and K. Burridge. 2011. Rho protein crosstalk: another social network? *Trends Cell Biol*. 21:718-726.

Haddad, E., J.L. Zugaza, F. Louache, N. Debili, C. Crouin, K. Schwarz, A. Fischer, W. Vainchenker, and J. Bertoglio. 2001. The interaction between Cdc42 and WASP is required for SDF-1-induced T-lymphocyte chemotaxis. *Blood*. 97:33-38.

Harris, K.P., and U. Tepass. 2010. Cdc42 and vesicle trafficking in polarized cells. *Traffic*. 11:1272-1279.

Hartsock, A., and W.J. Nelson. 2008. Adherens and tight junctions: structure, function and connections to the actin cytoskeleton. *Biochim Biophys Acta*. 1778:660-669.

Hattori, M., and N. Minato. 2003. Rap1 GTPase: functions, regulation, and malignancy. *J Biochem*. 134:479-484.

Hauzenberger, D., J. Klominek, and K.G. Sundqvist. 1994. Functional specialization of fibronectin-binding beta 1-integrins in T lymphocyte migration. *J Immunol*. 153:960-971.

Hayday, A.C., and D.J. Pennington. 2007. Key factors in the organized chaos of early T cell development. *Nat Immunol*. 8:137-144.

Heasman, S.J., L.M. Carlin, S. Cox, T. Ng, and A.J. Ridley. 2010. Coordinated RhoA signaling at the leading edge and uropod is required for T cell transendothelial migration. *J Cell Biol*. 190:553-563.

Heasman, S.J., and A.J. Ridley. 2008. Mammalian Rho GTPases: new insights into their functions from in vivo studies. *Nat Rev Mol Cell Biol*. 9:690-701.

Hehnly, H., W. Xu, J.L. Chen, and M. Stamnes. 2010. Cdc42 regulates microtubule-dependent Golgi positioning. *Traffic*. 11:1067-1078.

Hoebe, R.A., C.H. Van Oven, T.W. Gadella, Jr., P.B. Dhonukshe, C.J. Van Noorden, and E.M. Manders. 2007. Controlled light-exposure microscopy reduces photobleaching and phototoxicity in fluorescence live-cell imaging. *Nat Biotechnol*. 25:249-253.

Hogg, N., R. Henderson, B. Leitinger, A. McDowall, J. Porter, and P. Stanley. 2002. Mechanisms contributing to the activity of integrins on leukocytes. *Immunol Rev*. 186:164-171.

Hsiao, H.W., W.H. Liu, C.J. Wang, Y.H. Lo, Y.H. Wu, S.T. Jiang, and M.Z. Lai. 2009. Deltex1 is a target of the transcription factor NFAT that promotes T cell anergy. *Immunity*. 31:72-83.

Huang, M., and G.C. Prendergast. 2006. RhoB in cancer suppression. *Histol Histopathol*. 21:213-218.

Huo, Y., A. Schober, S.B. Forlow, D.F. Smith, M.C. Hyman, S. Jung, D.R. Littman, C. Weber, and K. Ley. 2003. Circulating activated platelets exacerbate atherosclerosis in mice deficient in apolipoprotein E. *Nat Med*. 9:61-67.

Iden, S., and J.G. Collard. 2008. Crosstalk between small GTPases and polarity proteins in cell polarization. *Nat Rev Mol Cell Biol*. 9:846-859.

Infante, E., S.J. Heasman, and A.J. Ridley. 2011. Statins inhibit T-acute lymphoblastic leukemia cell adhesion and migration through Rap1b. *J Leukoc Biol*. 89:577-586.

Ishida, D., K. Kometani, H. Yang, K. Kakugawa, K. Masuda, K. Iwai, M. Suzuki, S. Itohara, T. Nakahata, H. Hiai, H. Kawamoto, M. Hattori, and N. Minato.

2003. Myeloproliferative stem cell disorders by deregulated Rap1 activation in SPA-1-deficient mice. *Cancer Cell*. 4:55-65.

Jaffe, A.B., and A. Hall. 2005. Rho GTPases: biochemistry and biology. *Annu Rev Cell Dev Biol*. 21:247-269.

Jankovic, M., R. Casellas, N. Yannoutsos, H. Wardemann, and M.C. Nussenzweig. 2004. RAGs and regulation of autoantibodies. *Annu Rev Immunol*. 22:485-501.

Janssen, J.W., W.D. Ludwig, W. Sterry, and C.R. Bartram. 1993. SIL-TAL1 deletion in T-cell acute lymphoblastic leukemia. *Leukemia*. 7:1204-1210.

Jiang, Z.Y., A. Chawla, A. Bose, M. Way, and M.P. Czech. 2002. A phosphatidylinositol 3-kinase-independent insulin signaling pathway to N-WASP/Arp2/3/F-actin required for GLUT4 glucose transporter recycling. *J Biol Chem*. 277:509-515.

Johnson-Leger, C., M. Aurrand-Lions, and B.A. Imhof. 2000. The parting of the endothelium: miracle, or simply a junctional affair? *J Cell Sci*. 113 (Pt 6):921-933.

Johnson-Leger, C.A., M. Aurrand-Lions, N. Beltraminelli, N. Fasel, and B.A. Imhof. 2002. Junctional adhesion molecule-2 (JAM-2) promotes lymphocyte transendothelial migration. *Blood*. 100:2479-2486.

Kadono, T., G.M. Venturi, D.A. Steeber, and T.F. Tedder. 2002. Leukocyte rolling velocities and migration are optimized by cooperative L-selectin and intercellular adhesion molecule-1 functions. *J Immunol*. 169:4542-4550.

Kaibuchi, K., S. Kuroda, and M. Amano. 1999. Regulation of the cytoskeleton and cell adhesion by the Rho family GTPases in mammalian cells. *Annu Rev Biochem*. 68:459-486.

Kallen, J., K. Welzenbach, P. Ramage, D. Geyl, R. Kriwacki, G. Legge, S. Cottens, G. Weitz-Schmidt, and U. Hommel. 1999. Structural basis for LFA-1 inhibition upon lovastatin binding to the CD11a I-domain. *J Mol Biol*. 292:1-9.

Kang, P.J., L. Beven, S. Hariharan, and H.O. Park. 2010. The Rsr1/Bud1 GTPase interacts with itself and the Cdc42 GTPase during bud-site selection and polarity establishment in budding yeast. *Mol Biol Cell*. 21:3007-3016.

Karp, J.E., and J.E. Lancet. 2005. Targeting the process of farynesylation for therapy of hematologic malignancies. *Curr Mol Med*. 5:643-652.

Katagiri, K., A. Maeda, M. Shimonaka, and T. Kinashi. 2003. RAPL, a Rap1-binding molecule that mediates Rap1-induced adhesion through spatial regulation of LFA-1. *Nat Immunol*. 4:741-748.

Katoh, M. 2002. Molecular cloning and characterization of WRCH2 on human chromosome 15q15. *Int J Oncol*. 20:977-982.

Kebriaei, P., J. Anastasi, and R.A. Larson. 2002. Acute lymphoblastic leukaemia: diagnosis and classification. *Best Pract Res Clin Haematol*. 15:597-621.

Khan, W.N. 2009. B cell receptor and BAFF receptor signaling regulation of B cell homeostasis. *J Immunol*. 183:3561-3567.

Kiuchi, T., K. Ohashi, S. Kurita, and K. Mizuno. 2007. Cofilin promotes stimulus-induced lamellipodium formation by generating an abundant supply of actin monomers. *J Cell Biol*. 177:465-476.

Klemm, J.D., S.L. Schreiber, and G.R. Crabtree. 1998. Dimerization as a regulatory mechanism in signal transduction. *Annu Rev Immunol*. 16:569-592.

Konig, R., and W. Zhou. 2004. Signal transduction in T helper cells: CD4 coreceptors exert complex regulatory effects on T cell activation and function. *Curr Issues Mol Biol*. 6:1-15.

Kress, H., E.H. Stelzer, D. Holzer, F. Buss, G. Griffiths, and A. Rohrbach. 2007. Filopodia act as phagocytic tentacles and pull with discrete steps and a load-dependent velocity. *Proc Natl Acad Sci U S A*. 104:11633-11638.

Kulkarni, R., S. Behboudi, and S. Sharif. 2011. Insights into the role of Toll-like receptors in modulation of T cell responses. *Cell Tissue Res*. 343:141-152.

Kuoppala, J., A. Lamminpaa, and E. Pukkala. 2008. Statins and cancer: A systematic review and meta-analysis. *Eur J Cancer*. 44:2122-2132.

Lafuente, E.M., A.A. van Puijenbroek, M. Krause, C.V. Carman, G.J. Freeman, A. Berezovskaya, E. Constantine, T.A. Springer, F.B. Gertler, and V.A. Boussiotis. 2004. RIAM, an Ena/VASP and Profilin ligand, interacts with Rap1-GTP and mediates Rap1-induced adhesion. *Dev Cell*. 7:585-595.

Larson, R.C., I. Lavenir, T.A. Larson, R. Baer, A.J. Warren, I. Wadman, K. Nottage, and T.H. Rabbitts. 1996. Protein dimerization between Lmo2 (Rbtn2) and Tal1 alters thymocyte development and potentiates T cell tumorigenesis in transgenic mice. *EMBO J*. 15:1021-1027.

Laubli, H., and L. Borsig. 2010. Selectins promote tumor metastasis. *Semin Cancer Biol*. 20:169-177.

Le Clainche, C., and M.F. Carlier. 2008. Regulation of actin assembly associated with protrusion and adhesion in cell migration. *Physiol Rev*. 88:489-513.

Lee, H.S., C.J. Lim, W. Puzon-McLaughlin, S.J. Shattil, and M.H. Ginsberg. 2009. RIAM activates integrins by linking talin to ras GTPase membrane-targeting sequences. *J Biol Chem*. 284:5119-5127.

Lee, K., K.T. Nam, S.H. Cho, P. Gudapati, Y. Hwang, D.S. Park, R. Potter, J. Chen, E. Volanakis, and M. Boothby. 2012. Vital roles of mTOR complex 2 in Notch-driven thymocyte differentiation and leukemia. *J Exp Med*. 209:713-728.

Leitinger, B., A. McDowall, P. Stanley, and N. Hogg. 2000. The regulation of integrin function by Ca(2+). *Biochim Biophys Acta*. 1498:91-98.

Leung, S.M., R. Rojas, C. Maples, C. Flynn, W.G. Ruiz, T.S. Jou, and G. Apodaca. 1999. Modulation of endocytic traffic in polarized Madin-Darby canine kidney cells by the small GTPase RhoA. *Mol Biol Cell*. 10:4369-4384.

Lewis, K.A., S.A. Holstein, and R.J. Hohl. 2005. Lovastatin alters the isoprenoid biosynthetic pathway in acute myelogenous leukemia cells in vivo. *Leuk Res*. 29:527-533.

Ley, K., C. Laudanna, M.I. Cybulsky, and S. Nourshargh. 2007. Getting to the site of inflammation: the leukocyte adhesion cascade updated. *Nat Rev Immunol*. 7:678-689.

Liao, J.K., and U. Laufs. 2005. Pleiotropic effects of statins. *Annu Rev Pharmacol Toxicol*. 45:89-118.

Lin, J., and A. Weiss. 2001. T cell receptor signalling. *J Cell Sci*. 114:243-244.

Lipp, M., and G. Muller. 2003. Shaping up adaptive immunity: the impact of CCR7 and CXCR5 on lymphocyte trafficking. *Verh Dtsch Ges Pathol*. 87:90-101.

Liu, Y., S.K. Shaw, S. Ma, L. Yang, F.W. Luscinskas, and C.A. Parkos. 2004. Regulation of leukocyte transmigration: cell surface interactions and signaling events. *J Immunol*. 172:7-13.

Lu, C., M. Shimaoka, Q. Zang, J. Takagi, and T.A. Springer. 2001. Locking in alternate conformations of the integrin alphaLbeta2 I domain with disulfide

bonds reveals functional relationships among integrin domains. *Proc Natl Acad Sci U S A*. 98:2393-2398.

Ludford-Menting, M.J., J. Oliaro, F. Sacirbegovic, E.T. Cheah, N. Pedersen, S.J. Thomas, A. Pasam, R. Iazzolino, L.E. Dow, N.J. Waterhouse, A. Murphy, S. Ellis, M.J. Smyth, M.H. Kershaw, P.K. Darcy, P.O. Humbert, and S.M. Russell. 2005. A network of PDZ-containing proteins regulates T cell polarity and morphology during migration and immunological synapse formation. *Immunity*. 22:737-748.

Mackay, C.R. 2001. Chemokines: immunology's high impact factors. *Nat Immunol*. 2:95-101.

Maddur, M.S., P. Miossec, S.V. Kaveri, and J. Bayry. 2012. Th17 cells: biology, pathogenesis of autoimmune and inflammatory diseases, and therapeutic strategies. *Am J Pathol*. 181:8-18.

Malinin, N.L., L. Zhang, J. Choi, A. Ciocea, O. Razorenova, Y.Q. Ma, E.A. Podrez, M. Tosi, D.P. Lennon, A.I. Caplan, S.B. Shurin, E.F. Plow, and T.V. Byzova. 2009. A point mutation in KINDLIN3 ablates activation of three integrin subfamilies in humans. *Nat Med*. 15:313-318.

Mamdouh, W., R.E. Kelly, M. Dong, L.N. Kantorovich, and F. Besenbacher. 2008. Two-dimensional supramolecular nanopatterns formed by the coadsorption of guanine and uracil at the liquid/solid interface. *J Am Chem Soc*. 130:695-702.

Mamdouh, Z., X. Chen, L.M. Pierini, F.R. Maxfield, and W.A. Muller. 2003. Targeted recycling of PECAM from endothelial surface-connected compartments during diapedesis. *Nature*. 421:748-753.

Manevich, E., V. Grabovsky, S.W. Feigelson, and R. Alon. 2007. Talin 1 and paxillin facilitate distinct steps in rapid VLA-4-mediated adhesion strengthening to vascular cell adhesion molecule 1. *J Biol Chem*. 282:25338-25348.

Mathisen, M.S., E. Jabbour, D. Thomas, S. O'Brien, and H. Kantarjian. 2013. Acute Lymphoblastic Leukemia (ALL) in Adults: Encouraging Developments on the Way to Higher Cure Rates. *Leuk Lymphoma*.

Matter, K., and M.S. Balda. 2003. Signalling to and from tight junctions. *Nat Rev Mol Cell Biol*. 4:225-236.

Mattila, P.K., and P. Lappalainen. 2008. Filopodia: molecular architecture and cellular functions. *Nat Rev Mol Cell Biol*. 9:446-454.

Mazieres, J., A. Pradines, and G. Favre. 2004. Perspectives on farnesyl transferase inhibitors in cancer therapy. *Cancer Lett*. 206:159-167.

McCormack, M.P., L.F. Young, S. Vasudevan, C.A. de Graaf, R. Codrington, T.H. Rabbitts, S.M. Jane, and D.J. Curtis. 2010. The Lmo2 oncogene initiates leukemia in mice by inducing thymocyte self-renewal. *Science*. 327:879-883.

Menetrier-Caux, C., T. Curiel, J. Faget, M. Manuel, C. Caux, and W. Zou. 2012. Targeting regulatory T cells. *Target Oncol*. 7:15-28.

Meng, Y.S., H. Khoury, J.E. Dick, and M.D. Minden. 2005. Oncogenic potential of the transcription factor LYL1 in acute myeloblastic leukemia. *Leukemia*. 19:1941-1947.

Miaczynska, M., and D. Bar-Sagi. 2010. Signaling endosomes: seeing is believing. *Curr Opin Cell Biol*. 22:535-540.

Millan, J., L. Hewlett, M. Glyn, D. Toomre, P. Clark, and A.J. Ridley. 2006. Lymphocyte transcellular migration occurs through recruitment of

endothelial ICAM-1 to caveola- and F-actin-rich domains. *Nat Cell Biol*. 8:113-123.

Millan, J., and A.J. Ridley. 2005. Rho GTPases and leucocyte-induced endothelial remodelling. *Biochem J*. 385:329-337.

Miller, D.H., O.A. Khan, W.A. Sheremata, L.D. Blumhardt, G.P. Rice, M.A. Libonati, A.J. Willmer-Hulme, C.M. Dalton, K.A. Miszkiel, P.W. O'Connor, and G. International Natalizumab Multiple Sclerosis Trial. 2003. A controlled trial of natalizumab for relapsing multiple sclerosis. *N Engl J Med*. 348:15-23.

Mor, A., M.L. Dustin, and M.R. Philips. 2007. Small GTPases and LFA-1 reciprocally modulate adhesion and signaling. *Immunol Rev*. 218:114-125.

Mor, A., J.P. Wynne, I.M. Ahearn, M.L. Dustin, G. Du, and M.R. Philips. 2009. Phospholipase D1 regulates lymphocyte adhesion via upregulation of Rap1 at the plasma membrane. *Mol Cell Biol*. 29:3297-3306.

Morita, K., H. Sasaki, M. Furuse, and S. Tsukita. 1999. Endothelial claudin: claudin-5/TMVCF constitutes tight junction strands in endothelial cells. *J Cell Biol*. 147:185-194.

Morton, P.E., and M. Parsons. 2011. Measuring FRET using time-resolved FLIM. *Methods Mol Biol*. 769:403-413.

Moser, M., K.R. Legate, R. Zent, and R. Fassler. 2009. The tail of integrins, talin, and kindlins. *Science*. 324:895-899.

Mullally, A., and B.L. Ebert. 2010. NF1 inactivation revs up Ras in adult acute myelogenous leukemia. *Clin Cancer Res*. 16:4074-4076.

Muller, W.A. 2003. Leukocyte-endothelial-cell interactions in leukocyte transmigration and the inflammatory response. *Trends Immunol*. 24:327-334.

Muller, W.A., S.A. Weigl, X. Deng, and D.M. Phillips. 1993. PECAM-1 is required for transendothelial migration of leukocytes. *J Exp Med*. 178:449-460.

Naji, L., D. Pacholsky, and P. Aspenstrom. 2011. ARHGAP30 is a Wrch-1-interacting protein involved in actin dynamics and cell adhesion. *Biochem Biophys Res Commun*. 409:96-102.

Nakamura, N., C. Rabouille, R. Watson, T. Nilsson, N. Hui, P. Slusarewicz, T.E. Kreis, and G. Warren. 1995. Characterization of a cis-Golgi matrix protein, GM130. *J Cell Biol*. 131:1715-1726.

Navarro-Lerida, I., S. Sanchez-Perales, M. Calvo, C. Rentero, Y. Zheng, C. Enrich, and M.A. Del Pozo. 2012. A palmitoylation switch mechanism regulates Rac1 function and membrane organization. *EMBO J*. 31:534-551.

Newton, P., G. O'Boyle, Y. Jenkins, S. Ali, and J.A. Kirby. 2009. T cell extravasation: demonstration of synergy between activation of CXCR3 and the T cell receptor. *Mol Immunol*. 47:485-492.

Nwabo Kamdje, A.H., and M. Krampera. 2011. Notch signaling in acute lymphoblastic leukemia: any role for stromal microenvironment? *Blood*. 118:6506-6514.

O'Neil, J., J. Grim, P. Strack, S. Rao, D. Tibbitts, C. Winter, J. Hardwick, M. Welcker, J.P. Meijerink, R. Pieters, G. Draetta, R. Sears, B.E. Clurman, and A.T. Look. 2007. FBW7 mutations in leukemic cells mediate NOTCH pathway activation and resistance to gamma-secretase inhibitors. *J Exp Med*. 204:1813-1824.

Ocio, E.M., M.V. Mateos, P. Maiso, A. Pandiella, and J.F. San-Miguel. 2008. New drugs in multiple myeloma: mechanisms of action and phase I/II clinical findings. *Lancet Oncol*. 9:1157-1165.

Ono, Y., N. Fukuhara, and O. Yoshie. 1997. Transcriptional activity of TAL1 in T cell acute lymphoblastic leukemia (T-ALL) requires RBTN1 or -2 and induces TALLA1, a highly specific tumor marker of T-ALL. *J Biol Chem*. 272:4576-4581.

Oppenheimer-Marks, N., L.S. Davis, D.T. Bogue, J. Ramberg, and P.E. Lipsky. 1991. Differential utilization of ICAM-1 and VCAM-1 during the adhesion and transendothelial migration of human T lymphocytes. *J Immunol*. 147:2913-2921.

Osmani, N., F. Peglion, P. Chavrier, and S. Etienne-Manneville. 2010. Cdc42 localization and cell polarity depend on membrane traffic. *J Cell Biol*. 191:1261-1269.

Ostermann, G., K.S. Weber, A. Zernecke, A. Schroder, and C. Weber. 2002. JAM-1 is a ligand of the beta(2) integrin LFA-1 involved in transendothelial migration of leukocytes. *Nat Immunol*. 3:151-158.

Palamidessi, A., E. Frittoli, M. Garre, M. Faretta, M. Mione, I. Testa, A. Diaspro, L. Lanzetti, G. Scita, and P.P. Di Fiore. 2008. Endocytic trafficking of Rac is required for the spatial restriction of signaling in cell migration. *Cell*. 134:135-147.

Palfy, M., A. Remenyi, and T. Korcsmaros. 2012. Endosomal crosstalk: meeting points for signaling pathways. *Trends Cell Biol*.

Palomero, T., D.T. Odom, J. O'Neil, A.A. Ferrando, A. Margolin, D.S. Neuberg, S.S. Winter, R.S. Larson, W. Li, X.S. Liu, R.A. Young, and A.T. Look. 2006. Transcriptional regulatory networks downstream of TAL1/SCL in T-cell acute lymphoblastic leukemia. *Blood*. 108:986-992.

Palomero, T., M.L. Sulis, M. Cortina, P.J. Real, K. Barnes, M. Ciofani, E. Caparros, J. Buteau, K. Brown, S.L. Perkins, G. Bhagat, A.M. Agarwal, G. Basso, M. Castillo, S. Nagase, C. Cordon-Cardo, R. Parsons, J.C. Zuniga-Pflucker, M. Dominguez, and A.A. Ferrando. 2007. Mutational loss of PTEN induces resistance to NOTCH1 inhibition in T-cell leukemia. *Nat Med*. 13:1203-1210.

Park, H., Z. Li, X.O. Yang, S.H. Chang, R. Nurieva, Y.H. Wang, Y. Wang, L. Hood, Z. Zhu, Q. Tian, and C. Dong. 2005. A distinct lineage of CD4 T cells regulates tissue inflammation by producing interleukin 17. *Nat Immunol*. 6:1133-1141.

Park, S.J., S. Suetsugu, H. Sagara, and T. Takenawa. 2007. HSP90 cross-links branched actin filaments induced by N-WASP and the Arp2/3 complex. *Genes Cells*. 12:611-622.

Parri, M., and P. Chiarugi. 2010. Rac and Rho GTPases in cancer cell motility control. *Cell Commun Signal*. 8:23.

Peifer, M., and P. Polakis. 2000. Wnt signaling in oncogenesis and embryogenesis--a look outside the nucleus. *Science*. 287:1606-1609.

Pellinen, T., S. Tuomi, A. Arjonen, M. Wolf, H. Edgren, H. Meyer, R. Grosse, T. Kitzing, J.K. Rantala, O. Kallioniemi, R. Fassler, M. Kallio, and J. Ivaska. 2008. Integrin trafficking regulated by Rab21 is necessary for cytokinesis. *Dev Cell*. 15:371-385.

Peter, M., S.M. Ameer-Beg, M.K. Hughes, M.D. Keppler, S. Prag, M. Marsh, B. Vojnovic, and T. Ng. 2005. Multiphoton-FLIM quantification of the EGFP-mRFP1 FRET pair for localization of membrane receptor-kinase interactions. *Biophys J*. 88:1224-1237.

Petri, B., and M.G. Bixel. 2006. Molecular events during leukocyte diapedesis. *FEBS J*. 273:4399-4407.

Phillipson, M., B. Heit, P. Colarusso, L. Liu, C.M. Ballantyne, and P. Kubes. 2006. Intraluminal crawling of neutrophils to emigration sites: a molecularly distinct process from adhesion in the recruitment cascade. *J Exp Med*. 203:2569-2575.

Phillipson, M., J. Kaur, P. Colarusso, C.M. Ballantyne, and P. Kubes. 2008. Endothelial domes encapsulate adherent neutrophils and minimize increases in vascular permeability in paracellular and transcellular emigration. *PLoS One*. 3:e1649.

Pieters, R., and W.L. Carroll. 2010. Biology and treatment of acute lymphoblastic leukemia. *Hematol Oncol Clin North Am*. 24:1-18.

Puri, K.D., T.A. Doggett, C.Y. Huang, J. Douangpanya, J.S. Hayflick, M. Turner, J. Penninger, and T.G. Diacovo. 2005. The role of endothelial PI3Kgamma activity in neutrophil trafficking. *Blood*. 106:150-157.

Raaijmakers, J.H., and J.L. Bos. 2009. Specificity in Ras and Rap Signaling. *Journal of Biological Chemistry*. 284:10995-10999.

Radhakrishna, H., O. Al-Awar, Z. Khachikian, and J.G. Donaldson. 1999. ARF6 requirement for Rac ruffling suggests a role for membrane trafficking in cortical actin rearrangements. *J Cell Sci*. 112 (Pt 6):855-866.

Radtke, F., A. Wilson, S.J. Mancini, and H.R. MacDonald. 2004. Notch regulation of lymphocyte development and function. *Nat Immunol*. 5:247-253.

Ratner, S., M.P. Piechocki, and A. Galy. 2003. Role of Rho-family GTPase Cdc42 in polarized expression of lymphocyte appendages. *J Leukoc Biol*. 73:830-840.

Rattan, S. 2010. 3-Hydroxymethyl coenzyme A reductase inhibition attenuates spontaneous smooth muscle tone via RhoA/ROCK pathway regulated by RhoA prenylation. *Am J Physiol Gastrointest Liver Physiol*. 298:G962-969.

Real, P.J., and A.A. Ferrando. 2009. NOTCH inhibition and glucocorticoid therapy in T-cell acute lymphoblastic leukemia. *Leukemia*. 23:1374-1377.

Ridley, A.J. 2006. Rho GTPases and actin dynamics in membrane protrusions and vesicle trafficking. *Trends Cell Biol*. 16:522-529.

Ridley, A.J., H.F. Paterson, C.L. Johnston, D. Diekmann, and A. Hall. 1992. The small GTP-binding protein rac regulates growth factor-induced membrane ruffling. *Cell*. 70:401-410.

Riou, P., P. Villalonga, and A.J. Ridley. 2010. Rnd proteins: multifunctional regulators of the cytoskeleton and cell cycle progression. *Bioessays*. 32:986-992.

Robb, L. 2007. Cytokine receptors and hematopoietic differentiation. *Oncogene*. 26:6715-6723.

Roberts, P.J., N. Mitin, P.J. Keller, E.J. Chenette, J.P. Madigan, R.O. Currin, A.D. Cox, O. Wilson, P. Kirschmeier, and C.J. Der. 2008. Rho Family GTPase modification and dependence on CAAX motif-signaled posttranslational modification. *J Biol Chem*. 283:25150-25163.

Roberts, W.G., and G.E. Palade. 1997. Neovasculature induced by vascular endothelial growth factor is fenestrated. *Cancer Res*. 57:765-772.

Rossman, K.L., C.J. Der, and J. Sondek. 2005. GEF means go: turning on RHO GTPases with guanine nucleotide-exchange factors. *Nat Rev Mol Cell Biol*. 6:167-180.

Rothenberg, E.V., J.E. Moore, and M.A. Yui. 2008. Launching the T-cell-lineage developmental programme. *Nat Rev Immunol*. 8:9-21.

Rougerie, P., and J. Delon. 2012. Rho GTPases: Masters of T lymphocyte migration and activation. *Immunol Lett*. 142:1-13.

Roy, S., S. Plowman, B. Rotblat, I.A. Prior, C. Muncke, S. Grainger, R.G. Parton, Y.I. Henis, Y. Kloog, and J.F. Hancock. 2005. Individual palmitoyl residues serve distinct roles in H-ras trafficking, microlocalization, and signaling. *Mol Cell Biol*. 25:6722-6733.

Ruffell, B., D.G. DeNardo, N.I. Affara, and L.M. Coussens. 2010. Lymphocytes in cancer development: polarization towards pro-tumor immunity. *Cytokine Growth Factor Rev*. 21:3-10.

Ruusala, A., and P. Aspenstrom. 2008. The atypical Rho GTPase Wrch1 collaborates with the nonreceptor tyrosine kinases Pyk2 and Src in regulating cytoskeletal dynamics. *Mol Cell Biol*. 28:1802-1814.

Ryan, S.O., and B.A. Cobb. 2012. Roles for major histocompatibility complex glycosylation in immune function. *Semin Immunopathol*. 34:425-441.

Saldanha, A.J. 2004. Java Treeview--extensible visualization of microarray data. *Bioinformatics*. 20:3246-3248.

Sanchez-Madrid, F., and J.M. Serrador. 2009. Bringing up the rear: defining the roles of the uropod. *Nat Rev Mol Cell Biol*. 10:353-359.

Santos, E., A.R. Nebreda, T. Bryan, and E.S. Kempner. 1988. Oligomeric structure of p21 ras proteins as determined by radiation inactivation. *J Biol Chem*. 263:9853-9858.

Sanz-Moreno, V., G. Gadea, J. Ahn, H. Paterson, P. Marra, S. Pinner, E. Sahai, and C.J. Marshall. 2008. Rac activation and inactivation control plasticity of tumor cell movement. *Cell*. 135:510-523.

Saras, J., P. Wollberg, and P. Aspenstrom. 2004. Wrch1 is a GTPase-deficient Cdc42-like protein with unusual binding characteristics and cellular effects. *Exp Cell Res*. 299:356-369.

Sassano, A., E. Katsoulidis, G. Antico, J.K. Altman, A.J. Redig, S. Minucci, M.S. Tallman, and L.C. Platanias. 2007. Suppressive effects of statins on acute promyelocytic leukemia cells. *Cancer Res*. 67:4524-4532.

Satoh, K., K. Ichihara, E.J. Landon, T. Inagami, and H. Tang. 2001. 3-Hydroxy-3-methylglutaryl-CoA reductase inhibitors block calcium-dependent tyrosine kinase Pyk2 activation by angiotensin II in vascular endothelial cells. involvement of geranylgeranylation of small G protein Rap1. *J Biol Chem*. 276:15761-15767.

Schafer, C., B. Borm, S. Born, C. Mohl, E.M. Eibl, and B. Hoffmann. 2009. One step ahead: role of filopodia in adhesion formation during cell migration of keratinocytes. *Exp Cell Res*. 315:1212-1224.

Schenkel, A.R., Z. Mamdouh, X. Chen, R.M. Liebman, and W.A. Muller. 2002. CD99 plays a major role in the migration of monocytes through endothelial junctions. *Nat Immunol*. 3:143-150.

Schiefelbein, D., I. Goren, B. Fisslthaler, H. Schmidt, G. Geisslinger, J. Pfeilschifter, and S. Frank. 2008. Biphasic regulation of HMG-CoA reductase expression and activity during wound healing and its functional role in the control of keratinocyte angiogenic and proliferative responses. *J Biol Chem*. 283:15479-15490.

Schmidt, A., and A. Hall. 2002. Guanine nucleotide exchange factors for Rho GTPases: turning on the switch. *Genes Dev*. 16:1587-1609.

Schmittgen, T.D., and K.J. Livak. 2008. Analyzing real-time PCR data by the comparative C(T) method. *Nat Protoc*. 3:1101-1108.

Segev, N. 2011. GTPases in intracellular trafficking: an overview. *Semin Cell Dev Biol*. 22:1-2.

Sekar, R.B., and A. Periasamy. 2003. Fluorescence resonance energy transfer (FRET) microscopy imaging of live cell protein localizations. *J Cell Biol*. 160:629-633.

Shamri, R., V. Grabovsky, J.M. Gauguet, S. Feigelson, E. Manevich, W. Kolanus, M.K. Robinson, D.E. Staunton, U.H. von Andrian, and R. Alon. 2005. Lymphocyte arrest requires instantaneous induction of an extended LFA-1 conformation mediated by endothelium-bound chemokines. *Nat Immunol*. 6:497-506.

Shaw, S.K., P.S. Bamba, B.N. Perkins, and F.W. Luscinskas. 2001. Real-time imaging of vascular endothelial-cadherin during leukocyte transmigration across endothelium. *J Immunol*. 167:2323-2330.

Shepelev, M.V., J. Chernoff, and I.V. Korobko. 2011. Rho family GTPase Chp/RhoV induces PC12 apoptotic cell death via JNK activation. *Small Gtpases*. 2:17-26.

Shirsat, N.V., R.J. Pignolo, B.L. Kreider, and G. Rovera. 1990. A member of the ras gene superfamily is expressed specifically in T, B and myeloid hemopoietic cells. *Oncogene*. 5:769-772.

Shutes, A., A.C. Berzat, A.D. Cox, and C.J. Der. 2004. Atypical mechanism of regulation of the Wrch-1 Rho family small GTPase. *Curr Biol*. 14:2052-2056.

Simeoni, L., S. Kliche, J. Lindquist, and B. Schraven. 2004. Adaptors and linkers in T and B cells. *Curr Opin Immunol*. 16:304-313.

Singbartl, K., J. Thatte, M.L. Smith, K. Wethmar, K. Day, and K. Ley. 2001. A CD2-green fluorescence protein-transgenic mouse reveals very late antigen-4-dependent CD8+ lymphocyte rolling in inflamed venules. *J Immunol*. 166:7520-7526.

Sommers, C.L., J.B. Dejarnette, K. Huang, J. Lee, D. El-Khoury, E.W. Shores, and P.E. Love. 2000. Function of CD3 epsilon-mediated signals in T cell development. *J Exp Med*. 192:913-919.

Spilker, C., and M.R. Kreutz. 2010. RapGAPs in brain: multipurpose players in neuronal Rap signalling. *Eur J Neurosci*. 32:1-9.

Stephens, L., C. Ellson, and P. Hawkins. 2002. Roles of PI3Ks in leukocyte chemotaxis and phagocytosis. *Curr Opin Cell Biol*. 14:203-213.

Stephens, L., L. Milne, and P. Hawkins. 2008. Moving towards a better understanding of chemotaxis. *Curr Biol*. 18:R485-494.

Stewart, M., and N. Hogg. 1996. Regulation of leukocyte integrin function: affinity vs. avidity. *J Cell Biochem*. 61:554-561.

Symons, M., and J.E. Segall. 2009. Rac and Rho driving tumor invasion: who's at the wheel? *Genome Biol*. 10:213.

Takahashi, K., H. Nakanishi, M. Miyahara, K. Mandai, K. Satoh, A. Satoh, H. Nishioka, J. Aoki, A. Nomoto, A. Mizoguchi, and Y. Takai. 1999. Nectin/PRR: an immunoglobulin-like cell adhesion molecule recruited to cadherin-based adherens junctions through interaction with Afadin, a PDZ domain-containing protein. *J Cell Biol*. 145:539-549.

Takaishi, K., T. Sasaki, H. Kotani, H. Nishioka, and Y. Takai. 1997. Regulation of cell-cell adhesion by rac and rho small G proteins in MDCK cells. *J Cell Biol*. 139:1047-1059.

Takesono, A., S.J. Heasman, B. Wojciak-Stothard, R. Garg, and A.J. Ridley. 2010. Microtubules regulate migratory polarity through Rho/ROCK signaling in T cells. *PLoS One*. 5:e8774.

Tang, W.H., and G.S. Francis. 2010. Statin treatment for patients with heart failure. *Nat Rev Cardiol*. 7:249-255.

Tao, W., D. Pennica, L. Xu, R.F. Kalejta, and A.J. Levine. 2001. Wrch-1, a novel member of the Rho gene family that is regulated by Wnt-1. *Genes Dev*. 15:1796-1807.

Tavor, S., and I. Petit. 2010. Can inhibition of the SDF-1/CXCR4 axis eradicate acute leukemia? *Semin Cancer Biol*. 20:178-185.

Tybulewicz, V.L.J., and R.B. Henderson. 2009. Rho family GTPases and their regulators in lymphocytes. *Nature Reviews Immunology*. 9:630-644.

Uchiyama, T., T. Ishikawa, and A. Imura. 1995. Adhesion properties of adult T cell leukemia cells. *Leuk Lymphoma*. 16:407-412.

van Dam, T.J., H. Rehmann, J.L. Bos, and B. Snel. 2009. Phylogeny of the CDC25 homology domain reveals rapid differentiation of Ras pathways between early animals and fungi. *Cell Signal*. 21:1579-1585.

van der Merwe, P.A., and O. Dushek. 2011. Mechanisms for T cell receptor triggering. *Nat Rev Immunol*. 11:47-55.

van Grotel, M., J.P. Meijerink, E.R. van Wering, A.W. Langerak, H.B. Beverloo, J.G. Buijs-Gladdines, N.B. Burger, M. Passier, E.M. van Lieshout, W.A. Kamps, A.J. Veerman, M.M. van Noesel, and R. Pieters. 2008. Prognostic significance of molecular-cytogenetic abnormalities in pediatric T-ALL is not explained by immunophenotypic differences. *Leukemia*. 22:124-131.

Van Hennik, P.B., and P.L. Hordijk. 2005. Rho GTPases in hematopoietic cells. *Antioxid Redox Signal*. 7:1440-1455.

van Hennik, P.B., J.P. ten Klooster, J.R. Halstead, C. Voermans, E.C. Anthony, N. Divecha, and P.L. Hordijk. 2003. The C-terminal domain of Rac1 contains two motifs that control targeting and signaling specificity. *J Biol Chem*. 278:39166-39175.

van Wetering, S., J.D. van Buul, S. Quik, F.P. Mul, E.C. Anthony, J.P. ten Klooster, J.G. Collard, and P.L. Hordijk. 2002. Reactive oxygen species mediate Rac-induced loss of cell-cell adhesion in primary human endothelial cells. *J Cell Sci*. 115:1837-1846.

Vega, F.M., and A.J. Ridley. 2008. Rho GTPases in cancer cell biology. *FEBS Lett*. 582:2093-2101.

Vestweber, D. 2007. Adhesion and signaling molecules controlling the transmigration of leukocytes through endothelium. *Immunol Rev*. 218:178-196.

Vestweber, D. 2008. VE-cadherin: the major endothelial adhesion molecule controlling cellular junctions and blood vessel formation. *Arterioscler Thromb Vasc Biol*. 28:223-232.

Vicente, R., L. Swainson, S. Marty-Gres, S.C. De Barros, S. Kinet, V.S. Zimmermann, and N. Taylor. 2010. Molecular and cellular basis of T cell lineage commitment. *Semin Immunol*. 22:270-275.

Vielkind, S., M. Gallagher-Gambarelli, M. Gomez, H.J. Hinton, and D.A. Cantrell. 2005. Integrin regulation by RhoA in thymocytes. *J Immunol*. 175:350-357.

Vignjevic, D., S. Kojima, Y. Aratyn, O. Danciu, T. Svitkina, and G.G. Borisy. 2006. Role of fascin in filopodial protrusion. *J Cell Biol*. 174:863-875.

Vignjevic, D., M. Schoumacher, N. Gavert, K.P. Janssen, G. Jih, M. Lae, D. Louvard, A. Ben-Ze'ev, and S. Robine. 2007. Fascin, a novel target of beta-catenin-TCF signaling, is expressed at the invasive front of human colon cancer. *Cancer Res*. 67:6844-6853.

Wang, B., J.X. Zou, B. Ek-Rylander, and E. Ruoslahti. 2000. R-Ras contains a proline-rich site that binds to SH3 domains and is required for integrin activation by R-Ras. *J Biol Chem*. 275:5222-5227.

Wang, C.Y., P.Y. Liu, and J.K. Liao. 2008. Pleiotropic effects of statin therapy: molecular mechanisms and clinical results. *Trends Mol Med*. 14:37-44.

Wang, H., X. Zeng, Z. Fan, and B. Lim. 2010. RhoH plays distinct roles in T-cell migrations induced by different doses of SDF1 alpha. *Cell Signal*. 22:1022-1032.

Wang, Q., and C.M. Doerschuk. 2000. Neutrophil-induced changes in the biomechanical properties of endothelial cells: roles of ICAM-1 and reactive oxygen species. *J Immunol*. 164:6487-6494.

Wedepohl, S., F. Beceren-Braun, S. Riese, K. Buscher, S. Enders, G. Bernhard, K. Kilian, V. Blanchard, J. Dernedde, and R. Tauber. 2012. L-Selectin - a dynamic regulator of leukocyte migration. *Eur J Cell Biol*. 91:257-264.

Weerkamp, F., J.J. van Dongen, and F.J. Staal. 2006. Notch and Wnt signaling in T-lymphocyte development and acute lymphoblastic leukemia. *Leukemia*. 20:1197-1205.

Wegmann, F., B. Petri, A.G. Khandoga, C. Moser, A. Khandoga, S. Volkery, H. Li, I. Nasdala, O. Brandau, R. Fassler, S. Butz, F. Krombach, and D. Vestweber. 2006. ESAM supports neutrophil extravasation, activation of Rho, and VEGF-induced vascular permeability. *J Exp Med*. 203:1671-1677.

Weisz Hubsman, M., N. Volinsky, E. Manser, D. Yablonski, and A. Aronheim. 2007. Autophosphorylation-dependent degradation of Pak1, triggered by the Rho-family GTPase, Chp. *Biochem J*. 404:487-497.

Weitz-Schmidt, G., K. Welzenbach, V. Brinkmann, T. Kamata, J. Kallen, C. Bruns, S. Cottens, Y. Takada, and U. Hommel. 2001. Statins selectively inhibit leukocyte function antigen-1 by binding to a novel regulatory integrin site. *Nat Med*. 7:687-692.

Welch, H.C., W.J. Coadwell, L.R. Stephens, and P.T. Hawkins. 2003. Phosphoinositide 3-kinase-dependent activation of Rac. *FEBS Lett*. 546:93-97.

Weng, A.P., A.A. Ferrando, W. Lee, J.P.t. Morris, L.B. Silverman, C. Sanchez-Irizarry, S.C. Blacklow, A.T. Look, and J.C. Aster. 2004. Activating mutations of NOTCH1 in human T cell acute lymphoblastic leukemia. *Science*. 306:269-271.

Wennerberg, K., K.L. Rossman, and C.J. Der. 2005. The Ras superfamily at a glance. *J Cell Sci*. 118:843-846.

Whyte, D.B., P. Kirschmeier, T.N. Hockenberry, I. Nunez-Oliva, L. James, J.J. Catino, W.R. Bishop, and J.K. Pai. 1997. K- and N-Ras are geranylgeranylated in cells treated with farnesyl protein transferase inhibitors. *J Biol Chem*. 272:14459-14464.

Willems, L., J. Tamburini, N. Chapuis, C. Lacombe, P. Mayeux, and D. Bouscary. 2012. PI3K and mTOR signaling pathways in cancer: new data on targeted therapies. *Curr Oncol Rep*. 14:129-138.

Williams, C.L. 2003. The polybasic region of Ras and Rho family small GTPases: a regulator of protein interactions and membrane association and a site of nuclear localization signal sequences. *Cell Signal*. 15:1071-1080.

Wilson, A., H.R. MacDonald, and F. Radtke. 2001. Notch 1-deficient common lymphoid precursors adopt a B cell fate in the thymus. *J Exp Med*. 194:1003-1012.

Wittchen, E.S. 2009. Endothelial signaling in paracellular and transcellular leukocyte transmigration. *Front Biosci*. 14:2522-2545.

Wittchen, E.S., A. Aghajanian, and K. Burridge. 2011. Isoform-specific differences between Rap1A and Rap1B GTPases in the formation of endothelial cell junctions. *Small Gtpases*. 2:65-76.

Wittchen, E.S., J.D. van Buul, K. Burridge, and R.A. Worthylake. 2005. Trading spaces: Rap, Rac, and Rho as architects of transendothelial migration. *Curr Opin Hematol*. 12:14-21.

Wolfe, M.S. 2009. gamma-Secretase in biology and medicine. *Semin Cell Dev Biol*. 20:219-224.

Wouters, F.S., P.J. Verveer, and P.I. Bastiaens. 2001. Imaging biochemistry inside cells. *Trends Cell Biol*. 11:203-211.

Xiong, Y., and R. Bosselut. 2012. CD4-CD8 differentiation in the thymus: connecting circuits and building memories. *Curr Opin Immunol*. 24:139-145.

Yamashiro, S., Y. Yamakita, S. Ono, and F. Matsumura. 1998. Fascin, an actin-bundling protein, induces membrane protrusions and increases cell motility of epithelial cells. *Mol Biol Cell*. 9:993-1006.

Zarbock, A., K. Ley, R.P. McEver, and A. Hidalgo. 2011. Leukocyte ligands for endothelial selectins: specialized glycoconjugates that mediate rolling and signaling under flow. *Blood*. 118:6743-6751.

Zeiser, R., K. Maas, S. Youssef, C. Durr, L. Steinman, and R.S. Negrin. 2009. Regulation of different inflammatory diseases by impacting the mevalonate pathway. *Immunology*. 127:18-25.

Zhang, H., J.S. Berg, Z. Li, Y. Wang, P. Lang, A.D. Sousa, A. Bhaskar, R.E. Cheney, and S. Stromblad. 2004. Myosin-X provides a motor-based link between integrins and the cytoskeleton. *Nat Cell Biol*. 6:523-531.

Zhang, J., L. Ding, L. Holmfeldt, G. Wu, S.L. Heatley, D. Payne-Turner, J. Easton, X. Chen, J. Wang, M. Rusch, C. Lu, S.C. Chen, L. Wei, J.R. Collins-Underwood, J. Ma, K.G. Roberts, S.B. Pounds, A. Ulyanov, J. Becksfort, P. Gupta, R. Huether, R.W. Kriwacki, M. Parker, D.J. McGoldrick, D. Zhao, D. Alford, S. Espy, K.C. Bobba, G. Song, D. Pei, C. Cheng, S. Roberts, M.I. Barbato, D. Campana, E. Coustan-Smith, S.A. Shurtleff, S.C. Raimondi, M. Kleppe, J. Cools, K.A. Shimano, M.L. Hermiston, S. Doulatov, K. Eppert, E. Laurenti, F. Notta, J.E. Dick, G. Basso, S.P. Hunger, M.L. Loh, M. Devidas, B. Wood, S. Winter, K.P. Dunsmore, R.S. Fulton, L.L. Fulton, X. Hong, C.C. Harris, D.J. Dooling, K. Ochoa, K.J. Johnson, J.C. Obenauer, W.E. Evans, C.H. Pui, C.W. Naeve, T.J. Ley, E.R. Mardis, R.K. Wilson, J.R. Downing, and C.G. Mullighan. 2012. The genetic basis of early T-cell precursor acute lymphoblastic leukaemia. *Nature*. 481:157-163.

Zhang, J.S., A. Koenig, C. Young, and D.D. Billadeau. 2011. GRB2 couples RhoU to epidermal growth factor receptor signaling and cell migration. *Mol Biol Cell*. 22:2119-2130.

Zhang, X., J. Jin, X. Peng, V.S. Ramgolam, and S. Markovic-Plese. 2008. Simvastatin inhibits IL-17 secretion by targeting multiple IL-17-regulatory

cytokines and by inhibiting the expression of IL-17 transcription factor RORC in CD4+ lymphocytes. *J Immunol*. 180:6988-6996.

Zhang, Y., and H. Wang. 2012. Integrin signalling and function in immune cells. *Immunology*. 135:268-275.

Zlotnik, A., and O. Yoshie. 2000. Chemokines: a new classification system and their role in immunity. *Immunity*. 12:121-127.

Acknowledgments

First and foremost, I would like to express my greatest gratitude to my supervisor Professor Anne Ridley for giving me the opportunity to conduct my PhD in her laboratory. I am grateful for her unlimited patience, constant support and direction. I also wish to thank my second supervisor Dr Shaun Thomas for his advice and encouragement throughout my PhD.

I would like to thank all the past and present members of the laboratory. I will always be grateful to my dear Ritu for being my family during these four years. A big, big thank you goes to Barbara, Silvia M. and Christina for making every single day of this journey so special. It would have been difficult without you girls! Thanks for all the positive words and constant support.
Many thanks to my fellow PhD student Naren for his help in the lab and for being a good friend. Thanks to Silvia G. for the energetic chats and scientific discussions.
A big thanks goes to Sarah for being a fantastic mentor and a great friend. I am grateful to Parag, Francisco, Philippe, Nico, Audrey, Virginia, Mariana for their scientific support and for the great time we shared inside and outside the lab.
I am also thankful to Dr Jonathan Morris for his career advice and his expertise in molecular biology.

I have to thank my friends from Cosenza for always believing in me. Also thanks to Raja, Jack and Ciccio for the warmest welcome back.

A special thanks goes to Mattia for always sticking by my side. Thank you for being my constant source of strength and motivation.

Most importantly, I thank my beloved parents and brother. Thank you for always being there, for guiding me and encouraging me to reach my dreams. Without you I would be nowhere.

I would like to dedicate this work to the memory of Flavia.